FUNCTIONAL ANALYSIS OF ACYL-COA BINDING PROTEIN IN SKIN AND SEBACEOUS GLANDS

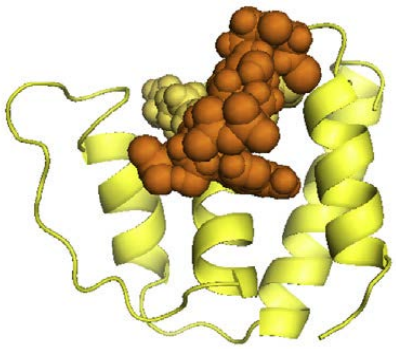

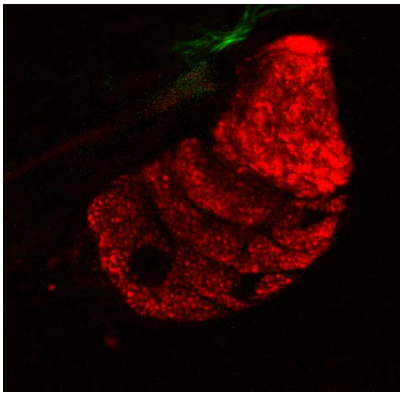

Ph.D. Thesis
Hanne Engelsby

Supervisor Nils J. Færgeman

Department of Biochemistry and Molecular Biology
Faculty of Science, University of Southern Denmark

March 2017

PREFACE

The work presented in this PhD thesis was performed in Professor Nils J. Færgemans laboratory, Department of Biochemistry and Molecular Biology, University of Southern Denmark. Many people and research groups were involved in the successful obtainment of the results presented here and I would like to express my gratitude and thankfulness to them.

First I would like to thank my supervisor Nils J. Færgeman for providing me with the opportunity to carry out this PhD. He has been an excellent guidance and I have enjoyed our fruitful discussions regarding this project.

Professor Carien M. Niessen, Department of Dermatology and CECAD Cologne, University of Cologne provided me with an excellent opportunity to carry out my environmental exchange in her laboratory. I am highly grateful for that and for the many fruitful discussions we have had. The members of the Niessen lab always provided me with the help I needed and invited me to their gatherings, which made me feel very welcome in their group. I would especially like to thank Emmi Wachsmuth and Franziska Peters for their excellent guidance in the lab and for introducing me to the many aspects of skin science.

I would like to thank present and former members of the Nils J. Færgeman laboratory, who have created a wonderful environment. Especially I would like to thank Ditte Neess and Signe Bek Sørensen for introducing me to the ACBP project and for many rich discussions regarding this project.

I would like to thank Dr. Roger Sandhoff, Professor Klaus Willecke, Professor Saverio Cinti Blaise, and Professor Torben Steiniche for their collaboration during this project.

Finally I would like to thank my family and friends for their invaluable support during my study. Special thanks to my kids, Kasper and Nanna, for your patience, understanding and encouragements, and for your kisses and your smiles, you mean the world to me. Sometimes the challenges of life makes me stumble, but my two best friends Lilo and Sofie always helped me through the tough times and for that I will be forever grateful. Randi, my dearest mom, you are there for me and the kids, always and at any hour of the day. Thank you so much for being the best mom ever. Finally, to my beloved dad Erik, I am so sad you are no longer here but I know you would have been so proud of me.

SUMMARY

The acyl-CoA binding protein (ACBP) is a small intracellular protein, which binds C14-C22 acyl-CoA esters with high affinity and specificity. ACBP is highly conserved through evolution and expressed in all eukaryotic species investigated. Moreover, ACBP is expressed in all mammalian tissues investigated. ACBP was discovered in 1987 and since then the protein has been thoroughly investigated. *In vitro* studies have indicated, that ACBP acts as an acyl-CoA pool former that can transport acyl-CoA esters between different enzymatic systems; however, the knowledge about *in vivo* functions of ACBP remain sparse. In an effort to elucidate the *in vivo* function of ACBP, mice with a target disruption of the *Acbp* gene (ACBP$^{-/-}$) were generated. ACBP$^{-/-}$ mice are born in a normal Mendelian ratio and they are viable and fertile. At birth ACBP$^{-/-}$ mice are indistinguishable from their ACBP$^{+/+}$ littermates; however, around 16-18 days of age ACBP$^{-/-}$ mice develop a greasy and tousled fur, which persists throughout their life. With age ACBP$^{-/-}$ mice display alopecia and scaling of the skin. Furthermore, the transepidermal water loss (TEWL) is elevated in ACBP$^{-/-}$ mice, demonstrating that the epidermal barrier function is defect.

Around the time of weaning ACBP$^{-/-}$ mice experience a delayed induction of the sterol regulatory element binding protein (SREBP)-driven lipogenic and cholesterogenic gene programs in the liver, which is likely to be caused by accumulation of triacylglycerol (TAG) and cholesterol ester (CE) in the liver. Surprisingly, mice with liver specific depletion of ACBP (Alb-ACBP$^{-/-}$) did not recapitulate this liver phenotype; however, the liver phenotype was recapitulated in mice with keratinocyte specific depletion of ACBP (K14-ACBP$^{-/-}$). Interestingly, this demonstrates that it is the depletion of ACBP in the keratinocytes rather that endogenous lack of ACBP in the liver, which causes the liver phenotype. Furthermore, the application of an artificial barrier on the skin of ACBP$^{-/-}$ mice rescued the liver phenotype, which indicates that it is the impaired epidermal barrier of ACBP$^{-/-}$ mice that causes the liver phenotype.

The work presented in this thesis aimed at elucidating the molecular and cellular mechanisms in the skin upon ACBP depletion. We showed that epidermal proliferation was increased upon ACBP depletion. Additionally, ACBP depletion decreased the level of protein bound [OS] ceramides in stratum corneum (SC). We also found the sebaceous gland to be enlarged in ACBP depleted mice, which was due to elevated differentiation of the sebaceous gland cells. Interestingly, the elevated differentiation of the sebaceous glands was accompanied by increased secretion of sebum lipids onto the fur of ACBP depleted mice.

Collectively, these results suggest that the reported impaired epidermal barrier in ACBP depleted mice is caused by reduced amounts of [OS] ceramides. Therefore, we hypothesize that the epidermal proliferation and differentiation are likely to be increased to compensate the epidermal barrier impairment upon ACBP depletion. Furthermore, the sebaceous gland hypertrophy indicates that ACBP is involved in regulation of sebaceous gland lipid synthesis and homeostasis.

Additionally, we have investigated the involvement of ACBP in the synthesis of ceramides. We found that ACBP is a very potent stimulator of CerS2 and CerS3 activity both *in vitro* and *in vivo*. Furthermore, we showed that ACBP interacts with CerS2-6. Taken together, these results indicate that ACBP is an important regulator of ceramide synthesis.

SUMMARY IN DANISH (DANSK RESUME)

Acyl-CoA bindende protein (ACBP) er et lille intracellulært protein, der binder C14-C22 acyl-CoA estre med høj affinitet og specificitet. ACBP er stærkt bevaret gennem evolutionen og udtrykkes i alle undersøgte eukaryote arter. Desuden er ACBP udtrykt i alle undersøgte pattedyrsvæv. ACBP blev opdaget i 1987 og er siden blevet grundigt undersøgt. Studier *in vitro* har indikeret, at ACBP kan opretholde en pulje af acyl-CoA estre og at ACBP kan transportere acyl-CoA estre mellem forskellige enzymsystemer. Alligevel er viden om ACBPs funktion i pattedyrsceller fortsat sparsom. For at belyse ACBPs funktion i pattedyrsceller, er der blevet genereret mus som mangler et funktionelt *Acbp* gen (ACBP$^{-/-}$). ACBP$^{-/-}$ mus fødes i normal Mendelsk fordeling og de er både levedygtige og fertile. Ved fødslen ligner ACBP$^{-/-}$ mus deres ACBP$^{+/+}$ søskende; imidlertid udvikler ACBP$^{-/-}$ mus en fedtet og strittende pels når de er omkring 16-18 dage gamle, hvilket varer ved i resten af deres levetid. ACBP$^{-/-}$ mus udvikler pletskaldethed og skællende hud med alderen. Desuden er det transepidermale vandtab (TEWL) øget i ACBP$^{-/-}$ mus, hvilket viser, at deres hud barrierer er defekt.

Omkring fravænningstidspunktet har ACBP$^{-/-}$ mus en forsinket induktion af de hepatiske lipogene og kolesterogene genprogrammer, som er drevet af sterol regulatorisk element bindende protein (SREBP), hvilket sker på grund af akkumulering af triacylglycerol (TAG) og kolesterolestre (CE) i leveren. Denne leverfænotype ses ikke hos mus med leverspecifik mangel på ACBP (Alb-ACBP$^{-/-}$), imidlertid er leverfænotypen bevaret hos mus som mangler ACBP i hudcellerne (K14-ACBP$^{-/-}$). Dette viser, at det er mangel på ACBP i hudceller, fremfor endogen mangel på ACBP i leveren, der forårsager lever fænotypen. Ydermere forhindrer applikation of af en kunstig barrierer på huden af ACBP$^{-/-}$ musene, at de udvikler leverfænotypen, hvilket indikerer, at det specifikt er den svækkede hudbarrierer hos ACBP$^{-/-}$ musene der forsager lever fænotypen.

Arbejdet, der er præsenteret i denne afhandling, har til formål, at belyse de molekylære og cellulære mekanismer som opstår i huden på grund af ACBP mangel. Vi har vist, at mangel på ACBP fører til øget prolifereringen i det yderste lag af huden, epidermis. Ydermere leder mangel på ACBP til nedsat mængde af proteinbundne [OS] ceramider i stratum corneum (SC). Vi fandt desuden at talgkirtlerne var forstørrede i mus, som mangler ACBP, hvilket øger differentiering af talgkirtelcellerne. Den øgede differentiering af talgkirtlerne førte til øget sekretion af sebum på musenes pels ved mangel på ACBP.

Tilsammen indikerer disse resultater, at det er den reducerede mængde [OS] ceramider, der er skyld i barriere defekten hos mus der mangler ACBP. Derfor foreslår vi, at talgkirtlernes proliferering og differentiering er øget for at kompensere for den svækkede barriere som mangel på ACBP fører til. Ydermere indikerer talgkirtel hypertrofien at ACBP formentlig er involveret i reguleringen af talgkirtlernes sebumproduktion og homeostase.

Vi har ydermere undersøgt ACBPs indflydelse på syntesen af ceramider. Vi fandt, at ACBP interagerer med CerS2-6, og at ACBP stimulerer aktiviteten af ceramid synthase (CerS) 2 og CerS3 kraftigt i både *in vitro* systemer og i levende pattedyrsceller. . Sammenfattet indikerer disse resultater, at ACBP er en vigtig regulator af ceramid syntesen.

TABLE OF CONTENTS

PUBLICATIONS AND MANUSCRIPTS

This thesis is based on the following manuscripts:

SUPPLEMENT 1

Acyl-CoA binding protein sustains normal sebaceous gland differentiation and sebum production in mice. Engelsby, H., Neess, D., Sandhoff, R., Niessen, C., Færgeman, N. J. (2017). Manuscript in preparation.

SUPPLEMENT 2

Regulation of Very-Long Acyl Chain Ceramide Synthesis by Acyl-CoA Binding Protein. Ferreira, N. S., **Engelsby, H.**, Neess, D., Kelly, S. L., Volpert, G., Merrill, A. H., Færgeman, N. J., Futerman, A. H. (2017). J Biol Chem, 2017 Mar 19. pii: jbc.M117.785345. doi: 10.1074/jbc.M117.785345. [Epub ahead of print]

ADDITIONAL PUBLICATION

Long-chain acyl-CoA esters in metabolism and signaling: Role of acyl-CoA binding proteins. Neess, D., Bek, S., **Engelsby, H.**, Gallego, S. F., Færgeman, N. J. (2015). Prog Lip Res. 2015 Jul;59:1-25.

ABBREVIATIONS

3-KR	3-ketodihydrosphingosine reductase
3-KSph	3-ketosphinganine
3T3-L1	Murine pre-adipocyte cell line
12R-LOX	12R lipoxygenase
ABCA12	ATP binding cassette transporter 12
ACAT	Acyl-CoA:cholesterol acyltransferase
Acb1	ACBP orthologue in *Saccharomyces cerevisiae*
ACBD	Acyl-CoA binding domain
ACBP	Acyl-CoA binding protein
$ACBP^{-/-}$	Mice with targeted disruption of the *Acbp* gene
$ACBP^{+/+}$	Control mice to $ACBP^{-/-}$ mice
ACC	Acetyl-CoA carboxylase
ACS	Acyl-CoA synthetase
ADAM	A disintegrin and metalloprotease
Alb-$ACBP^{-/-}$	Liver specific ACBP depleted mice
Alb-$ACBP^{+/+}$	Control mice to Alb-$ACBP^{-/-}$ mice
ANT	Adenine nucleotide translocase
[ADS]	α-hydroxy dihydrosphingosine
[AH]	α-hydroxy 6-hydroxysphingosine
[AP]	α-hydroxy phytosphingosine
ApoC1	Apolipoprotein C1
[AS]	α-hydroxy sphingosine
ATGL	Adipose triglyceride lipase
Blimp1	B lymphocyte-induced maturation protein-1
BMP	Bone morphogenetic protein
Bmpr1a	BMP receptor 1a
CARS	Coherent anti-stokes raman scattering
CAT	Carnitine acyltransferase
CE	Cholesterol ester
CerS	Ceramide synthase
CERT	Ceramide transfer protein
C/EBP	CCAAT-enhancer-binding protein
C. elegans	*Caenorhabditis elegans*
CerS	Ceramide synthase
CGI-58	Comparative gene identification-58
CPT	Carnitine palmitoyl transferase
CYP4F22	Cytochrome P450, family 4, subfamily F, polypeptide 22
CoA	Coenzyme A
DAG	Diacylglycerol
DBI	Diazepam-binding inhibitor

DES	Dihydroceramide desaturase
DGAT	Diacylglycerol acyltransferase
dHCer	Dihydroceramide
dHSph	Dihydrosphingosine
DNA	Deoxyribonucleic acid
DSC	Desmocollin
DSG	Desmoglein
E	Embryo age
E. coli	*Escherichia coli*
EGFR	Epidermal growth factor receptor
ELOVL	Elongation-of-very-long-chain-fatty-acid
eLOX3	epidermal lipogenase 3
[EODS]	Esterified ω-hydroxy dihydrosphingosine
[EOH]	Esterified ω-hydroxy 6-hydroxy sphingosine
[EOP]	Esterified ω-hydroxy phytosphingosine
[EOS]	Esterified ω-hydroxy sphingosine
ER	Endoplasmic reticulum
FA	Fatty Acid
FABP	Fatty acid binding protein
FADS2	Fatty acid desaturase-2
FA2H	Fatty acid 2-hydrolase
FAR	Fatty acid reductase
FAS	Fatty acid synthase
FATP	Fatty acid transport protein
FFA	Free fatty acid
GBA1	β-glucocerebrosidase
Gly	Glysine
GPAT	Glycerol-3-phosphate acyltransferase
HepG2	Human hepatocellular carcimoma cell line
HPTLC	High performance thin layer chomatrography
IFE	Interfollicular epidermis
IGF	Insulin growth factor
K	Keratin
K14-ACBP$^{-/-}$	Mice with depletion of ACBP in keratinocytes
K14-ACBP$^{+/+}$	Control mice to K14-ACBP$^{-/-}$ mice
LCB	Long chain base
LC	Long chain (C14-C22)
Lef1	Lymphoid enhancer-binding factor 1
Lrig1	Immunoglobulin-like domains 1
MADAG	monoalkyl diacylglycerol
MFAT	Human multifunctional O-acyltransferase
mRNA	messenger ribonucleic acid

MS	Mass spectrometry
MZ	Maturation zone
NFATc1	Nuclear factor of activated T-cells 1
nm1054	A spontaneous deletion of 400 kb on chromosome 1
[NDS]	Non-hydroxy dihydrosphingosine
[NH]	Non-hydroxy 6-hydroxy sphingosine
[NP]	Non-hydroxy phytosphingosine
[NS]	Non-hydroxy sphingosine
NZ	Necrosis zone
[OH]	Proteinbound ω-hydroxy 6-hydroxy sphingosine
[OP]	Proteinbound ω-hydroxy phytosphingosine
[OS]	Proteinbound ω-hydroxy sphingosine
P	Postnatal age
PI3K	Phosphoinositol 3 kinase
PKC	Protein kinase C
PM	Plasma membrane
PNPLA1	Patatin-like phospholipase domain-containing protein 1
PPAR	Peroxisome proliferator activated receptor
PPRE	Peroxisome proliferator-activated receptor response element)
pSap	Prosaposin
PSU	Pilosebaceous unit
PZ	Peripheral zone
RNA	Ribonucleic acid
RT-PCR	Real time polymerase chain reaction
RXRα	Retinoid X receptor α
SB	Stratum basale
SC	Stratum corneum
SCD	Stearoyl-CoA desaturase
S. cerevisiae	*Saccharomyces cerevisiae*
SEB-1	Immortalized sebocyte cell line
Ser	Serine
SG	Stratum granulosum
siRNA	Small interference RNA
SK1	Sphingosine kinase
SL	Sphingolipids
SM	Sphingomyelin
S1P	Sphingosine 1-phosphate
Sp1	Specificity protein 1
SPRR	Small proline rich protein
SPT	Serine palmitoyl transferase
SRE	Sterol regulatory element
SREBP	Sterol regulatory element-binding proteins

SS	Stratum spinosum
TAG	Triacylglycerol
Tcf	Transcription factor
TEM	Transmission electron microscopy
TEWL	Transepidermal water loss
TGF	Transforming growth factor
Ugcg	UDP-glucose:ceramide glucosyltransferase
ULC	Ultra-long chain (>C26)
VLC	Very-long chain (C22-C26)
Wnt	Wingless
WT	Wild type

AIM OF PROJECT

Since the discovery of ACBP in 1987, the structure and the biochemical properties of the protein have been thoroughly investigated. The majority of the studies of ACBP function have until recently been conducted *in vitro*, and in simple model organisms such as; e.g. yeast and *C. elegans*. However, reports about the *in vivo* functions of ACBP are sparse. Recently, the first investigations of ACBP function *in vivo* in mice were published. These publications descried that ACBP depletion causes delayed adaption to weaning and impaired epidermal barrier integrity.

The aim of this PhD project was to further elucidate the molecular and cellular mechanisms that cause the epidermal barrier defect upon ACBP depletion. Concomitantly, we wanted to study the involvement of ACBP in synthesis of ceramides to get a better understanding of whether ceramide synthesis in the skin might be affected by ACBP depletion.

1 INTRODUCTION

The following section provides introduction to acyl-Coenzyme A (CoA) binding protein (ACBP), including the structural and functional functions of ACBP together with known *in vitro* and *in vivo* properties. Furthermore, a short introduction to sphingolipids with emphasis on ceramides, ceramide synthases (CerS) and ceramide synthesis will be presented, to help understand our findings that ACBP induces CerS2 and CerS3 activity and interacts with CerS2-6. Since the ACBP depleted mice show a characteristic skin and fur phenotype, the general physiology of epidermis, hair follicles, sebaceous glands, and selected regulations hereof will briefly introduced as well. Finally a short introduction to epidermal lipids will follow, since ACBP depleted mice display alterations in some epidermal lipid species.

1.1 ACYL COA ESTERS

Fatty acids (FAs) play an important role in a variety of cellular functions; they function as energy supply, are important for cellular membranes, and serve signaling and regulatory purposes. FA derive from dietary sources, *de novo* synthesis or degradation of complex lipids. In order for the cell to utilize FA, the FA need to be converted into fatty acyl-CoA esters, by the action of one of 13 acyl-CoA synthetases (ACS).

Long-chain (LC) acyl-CoA esters are important intermediates in lipid metabolism and they also serve as regulators of a number of cellular functions (reviewed by [1, 2]). Due to the important regulatory function of LC acyl-CoA esters, the intracellular concentration needs to be tightly regulated. Therefor the cellular concentration of LC acyl-CoA ester is kept between 5-160 μM, depending on tissue type and metabolic state of the tissue, the free LC acyl-CoA ester concentration is not known but estimated to be below 0.2 μM [1]. A number of proteins capable of binding LC acyl-CoA esters and thereby sequestering them has been identified; e.g. fatty acid binding protein 1 (FABP1), sterol carrier protein 2 (SCP2), acyl-CoA binding protein (ACBP) (also known as diazepam-binding inhibitor (DBI)). From these ACBP singles out as the only protein that solely binds LC acyl-CoA esters. However, the last few years several proteins carrying an acyl-CoA binding protein domain (ACBD) has been identified. These are named ACBD1-7 and of these ACBD1 is synonymous with ACBP. Very little is known about the function of ACBD2-7 and they will not be discussed in further detail in the context of this thesis. Throughout this thesis, the term ACBP will be used when describing the acyl-CoA binding protein as the independent single-domain protein known as ACBP, DBI or ACBD1.

1.2 ACYL-COA BINDING PROTEIN

ACBP was first identified in bovine liver in 1987, by its ability to stimulate the synthesis of medium-chain acyl-CoA esters, when incubated with goat mammary gland fatty acid synthase (FAS) [3]. Subsequently ACBP was isolated from bovine and rat liver [4, 5], and the amino acid sequences were identical to the already known DBI. DBI was identified in rat brain in 1983 [6] where it was suggested to play a role in neurotransmission. Three more groups have independently discovered ACBP; as an adrenal peptide stimulating transport of cholesterol into Leydig cell mitochondria [7], a peptide that regulates insulin release in pig intestine [8], and a cholecystokinin-releasing peptide [9].

1.2.1 *ACBP* GENE

The *Acbp* gene was first cloned and characterized from rat [10], where four pseudogenes and one expressed gene were identified. The size of the functional rat *Acbp* gene is approximately 8 kb and

comprises four exons and three introns. The *Acbp* gene promotor region contains a cytosine-guanine rich region (CpG island) but no canonical TATA box. Furthermore, two major and several minor transcription initiation sites are identified [10, 11], suggesting that *Acbp* is a typical housekeeping gene. In keeping with this, ACBP is highly conserved throughout the four eukaryotic kingdoms (Animalia, Plantae, Fungi and Protista) [12, 13]. ACBP is generally found absent in prokaryotes, it has only been found expressed in a very small number of prokaryotic species.

All though ACBP is expressed in all eukaryotic cell types investigated [14], the expression level differs, with the highest expression in lipogenic tissues such as liver, white adipose tissue (WAT), brown adipose tissue (BAT), and Harderian gland [15] (figure 1). The cellular expression level of ACBP within specific tissues also varies, e.g. in skin, ACBP expression is more pronounced in epidermis and in the cells lining the hair shafts [16].

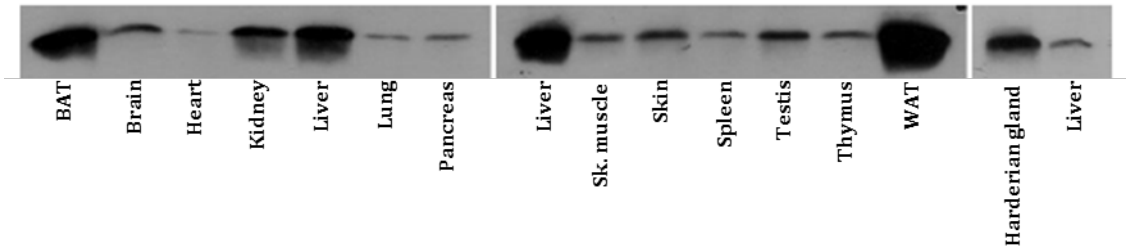

Figure 1: *ACBP* expression is ubiquitous, with highest expression in lipogenic tissues. ACBP is expressed in all tissues investigated, with highest expression in lipogenic tissues. Figure adapted and modified from [15, 17].

Several different regulatory elements are present in the promotor region of the *Acbp* gene; e.g. binding sites for nuclear factor γ (NF-γ)/CCAAT-binding transcription factor (CTF), specificity protein 1 (Sp1), activator protein 1 (AP-1), CCAAT-enhancer-binding protein (C/EBP), peroxisome proliferator-activated receptor response element (PPRE), sterol regulatory element (SRE), hepatocyte nuclear factor 3 (HNF-3), glucocorticoid response element (GRE) and insulin receptor substrate (IRS) [11, 18-21]. This indicates that the *Acbp* gene might be subject to complex regulation by many factors, which is likely to contribute to the differential tissue and specific cell type expression of *Acbp*.

Expression of the *Acbp* gene is metabolically regulated by both peroxisome proliferator-activated receptor (PPAR) and sterol regulatory element binding protein (SREBP) [15, 19, 22]. Early reports suggested *Acbp* expression in rat liver to be increased upon high fat feeding and decreased upon fasting [23], and furthermore increased during 3T3-L1 pre-adipocyte differentiation [24], which is accompanied by FA synthesis and triacylglycerol (TAG) accumulation, indicating *Acbp* expression to be correlated with lipogenesis and lipid accumulation. PPRE is highly conserved between rodents and humans, and is present in intron 1 of the *Acbp* gene. PPAR dimerizes with retionoic X receptor α (RXRα), and both RXRα/PPARα and RXRα/PPARγ dimerization induces expression of *Acbp*, whereas RXRα/PPARδ dimerization does not [19]. Additionally, the PPARγ ligand BRL49653 induces *Acbp* expression in murine adipocytes [19], suggesting *Acbp* to be a PPARγ target gene. The activation of *Acbp* upon PPARα/RXRα dimerization, suggests *Acbp* to be a PPARα target gene however PPARα target genes are induced by fasting [25]. This together with the reported decreased expression of *Acbp* upon fasting indicates that the *Acbp* gene is under

complex control of additional transcription factors, possibly activated by insulin and/or glucose under various metabolic conditions. In line with this assumption a functional SRE, conserved between rat and human, exists in the proximal promotor of the *Acbp* gene, and NF-γ and Sp1 sites located near SRE acts as auxiliary factors [22]. This suggests *Acbp* to be a SREBP-1 target gene, which is further supported by the finding that SREBP-1 and its target genes is decreased in mice liver upon fasting and increased when mice were fed a high carbohydrate diet [26]. Functional investigations in rat hepatocytes show that SREBPs mediate activation of the *Acbp* gene through the conserved SRE in response to insulin [22].
In conclusion, the *Acbp* gene is subject to PPARα, PPARγ and SREBP regulation in the liver: SREBP induce activation upon feeding and decreased activation upon fasting, as SREBP regulation dominates over PPARα regulation under these conditions. During fasting, removal of PPARα, further decreases *Acbp* expression, indicating that PPARα is responsible for keeping the *Acbp* expression relatively high under these conditions [15, 22]. This strongly suggests that *Acbp* expression needs to be tightly balanced under different metabolic conditions.

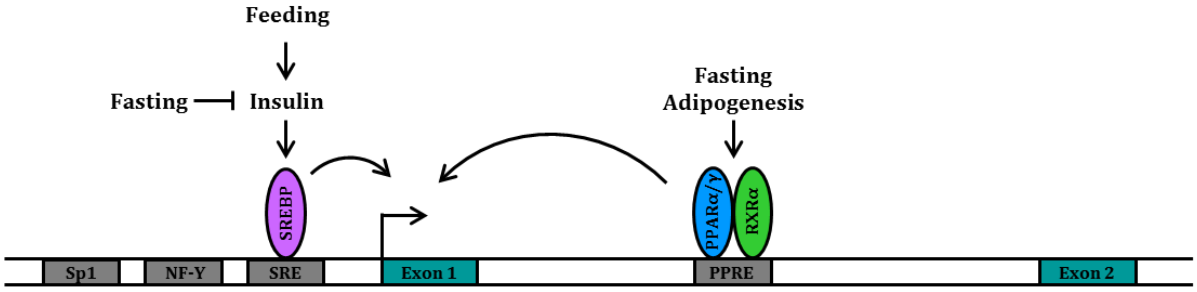

Figure 2: The *Acbp* gene is regulated by opposite metabolic stimuli. The expressed *Acbp* gene is approximately 8 kb in size and comprises four exons and three introns. Transcription initiation is regulated by a number of regulatory elements; e.g. specificity protein 1 (Sp1), nuclear factor γ (NF- γ), sterol regulatory element (SRE) and peroxisome proliferator-activated receptor response element (PPRE). Sp1 and NF-Y function as auxiliary transcription factors. Transcription is positively regulated by insulin which stimulates sterol regulatory element binding protein 1 (SREBP-1) binding to SRE in the proximal promotor of the *Acbp* gene. Fasting induces expression by stimulating PPARα and RXRα dimerization and binding to PPRE, but inhibits SREBP-1c activity and combined the *Acbp* expression is reduced. Figure adapted and modified from [15].

1.2.2 ACBP STRUCTURE AND LIGAND BINDING

The structure of ACBP is resolved by nuclear magnetic resonance (NMR) spectroscopy in bovine and yeast, and by X-ray crystallography in human and *Plasmodium falciparum* [27-30]. Independent of the method used, the structures resolved are very similar and consist of four α-helices oriented in an up-down-down-up manner. The four α-helices; A1, A2, A3 and A4, are running parallel in pairs; A1/A4 and A2/A3, with a 13-residue loop intersection between helix A2 and A3. The A2 helix is disjoint to helices A1 and A4, resulting in four helix-helix interfaces and not six interfaces as commonly found in super-coiled four-helix bundles. The four α-helices; A1 (Ala3-Leu15), A2 (Ala20-Val36), A3 (Gly51-Lys62) and A4 (Ser65-Tyr84) forms a bowl-like structure, primarily through hydrophobic interactions. The bowl-like structure has a highly polar rim and a predominantly non-polar inside, where the acyl-CoA ligand binds. The acyl-CoA

ligand is placed with the acyl chain in the bowl-like structure and the CoA part functioning as a lid, protecting the acyl-CoA ester from the aqueous surroundings (Figure 3).
In vitro ACBP binds both saturated and unsaturated C8-C26 acyl-CoA esters with highest affinity towards C14-C22 acyl-CoA esters. ACBP do not bind un-esterified FA, cholesterol, palmitoyl-carnitine or any other ligand tested and ACBP displays only low affinity towards free CoA [3, 5, 31, 32]. ACBP binds acyl-CoA esters with a binding stoichiometry of 1:1 [4].

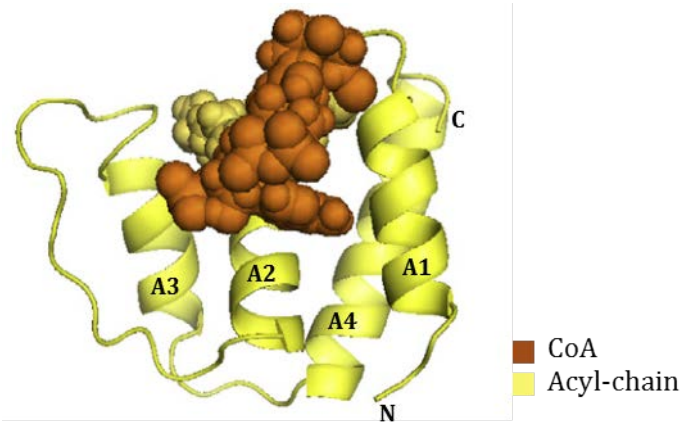

Figure 3: ACBP structure and ligand binding. The ACBP protein consists of four α-helices (A1, A2, A3 and A4) that are oriented in an up-down-down-up manner, forming a bowl-like structure where the acyl-CoA ligand binds. Yellow represents ACBP with N and C terminus indicated. Brown/yellow represents palmitoyl-CoA; yellow represents the acyl chain and brown represents CoA. Figure adapted and modified from [2].

1.2.3 *IN VITRO* FUNCTIONS OF ACBP

LC acyl-CoA esters are involved in the regulation of many cellular functions, which highlights the importance of keeping the cytosolic concentration of free LC acyl-CoA esters under tight regulation and in the low nano molar range. As described above, ACBP binds LC acyl-CoA esters with high affinity [4, 5, 32], and the ability of ACBP to function as an acyl-CoA pool former are established in studies in yeast, as the amount of intercellular LC acyl-CoA esters are increased by ACBP overexpression [33, 34]. This indicates that ACBP maintains a pool of LC acyl-CoA esters, which are accessible to be utilized in different cellular processes, and at the same time protects the acyl-CoA ester from hydrolysis and keeps the intra cellular concentration of free LC acyl-CoA esters very low. The ability of ACBP to sequester LC acyl-CoA esters also prevents product inhibition of different enzymes; mitochondrial acyl-CoA synthetase (ACS) [33], acetyl-CoA carboxylase (ACC) [35], mitochondrial adenine nucleotide translocase (ANT) [35], FAS [3], carnitine palmitoyl transferase (CPT) [3, 36], acyl-CoA lysophospholipid acyltransferase (LAT) [37] and acyl-CoA:cholesterol acyltransferase (ACAT) [38, 39]. Furthermore, ACBP affects the activity of several enzymes, that uses LC acyl-CoA esters as substrate, by delivering LC acyl-CoA esters to them; ACAT [39], glycerol-3-phosphate acyltransferase (GPAT) [37, 40]. In addition ACBP delivers LC acyl-CoA esters to carnitine acyltransferase (CAT) [41] and CPT [42]. This suggests that ACBP might play a role in cholesterol synthesis [39], triacylglycerol synthesis [40], phospholipid synthesis [37], glycerolipid synthesis [41], and FA β-oxidation [41, 42] by delivering LC acyl-CoA esters to enzymes involved in the different enzymatic pathways. In addition ACBP donates and/or extracts LC acyl-CoA esters to/from the outer mitochondrial membrane [5, 39, 42].

1.2.4 ACBP FUNCTION IN MAMMALIAN CELL CULTURES

ACBP function has been investigated by small interference RNA (siRNA) mediated knock down in several cell lines and abolished expression of ACBP results in growth arrest and cell death, indicating an essential function of ACBP [43]. However, siRNA mediated knock down of ACBP in 3T3-L1 pre-adipocytes and HepG2 cells results in viable cells, despite the reduced levels of ACBP [44, 45]. ACBP knock down in 3T3-L1 cells results in impaired differentiation and accumulation of triglyceride and decreased expression pattern of the adipogenic transcription factors PPARγ and C/EBPα. The impaired differentiation status is partly rescued by treating the cells with a PPARγ agonist and synthetic glucocorticoid dexamethasone, which are both adipogenic inducers [45].

1.2.5 Acb1p FUNCTION IN *SACCHAROMYCES CEREVISIAE*

The function of ACBP has been thoroughly studied in the yeast *Saccharomyces cerevisiae* (*S. cerevisiae*) by disruption of the *ACB1* gene encoding Acb1, the yeast ACBP orthologue. The Acb1 protein in *S. cerevisiae* comprises of 86 amino acids which show 48% sequence identity with human ACBP and very similar structure (reviewed by [2]). Acb1 depletion in *S. cerevisiae* results in reduced growth rate, altered plasma membrane structures and vesicle accumulation [46-48]. The impaired growth rate in *S. cerevisiae* upon Acb1 depletion can be complemented by expression of human or murine ACBP, which suggests similar functions of ACBP in human, mice and yeast [13]. Acb1 depletion in yeast results in multilayered plasma membranes and accumulation of both autophagocytotic-like bodies and vesicles [46, 48]. This indicates a function of ACBP in membrane biogenesis and vesicle formation/trafficking. Acb1 depleted yeast display multi-lobed vacuoles, which is rescued by re-induction of Acb1 [48]. Additionally, isolated vacuoles from Acb1 depleted yeast display impaired fusion probabilities both with other vacuoles isolated from Acb1 depleted yeast and vacuoles isolated from control yeast. Interestingly, addition of Acb1, acyl-CoA or Acb1-acyl-CoA complex did not restore the vacuole fusion abnormalities in Acb1 depleted yeast [48]. This indicates that Acb1, acyl-CoA and Acb1-acyl-CoA are not directly involved in the fusion process, but more likely in assembly of the vacuole fusion machinery.

Acb1 depletion in *S. cerevisiae* does not affect the total acyl-CoA ester level. However, the relative stearoyl-CoA level is increased by 3.5-fold and the level of C14:0 acyl-CoA, C16:1 acyl-CoA and C18:1 acyl-CoA esters are decreased by 2-fold in Acb1 depleted yeast compared with wild type (WT) [46, 47]. In keeping with this, Acb1 facilitates removal of acyl-CoA esters from yeast FAS [47], altogether implying that Acb1 is involved in termination of FA synthesis in yeast. Furthermore, overexpression of either bovine *ACBP* or yeast *ACB1* in Acb1 depleted yeast, results in accumulation of C14:0 acyl-CoA, C16:0 acyl-CoA and C16:1 acyl-CoA esters, indicating the capability of ACBP to act as an acyl-CoA pool former *in vivo* [34, 49].

Lipidomic analyses of Acb1 depleted cells reveals an increase in total level of phosphatidylinositol and phosphatidylglycerol, possibly due to a significant induction of the expression of the inositol 3-phosphate synthase (*INO1*) gene. The expression of *INO1* is normalized by addition of exogenous FAs or by overexpression of *FAS1* or *ACC1*, indicating that Acb1 links FA metabolism to transcriptional regulation of glycerophospholipid biosynthesis [50].

Acb1 depleted yeast show a small reduction in the total level of FAs, however a dramatic reduction is observed in C26:0 FAs compared with WT. Addition of exogenous C16:0 FA do not complement the reduced level of very-long chain FA (VLCFA), thus suggesting an involvement of Acb1 in synthesis and elongation of VLCFAs [46].

Yeast depleted of Acb1 display reduced levels of the short chain bases phytosphingosine and dihydrosphingosine (dHSph) (reviewed by [2]). Furthermore, Acb1 depleted yeast have reduced levels of ceramides, inositol phosphoryl ceramide and mannosyl inositol phosphoryl ceramide, suggesting a role of Acb1 in sphingolipid synthesis [46, 48].

1.2.6 ACBP FUNCTION IN *CAENORHABDITIS ELEGANS*

The nematode *Caenorhabditis elegans* (*C. elegans*) express seven ACBP paralogues of which ACBP-1, ACBP-3, ACBP-4, and ACBP-6 only contain the ACBP domain. ACBP-2 contains an enoyl-CoA hydratase/isomerase and ACBP-5 contains two Ankyrin repeats besides the ACBP domain. The membrane associated ACBP domain-containing protein-1 (MAA-1) additionally contains a coiled-coil and a transmembrane domain besides the ACBP domain [51]. All of the *C. elegans* ACBP isoforms are capable of rescuing the slow growth phenotype in Acb1 depleted yeast [51]. ACBP-1 is considered to be the *C. elegans* paralogue with highest similarity to mammalian ACBP and yeast Acb1.

ACBP-1 localizes to the intestine, ACBP-2 to the intestine and the hypodermis, ACBP-3 to the hypodermis, body wall muscles and pharynx, ACBP-5 to the pharynx and intestine. ACBP-4 and ACBP-6 are weakly expressed in granular structures of the intestine and in neurons in the head, body and tail, respectively [51].

In *C. elegans,* depletion of *acbp-1* results in significantly decreased lifespan and an increase in lipid droplet size, although the number of lipid droplets are decreased. *C. elegans* depleted of *acbp-2* and *acbp-3* display reduced size and number of lipid droplets compared with WT. Additionally, *acbp-1*, *acbp-2* and *acbp-3* depleted *C. elegans* show decreased accumulation of TAG. Taken together, this suggests that acyl-CoA binding proteins are involved in lipid droplet morphology and TAG storage in *C. elegans* [51].

1.2.7 ACBP FUNCTION IN MAMMALS

Several studies have used genetically modified mice and rat models to elucidate more about the function of ACBP in mammals. Overexpression of ACBP in mice causes accumulation of saturated and polyunsaturated, but not monounsaturated LC acyl-CoA esters in the liver. Furthermore, the LC acyl-CoA esters level in membranes and organelles, especially in microsomes, increased in mice overexpressing ACBP compared with control mice [52]. Moreover, overexpression of ACBP in rats leads to accumulation of acyl-CoA esters in adipose tissue and in the liver [53]. Taken together, these data supports the suggested function of ACBP as an acyl-CoA pool former. The increased level of LC acyl-CoA esters in the microsomes of mice overexpressing ACBP increases at the expense of the LC acyl-CoA ester level in the cytosol, indicating that ACBP may donate their cargo into membranes [52]. Additionally, the level of TAG and GPAT activity increases in mice overexpressing ACBP, suggesting that ACBP might deliver LC acyl-CoA esters for TAG synthesis.

ACBP overexpression in rat causes decreased gene expression of the transcription factors *Pparγ*, *Pparδ* and *Srebp-1* in both adipose tissue and in the liver, in the fed state. When these rats are fasted, the expression of all PPARs increases whereas the level of SREBP remains similar to that of control rats [53]. *Acbp* expression is regulated by PPARs and SREBP and this study suggests that ACBP is indirectly involved in regulation of *Ppar* and *Srebp* expression, indicating a regulatory feedback mechanism between ACBP and PPARs and SREBP.

Recently, Landrock *et al*. suggested that ACBP depletion in mice causes embryonic preimplantation lethality [54]. However, this contradicts earlier findings, where mice carrying a spontaneous deletion of 400 kb on chromosome 1 (*nm1054*), including the *Acbp* sequence, was characterized [55]. These mice are smaller in body size than their WT littermates and their appearance are pale due to anemia. On a C57BL/6J background the *nm1054* mutation are prenatally lethal, as only 15 mutants out of 220 births in total survived. [56]. However when bred on a mixed background (129S6/SvEvTAC x C57BL/6J) the *nm1054* deletion appears to be non-lethal and these mice display a phenotype with matted, sparse, reddish and greasy fur together with sebocyte hyperplasia [55]. High performance thin layer chromatography (HPTLC) analysis of fur lipids reveals a decrease in TAG and an appearance of an unidentified lipid species with similar migration pattern, confirming the suggested involvement of ACBP in TAG synthesis.
Recently a mouse model with target disruption of *Acbp* (ACBP$^{-/-}$) was reported [57]. The ACBP$^{-/-}$ mice were generated on a C57BL/6JBom background and in contrast to the *nm1054* mice, these mice are viable. Importantly, the *nm1054* deletion includes 5 other genes besides *Acbp*, which makes it difficult to evaluate the contribution from ACBP to the observed lethality. Furthermore, the *Acbp* deletion generated by Landrock *et al*. included a large part of the *Acbp* gene promoter region [54]. It is likely that the deletion of regulatory elements contributes to the observed lethality in this and in the *nm1054* mice mutants.
The ACBP$^{-/-}$ mice reported by the Mandrup lab [57] are viable and fertile, and the pups are born in a normal Mendelian ratio [57]. At birth the ACBP$^{-/-}$ pups are indistinguishable from their WT littermates (ACBP$^{+/+}$); however around 16-18 days of age the ACBP$^{-/-}$ mice develop a characteristic macroscopic phenotype, which is characterized by greasy and tousled fur as well as swollen eyelids. With age ACBP$^{-/-}$ mice develop alopecia, scaling of the skin and de-pigmentation of the fur [57] (figure 4).

Figure 4: ACBP depleted mice display distinct skin/fur phenotypes. A) 3 weeks old ACBP depleted mice (ACBP$^{-/-}$) display a tousled and greasy fur phenotype. **B)** At 12 weeks of age the fur of ACBP$^{-/-}$ mice has becomes de-pigmented. **C)** The fur of ACBP$^{-/-}$ mice remains greasy and tousled and with age they develop alopecia and scaling of the skin. Figure adapted from [16]

The ACBP$^{-/-}$ mice show delayed adaption to weaning, which occurs when the pups are taken away from their mother at postnatal day 21 (P21). The delayed adaption to weaning is determined by a slightly decreased growth rate and increased mortality around weaning. Furthermore, the expression of genes involved in cholesterolgenesis and FA synthesis show a delayed upregulation in the liver of P21 ACBP$^{-/-}$ mice compared with that of ACBP$^{+/+}$ mice, possibly due to a delayed induction of SREBP transcription factor activity. The delayed induction of the lipogenic pathway causes a 50% reduction in *de novo* synthesis

of cholesterol at P21 in ACBP$^{-/-}$ mice liver, but no difference in *de novo* TAG synthesis at P21 in ACBP$^{-/-}$ mice liver compared with ACBP$^{+/+}$. Moreover, hepatic cholesterol ester and TAG levels are elevated in ACBP$^{-/-}$ mice, but no increase in free cholesterol is observed [57]. Mice with target deletion of ACBP in the liver (Alb-ACBP$^{-/-}$) show normal adaption to weaning, whereas mice with targeted deletion of ACBP in keratinocytes (K14-ACBP$^{-/-}$) show delayed adaption to weaning [58]. Therefore, the delayed adaption to weaning is caused by an impaired epidermal barrier due to ACBP depletion in the keratinocytes rather than ACBP deficiency in the liver. In keeping with this, the liver phenotype is abolished by applying an artificial barrier on the skin surface of ACBP$^{-/-}$ mice, indicating that the reported increase in transepidermal water loss (TEWL) in ACBP$^{-/-}$ mice [16] most likely causes the suppression of the hepatic SREBP gene program at weaning, possibly through lipid accumulation in the liver [58]. Interestingly, the K14-ACBP$^{-/-}$ mice display a macroscopic phenotype similar to that of ACBP$^{-/-}$ mice, with a greasy and tousled fur accompanied by de-pigmentation, alopecia and scaling of the skin with age [58] (figure 5). This suggests that it is the depletion of ACBP in the keratinocytes, which causes the skin/fur phenotype.
Unpublished data from our lab (PhD student Vibeke Kruse) show that the food intake is elevated in ACBP$^{-/-}$ mice and K14-ACBP$^{-/-}$ mice compared with that of control mice, suggesting a relatively higher metabolic rate in ACBP depleted mice. Furthermore, ACBP$^{-/-}$ and K14-ACBP$^{-/-}$ mice are protected against high fat diet induced obesity and from developing glucose insensitivity when fed a high fat diet. We speculate that these findings are caused by the disrupted epidermal barrier.

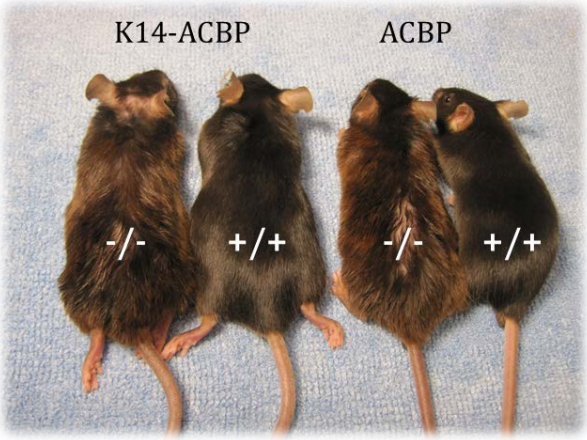

Figure 5: Keratinocyte specific ACBP depletion recapitulates the skin/fur phenotype of full body ACBP depleted mice. ACBP depleted mice (ACBP$^{-/-}$) display a fur phenotype with tousled and greasy fur. With age the fur becomes depigmented and alopecia occurs together with scaling of the skin. Keratinocyte specific ACBP depleted mice (K14-ACBP$^{-/-}$) mice display a phenotype similar to that of ACBP$^{-/-}$ mice.

Further investigations of the skin/fur phenotype in ACBP$^{-/-}$ mice, indicates that there is a reduced water content and pH in stratum corneum (SC) of ACBP$^{-/-}$ mice compared with ACBP$^{+/+}$ mice. Additionally, the total level of free FA (FFA) and cholesterol are unaltered in SC and epidermis from ACBP$^{-/-}$ mice compared with ACBP$^{+/+}$ mice, although the level of VLCFA are highly decreased in SC [16]. Furthermore, the epidermal level of C20:1 FA is increased in ACBP$^{-/-}$ mice compared with ACBP$^{+/+}$ mice. The monoacyl diacylglycerol (MADAG) content in SC and epidermis are significantly increased, whereas TAG is

unchanged in ACBP$^{-/-}$ mice compared with ACBP$^{+/+}$ mice. However, lipids extracted from the fur show decreased levels of TAG and increased levels of MADAG. Importantly, ACBP$^{-/-}$ mice display increased TEWL compared with ACBP$^{+/+}$ mice, indicating an impaired epidermal barrier, which seems to worsen with age [16]. Taken together, this indicates an important role for ACBP in maintaining the integrity of the epidermal barrier function and that ACBP is important for normal epidermal lipid synthesis.
As mentioned previously, disruption of ACBP in mice causes a phenotype with swollen eyelids. This was further investigated [17] and studies revealed that ACBP depletion leads to significant enlargement of Harderian glands; a small gland which is located behind the eye ball and involved in production of fur lipids and lipids used for lubrication of the eye lid. ACBP$^{-/-}$ mice display hypertrophy of the acinar cells of the Hadrian gland, together with increased *de novo* synthesis of MADAG, compared with ACBP$^{+/+}$ mice. K14-ACBP$^{-/-}$ mice show a similar Harderian gland phenotype as ACBP$^{-/-}$ mice and interestingly, application of an artificial barrier rescues this phenotype, indicating that the impaired barrier causes the observed phenotype in the Harderian gland [17]. These findings indicate that ACBP is important for Harderian gland homeostasis and lipid production.
ACBP$^{-/-}$ mice show increased water intake, and after 20 h of water deprivation ACBP$^{-/-}$ mice have increased diuresis, reduced urine osmolality, elevated hematocrit and higher relative weight loss [59]. It is not known whether this is linked to the impaired epidermal barrier integrity or caused by loss of ACBP in the kidneys.

1.2.8 SUMMARY OF ACBP FUNCTION

ACBP binds acyl-CoA esters and function as an acyl-CoA pool former both *in vitro* and *in vivo*. By binding acyl-CoA esters, ACBP abolish product inhibition of a number of enzymes utilizing acyl-CoA esters (e.g. ACS, FAS, ACC, ANT, CPT and ACAT) *in vitro*. Furthermore, ACBP delivers acyl-CoA esters to enzymes (e.g. CPT, ACAT, GPAT and CAT) *in vitro* and is capable of donating and extracting acyl-CoA esters to/from mitochondrial membranes *in vitro*.
Depletion of Acb1 in yeast causes altered membrane structures and vesicle accumulation, together with alterations of FA and ceramide level and distribution. Depletion of *acbp-1* in *C. elegans* results in decreased lifespan, together with increased lipid droplet size and a decrease in lipid droplet number. Depletion of *acbp-1*, *acbp-2* and *acbp-3* in *C. elegans* leads to decreased TAG accumulation.
In rodents, ACBP depletion causes impaired barrier function, which results in increased lipid accumulation in the liver. The increased hepatic lipid content deregulates the lipogenic gene program in the liver which eventually results in delayed adaption to weaning. ACBP depletion results in decreased levels of VLCFA in SC and alterations in the fur lipid composition. Finally ACBP depletion in mice leads to hypertrophy of the Harderian glands and increased *de novo* MADAG synthesis in Harderian glands.

1.3 SPHINGO LIPIDS

Sphingolipids (SL) was first described in 1884 by J. L. W. Thudichum [60], as he isolated a compound from brain, which was given the name “sphingosin” after the Greek mythology creature, the Sphinx. The compound isolated by J. L. W. Thudichum, was later structurally characterized by H. E. Carter as 2S,3R,4E-2-aminooctadec-4-ene-1,3-diol [61]. H. E. Carter was the first to elucidate the structure of both sphingosine and dihydrosphingosine (dHSph) and he proposed to designate lipids derived from sphingosine as sphingolipids [61].

Sphingolipids (SL) is a class of lipids predominately defined by an 18 carbon amino backbone called the long chain base (LCB), although LCBs with alternative backbone length ranging from 12-26 carbons also exists [62, 63]. During 1970 it was proposed that more than 60 structural variations of the LCBs exist [64, 65]. SL in their simplest forms; sphingosine, phytosphingosine and dHSph (also known as sphinganine) are designated LCBs and can be modified in various ways; e.g. phosphorylated, acylated, glycosylated, bridged to a number of head groups through phosphordiester linkage and/or acylated with acyl-CoA esters of varying chain lengths to form more complex SLs. Sphingosine and dHSph are the most abundant LCBs in mammalian cells, whereas phytosphingosine are found mostly in plants and fungi. Both LCBs and more complex sphingolipids; e.g. ceramides, sphingomyelin (SM), glycosphingolipids and galactosphingolipids play important roles in the biology of cell membranes and participate in regulation of cell function. The specific function of the diverse SLs does not only depend on their SL class, as it has become apparent that specific SL within various classes carry out unique biological functions depending on their specific structure; e.g. modifications and chain lengths. SLs are associated with a high number of different cellular processes; e.g. cell membrane structure, apoptosis, migration, cell proliferation and signal transduction. In addition numerous diseases are linked to dysfunction in SL metabolism; e.g. diabetes, cancer, Parkinson's disease, Alzheimer's disease, epilepsy and several types of skin diseases (reviewed by [66-70]).
Although the existence of SLs has been known for more than a century, the high number, their diverse function and interconnected metabolism have made the understanding of their involvement in cell biology complex. In this thesis only ceramides and synthesis hereof will be discussed in detail, see section 1.3.1 and 1.3.2.

1.3.1 CERAMIDES

Ceramides is a class of SLs that is composed of a simple LCB, which is *N*-acylated with acyl-CoA esters of varying chain lengths. They play a central role in SL metabolism since they function as precursors for all complex SLs. Ceramides are synthesized at the cytosolic leaflet of the endoplasmic reticulum (ER), either in the *de novo* synthesis pathway or via the salvage pathway.
The synthesis of ceramides is carried out by a family of six ceramide synthases (CerS), CerS1-6, in mammalian cells. The different CerS isoforms display differential cellular expression and varying affinity for acyl-CoA esters with different chain lengths (reviewed by [71, 72]). Although the differential expression of the CerS isoforms in various cell types and the involvement of ceramides in an array of cellular processes, emphasize the importance of ceramides and their synthesis, the information regarding CerS structure and regulation is sparse. The CerS localize to the ER membrane [73-75], and are believed to have six trans membrane spanning domains [76, 77]. CerS have a unique C-terminal TLC domain which is named after the three protein families in which it was originally found (Tram, Lag and CLN8) [78]. Additionally, all CerS, except from CerS1, have a homebox (Hox)-like domain, which lacks the 15 first aa compared with full length Hox domains (reviewed by [79]). The majority of the Hox-like domain is not required for CerS activity, but a 12 aa residue flanking the Hox and TLC domain is important for CerS activity [80]. Additionally, a longevity assurance gene (Lag1p) motif within the TLC domain is essential for catalytically activity, as two histidine residues in the Lag1p motif are important for catalysis and/or substrate binding [78, 81-83]. Phosphorylation, homo- and hetero-dimerization, and/or interaction with elongation-of-very-long-chain-fatty-acids (ELOVL) regulate CerS activity [84-86].

CerS1 is functionally and structurally different from the other CerS enzymes and is located on an entirely different branch of the phylogenetic three [87]. CerS1 is predominantly expressed the central nervous system in mice [88] and have highest affinity towards C18 acyl-CoA esters [89]. CerS2 display highest expression in kidney and liver, and has highest affinity towards C20-C26 acyl-CoA esters [90]. CerS3 produces ceramides with acyl chains ≥C24 and are highly expressed in testis and in the skin [91-93]. CerS4 displays affinity towards C18-C22 acyl-CoA esters and CerS5 towards C16 acyl-CoA esters [94]. CerS4 display highest expression in skin, heart, liver and in leukocytes [90], whereas CerS5 is mainly expressed in lung epithelium, and in white and grey matter in the brain [95, 96]. CerS6 synthesizes ceramides with C14 and C16 acyl chains [92] and the highest expression in mice are observed in kidney, intestine and brain [97].

Ceramides are important components of eukaryotic membranes and involved in alterations of membrane biophysical properties. Importantly, ceramides are essential for maintaining the epidermal barrier function (reviewed by [98]) and ceramides serve as signaling molecules (reviewed by [99, 100]). Additionally, ceramides are involved in several aspects of development of the metabolic syndrome and elevated ceramide levels lead to insulin resistance and type II diabetes (reviewed by [101]). For example, mechanistic studies reveal that upon CerS2 deficiency a compensatory induction of C16 ceramide level causes impaired β-oxidation. Additionally, inhibition of global ceramide synthesis abolish the effects of CerS2 deficiency *in vivo*, whereas overexpression of CerS6 recapitulates the phenotype, indicating that the ceramide acyl chain length impact hepatic steatosis and insulin sensitivity [102].

1.3.1.1 CERAMIDE SYNTHESIS

Ceramides are synthesized in either the *de novo* pathway or in the salvage pathway. The *de novo* pathway consists of a set of four enzyme; serine palmitoyltransferase (SPT), 3-ketodihydrosphingosine reductase (3-KR), CerS and dihydroceramide desaturase (DES) (figure 5). SPT catalyze the condensation of cytosolic serine and palmitoyl-CoA to form 3-ketodihydrosphingosine (3-KSph) [73]. 3-KR catalyze the reduction of 3-KSph to form dHSph. [103]. The formed dHSph becomes acylated with an acyl-CoA ester by the action of CerS [104]. Six distinct CerS isoforms (CerS1-6) exists, each with different but overlapping preference of acyl-CoA esters, see section 1.3.1. DES catalyze the desaturation of dHSph forming ceramide [105]. Ceramides can be further metabolized in the ER to galactosylceramide (GalCer) [106], ceramide phosphoethanolamine (CPE) [107] or to other complex sphingolipids. Ceramides have very low solubility in aqueous environments and as such they are membrane bound molecules. The cell uses two major mechanisms for the transport of ceramides from one membrane to another either vesicular transport or by the ceramide transfer protein (CERT) [108, 109]. In Golgi, ceramides can be further processed into glucosylceramide (GlcCer) and SM in a reaction that is catalyzed by glucosylceramide synthase (GCS) [110] and sphingomyelin synthase 1 (SMS1) [111], respectively. The synthesized GlcCer serves as precursor for the majority (300-400 different species) of all glycosphingolipids (GLS) (reviewed by [112]). At the trans-Golgi apparatus or in the plasma membrane (PM), SM can be converted into ceramide and ceramide 1-phosphate (C1P) via neutral sphingomyelinase (nSMase) [113] and ceramide kinase (CERK) [114], respectively.

For degradation of complex sphingolipids several pathways exists. At the PM, SM is degraded to ceramide, sphingosine (Sph) and finally sphingosine 1-phosphate (S1P) via secretory sphingomyelinase (sSMase), neutral ceramidase (nCDase) and sphingosine kinase (SK1), respectively. The endolysosome pathway

degrades SM or glycosphingolipids (GSL) to ceramide via acidic sphingomyelinase (aSMase) [113] and glycosidase (GCase), respectively. In the cytosol, acid ceramidase (aCDase) converts ceramide into free Sph, which can be used to re-synthesize ceramide via CerS in ER (salvage pathway) or be converted into S1P by SK1/2 in the cytosol. S1P can be hydrolyzed back into Sph via S1P phosphatase (Spp). Finally S1P can be degraded into ethanolamine 1-phosphate (EA1P) and hexadecenal via S1P lyase (SPL) (Figure 6).

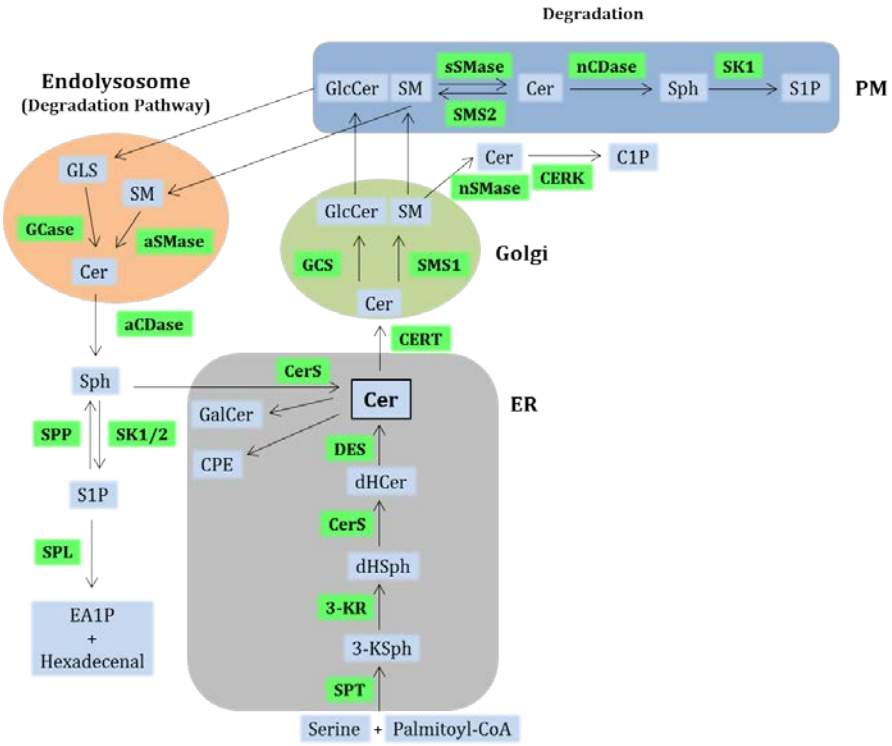

Figure 6: *De novo* ceramide synthesis. The detailed *de novo* synthesis of ceramides is described in the text. Abbreviations: Endoplasmic reticulum (ER), plasma membrane (PM), serine palmitoyltransferase (SPT), 3-ketodihydrosphingosine (3-KSph), 3-ketodihydrosphingosine reductase (3-KR), dihydrosphingosine (dHSph), ceramide synthase (CerS), ceramide (Cer) and dihydroceramide desaturase (DES), galactosylceramide (GalCer), ceramide phosphoethanolamine (CPE), ceramide transfer protein (CERT), glucosylceramide (GlcCer), sphingomyelin (SM), glucosylceramide synthase (GCS), sphingomyelin synthase 1 (SMS1), glycosphingolipids (GLS), ceramide 1-phosphate (C1P), neutral sphingomyelinase (nSMase), ceramide kinase (CERK), sphingosine (Sph), sphingosine 1-phosphate (S1P), secretory sphingomyelinase (sSMase), neutral ceramidase (nCDase) and sphingosine kinase (SK1), acidic sphingomyelinase (aSMase), glycosidase (GCase), acid ceramidase (aCDase), ethanolamine 1-phosphate (EA1P), hexadecenal and S1P lyase (SPL), S1P phosphatase (Spp).

1.3.2 SUMMARY OF CERAMIDES

Ceramides comprises of a LCB, which is *N*-acylated with an acyl-CoA ester and play important roles as PM components and as signaling molecules. Additionally, ceramides are important for maintaining epidermal barrier integrity. Ceramides are synthesized in the ER either by *de novo* synthesis or via the salvage pathway and they serve as precursors for more complex SL. CerS are key enzymes in the synthesis of ceramides and there exists six different isoforms displaying different cellular localization and acyl-CoA chain length specificity.

1.4 THE EPIDERMIS

The skin is the largest organ of the human body and is subdivided into two main layers; the lower dermis and the upper epidermis. The dermis is a flexible connective layer that is buildup of a fibrous network mainly consisting of collagen and elastin, which accounts for the elasticity and the tension strength of the skin. Nerves and blood vessels residing in the dermis are responsible for the sensing and thermoregulatory functions of the skin. The epidermis and its appendages provides a barrier between the internal milieu and the external environment and protect the body against e.g. physical stress, chemical injury, ultraviolet radiation, biological attacks, immunological impairment, heat loss and loss of water and electrolytes. The epidermis is further divided into four different layers; stratum basale (SB), stratum spinosum (SS), stratum granulosum (SG) and stratum corneum (SC) and the majority of epidermal cells are referred to as keratinocytes (figure 7).

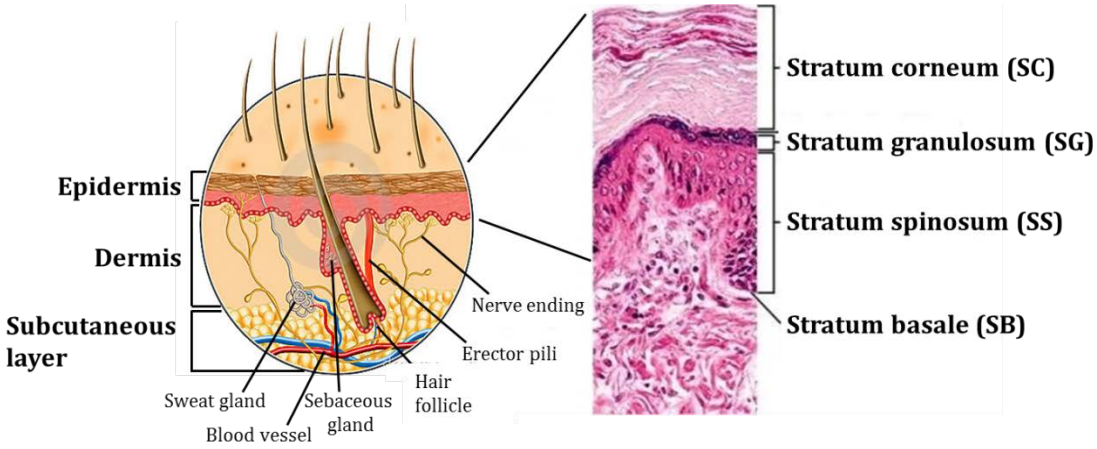

Figure 7: Human skin and epidermis. The subcutaneous layers below the dermis function as isolation and additionally it provides the layers above with nutrients due to the presence of blood vessels. The dermis provides the skin with flexibility due to the content of collagen and elastin. The sweat glands, erector pili and nerve endings span through the dermis layer. The hair follicle resides in all skin layers depending on growth cycle status. The sebaceous gland is attached to the upper part of the hair follicle. The epidermis is the outermost skin layer and is further divided in stratum basale (SB), stratum spinosum (SS), stratum granulosum (SG) and stratum corneum (SC). Figure adapted and modified from www.dreamstime.com\oyalty-free-stock-photography-human-skin-inside-structure-image10262887 and http://faculty.southwest.tn.edu/rburkett/integumentary_system.htm.

The hair follicles reside in the dermis and together with the sebaceous gland, the apocrine gland and the erector pili muscle; it forms the pilosebaceous unit (PSU). The parts of epidermis, which is in between the PSU are referred to as the interfolllicular epidermis (IFE). In order for the epidermis, hair follicles and sebaceous glands to carry out their pivotal protective functions, these tissues continuously need to renew themselves. The skin homeostasis process relies on stem cells and progenitor cells (also named transient amplifying cells) in the basal layers of epidermis, hair follicles and sebaceous glands.

The epidermis and dermis are separated by a basement membrane where the epidermal stem cells and progenitor cells of the SB adhere to. The stem cells ensure lifelong maintenance of the epidermis due to their unlimited self-renewal capacity and their ability to differentiate (reviewed by [115]). The basement membrane is composed of a specialized layer of extracellular matrix proteins; e.g. collagen IV, nidogens and

laminin 5 which provides a platform for growth factors and nutrients together with structural support for the epidermis (reviewed by [116, 117]). The basal cells in SB are anchored to the basement membrane by heterodimeric transmembrane receptors, consisting of α- and β-integrin subunits. These heterodimeric transmembrane receptors bind specific extracellular matrix components through their extracellular domains (reviewed by [118]). When the keratinocytes lose contact with the basement membrane, they are committed to terminal differentiation and they therefor migrate through the SS, SG and SC. Eventually they are shed off as death cells at the surface of the skin. The epidermal homeostasis process is thoroughly reviewed by [119-122].

The majority of knowledge about epidermal homeostasis and regulation hereof almost entirely rely on observations from genetically modified mouse models and human skin differs from mouse skin, therefor caution should be taken in applying these observations directly to human epidermal homeostasis. The epidermis layers in human skin consist of more cell layers than in mouse skin, resulting in an overall thicker epidermis in humans. Additionally, human skin display less frequency of hair follicles (figure 8).

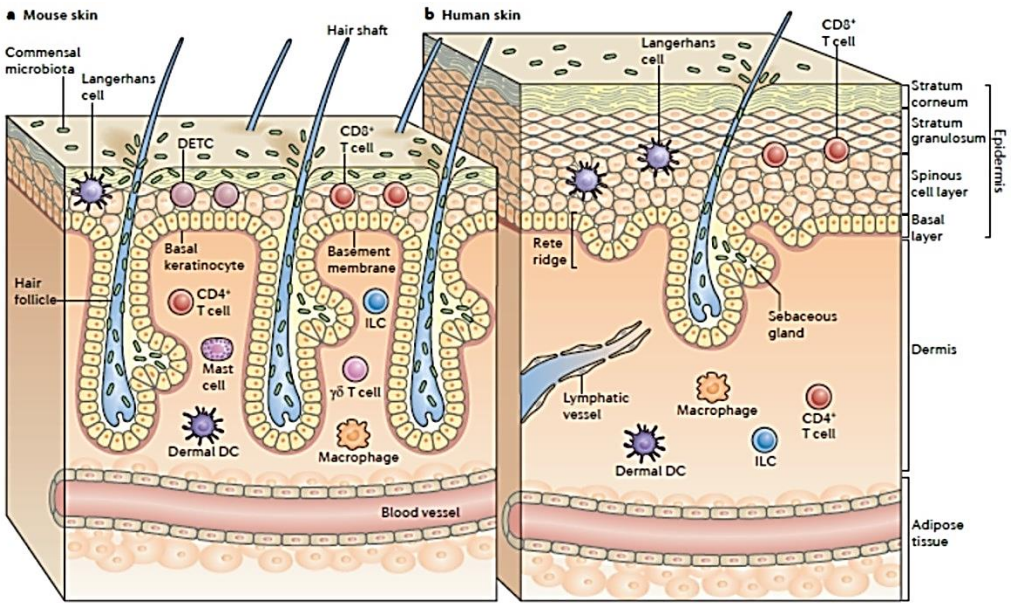

Figure 8: Structure of mouse vs. human skin: a) The density of hair follicles is higher in mouse skin and the epidermal layers; stratum basal, stratum spinosum, stratum granulosum and stratum corneum display less cell layers compared with human skin. **b)** Human skin has larger areas of inter follicular epidermis (IFE) between the hair follicles and the epidermis is thicker in human skin, with more layers of cells within different epidermal layers. Immune cell types are indicated: Langerhans cells, $CD8^+$ T cells, $V\gamma5^+$ dendritic epidermal T cells (DETCs), $CD4^+$ T cells, macrophages, mast cells, conventional αβ T cells, innate lymphoid cells (ILCs), γδ T cells and dermal DC cells. Figure adapted from [123].

1.4.1 EPIDERMAL DEVELOPMENT

During embryogenesis, at embryo (E) age 8.5, the IFE develops from a single layered ectoderm, when surface ectoderm cells commit to an epidermal fate and form the SB (reviewed by [124]). Wingless (Wnt) signaling plays a significant role in this cell commitment, as Wnt signaling blocks the fibroblast growth factor signaling to the ectoderm cells. This causes the ectoderm cells to express bone morphogenetic proteins (BMPs), which determines their development into epidermis (reviewed by [125]). At E9-E13.5 the first suprabasal layer; the periderm is formed [126]. Next, an intermediate cell layer forms between the basal layer and the periderm, which is associated with asymmetric cell division of basal cells. At E12.5 the basal cells are single layered throughout the embryo surface and the proportion of perpendicular asymmetric cell divisions are 0%. The proportion of perpendicular asymmetric cell divisions rises to 70% between E14.5-E17.5, when the stratified epidermis is formed [127, 128]. Subsequently, the proportion of perpendicular asymmetric cell divisions is expected to decrease, as the need to generate suprabasal cells decline [127, 129].

When basal cells lose their proliferative capacity they mature into spinous cells and undergo further maturation into granular cells and cornified cells [127, 130]. However, this first periderm is shed off before birth in conjunction with formation of the epidermal barrier which is fully developed at E16 [131]. The epidermal barrier formation is strongly correlated to formation of the SC, which also occurs at E16 [132].

1.4.2 EPIDERMAL PROLIFERATION

All though the epidermal proliferation processes and the involved regulatory processes are not fully elucidated yet, recent studies suggest that epidermal homeostasis highly rely on asymmetric divisions of both stem cells and progenitor cells in SB [128, 129]. The stem cells divide asymmetrically resulting in one daughter cell remaining attached to the basement membrane and the other daughter cell commits to a progenitor differentiation fate [128]. The stem cells also support the proportion of progenitor cells in SB. The progenitor cells share a similar pattern of asymmetric self-renewal, where the balance between proliferation and differentiation rely on stochastic fate choice [133]. The progenitor cells in SB eventually withdraw from the cell cycle, detach from the basement membrane and commit to terminal differentiation [134].

In adult mice, the epidermal homeostasis process is subject to tight regulation, and the generation of suprabasal cells is strongly correlated with the number of cells that are lost by shedding or injury. This regulation is crucial since unbalances results in either hypoproliferation or hyperproliferation with epidermal defects as outcome. In mice, several control mechanisms involved in epidermis proliferation and differentiation has been identified; e.g. multiple differentiation factors, chromatin remodeling complexes and small non-coding RNAs (reviewed by [119]). Even the mechano-physical properties of the basement membrane impacts the proliferative potentials of basal cells [135]. Additionally, the basement membrane is composed of an array of extracellular matrix polymers and growth factors, that provide the basal cells with a complex repertoire of stimuli (reviewed by [121]). A selection of the regulatory mechanism's involved in the epidermal self-renewal process will be discussed in further detail below (1.4.6).

1.4.3 EPIDERMAL DIFFERENTIATION

The epidermal differentiation process involves an increasing level of stratification through differential expression of keratins together with breaking and formation of specialized cell-cell contacts. The complex

differentiation process ultimately results in terminally differentiated keratinocytes, termed corneocytes, in SC, which sustains the primordial frontline of the epidermal barrier defense.

Terminal differentiation initiates when proliferative keratinocytes in SB detach from the basement membrane, becomes mitotically inactive and initiate migration towards SC. At this point the keratinocytes are committed to terminal differentiation and migrate through the three layers of differentiation; SS, SG and SC, while undergoing major changes in transcription, morphology and function, before they eventually are shed from the skin surface by a process named desquamation.

As the keratinocytes leave SB the expression of keratin (K) 5 and K14 is switched to expression of K1 and K10 [136]. In SS K1 and K10 interlinks with desmosomes to form a robust network that provides protection against mechanical stress at the body surface [136]. All though the network is robust, the bridges between keratin and desmosomes constantly break and reforms as the keratinocytes migrate towards the skin surface, contributing to the flexibility and strength of the skin. Molecular aspects of cell-cell adherence and the differential expression of structural proteins will be discussed in further detail below (1.4.4 and 1.4.5, respectively).

When the keratinocytes reach the SG, the lamellar bodies (also known as lamellar granules or Oland bodies) and keratohyalin granules are formed [137]. The lamellar bodies are coordinately packed with polar lipids (e.g. glucosylceramides, phospholipids and cholesterol) and hydrolytic enzymes (e.g. β-glucocerebrosidase, acidic sphingomyelinase, secretory phospholipase A_2, neutral lipases and proteases) which are needed for the formation of the cornified envelope and lipid lamella in SC (reviewed in [138, 139]). The keratohyalin granules contain different histidine- and cysteine-rich structural proteins that are involved in ligation of keratin filaments and formation of the cornified envelope. A major component of the keratohyalin granules is profilaggrin, which is processed to filaggrin and causes the dense packing of keratin filaments in corneocytes [140].

The keratinocytes in SG undergo a unique form of programmed cell death, named cornification. In this process the intracellular organelles and their content are replaced by a compact cytoskeleton and the proteins on the corneocyte periphery are cross-linked to form the protein envelope. The protein envelope is further crosslinked to lipids, together generating the cornified envelope, which replaces the plasma membrane. Finally the intercellular spaces between the corneocytes are filled with lipids originating from the lamellar bodies, forming the lipid lamella. All together these structural changes form the brick-mortar structure of the SC (reviewed by [141, 142]).

During the differentiation process the keratinocytes initiate the expression of terminal differentiation markers, such as filaggrin and loricrin [137] which are encoded by genes of the epidermal differentiation complex. The epidermal differentiation complex is a 2 Mb region located on human chromosome 1q21, which comprises a number of genes encoding structural and regulatory proteins that are crucial for proper keratinocyte differentiation and SC integrity (reviewed by [143]). The genes of the epidermal differentiation complex are organized into four families encoding the following proteins; the EF-hand calcium-binding proteins of the S100A family, the small proline rich protein (SPRR), the late cornified envelope proteins and the S100-fused type proteins. Additionally the genes encoding involucrin and loricrin are both included in the epidermal differentiation complex.

1.4.4 EPIDERMAL CELL-CELL ADHERENCE

Keratinocytes adhere to neighboring cells through desmosomes, adherence junctions and tight junctions (reviewed by [144, 145]).

1.4.4.2 DESMOSOMES

Desmosomes are structures that are formed by cadherins, armadillo proteins and plakins to connect keratin intermediate filaments from one cell to another cell. The cadherins desmoglein (Dsg) and desmocollin (Dsc) span the membranes in pairs and interconnect with the Dsg/Dsc pairs from the neighboring cells. The cytosolic tails provide a binding site for the armadillo family member's plakoglobin and plakophilins. Furthermore, the plakin family member desmoplakin links the keratin intermediate filaments to the specialized area of the plasma membrane. The dominant cadherins expressed in differentiating keratinocytes are Dsg1/3 and Dsc1/3 whereas Dsg2/Dsc2 are expressed at low levels in SB. Dsg4 are expressed solely in SG and SC [146, 147].

1.4.4.2 ADHERENCE JUNCTIONS

Adherence junctions connect actin filament bundles between neighboring cells and consist of the nectin-afadin complex and the classical cadherin-catenin complex. Nectin spans the membrane and connects with afadin in the cytosol where actin binds. The type I classical cadherins belong to the same superfamily as desmosomal cadherins and also span the membrane. In the cytosol cadherin connects directly with p120 catenin and β-catenin, whereas α-catenin binds to β-catenin and connects actin to the complex. Both E-cadherin and P-cadherin are involved in adherence junctions in SB, but only E-cadherin is involved in adherence junctions in differentiating keratinocytes [148].

1.4.4.3 TIGHT JUNCTIONS

Tight junctions are as their name indicates tighter than both desmosomes and adherence junctions and are highly involved in epidermal barrier integrity in SG. Three types of transmembrane components are involved in tight junction formation; the IgG like family of junctional adhesion molecules (JAM), claudin and occluding (reviewed by [149]).

1.4.5 EPIDERMAL STRUCTURAL PROTEINS

Keratinocytes express an array of structural proteins such as keratin (K), filaggrin, trichohyalin, loricrin, small proline rich proteins (SPRR), envoplakin, periplakin and involucrin (reviewed by [150-152]). The expressed structural proteins support the differentiating keratinocytes to make a mechanically resistant surface ensuring proper protection of the underlying tissues. Differentiating keratinocytes accumulate keratins to make a keratin cytoskeleton that replaces the cytosolic intercellular components and organelles. The keratins are linked to desmosomes, thereby ensuring cell-cell adherence in SC. During terminal differentiation, filaggrin and trichohyalin associate with the keratin skeleton to insure its integrity. Loricrin and SPRR are crosslinked by transglutaminases in the cytosolic side of the cornified envelope, whereas and involucrin, envoplakin and periplakin are crosslinked in the cornified envelope facing outward. SC Lipids, especially ceramides, crosslink to involucrin, envoplakin and periplakin thereby forming the lipid envelope. Together these structures form the cornified envelope (figure 9).

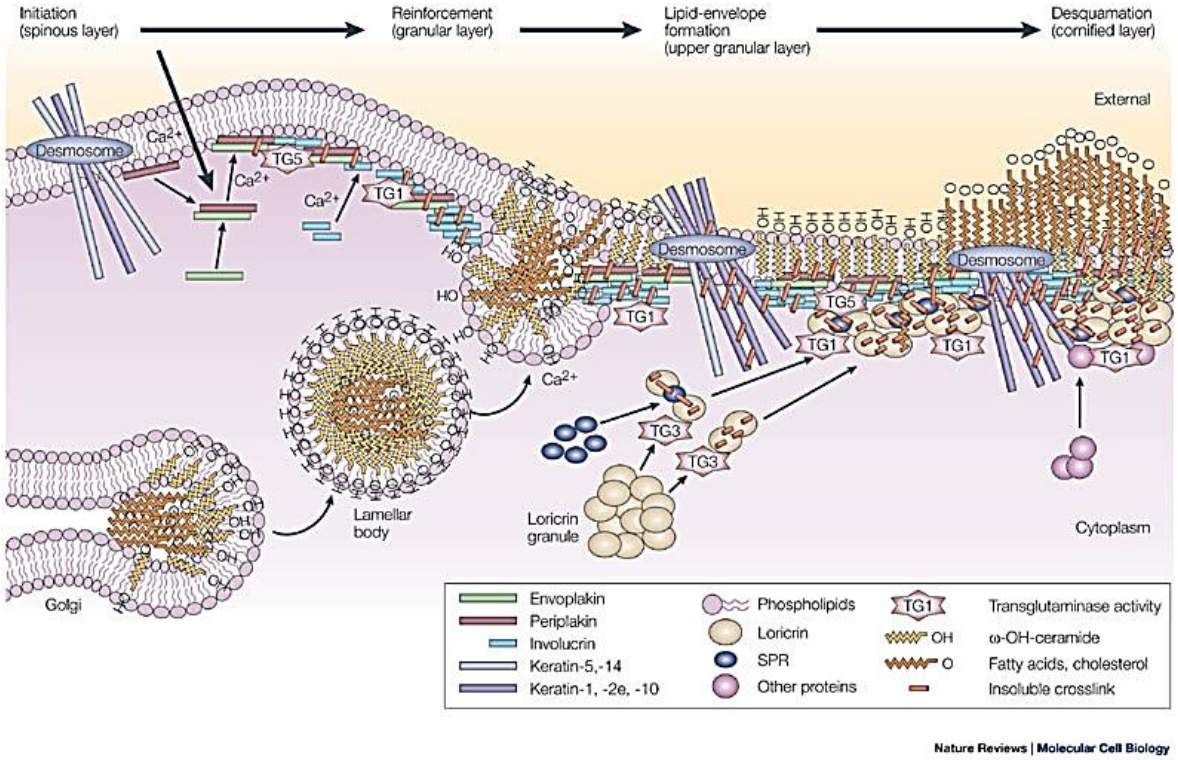

Figure 9: Cornified envelope formation. The differentiation process is initiated in SS with synthesis of several structural proteins needed for cornified envelope formation. Transglutaminase (TG) 1 and TG5 crosslink envoplakin and periplakin on the cytosolic side of the plasma membrane. In SG the keratinocytes are reinforced by crosslink of loricrin to SPRRs by TG3 and TG1. Additionally, lipids included in the lamellar bodies are covalently attached to cornified envelope proteins. Induced crosslink occurs on desmosomes and function as substrates for TGs. The formation of the lipid envelope is also initiated in SG, where lamellar body lipids are crosslinked to envoplakin, periplakin and involucrin by TG5 and TG1. The crosslinked lipids are exposed on the outside of the plasma membrane. Finally, in SC loricrin and other proteins are further crosslinked by TG1, and ω-hydroxy ceramides, FA and cholesterol are extruded from the lamellar bodies into the extracellular space between the corneocytes. Figure adapted from [141].

1.4.5.1 KERATINS

In total, 54 mammalian keratin genes have been identified. These express two types of keratins; Type I keratins (K9-K28 and K31-K86) are acidic proteins and type II keratins (K1-K8 and K71-K86) are basic or neutral proteins. 2/3 of all keratin types are expressed in keratinocytes and make up 85% of the total cellular protein content of keratinocytes [153]. All keratins have a central α-helical rod domain which is essential for filament assembly. The α-helical rod domain is flanked by variable non helical end-domains involved in filament assembly and/or interactions with other proteins (reviewed by [154]). Keratins are most commonly co-expressed in pairs, one of each type, which assemble into keratin intermediate filaments. Un-committed ectoderm cells express K8 and K18 [155]. Cells in SB express K5 and K14, which are frequently used as markers for cells in SB. When the keratinocytes start to differentiate and migrate into SS, the expression of K5 and K14 are shifted to expression of K1 and K10 [136]. K6 and K16 are not expressed in keratinocytes under normal conditions, but their expression is increased in skin with epidermal barrier function disorders and during wound healing [156-158], indicating a function for K6 and K16 during hyperproliferation situations.

Keratins are linked to several skin diseases in humans. Epidermolysis bollosa, a rare skin disease with blistering all over the body, is linked to *K5/K14* mutations [159]. In support of this, lessons from transgene mice depleted of K14, show that in absence of K14, K15 levels are increased possibly causing cytolysis in SB, leading to skin blistering [160]. In addition epidermolytic ichthyosis is linked to *K1/K10* mutations [161] and in mice depleted of K10, the level of K5/K14 is increased and K1 decreased [162]. Taken together, this indicates some degree of redundancy between keratins and compensatory induction of expression of other keratins in case of depletion of one keratin.

1.4.5.2 FILAGGRIN

Filaggrin is a histidine-rich basic protein, which is involved in aggregating keratin intermediate filaments into bundles and macrofibrils in SC [140, 163]. Expression of profilaggrin is initiated in SG [164]. In humans profilaggrin consists of 10-12 filaggrin repeats that are linked together by short hydrophobic linker peptides [165]. In rodents profilaggrin consists of at least twenty filaggrin repeats [166]. Profilaggrin is packed into keratohyalin granules as phosphorylated precursors and in the lower part of SC profilaggrin is modified and cleaved to yield filaggrin. Subsequently, filaggrin is degraded into free amino acids, which function as moisturizers due to their ability to bind water [167, 168]. Profilaggrin is a member of the S-100 calcium-binding protein family, and it is suggested that the Ca^{2+} binding domain may function to sustain a Ca^{2+} reservoir in SG keratinocytes, allowing profilaggrin to self-regulate its processing into filaggrin [169]. Filaggrin depletion in humans is linked to ichthyosis vulgaris and predisposition to atopic dermatitis [170-172]. Mice depleted of filaggrin (flaky tail mouse) serve as an animal model for ichthyosis vulgaris/atopic dermatitis [173]. These mice lack profilaggrin packed keratohyalin granules and the expression of involucrin and loricrin are increased, indicating a compensatory mechanism.

1.4.5.3 TRICHOHYALIN

Trichohyalin is a member of the S-100 calcium-binding protein family and is predicted to form a single α-helical rod that might bind keratins and function as a scaffold protein in cell envelope organization [174].

1.4.5.4 LORICRIN

Loricrin is a major component of the cornified envelope and the protein is rich in glycine, serine and cysteine. Loricrin is expressed in SG and packed into keratohyaline granules. In SC loricrin localizes to the cornified envelope [164, 175]. Sequence analysis of loricrin predicts a flexible structure consisting of glycine-rich loop motifs separated by glutamine-rich linker sequences [176]. In humans loricrin crosslinks to a number of cornified envelope proteins including K1, K10, SPRR1, SPRR2, and filaggrin [177], which highlights the importance for loricrin in cornified envelope formation. In mice, loricrin depletion leads to skin abnormalities with shiny, translucent and fragile skin. Surprisingly, the epidermal skin barrier remains intact upon loricrin depletion, possibly due to increased expression of other cornified envelope proteins, which may compensate for the lack of loricrin to maintain epidermal barrier integrity [178].
Involucrin consists of short peptide repeats rich in glycine, lysine and glutamin [179]. Involucrin, envoplakin and periplakin are all part of the cornified envelope and are crosslinked to lipids of the lipid envelope, especially ceramides [180].

1.4.5.5 SPRR

The small proline-rich proteins (SPRR) consist of up to 40% proline and their expression is highly induced during epidermal differentiation, upon UV treatment and wound healing [176, 181]. SPRR mainly crosslink to loricrin, but also to other cornified envelope proteins [182-184].

All the mentioned structural proteins involved in cornified envelope formation, play important roles in epidermal barrier integrity. There is an array of compensatory mechanisms involved in sustaining the epidermal barrier integrity upon depletion of one or more proteins. All together this emphasizes the importance for proper epidermal barrier function for mammalian survival.

1.4.6 PATHWAYS INVOLVED IN EPIDERMAL HOMEOSTASIS

The regulations of epidermal homeostasis rely on numerous pathways and the understanding of the complex interplay is only emerging. Here a few important pathways will be discussed.

1.4.6.1 THE EPIDERMAL GROWTH FACTOR RECEPTOR PATHWAY

The epidermal growth factor receptor (EGFR) signaling pathway plays a pivotal role in keratinocyte stem cell regulation. Excessive induction of EGFR signaling results in various types of human tumors and aberrant induction causes non-melanoma skin cancer and chronic inflammatory disorders such as atopic dermatitis, psoriasis and allergic contact dermatitis (reviewed by [185-188]).

Experiments with transgenic mice expressing a dominant form of Son of Sevenless (SOS), an adapter protein involved in the downstream EGFR signaling cascade, reveals that increased EGFR signaling induces proliferation and differentiation of the IFE [189]. This is supported by findings in a mice model lacking leucine-rich repeats and immunoglobulin-like domains 1 (Lrig1), which is an EGFR ligand inhibiting EGFR signaling. In mice depleted of Lrig1, the IFE hyper-proliferates [190]. Furthermore, the EGFR ligand transforming growth factor (TGF) inhibits EGFR signaling in SB as compromised TGFβ signaling causes increased proliferation in mice epidermis [191]. The A disintegrin and metalloprotease (ADAM) proteins are highly involved in ligand shedding for the EGFR and mice depleted of ADAM17 have epidermal barrier defects, with elevated TEWL and altered expression of markers for terminal differentiation. This further underlines the pivotal role of EGFR signaling in epidermal homeostasis [192].

1.4.6.2 TUMOR SUPRESSER p63

The transcription factor p63 is a homolog of the tumor suppressor p53 [193]. The ΔNp63 isoform is preferential expressed in basal cells [194] and knock down of ΔN isoforms of p63, but not TA isoforms, decreases EGFR expression in human mammary epithelia cell line MCF-10A [195]. Furthermore, EGFR activation increases ΔNp63α expression in human keratinocytes through the phosphoinositol 3 kinase (PI3K)/Akt pathway [196], indicating a complex interplay between p63 and EGFR.

Lack of tumor protein p63 in mice causes impairment of IFE stratification and differentiation, resulting in a very thin epidermis and severe defects in epidermal proliferation [197, 198]. Furthermore, knock down experiments have highlighted the important role of p63 in epidermal homeostasis [199].

1.4.6.3 Ca^{2+} SIGNALING

The Ca^{2+} gradient increases as the keratinocytes migrate from SB to SG [200-202]. In keeping with this, *in vitro* studies have demonstrated that keratinocytes exposed to low Ca^{2+} concentrations (e.g. 0.03 mM) fail

to differentiate, but initiates differentiation when switched to Ca^{2+} concentrations above 0.1 mM [203]. When the cells start to differentiate, they rapidly initiate cell-cell adhesion, by recruitment of desmoplakin, occludins, claudins, E-cadherin and catenins to the plasma membrane. This is important for the correct formation of desmosomes, tight junctions and adherens junctions. The formed adherence complexes participate in altering the actin distribution, which is involved in sustaining the increased intracellular Ca^{2+} concentration [204, 205]. The elevated intracellular Ca^{2+} concentration promotes sequential expression of the differentiation markers K1, K10, involucrin, transglutaminase, loricrin and filaggrin [206-210]. In the genes expressing K1 and involucrin, there have been identified calcium responsive gene elements, which may be involved in Ca^{2+} induced expression of K1 and involucrin [211, 212]. In conclusion, increases in both extracellular and intracellular Ca^{2+} concentrations induce epidermal differentiation.
The Ca^{2+} induced differentiation is partly mediated by activation of protein kinase C (PKC). Ca^{2+} promotes synthesis of phosphatidylinositol and diacylglycerol which causes activation of PKC. Subsequently expression of early differentiation markers are downregulated and expression of late differentiation markers are upregulated, as the keratinocytes transition from SS to SG [213]. The above mentioned *in vitro* observations only reveal partly how calcium controls the transcription of genes involved in terminal differentiation and the exact mechanisms remain elusive.

1.4.7 SUMMARY OF EPIDERMIS

The human epidermis is divided into four layers: stratum basale (SB), stratum spinosum (SS), stratum granulosum (SG) and stratum corneum (SC). Within the dermis the hair follicle, the sebaceous gland, the apocrine gland and the erector pili muscle forms the pilosebaceous unit (PSU). Basal keratinocytes in SB proliferates and as they move through SS, SG and SC they terminally differentiate. The differentiation process involves accumulation of keratin filaments, replacement of the PM with the cornified envelope and assembly of the lipid lamella. The cell-cell adherences by desmosomes, adherence junctions and tight junctions constantly break and form to ensure proper barrier function as the keratinocytes migrate. The cornified envelope consists of proteins such as loricrin involucrin, periplakin and envoplakin which are crosslinked to lipids. Multiple pathways are involved in the regulation of the epidermal homeostasis process; e.g. EGFR, p63 and Ca^{2+} signaling.

1.5 HAIR FOLLICLES

The presence of hair is a unique feature of mammals which has many functions; e.g. physical protection, thermal insulation, camouflage, sensory perception and social interaction.
The hair follicle is part of the PSU together with the sebaceous gland, the apocrine gland and the erector pili muscle. The hair follicle is a very dynamic mini organ which undergoes continuously regeneration through cycling. During cycling, the upper part of the hair follicle remains permanent, whereas the lower part cycles through the three phases of regeneration: anagen, catagen and telogen. Anagen defines the growth phase, catagen is the apoptosis driven regression phase and telogen is a phase of relative quiescence.
The PSU is defined by distinct compartmentalized stem cell populations. The lowest part, the dermal papilla, is where the hair germ cells origin from and wherefrom the hair shafts grow out. The bulge separates the lower cycling part of the hair follicle from the upper permanent part. The Istmus designates the part between the bulge and where the sebaceous gland is located and the junctional zone is the upper part of the isthmus where the sebaceous gland is placed. Finally, the infundibulum designates the upper

part that is in connection with the IFE (figure 10) (reviewed by [214]). The current knowledge about hair follicle morphogenesis and cycling almost entirely rely on exceptionally informative observations from genetically modified mouse models and therefor caution should be taken in applying these observations directly to human hair follicle morphogenesis and cycling.

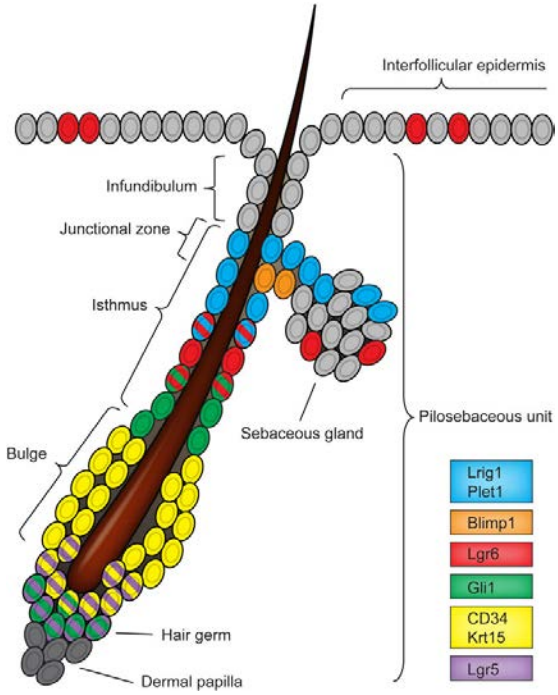

Figure 10: Hair follicle compartments and stem cell populations. The hair follicle and the sebaceous gland are part of the pilosebaceous unit (PSU). The hair follicle is further divided into the dermal papilla, the hair germ, the bulge, the isthmus, the junctional zone and the infundibulum. Distinct stem cell populations reside in the different compartments designated by expression of specific markers indicated by colors and key to the right. Figure adapted from [214].

1.5.1 HAIR FOLLICLE MORPHOGENESIS

Murine hair follicle morphogenesis initiates at an early embryonic state due to Wnt mediated signaling in mesenchymal cells. Essentially this causes thickening of epidermal keratinocytes, which form a hair placode, the hair placode is visible at E15.5. Subsequently the dermal condensate is formed due to condensation of specialized fibroblasts in the underlying mesenchyme. The dermal condensate signals to epidermal cells to initiate proliferation which causes them to grow down wards into the dermis. Next the dermal papilla is formed via enveloping of the dermal condensate with follicular epithelia cells. Hereafter, the entire hair follicle is formed as a consequence of stimulations from the dermal papilla.

Hair follicle morphogenesis involves a defined crosstalk between several signaling pathways including Wnt/β-catenin, Sonic hedgehog (Shh), ectodysplasin (Eda)/ectodysplasin receptor (EdaR), Notch and TGF-β/BMP (reviewed by [215-218]).

1.5.2 HAIR FOLLICLE CYCLING

Land mark publications describing the cycling of hair follicles were published decades ago [219, 220]. The majority of information regarding hair follicle cycling and control hereof, is derived from genetically modified mice models. Today it is generally appreciated, that in mice the first two hair cycles are synchronous. There might be small variations regarding the exact time points for when the hair follicles leave one phase to enter another, but generally the first catagen phase is initiated at P16, right after morphogenesis. During catagen the hair follicle undergo controlled apoptosis, causing regression of the hair follicle. At P18 the first telogen phase is initiated and during telogen the hair rests in the upper permanent part of the hair follicle. The first anagen phase is initiated at P22 with activation of stem cells in the bulge and hair germ causing proliferation and downward growth of the hair follicle. When the hair follicle reaches a defined depth in dermis the keratinocytes in the lower end of the hair follicle reverse their growth direction. This gives rise to the differentiated layers of the hair follicle, the inner root shaft and the hair shaft. The cycling of the hair follicles continues throughout the lifetime of the mice and is under the control of an array of signaling pathways including Wnt/βcatenin, Sonic hedgehog (Shh), Eda/EdaR, Notch and TGF-β/BMP (reviewed by [217, 221-223]).

1.5.3 PATHWAYS INVOLVED IN HAIR FOLLICLE MORPHOGENESIS AND CYCLING

Hair follicle morphogenesis and the continuous cycling of the hair follicle are tightly regulated through a refined interplay between numerous factors. Here a few of the involved signaling pathways will be discussed in brief.

1.5.3.1 WNT/β-CATENIN

Canonical Wnt/β-catenin signaling plays a major role in hair follicle morphogenesis and cycling. Epidermal Wnt10b expression correlates with initiation of hair follicle morphogenesis in mice [224]. Both Wnt10a and Wnt10b expression is upregulated in placodes during hair follicle morphogenesis onset [225]. Additionally, blocking of Wnt signaling with topical expression of Dickkopf 1 (a potent inhibitor of Wnt signaling) caused complete placode formation failure [226]. Furthermore, Wnt signaling directs epidermal cell fate during hair follicle morphogenesis [227]. Altogether, this emphasizes the essential role of Wnt/β-catenin signaling in onset of hair follicle morphogenesis and hair placode formation in mice.

During adult hair follicle cycling β-catenin accumulates in the hair germ at anagen onset. Additionally, dermal papilla specific depletion of β-catenin reduces hair follicle progenitor cell proliferation and differentiation, which causes premature entry into catagen [228]. On the contrary, overexpression of β-catenin increases bulge stem cell activation resulting in shortening of the telogen phase [229]. Taken together, this indicates that Wnt/β-catenin signaling function in adult hair follicle cycling by mediating crosstalk between the dermal papilla and the hair germ, thereby inducing hair follicle stem cell activation.

1.5.3.2 TGF-β/BMP

BMP signaling plays an inhibitory role in embryonic skin. During hair follicle morphogenesis BMP4 expression in dermal condensates is upregulated [230] and epidermal deletion of the BMP receptor 1a (Bmpr1a) results in large placode-like structures; however hair follicle differentiation is prevented and instead tumor formation is induced [231]. Additionally, when BMP signaling is elevated in mice, by ectopically expression of BMP4, the induction of hair follicle morphogenesis is impaired, causing

progressive baldness. A similar progressive baldness phenotype appears when the BMP antagonist Noggin is inactivated. [232]. These results suggest an important role for BMP signaling in both hair follicle formation and differentiation during morphogenesis, and thereby underline the inhibitor role of BMP signaling in hair follicle morphogenesis.

In adult hair follicles, BMP2 and BMP4 expression is elevated in the dermal papilla and hair germ during telogen. This promotes the quiescence of stem cells through nuclear factor of activated T-cells 1 (NFATc1) [233]. Towards the end of telogen the BMP levels decrease [234] and expression of the BMP inhibitor Noggin is increased in the bulge [235], which together facilitates the onset of anagen. Additionally, overexpression of BMP4 in the outer root sheath results in inhibited proliferation in hair germ and dermal papilla compartments, leading to impaired hair follicles, which are unable to regenerate [236]. Furthermore, overexpression of the BMP inhibitor, Noggin, in proliferating hair matrix cells and differentiating hair precursor cells results in excessive proliferation of matrix cells and impaired differentiation of the hair shaft, which prevents maturation of the hair shaft [237]. Ablation of Bmpr1a in purified dermal papilla cells, abolish their ability to organize hair growth in a novel *in vitro*/*in vivo* hybrid knockout assay [238]. Altogether this suggests the involvement of BMP signaling in both proliferation and differentiation during hair follicle regeneration and in dermal papilla function.

1.5.4 SUMMARY OF HAIR FOLLICLES

Hair follicle is subdivided into different compartments including the dermal papilla, the bulge, the Istmus, the junctional zone and the infundibulum. Hair follicle cycling involves three distinct phases: anagen (growth), catagen (regression) and telogen (rest) of which the two first hair cycles are synchronous in mice. The hair follicle morphogenesis and homeostatic cycling is regulated by numerous signaling pathways; e.g. Wnt/β-catenin and TGF-β/BMP.

1.6 EPIDERMAL LIPIDS

The mammalian epidermal barrier highly depends on SC lipids embedding the corneocytes. This lipid matrix is highly ordered and consists of 60% ceramides, 20% cholesterol and 20% free FA (FFA) [239].

The SC lipids originate from lamellar bodies that are produced in the upper part of SS and are highly abundant in SG. Lamellar bodies are packed with lipids used for the formation of the cornified envelope and the lipid lamella in SC. Additionally; lamellar bodies contain enzymes used for processing of these lipids. The epidermal fraction of FFA is mostly saturated long-chain FA. Human skin composes of 34-39% lignoceric acid (C24:0) and 23-25% hexacosanoic acid (C26:0) and smaller fractions of C32-C36 FFA (both saturated and un-saturated) [240, 241]. The epidermal ceramides are very important for the barrier function and will be discussed in detail in section 1.6.1.

1.6.1 EPIDERMAL CERAMIDES

Ceramides are the main lipid specie in SC and due to their highly hydrophobic nature; ceramides are key players in epidermal barrier integrity. Already in 1978 the ceramide composition of human SC were partly unraveled by HPTLC combined with gas and liquid chromatography [242]. Further analyses of the SC ceramide subclasses in the following years unraveled even more ceramide subclasses, and the esterified ω-hydroxy ceramide were identified in 1985 [243]. The expanding number of SC ceramides called for a new nomenclature introduced by Motta and colleagues [244], which will be used throughout this thesis. In

human SC, a total of 12 ceramide subclasses are known (figure 11a) including [EOS], [NS], [AS], [EOP], [NP], [AP], [EOH], [NH], [AH], [EODS], [NDS] and [ADS]. The last letters designate the different ceramide backbones; sphingosine (S), phytosphingosine (P), 6-hydroxy sphingosine (H) and dihydrosphingosine (DS) and the first letters defines the acyl chain; esterified ω-hydroxy (EO), non-hydroxy (N) and α-hydroxy (A) (reviewed by [245, 246]).

Comprehensive mass spectrometry (MS) studies of human SC ceramides reveal that the [NP] ceramide are the most abundant subclass in SC (22%) and that the ceramides with esterified ω-hydroxy acyl moiety ([EOS], [EOH] and [EODS]) only contribute with 8% (figure 11b). A total of 342 different ceramide species have been identified and within these the length of the acyl chain varies between C14 and C32 whereas the length of the LCB varies between C14 and C28. The very-long acyl chains are mostly detected in the esterified ω-hydroxy ceramides [241, 247, 248]. The esterified ω-hydroxy ceramides can be crosslinked to involucrin, periplakin and envoplakin in the cornified envelope and serves as scaffold for the lipid lamella [180]. These protein bound ceramides are designated [OS], [OH] and [OP] (figure 11a).

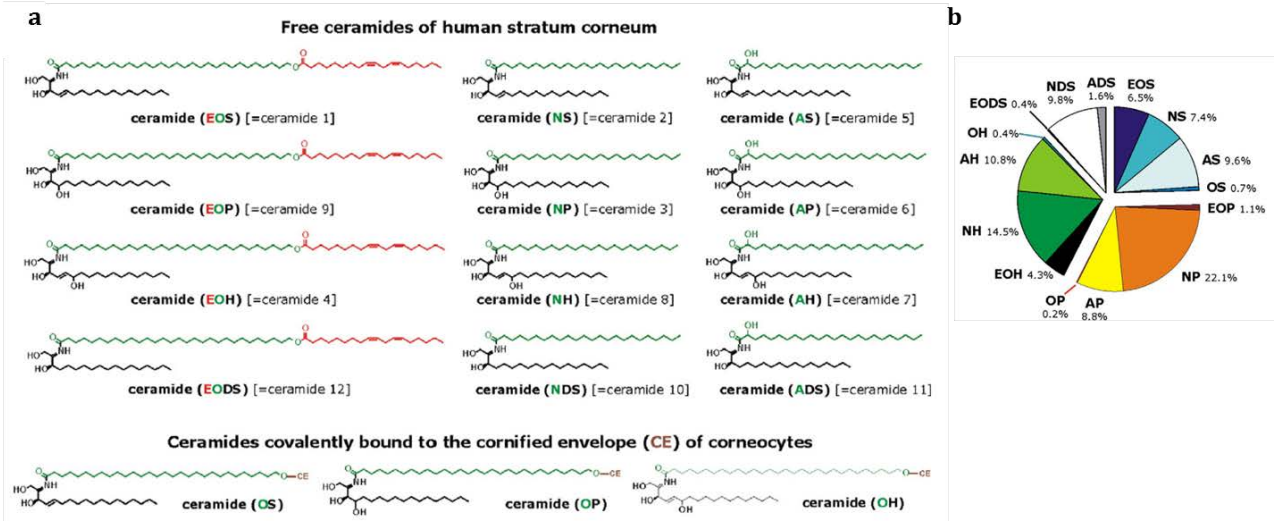

Figure 11: The epidermal ceramide subclasses and their distribution. a) 12 different ceramide subclasses have been identified in human epidermis including [EOS], [NS], [AS], [EOP], [NP], [AP], [EOH], [NH], [AH], [EODS], [NDS] and [ADS]. The first letters designates the acyl chain; esterified ω-hydroxy (EO), non-hydroxy (N) and α-hydroxy (A) and the last letters describes the different ceramide backbones; sphingosine (S), phytosphingosine (P), 6-hydroxy sphingosine (H) and dihydrosphingosine (DS). The [EOS], [EOP], [EOH] and [EODS] ceramides can be further processed in SC and thereby be crosslinked to proteins of the cornified envelope. The protein bound ceramides are designated [OS], [OH] and [OP]. **b)** The distribution of epidermal ceramides show highest content of [NP] ceramides (22.1%), whereas the contribution from ω-hydroxy esterified ceramides ([EOS], [EOP], [EOH] and [EODS]) is only 12.3% combined. Figure adapted from [245].

The esterified ω-hydroxy ceramides are by far the most important epidermal ceramides. These ceramides are very hydrophobic and play a pivotal role in the epidermal water permeability barrier. Recently, there have been identified yet another unique 1-O-acylceramide in mice and human epidermis [249].

The current knowledge regarding synthesis of the esterified ω-hydroxy ceramides and the steps leading to the linking of esterified ω-hydroxy ceramides to proteins in the cornified envelope will be described in the following section using [EOS] ceramides and [OS] ceramides as example (1.6.2).

1.6.2 SYNTHESIS OF [EOS] AND [OS] CERAMIDES

The synthesis of [EOS] and [OS] ceramides are not yet fully elucidated, but there is high evidence for the synthesis to progress as described in figure 12a. It has been proposed that the synthesis of these unique stratum corneum ceramides can follow both the *de novo* and the salvage pathways of ceramide synthesis as described above (1.3.1.1). Only the *de novo* synthesis pathway will be described here.

1.6.2.1 CERS3

The synthesis of [EOS] ceramides is initiated by the fusion of serine and palmitoyl-CoA to form 3KSph, a process catalyzed by SPT. Subsequently, 3KSph is reduced to form dHSph by the action of 3-KR (figure 12a). The acylation of dHSph to form ceramide involves CerS3, as this is the only CerS isoform that is capable of using ultra-long chain (ULC) acyl-CoA esters as substrate [91-93]. Importantly, and in keeping with this, CerS3 depleted mice display a total loss of epidermal ceramides with acyl chains ≥C26, including glucosylated ceramides, [EOS] ceramides and [OS] ceramides. [250]. CerS3 deficient mice die soon after birth due to increased TEWL and the skin of these mice is unwrinkled, erythematous, sticky, thick and compact. CerS3 depletion causes embryonic keratinocyte maturation arrest which leads to impairment of the lipid lamellae and the cornified lipid envelope [250]. Additionally, in humans, mutation in the *CerS3* gene causes autosomal recessive congenital ichthyosis with epidermal thickening and loss of epidermal-specific ceramide content with acyl chains ≥C26 [251, 252]. These observations highly illustrate the importance of CerS3 in the synthesis of [OS] ceramides and in maintaining normal epidermal morphology.

1.6.2.2 ELOVL

The ULC acyl-CoA esters used for ceramide synthesis are synthesized as follows (figure 12a). Palmitoyl is synthesized by FAS. Elongation of palmitoyl-CoA to very-long chain (VLC) acyl-CoA takes place on the cytoplasmic side of ER membranes and is catalyzed by different elongation-of-very-long-chain-fatty-acid (ELOVL) protein isoforms depending on their substrate specificity (reviewed by [253, 254]). The elongation process is a four-step cycle that elongates the acyl-CoA esters by two carbon atoms for each cycle. First, ELOVL are responsible for the condensation of acyl-CoA into 3-ketoacyl-CoA, next 3-ketoacyl-CoA reductase (KAR) reduces 3-ketoacyl-CoA to 3-hydroxyacyl-CoA. This is followed by the action of 3-hydroxyacyl-CoA dehydratase (HACD) which dehydrates 3-hydroxyacyl-CoA into trans-2-enoyl-CoA and last trans-2-enoyl-CoA reductase (TER) reduces trans-2-enoyl-CoA into acyl-CoA (reviewed by [255]). ELOVL1, 3, 6, and 7 are all capable of elongating both saturated and un-saturated acyl-CoA esters to a maximum chain length of C24. ELOVL1 and ELOVL4 catalyze the extended elongation to produce acyl-CoA esters with 28 carbon atoms, whereas ELOVL4 is the only isoform catalyzing the further elongation to produce acyl-CoA esters longer than C28 [256-258]. Interestingly, mice depleted of ELOVL1 dies shortly after birth due to severe epidermal barrier defects and display impairment of the SC lipid lamellae. Additionally, ceramides containing acyl chain ≥C26 (especially ω-hydroxy ceramides) are decreased whereas ceramides with acyl moiety ≤C24 are elevated in the epidermis of ELOVL1 depleted mice [259]. These findings underline the involvement of ELOVL1 in the synthesis of acyl-CoA esters ≥C26 used for ceramide synthesis in the epidermis and the importance of ceramides with acyl moiety ≥C26 for epidermal barrier integrity. Furthermore, postnatal death due to impaired barrier function is observed in ELOVL4 deficient mice [256-258, 260, 261]. ELOVL4 depleted mice display wrinkled and scaly skin with reduced epidermal thickness accompanied by impaired SC structure and lamellar body content. Lipid analyses

reveal depletion of ceramides with ω-hydroxy acyl chain ≥C28 in SC and accumulation of ceramides with acyl moiety C26 [256, 257]. These results sustain the important role of ELOVL4 in the synthesis of acyl-CoA esters ≥C28 which are used for production of ceramides with acyl chain ≥C28 in epidermis and the pivotal role of these ceramides in sustaining normal epidermal barrier function.

1.6.2.3 CYP4F22

Next the ULC acyl-CoA esters are ω-hydroxylated (figure 12a). It is believed that a monooxygenase belonging to the cytochrome P450 family; cytochrome P450, family 4, subfamily F, polypeptide 22 (CYP4F22) is responsible for this step. CYP4F22 is highly expressed in keratinocytes [262] and human mutations in *CYP4F22* causes autosomal recessive congenital ichthyosis (ARCI) [263]. Recently Ohno *et al.* have demonstrated that CYP4F22 localize to the outer ER membrane, and that CYP4F22 prefers FA ≥C28 as substrate [264]. The substrate specificity of CYP4F22 indicates that the ω-hydroxylation of the ULC acyl-CoA esters takes place after the elongation process and that the ULC acyl-CoA esters are converted into ULC FA prior to ω-hydroxylation. The CerS3 substrate specificity being ULC acyl-CoA esters, suggests that the ω-hydroxylated ULC FA is converted into ω-hydroxy ULC acyl-CoA esters by ACS before incorporation into ceramides.

CerS3 then catalyzes the acylation of dHSph with ω-hydroxy ULC acyl-CoA to form ω-hydroxy dihydroceramide (dHCer) as discussed in section 1.6.2.1 and DES desaturates ω-hydroxy dHCer to form ω-hydroxy ceramide.

1.6.2.4 DGAT2

The ω-hydroxy ceramide becomes acylated with linoleic acid and glucosylated before packing into lamellar bodies in Golgi. However currently it is not clear in which order the two modifications happen. Here the acylation is discussed first and followed by discussion of the glucosylation process.

Linoleic acid is an essential FA that needs to be taken up from the diet. Dietary lipids are degraded in the intestine, taken up over the intestinal wall and transported to various cell types for many purposes; e.g. synthesis of complex lipids, energy production and storage. The linoleic acid used for ω-esterification is suggested to originate from TAG storages in lipids droplets [265].

The final step in TAG biosynthesis involves the attachment of LC acyl-CoA esters to diacylglycerol and is catalyzed by diacylglycerol acyltransferase (DGAT) 2 (figure 12a). DGAT2 deficient mice display increased TEWL and increased weight loss, possible due to dehydration. DGAT2 depleted mice also show decreased epidermal thickness, impaired lamellar body content and impaired lamellar membranes in SC [266], indicating that the reduced barrier function originates from abnormalities in the lamellar body secretory system. Further investigation of the lipid composition of DGAT2 depleted mice skin reveals a marked decreased of linoleic acid in both TAG and FFA. Additionally, the levels of esterified ω-hydroxy ceramides are significantly decreased, suggesting DGAT2 to be highly involved in the pathway leading to linoleic acid production for incorporation into esterified ω-hydroxy ceramides. Furthermore, transplantation of skin draft from the DGAT2 depleted mice onto athymic nude mice restores TEWL, which indicates that expression of in-body DGAT2 restores the skin phenotype of DGAT2 deficient mice. This also indicates that the linoleic acid used for ω-esterification of ceramides derives from in-body storages [266].

1.6.2.5 PNPLA1/CGI-58

The synthesized TAG which is stored in lipid droplets needs to be hydrolyzed in order to release linoleic acid (figure 12a). Adipose triglyceride lipase (ATGL, also known as PNPLA2) is activated by comparative gene identification-58 (CGI-58, also known as ABHD-5) and catalyzes the hydrolysis of TAG [267]. Interestingly, there is no skin abnormalities reported in patients with mutations in *ATGL* in addition to neutral lipid storage disease. However, patients with mutations in CGI-58 display the hallmarks of lamellar ichthyosis and less frequently of neutral lipid storage disease [268]. These findings indicate a role of CGI-58 in skin lipid metabolism independently of ATGL. In thread with this, growth retardation, postnatal death, systemic TAG accumulation and impaired epidermal barrier development are observed in mice depleted of CGI-58 [269]. However, mice with ATGL deficiency accumulate TAG in multiple tissues but do not develop ichthyosis [270]. In addition, the accumulation of TAG in dermis is similar between ATGL and CGI-58 depleted mice, whereas in epidermis CGI-58 mice accumulate more TAG than the ATGL depleted mice [269]. These findings underline an ATGL independent function of CGI-58 in the maintenance of epidermal integrity. Additionally, protein bound ceramides and esterified ω-hydroxy ceramides are markedly decreased in epidermis from CGI-85 depleted mice. Furthermore, Keratinocyte specific disruption of CGI-58 in mice recapitulates the skin phenotype of full body CGI-58 depletion. Whereas restoring CGI-58 expression in differentiating keratinocytes reverses the skin phenotype [271]. This indicates that CGI-58 expression in suprabasal keratinocytes is essential for epidermal barrier function.

Very recently, Ohno and colleagues identified the long-sought acyltransferase, which is responsible for the esterification of ω-hydroxy ceramides with linoleic acid to produce [EOS] ceramides, to be the patatin-like phospholipase domain-containing protein 1 (PNPLA1) [272]. Interestingly, their findings indicate that PNPLA1 uses TAG as substrate rather that linoleoyl-CoA. Mutations in *PNPLA1* cause autosomal recessive congenital ichthyosis in humans [273]. In addition, mice depleted of PNPLA1 exhibit neonatal lethality due to severe epidermal barrier defects [274, 275]. PNPLA1 is expressed in differentiated keratinocytes and depletion hereof results in absence of epidermal lipids esterified with linoleic acid, including esterified ω-hydroxy ceramides and esterified ω-hydroxy GlcCer, in mice. Concomitantly, their putative precursors, ω-hydroxy ceramides, were increased in level and PNPLA1 depletion results in impairment of the SC lipid envelope and lipid lamellae [274, 275]. Keratinocyte specific depletion of PNPLA1 in mice recapitulates the skin phenotype of full body PNPLA1 depletion [274] and importantly, an identical defect in esterified ω-hydroxy ceramide synthesis was reported in a patient with mutated PNPLA1, which indicates that the function of PNPLA1 is conserved between mammalian species. Taken together, these results indicate that PNPLA1 may be involved in the esterification of ω-hydroxy ceramides using TAG as substrate and that CGI-58 might possibly activate PNPLA1.

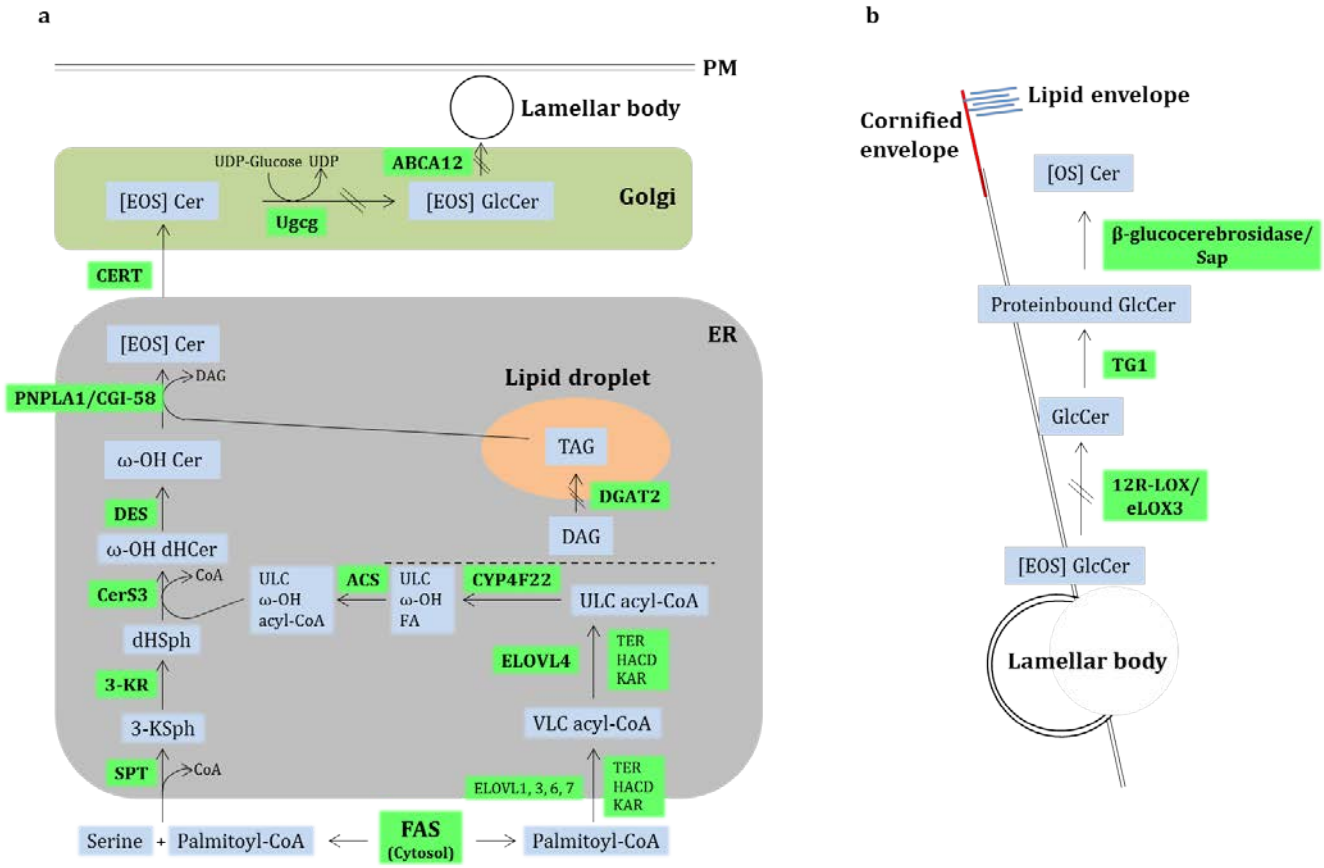

Figure 12: Proposed pathway for synthesis of [EOS] ceramides and covalent attachment of ceramides into the cornified envelope in SC. a) Palmitoyl-CoA is synthesized by FAS. Palmitoyl-CoA are condensed with serine to form 3KSph, catalyzed by SPT. 3-KR catalyzes the reduction of 3KSph to form dHSph. The acylation of dHSph with ULC ω-hydroxy acyl-CoA to form ω-hydroxy dHCer involves CERS3. The ULC ω-hydroxy acyl-CoA is synthesized from palmitoyl-CoA which gets elongated to VLC acyl-CoA in four step cycles involving ELOVL1, 3, 6, 7, KAR, HACD, TER and the further elongation involves ELOVL4, KAR, HACD, TER. The ULC acyl-CoA gets converted into ULC FA (step not shown) and then ω-hydroxy by CYP4F22. ACS converts the ULC ω-hydroxy FA to ULC ω-hydroxy acyl-CoA. Next the ω-hydroxy dHCer are reduced to ω-hydroxy ceramide by DES. PNPLA1 acylates the ω-hydroxy ceramide with linoleic acid originating from the TAG synthesis pathway where DGAT2 are involved in synthesis of the TAG found in lipid droplets. The synthesized [EOS] ceramide are transported to Golgi and are glycosylated by Ugcg before packing into lamellar bodies involving ABCA12. **b)** During terminal differentiation in SC, the lamellar body content and also [EOS] GlcCer are extruded into the intercellular space. The linoleic acid are removed first involving 12R-LOX/eLOX3 generating GlcCer, TG1 attaches the GlcCer to proteins in the cornified envelope and hereafter β-glucocerebrosidase and Sap-C removes the glycosylation and the [OS] Cer are now attached to proteins in the cornified envelope. Abbreviations: Endoplasmic reticulum (ER), fatty acid synthase (FAS), serine palmitoyltransferase (SPT), 3-ketodihydrosphingosine (3-KSph), 3-ketodihydrosphingosine reductase (3-KR), dihydrosphingosine (dHSph), ceramide synthase (CerS), ceramide (cer), elongation-of-very-long-chain-fatty-acid (ELOVL), 3-ketoacyl-CoA reductase (KAR), 3-hydroxyacyl-CoA dehydrase (HACD), trans-2-enoyl-CoA reductase (TER), very-long-chain (VLC), ultra-long-chain (ULC), cytochrome P450, family 4, subfamily F, polypeptide 22 (CYP4F22), fatty acid (FA), fatty acyl-CoA synthetase (ACS), esterified ω-hydroxy ceramide ([EOS] cer), diacylglycerol (DAG), diacylglycerol acyltransferase-2 (DGAT2), triacylglycerol (TAG), patatin-like phospholipase domain-containing protein 1 (PNPLA1), comparative gene identification-58 (CGI-58), long-chain (LC), ceramide transport protein (CERT), UDP-glucose:ceramide glucosyltransferase (Ugcg), glucosyl (Glc), ATP binding cassette transporter 12 (ABCA12), plasma membrane (PM), 12R lipoxygenase (12R-LOX), epidermal lipogenase 3 (eLOX3), transglutaminase 1 (TG1), β-glucocerebrosidase (GBA1), sphingolipid activator protein (Sap) and protein bound ceramide ([OS] cer).

1.6.2.6 [EOS] TRANSPORT

The transport pathway for [EOS] ceramides from ER to Golgi is not elucidated yet. Regularly the major transport pathway from ER to GOLGI is budding and fusion of membrane vesicles but another possible pathway involves CERT (reviewed by [276]).

1.6.2.7 UGCG

The glucosylation of ceramides with acyl chains of up to C26 is suggested to occur at the cytosolic surface of Golgi membranes and to be catalyzed by a membrane bound glucosyltransferase (also called glucosylceramide synthase) (figure 12a) [277, 278]. In support of this assumption, the messenger ribonucleic acid (mRNA) level of glucosylceramide synthase increases 40-fold during terminal differentiation in cultured keratinocytes [279] and the glucosylation of ceramides occur as they pass through Golgi in cultured keratinocytes [280]. Furthermore, GlcCer levels increase and glucosyltransferase activity is induced during differentiation of keratinocytes in culture [281].

The glucosylation of ceramides in epidermis is believed to be catalyzed by UDP-glucose:ceramide glucosyltransferase (Ugcg) since keratinocyte specific deletion of Ugcg in mice, causes pronounced desquamation of the SC. Additionally, the organization of the lamellar body content becomes irregularly arranged and postnatal death at P5 is observed due to extremely increased TEWL. Surprisingly, the [OS] ceramide amount remains unchanged even though the level of GlcCer is significantly decreased and the amount of ω-hydroxy ceramides is significantly increased in Ugcg depleted mice compared with control mice. Moreover, the ω-hydroxy SM content is increased to levels similar to the level of lost GlcCer [282]. To further study the molecular consequences of Ugcg depletion and to investigate the contribution of ω-hydroxy ceramides and [OS] ceramide to the epidermal water permeability barrier, a mouse model with Tamoxifen inducible Ugcg depletion in keratinocytes was generated [283]. This would circumvent the problem of postnatal death. Three weeks after inducing the Ugcg depletion in the skin, a significant decrease in GlcCer and protein bound GlcCer are observed together with an almost complete loss of [OS] ceramides. Furthermore, an increase in ω-hydroxy SM and free extractable ceramides are observed. These mice display increased TEWL and elevated pH, together with hyperproliferation and disordered differentiation in the skin. This leads to a severe ichthyosis-like skin phenotype, with significant delayed wound healing [283]. Taken together, these observations indicate that transient formation of GlcCer is important for the level of protein bound ceramides. Additionally, the inability to carry out glucosylation of the ceramides leads to accumulation of ω-hydroxy ceramides and channeling of ceramides into the synthesis of ω-hydroxy SM.

1.6.2.8 ABCA12

The packing of lipids into lamellar bodies is believed to involve ATP binding cassette transporter 12 (ABCA12) (figure 12a). Importantly, mutations in the human *ABCA12* gene are the cause of Harlequin ichthyosis, a rare autosomal recessive congenital ichthyosis skin disease with profound thickening of the skin [284]. In keeping with this, mice depleted of ABCA12 recapitulate the phenotype of Harlequin ichthyosis with hyperkeratosis. ABCA12 depleted mice display lamellar body abnormalities with no organized lamellar structure and severe increased TEWL. The hyperkeratosis arises due to lack of desquamation rather than increased proliferation. The level of total ceramides is reduced in ABCA12 deficient mice skin, with [EOS] ceramides being the most significantly reduced species. The content of

[EOS] GlcCer are increased, indicating that ABCA12 is important for packing of [EOS] GlcCer into lamellar bodies and that [EOS] ceramides are highly involved in epidermal barrier integrity [285, 286].

1.6.2.9 12R-LOX AND ELOX3

The facilitation and regulation of the secretion of lipid lamellar body content into the intercellular space at the transition zone between SG and SC is mostly unknown. The processing of the [EOS] GlcCer and other lamellar body lipids to yield the highly organized structure of the lipid envelope and lipid lamella rely on several enzymes [287-289], here only the proteins involved in the processing of [EOS] GlcCer to yeld [OS] ceramides will be discussed.

Most likely the linoleic acid of [EOS] GlcCer is stepwise oxidized by 12R lipoxygenase (12R-LOX) and epidermal lipogenase 3 (eLOX3) before attachment to the cornified envelope [290, 291]. Depletion of eLOX3 leads to a similar phenotype as 12R-LOX depletion in mice, and in both cases the TEWL is highly increased and leads to postnatal death. Additionally, the [OS] ceramide level is significantly decreased and the cornified envelope impaired in both mice models [290-293]. This suggests that the 12R-LOX/eLOX-3 pathway plays a key role in the processing of [EOS] GlcCer to [OS] ceramide. These findings are further supported by findings in humans where depletion of 12R-LOX/eLOX-3 leads to diminished protein bound ceramides in the skin and development of autosomal recessive congenital ichthyosis (ARCI) [294].

The ceramides are believed to be covalently linked to proteins of the cornified envelope prior to de-glucosylation [245, 295, 296], possibly by the action of transglutaminase 1 (TG1) [297].

1.6.2.10 GBA1

The hydrolysis of GlcCer is important for epidermal barrier integrity and involves both β-glucocerebrosidase (GBA1) and sphingolipid activator protein (Sap) (figure 12b) [296, 298-301]. Mice deficient of GBA1 display a phenotype similar to patients with Gaucher disease including impaired glycosphingolipid metabolism, increased TEWL and early death [296, 298, 302-304]. Additionally, protein bound GlcCer accumulates in mice deficient of GBA1 [296], which confirm the assumption that GlcCer are covalently linked to the cornified envelope prior to de-glucosylation. Accumulation of epidermal GlcCer accompanied by decreased [OS] ceramide levels is observed in mice deficient of pSap [300, 301]. Taken together both GBA1 and Sap are required for processing of GlcCer into [OS] ceramide and important for normal epidermal barrier function.

1.6.3 SUMMARY OF EPIDERMAL LIPIDS

The epidermal lipid matrix consists of 60% ceramides, 20% cholesterol and 20% FFA. Especially the ceramides play a pivotal role in epidermal barrier integrity and in human epidermis 12 ceramide subclasses exists including [EOS], [NS], [AS], [EOP], [NP], [AP], [EOH], [NH], [AH], [EODS], [NDS], and [ADS]. Additionally, the esterified ω-hydroxy ceramides can be covalently linked to cornified envelope proteins and are designated [OS], [OH] and [OP] ceramides. The synthesis of [EOS] and [OS] ceramides are not fully elucidated yet, but these ceramides are highly involved in epidermal barrier formation in SC. Depletion of several enzymes involved in stratum corneum ceramide synthesis affects the synthesis of [EOS] and [OS] ceramides. ELOVL1 and ELOVL4 are important for the elongation of acyl-CoA esters to yield ULC acyl-CoA esters and CYP4F22 is suggested to be involved in the ω-hydroxylation of ULC FA. DGAT2 is important for TAG synthesis and CGI-58 may activate an unidentified lipase involved in TAG hydrolysis. Especially CerS3 is important for ULC ω-hydroxy ceramide synthesis and PLPN1 is involved in the further acylation with

linoleic acid whereas Ugcg is involved in glucolysation of the [EOS] ceramides. ABCA12 is involved in the packing of [EOS] glucosylated ceramides into lamellar bodies. The processing of [EOS] glucosylated ceramides to [OS] ceramides possibly involves 12R-LOX, eLOX3, GBA1 and Sap.

1.7 SEBACEOUS GLANDS

Sebaceous glands are sebum-secreting glands consisting primarily sebocytes. Free sebaceous glands secrete their content directly onto the surface (e.g. Meibomian glands (eyelid), Tyson's glands (genitals), Fordyce's glands (oral), Montgomery glands (nipples), and Tyson's glands (ears)). However, sebaceous glands associated with the hair follicle, secrete their content into the hair follicle unit at the junctional zone and eventually the sebum reaches the skin surface. Sebaceous glands associated with the hair follicle, are the type of sebaceous glands referred to throughout this thesis.

The exact function of sebaceous glands remains to be determined, although a variety of theories regarding their function exists. Sebaceous glands are proposed to be involved in water resistance [305], UV radiation response [306], thermoregulation and anti-inflammatory function [307, 308], and pheromone transport.

Sebaceous glands are found throughout the human body except on the foot soles and on the palms of the hand. Sebaceous glands consist of highly specialized sebocytes which display different activity in the different zones of the gland (figure 13). The peripheral zone (PZ) consists of small mitotically active cells that continuously proliferate and are in contact with the basal lamina of the hair follicle via hemi-desmosomes. When the cells leave the PZ, they differentiate as they move through the maturation zone (MZ). As the cells differentiate, they increase in size and progressively accumulate lipids. When the sebocytes reach the necrosis zone (NZ), they disintegrate and release their content (sebum), via holocrine secretion into the junctional zone of the hair follicle [309].

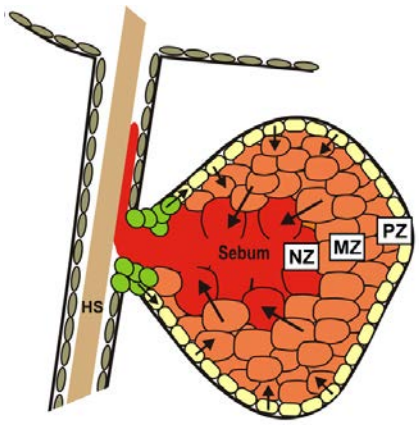

Figure 13: Sebaceous gland. Sebaceous glands are divided into three different zones; the peripheral zone (PZ), the maturation zone (MZ) and the necrosis zone (NZ). The sebocytes in the sebaceous glands originate from proliferating cells in the PZ, when reaching the MZ the sebocytes initiate differentiation accompanied by lipid accumulation. When the sebocytes reach the NZ, their content is released into the hair follicle by holocrine secretion. Figure adapted from [310].

1.7.1 SEBACEOUS GLAND FORMATION AND HOMEOSTASIS

Formation of sebaceous glands is initiated in the last stages of hair follicle morphogenesis. Sebaceous gland formation and homeostasis involves a number of signaling pathways and transcriptional regulations also involved in hair follicle homeostasis such as Wnt/β-catenin, hedgehog, Ras, Insulin growth factor (IGF), c-myc, PPARγ and B lymphocyte-induced maturation protein-1 (Blimp1) (reviewed by [311-313]). A selection of the involved pathways will be discussed in section 1.7.2 and a selection of the involved transcription factors will be discussed in section 1.7.3.

The majority of knowledge regarding sebaceous gland formation, homeostasis and lipid accumulation originates from genetically modified mice (reviewed by [314]).

Although the information is sparse, resent work has begun to reveal more information regarding sebaceous gland development. Recently stem cell compartments expressing the Sox9 transcription factor and leucine-rich repeats and immunoglobulin-like domains protein 1 (Lrig1) during hair follicle morphogenesis were linked to sebaceous gland formation. Sox9 and Lrig1 are initially co-expressed during early hair follicle morphogenesis. When the sebaceous glands are formed Lrig1 cells separate from Sox9 cells and Lrig1 positive cells remain at the upper part of the hair follicle, whereas Sox9 positive cells confines to the hair follicle bulge region. Both Sox9 and Lrig1 expressing cells are suggested to be important for sebocyte formation and in keeping with this Sox9 depleted mice fail to develop sebaceous glands [315-317]. Altogether, these findings suggest that both Sox9 and Lrig1 positive progenitor cells are capable of differentiating into sebocytes.

Sebaceous glans homeostasis relies on continuous proliferation of the sebocytes in the PZ combined with differentiation and lipid accumulation of the sebocytes in the MZ. Proteins involved in the sebocyte lipid accumulation will be discussed in further detail in section 1.7.4.

1.7.2 PATHWAYS INVOLVED IN SEBACEOUS GLAND FORMATION AND HOMEOSTASIS

Sebaceous gland formation and homeostasis involves numerous pathways and a selection of these will be discussed in the following.

1.7.2.1 WNT/β-CATENIN

As described in 1.5.3.1, Wnt/β-catenin signaling is important for hair follicle morphogenesis and cycling. In contrast, blocking of the downstream mediators of Wnt/β-catenin signaling TCF/Lef1 is essential for the commitment of hair follicle stem cells and progenitor cells to sebaceous gland lineage differentiation. This is demonstrated in mice expressing a dominant-negative Lef1, which develop sebaceous glands at the expense of hair follicles [318]. Furthermore, blocking of TCF/Lef1 in mice hair follicle bulge stem cells, results in development of ectopic sebaceous glands originating from the bulge cells [319]. Additionally, expression of TCF3 in mice epidermis results in suppression of transcriptional regulators and absence of sebaceous gland formation [320]. However, overexpression of Smad7, which causes degradation of β-catenin, leads to sebaceous gland hyperplasia [321]. All together these findings suggest that Wnt signaling inhibits differentiation towards sebocytes, since blocking of Wnt signaling promotes sebocyte development.

1.7.2.2 HEDGEHOG

Sebocyte formation is suppressed upon inhibition of hedgehog signaling, whereas activation of hedgehog increases both size and number of sebaceous glands [322]. Interestingly, overexpression of Lef1 in human

sebocytes induces expression of hedgehog and results in increased differentiation and proliferation *in vitro* [323]. Taken together, this suggests that hedgehog signaling induces sebocyte differentiation and differentiation.

1.7.2.3 RAS

In addition to hedgehog signaling, Ras signaling also promotes sebaceous gland formation. This is demonstrated by expression of an oncogenic constitutively active KRas mutant in bulge stem cells, which causes increased proliferation and enlargement of sebaceous glands [324], suggesting that small guanosine triphosphate (GTP)ases may play an important role in sebaceous gland homeostasis.

1.7.2.4 IGF

IGF plays a role in regulation of lipid production in sebaceous glands. When treating the immortalized sebocyte cell line SEB-1 with insulin in high doze and IGF-1 in a physiological doze, the sebocyte lipid synthesis increases together with levels of mature SREBP-1 [325]. Inhibition of the mitogen-activated protein kinase (MAPK) pathway in IGF-1 treated sebocytes has no effect on lipid synthesis or SREBP-1 expression, whereas inhibition of the PI3K pathway decreases lipid production and SREBP-1 expression [326]. This suggests that SREBP-1 is likely to be involved in transcription of lipid synthesizing genes in sebocytes through IGF activation of the PI3K pathway.

1.7.3 TRANSCRIPTONAL REGULATION OF SEBACEOUS GLAND FORMATION AND HOMEOSTASIS

Sebaceous gland homeostasis is also regulated on the transcriptional level and a selection of these will be discussed in the following.

1.7.3.1 ANDROGEN NUCLEAR RECEPTORS

Androgen nuclear receptors are well known regulators of sebaceous gland development. Hormonal regulation of sebaceous glands is evident during puberty, where sebum production is increased. Castrated men, unable to produce testosterone, exhibit impaired sebum production [327]. Sebocytes express androgen receptors, which indicate that androgens act directly on sebocytes [328, 329]. In addition testosterone induces proliferation and sebum production, whereas estrogens and anti-androgenic steroids blocks proliferation and sebum production [330-332].

1.7.3.2 BLIMP1

The transcription factor Blimp1 is expressed in cells residing adjacent to the sebaceous gland in the upper hair follicle. Genetic lineage tracing experiments in mice show, that the Blimp1 positive cells are progenitor cells for proliferative and differentiating cells in sebaceous glands. Additionally, Blimp1 depletion in mice epidermis results in increased proliferation of the sebaceous glands, resulting in increased cell number. Furthermore, Blimp1 depletion causes increased sebum production and oily skin upon ageing [333]. These observations are highly indicative of that Blimp1 regulates sebocyte proliferation and sebum production *in vivo*.

1.7.3.3 C-MYC

The transcription factor c-myc is an essential player in sebaceous gland development. Mice overexpressing c-myc in SB develop enlarged and more numerous sebaceous glands at the expense of hair follicles [334].

Furthermore, keratinocyte specific depletion of c-myc in mice impairs sebaceous gland development [335]. These findings indicate that c-myc promotes sebaceous gland development *in vivo*.

1.7.3.4 PPARγ

The transcription factor PPARγ, which also contributes to regulation of ACBP expression (1.2.1), is expressed in rat preputial sebocytes [336] and in human sebocytes [337, 338]. As PPARγ knock out mice are not viable, *in vivo* evidence for PPARγ function in sebaceous gland sebum production are inadequate. Interestingly treatment with PPARγ ligands increases sebocyte, but not keratinocyte differentiation in rat preputial cells [339] and increases sebum production in humans [340]. Surprisingly, K14-Cre transgenic mice with epidermal PPARγ knock out display a skin/fur phenotype similar to WT littermates [341]. In contrast K15-Cre targeted depletion of PPARγ in K15 positive bulge stem cells results in scarring alopecia and sebaceous gland atrophy [342]. Taken together, these results suggest a role for PPARγ in bulge stem cells required for sebaceous gland homeostasis.

1.7.4 SEBACEOUS GLAND LIPID PRODUCTION

The main function of the mammalian sebaceous gland is to produce lipids for subsequently secretion into the hair follicle. The secreted sebum varies among species, possibly due to different needs adapting varying environmental habitats. Human sebum is highly complex and consists of 30-50% TAG/diacylglycerol (DAG), 15-30% FFA, 26-30% wax esters, 12-20% squalene, 3-6% CE and 1.5-2.5% cholesterol [311, 343, 344]. Some of the lipids produced in sebaceous glands are unique and are only found in traceable amounts in other tissues; e.g. sapienic acid, wax esters, squalene and some VLC branched or hydroxylated FA.

The lipid droplet proteome is well characterized in many cell lines; however investigations in sebocyte cell lines remain sparse. Recently, the lipid droplet proteome was investigated in SZ95 sebocytes and 54 proteins are significantly enriched in the lipid droplet fraction. The majority of the identified proteins are well-known lipid droplet proteins such as perilipin, long-chain ACS and squalene monooxygenase; in addition, six novel lipid droplet proteins are identified [345].

The human sebum TAG is suggested to be partly hydrolyzed into FFA and glycerol before reaching the skin surface [346-348]. It is still controversial whether the same mechanism for TAG hydrolysis exists in other animals. However there are identified a number of unique FFA in human sebum; e.g. sapienic acid (C16:1, Δ6) and lauric acid (C12:0) [349, 350]. Sapienic acid and lauric acid may be involved in protection against bacteria [350, 351]. Sapienic acid is the most abundant FA in human sebum and is not present in sebum from other hair-bearing animals. There are identified a FA desaturase-2 (FADS2) with restricted expression in the human skin to differentiating sebocytes. FADS2 is a Δ6 desaturase which primarily desaturates linoleate but also capable of converting palmitate into sapienate [352].

Wax esters synthesis are suggested to be correlated with sebaceous gland differentiation, as impairment of wax ester biosynthesis correlates with sebaceous gland atrophy in animal models [353, 354]. Although wax ester biosynthesis is still unexplored in humans, there are identified two fatty acid reductase (FAR) enzymes capable of reducing FA to fatty alcohols needed for wax synthesis. One of the identified FAR, FAR1, localize to sebaceous glands and prefers saturated and unsaturated C16 and C18 FA [355]. Additionally, a mammalian wax synthase, suggested to be involved in the synthesis of wax monoesters from FA and fatty alcohol, are isolated and found abundant expressed in tissues rich in sebaceous glands [356]. Furthermore, *in vitro* experiments suggests that DGAT1, which catalyzes the final step of

triacylglycerol biosynthesis, may exhibit acyl-CoA:monoacylglycerol acyltransferase, acyl-CoA:fatty acyl alcohol acyltransferase (wax synthase) and acyl-CoA:retinol acyltransferase activities and thereby is capable of synthesizing diacylglycerols, wax esters, and retinyl esters, respectively [357]. Additionally, a human multifunctional O-acyltransferase (MFAT) are characterized, which belongs to the acyl-CoA:diacylglycerol acyltransferase 2/acyl-CoA:monoacylglycerol acyltransferase gene family. MFAT are highly expressed in human skin and exhibit acyl-CoA:fatty acyl alcohol acyltransferase and acyl-CoA:retinol acyltransferase activity capable of synthesizing diacylglycerols, wax monoesters, and retinyl esters, respectively [358]. These observations emphasize the complexity of sebaceous gland lipid synthesis, although the sebaceous gland wax ester biosynthesis remains elusive.

Squalene is synthesized from acetyl-CoA and acetoacetyl-CoA; both HMG-CoA synthase, HMG-CoA reductase and squalene synthase are involved in the synthesis of squalene. Squalene can be further processed to lanosterol and cholesterol which involves squalene expoidase enzyme among others (reviewed by [359]). The whole pathway are designated the mevalonate pathway and the transcription of the involved enzymes are highly regulated by SREBP2 (reviewed by [359, 360]). Cholesterol can be further processed to cholesterol ester (CE) and involves ACAT. Squalene accumulates in sebum and it is still puzzling why squalene is not processed to cholesterol in quantities as observed in other tissues.

The exact composition of mouse sebum still needs to be elucidated and may vary among strains. Several lipid species are identified in C57BL6 mice including CE, wax monoester, wax diester, TAG, and cholesterol [97, 353]. Furthermore, different MADAG species are identified on the skin surface of hairless mice, especially MADAG with eicosenoic acid (C20:1) acyl moiety are enriched [361].

A number of enzymes important for lipid synthesis in sebaceous glands are identified in experiments using transgene mice models and a selection of these will be discussed in the following.

1.7.4.1 FATP4

Targeted disruption of fatty acid transport protein (FATP) 4 in mice causes thickening of epidermis and disrupted epidermal barrier, which leads to neonatal death and impairments of the PSU including sebaceous glands [362, 363]. When sebaceous glands from FATP4 knock out mice are grafted onto nude mice, they exhibit abnormal development and the sebum composition display reduced levels of wax diester [362]. All together this indicates a pivotal function of FATP4 in sebaceous gland lipid transport, lipid synthesis and development. Additionally, depletion of FABP5 results in impairment of sebaceous glands and sebum alterations [364]. Thus further underlines the importance of FA metabolism in sebaceous gland function.

1.7.4.2 ACBP

The *nm1054* mouse strain with spontaneous deletion of a 400 kb region on chromosome 1 including the *Acbp* sequence, display sebocyte hyperplasia, accompanied by greasy and tousled fur, as well as alopecia [55]. A similar skin/fur phenotype is reported in mice with targeted disruption of the *Acbp* gene [16] although no sebocyte hyperplasia is reported in this model. In both studies expression of ACBP in the sebaceous glands are detected in WT control animals. Both groups analyzed the fur lipids and found the amount of TAG to be decreased on the fur [16, 55]. Additionally, the MADAG content on the fur, in stratum corneum and in epidermis is elevated in ACBP depleted mice compared WT type mice [16]. Furthermore, the levels of VLCFA are decreased in stratum corneum and C20:1 FA increased in epidermis of ACBP

deficient mice [16]. These results strongly suggest, that ACBP is involved in the sebocyte lipid synthesis, especially in TAG synthesis, although the epidermal/stratum corneum and sebocyte contribution to the fur lipids are difficult to distinguish.

1.7.4.3 ELOVL3

The fatty acid elongase ELOVL3 is expressed in mice sebaceous glands and hair follicle epithelia cells. Mice depleted of ELOVL3 have tousled fur and alopecia [365]. With age ELOVL3 depleted mice develop an irritated and eczematous skin phenotype. Disruption of ELOVL3 causes sebaceous gland hyperplasia with abnormal sebocyte lipid production. The fur lipids contain reduced amount of TAG and increased amounts of wax and sterol esters compared with that of control mice. In agreement with ELOVL3 involvement in synthesis of saturated and mono-unsaturated FA up to C24, the amount of C22-C24 FA is decreased in TAG and the level of C20:1 FA highly accumulates in both total FA and in TAG fur lipids. Additionally, ELOVL3 depleted mice display a defective water barrier [365]. Together, these data underlines the importance of FA elongation, and correct sebum lipid composition to maintain the epidermal barrier integrity.

1.7.4.4 SCD1

Stearoyl-CoA desaturase (SCD) enzymes (Δ9-desaturases) mediate the desaturation of FA, which is essential for the use of FA in sebaceous gland lipid synthesis. Several SCD isoforms are expressed in murine skin, but mainly SCD1 and SCD3 are expressed in sebaceous glands [354, 366-368]. A mutation in the *SCD1* gene results in sebocyte atrophy and alopecia in asebia mice [369]. Moreover, mice with target SCD1 depletion display a similar sebocyte phenotype, and in addition SCD1 deficient mice are resistant to diet induced obesity and insulin resistance [354, 370-374]. Interestingly, mice with keratinocyte specific deletion of SCD1 recapitulate the phenotype seen in mice with global SCD1 depletion. These mice have increased metabolic rate due to inability to maintain core body temperature caused by impaired barrier function [367]. The impaired epidermal barrier function is linked to depletion of the sebum lipids TAG and wax diester on the skin surface [367]. These results emphasize the important role of SCD1 in epidermal barrier integrity and in sebaceous gland lipid synthesis and that TAG and wax diesters are important for epidermal barrier integrity.

1.7.4.5 DGAT

DGAT catalyzes the final step in TAG synthesis. There exist two DGAT enzymes in humans, DGAT1 and DGAT2, which has differential sequences and localization [375]. Mice depleted of DGAT1 display sebaceous gland atrophy, dry fur and alopecia, which is associated with decreased level of wax diester in sebum [353]. Consistently, DGAT1 is suggested to be involved in wax ester synthesis [357]. Taken together, this suggests that TAG synthesis is important for sebaceous gland function and homeostasis, and sustains that DGAT1 is involved in wax ester synthesis.

1.7.4.6 FA2H

Fatty acid 2-hydrolase (FA2H) is highly expressed in human skin where it is required for the synthesis of sphingolipids containing 2-hydroxylated FA which are abundant in mammalian skin [376]. Sebaceous gland hyperproliferation during hair follicle morphogenesis and anagen hair follicle cycling are observed in mice deficient of FA2H [377]. Mice depleted of FA2H however, show no significant changes in sphingolipids containing hydroxylated FA. In mice expression of FA2H is restricted to sebaceous glands, where it is used

for synthesis of 2-hydroxylated glucosylceramide and wax diester. The observed enlargement of sebaceous glands in FA2H depleted mice is accompanied by a decrease in the amount of wax diesters and an increase in wax monoester, cholesterol and FFA, and cycling alopecia in telogen. Additionally, the EGFR ligand epigen is significantly upregulated in sebocytes [377]. Taken together, these results suggest a role for FA2H in sebaceous gland function which is linked to hair follicle cycling.

Overexpression of another EGFR ligand, amphiregulin, in mouse skin also causes enlarged sebaceous glands due to hyperproliferation [378]. Additionally, transgenic mice overexpressing epigen in keratinocytes, display enlarged sebaceous glands [379]. All together this strongly indicates a role for EGFR in proper regulation of sebaceous gland proliferation and size. This is further supported by the notion that mutant mice with a constitutive active EGFR receptor also display enlarged sebaceous glands [380].

1.7.4.7 CERS4

The role of CerS4 in the epidermis has been investigated by depletion of the protein in mice. CerS4 is expressed in differentiating keratinocytes and in the PSU, especially in sebaceous glands. CerS4 depletion causes enlargement of the sebaceous glands, increased sebum production, dilation of the infundibulum width and hair loss [381, 382]. Further analysis of the sebum composition reveals a decrease in wax diester and an increase in wax monoester in CerS4 depleted mice compared with controls. Concomitant with the finding that the major diol in mice sebum wax diester is C20 1,2-alkane diol, decreased levels of C20 1,2-alkane diol in sebum from CerS4 depleted mice are observed [381]. In line with the acyl-CoA affinity of CerS4 being C18-C22 [94], disruption of CerS4 results in decreased levels of C20 sphingolipids [381]. CerS4 depletion is suggested to alter the Lrig1 positive stem cell population in the hair follicle junctional zone, as CerS4 depletion causes the Lrig1 positive stem cell population to spread towards the sebaceous glands [382]. This leads to altered hair follicle cycling and possibly exhausts the hair follicle, which contributes to the hair loss [382]. These results indicate that CerS4 is important for PSU homeostasis, and in particular are important for sebaceous gland homeostasis.

1.7.4.8 APOC1

Transgenic mice depleted of apolipoprotein C1 (apoC1) display no obvious skin/fur phenotype [383]. However overexpression of human apoC1 in transgene mice results in thickened, dry and scaly skin, which is accompanied by sebaceous gland atrophy and alopecia. The sebum produced in mice overexpressing apoC1 display reduced TAG and wax diester levels [384], thus suggesting a role for ApoC1 in sebaceous gland lipid production, hair follicle homeostasis and possibly also in epidermal lipid production.

1.7.5 SUMMARY OF SEACEOUS GLANDS

Sebaceous glands are lipid producing glands, which are associated with the hair follicle. Cells in the peripheral zone (PZ) proliferate and as the sebocytes move through the maturation zone (MZ) they differentiate and accumulate lipids. These lipids are released by holocrine secretion in the necrosis zone (NZ) and extruded into the junctional zone of the hair follicle. Several signaling pathways and transcriptional regulations are involved in sebaceous gland formation and homeostasis including Wnt/β-catenin, hedgehog, Ras, IGF, c-myc, PPARγ and Blimp1. The main function of sebaceous glands is lipid production and a number of known proteins involved in lipid biosynthesis are important for sebaceous gland synthesis. Depletion of ACBP, ELOVL3, FA2H and CERS4 causes enlargement of the sebaceous glands accompanied by increased lipid production, whereas depletion of FATP4, SCD1 and DGAT results in

sebaceous gland atrophy. Additionally, overexpression of apoC1 causes sebaceous gland atrophy. These results highlights the importance of proteins involved in sebaceous gland lipid production, although the exact mechanisms leading to either sebaceous gland atrophy or enlargement needs to be elucidated further to fully understand their impact on sebaceous gland homeostasis.

2 RESULTS AND DISCUSSION

The manuscripts presented in Supplement 1 and Supplement 2 [385] represents the majority of the work performed during this PhD. Supplement 1 describes our investigations of the molecular and cellular mechanisms governing the alterations in the skin of ACBP depleted mice and Supplement 2 describes our functional analysis of ACBP involvement in ceramide synthesis.

2.1 SUPPLEMENT 1

Supplement 1 describes our investigation of the consequences of ACBP depletion on epidermal proliferation, differentiation, hair cycling, and sebaceous gland homeostasis. We have previously reported that the ACBP$^{-/-}$ pups are born in a normal Mendelian ratio and that they are fully viable and fertile [57]. Around 16 days of age the skin/fur phenotype becomes evident, as the fur of the pups looks greasy and tousled. This macroscopic phenotype is sustained throughout life, although the greasy appearance becomes less pronounced with age. As the mice become older, there is a shift in the fur color from black to brown/reddish and the mice develop alopecia and scaling of the skin [16].

2.1.1 DISRUPTION OF ACBP IMPAIRES DEVELOPMENT OF THE EPIDERMAL BARRIER

We have previously applied transepidermal water loss (TEWL) measurements to investigate the impaired epidermal barrier function in ACBP$^{-/-}$ and K14-ACBP$^{-/-}$ mice [16, 58]. TEWL measurements are used to evaluate the inside-out barrier, as it states the loss of body fluids through the skin. Additionally, TEWL correlates with the integrity of the epidermal barrier [386]. We wanted to further elucidate whether development of the epidermal barrier is delayed in ACBP$^{-/-}$ mice. Therefore, we performed an embryonic staining assay where the outside-in barrier is investigated by use of 5-bromo-4-chloro-3-indolyl-b, D-galactopyranoside (X-gal) [131]. Interestingly, we found that at E17.5 the barrier was not fully developed in ACBP$^{-/-}$ embryos compared with that of ACBP$^{+/+}$. However, at E18.5 both ACBP$^{-/-}$ and ACBP$^{+/+}$ embryos were resistant to X-gal staining, indicating that the barrier was fully developed (figure 16). These results indicate that the development of the epidermal barrier is delayed in ACBP$^{-/-}$ embryos. Whether the delayed development of the epidermal barrier in ACBP$^{-/-}$ embryos reflects the impaired barrier observed in ACBP$^{-/-}$ mice after birth remains unclear.

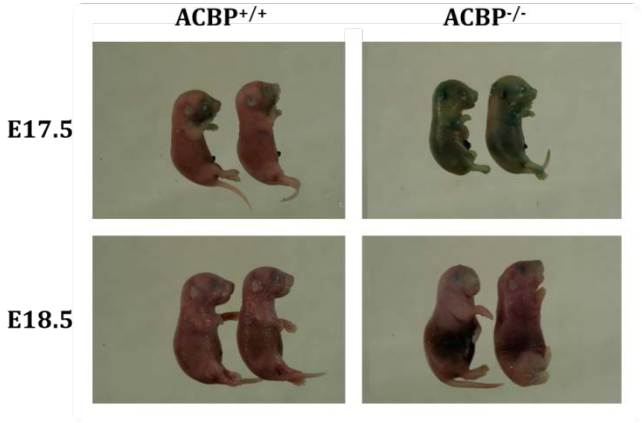

Figure 16: The development of the epidermal barrier is delayed in ACBP$^{-/-}$ embryos. ACBP$^{+/+}$ and ACBP$^{-/-}$ embryos at embryo (E) age 17.5 and E18.5 were stained with X-gal as described in [131], followed by incubation overnight a 37°C.

2.1.2 ACBP DEPLETION ALTERS MOUCE SKIN MORPHOLOGI

Since ACBP depleted mice are known to show alopecia during ageing [16], and alopecia has been associated with alterations in hair follicle cycling [382], this prompted us to investigate the hair follicle cycling in ACBP$^{-/-}$ and K14-ACBP$^{-/-}$ mice. We found that ACBP depletion leads to induced anagen-like state of the hair follicles in both ACBP$^{-/-}$ and K14-ACBP$^{-/-}$ mice at P58, and that this persists at P85 compared with that of WT control mice (Supplement 1, figure 1). Additionally, alopecia is thought to be linked to alterations in the sebaceous gland morphology as transgenic mice depleted of ELOVL3, CerS4 or FA2H all display alopecia concomitantly with enlarged sebaceous glands [365, 377, 381]. Furthermore, mice depleted of SCD1 or DGAT1 display alopecia, although the sebaceous glands are atrophic [353, 354]. These findings prompted us to investigate the sebaceous gland morphology in ACBP depleted mice. Interestingly, we found the sebaceous glands to be 2-fold increased in size in both ACBP$^{-/-}$ and K14-ACBP$^{-/-}$ mice compared with that of WT control mice at all ages investigated (Supplement 1, figure 1). This observation is consistent with findings in mice with a spontaneous deletion of 400 kb on chromosome 1 (*nm1054*) that includes the *Acbp* gene [55, 56], which also display sebaceous gland hypertrophy. Furthermore, we noticed clotting of sebum in the infundibulum of the hair follicles at P15 and P21 in ACBP$^{-/-}$ and K14-ACBP$^{-/-}$ mice (Supplement 1, figure 1). Sebum clotting in the infundibulum of the hair follicle is also reported in CerS4 depleted mice and is suggested to be causal for the alopecia in these mice [381]. Furthermore, in keeping with our observations from ACBP depleted mice, an anagen-like state of the hair follicle is also reported in the CerS4 depleted mice [382]. The anagen-like state in the hair follicles of the CerS4 depleted mice is suggested to exhaust the hair follicle stem cells and to thereby be involved in the alopecia. Whether the alopecia in the ACBP depleted mice is caused by exhaustion of the hair follicle stem cells due to the induced anagen-like state and/or caused by the sebum clotting in the infundibulum of the hair follicles remains elusive.

In the epidermis the lamellar bodies reside and to obtain a better knowledge of the structure and abundance of the lamellar bodies upon ACBP depletion we investigated this by use of transmission electron microscopy (TEM). Based on this we saw indications that there might be a decreased number of lamellar bodies in ACBP$^{-/-}$ epidermis compared with that of ACBP$^{+/+}$ mice (figure 14a and 14c). However, we observed no visual differences in the lipid organization inside the lamellar bodies upon ACBP depletion (figure 14b). These findings need to be elucidated further, although they suggest that ACBP depletion might affects the lamellar body abundance.

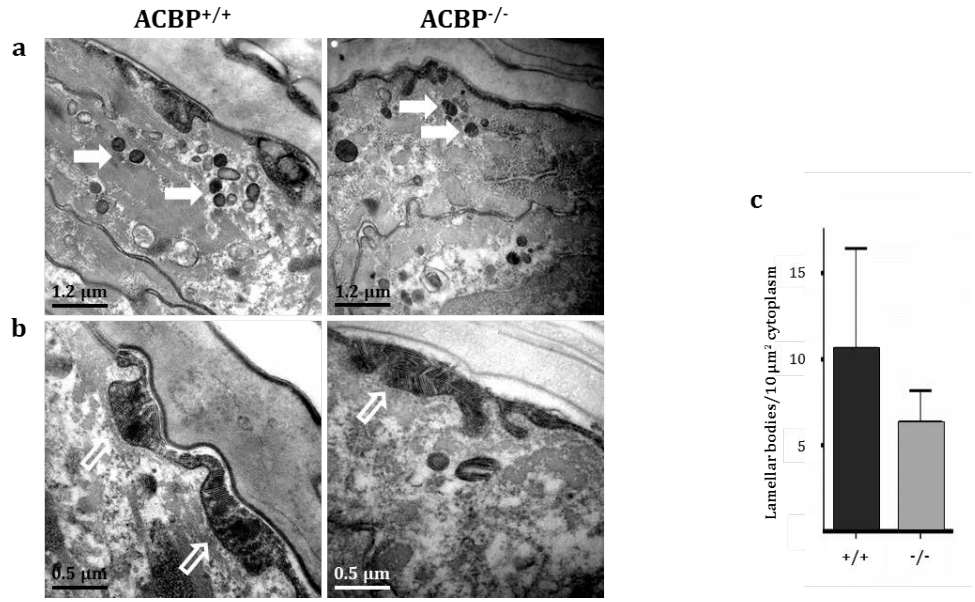

Figure 14: ACBP depletion affects the abundance of lamellar bodies. Adult ACBP$^{+/+}$ and ACBP$^{-/-}$ mice were anesthetized with 0.2 mL/10 g body weight (1:1:2 v/v/v Hypnorm/Dormicum/sterile H_2O) and perfused with 4% paraformaldehyde in 0.1 M phosphate buffer (pH 7.4). Skin biopsies were fixed for 12-15h in 4% paraformaldehyde in 0.1 M phosphate buffer (pH 7.4) at 4°C. Further processing and TEM was performed by Professor Saverio Cinti Blaise and colleagues, Director of obesity center, Università Politecnica delle Marche, Department of Clinical and Experimental Medicine, Ancona, Italy. **a)** and **b)** display different magnifications of ACBP$^{-/-}$ and ACBP$^{+/+}$ mice skin. White bold arrows indicate lamellar bodies and open white arrows indicate the lipid organization inside the lamellar bodies at the extrusion site between SG and SC. The pictures are representative of 3 individuals from each genotype **c)** Quantification of the number of lamellar bodies/10 µm^2 cytoplasm in ACBP$^{-/-}$ (-/-) and ACBP$^{+/+}$ (+/+) mice epidermis. Mean±SE. n=3/genotype.

2.1.3 ACBP DEPLETION INDUCES THE EPIDERMAL PROLIFERATION AND DIFFERENTIATION

Impaired epidermal barrier integrity is often accompanied by alterations in the epidermal differentiation and/or proliferation status as exemplified in mice depleted of CerS3 [250], Ugcg [283] or ELOVL4 [257]. This led us to investigate the epidermal proliferation and differentiation in ACBP depleted mice.

First we investigated the epidermal differentiation status of ACBP depleted mice by measuring the IFE thickness. We found the IFE thickness to be slightly increased at P47 and P58 in ACBP$^{-/-}$ mice and at P85 in K14-ACBP$^{-/-}$ mice compared with WT control mice (Supplement 1, figure 2a and 2b). The observed elevated IFE thickness is marginal and not consistent between the two different genotypes. This led us to further investigate the differentiation status by determining the mRNA expression level of various differentiation markers by real time polymerase chain reaction (RT-PCR). We analyzed the mRNA levels of *K10*, *loricrin*, *involucrin* and *profilaggrin* as they are frequently used as markers of epidermal differentiation. *K10* expression is initiated in differentiating keratinocytes [136], and *loricrin*, *involucrin* and *filaggrin* are all part of the epidermal differentiation complex [137, 143]. Interestingly, these data revealed that mRNA expression of *K10*, *loricrin*, *involucrin* and *profilaggrin* were not significant altered upon ACBP depletion (Supplement 1, figure 2c). Taken together, these results suggest that ACBP depletion leads to slightly elevated epidermal differentiation.

Filaggrin is synthesized from a large precursor protein, profilaggrin, which is 500 kDa in size in mice [166]. Profilaggrin is packed into keratohyalin granules and in SC profilaggrin becomes cleaved into single filaggrin filaments which are 28-34 kDa in size. In SC filaggrin filaments interacts with keratin intermediate filaments [140]. The processing of profilaggrin into filaggrin is highly associated with epidermal differentiation as discussed in section 1.4.3 and 1.4.5. The flaky tail mice display loss of profilaggrin and filaggrin content in epidermis leading to pronounced scaling on the skin [173]. These findings led us to further investigate the differentiation status in ACBP$^{-/-}$ mice by analyzing the processing of profilaggrin into filaggrin by use of Western blotting. We found a similar distribution pattern of the different filaggrin proteins between ACBP$^{-/-}$ and ACBP$^{+/+}$ mice. However, the level of all the filaggrin proteins were increased in amount ACBP$^{-/-}$ mice (figure 15a). These findings suggest that ACBP depletion in mice increases the level of filaggrin and that the epidermal differentiation is increased, although the mRNA level of *profilaggrin* were not significant elevated upon ACBP depletion.

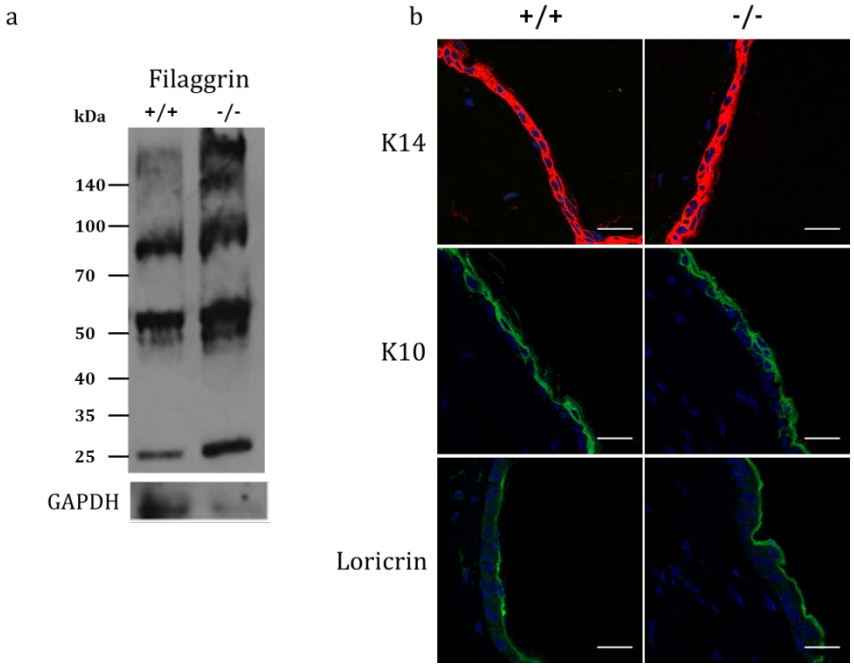

Figure 15: Increased level of epidermal filaggrin upon ACBP depletion. **a)** ACBP$^{+/+}$ (+/+) and ACBP$^{-/-}$ (-/-) epidermal splits from 5 + 5 mice at P85 were homogenized in 750 µL 8M Urea, the protein concentration were determined in the supernatant and equal amounts of proteins were pooled, followed by loading of equal amounts of protein onto a 4-12% Tris glycine gel. The proteins were separated using SDS running buffer followed by blotting onto a PVDF membrane and incubation with antibodies (anti-filaggrin (90581, Biolegend) and anti-rabbit HRP-conjugate (W402B, Promega)). The proteins were visualized using enhanced chemiluminescent. For loading control we used anti-GAPDH (sc-25778, Santa Cruz) and anti-rabbit HRP-conjugate (W402B, Promega). **b)** Mice at P85 were injected with BrdU 30 min. prior to scarification, the upper back skin were isolated, fixed with 4% PFA in PBS followed by paraffin embedding. Paraffin sections were de-paraffinized and incubated with following antibodies: K14 stain -Anti-BrdU (1:25) (347580, BD bioscience) and anti-K14 (1:1000) (PRB-155P, Covance) for 2h and Anti-mouse Alexa Flour 488 (1:500) (A21121, life science) and anti-Rabbit Alexa Flour 594 (1:500) (A21207, life science) for 1h. K10 stain - anti-K10 (1:500) (PRB-159P, Covance) for 2h and anti-rabbit (1:500) (A21206, Invitrogen) for 1h. Loricrin stain - anti-Loricrine (1:500) (PRB-145P, Covance) for 2h and anti-rabbit (1:500) (A21206, Invitrogen) for 1h. The pictures are representative of 5 individuals from each genotype. Scale bars represent 20 µm.

Next we determined the epidermal proliferation status upon ACBP depletion by quantifying the BrdU incorporation into K14 positive IFE cells. We detected an increased BrdU incorporation at P47 and P85 in ACBP$^{-/-}$ mice, and at P33, P47, P58, and P85 in K14-ACBP$^{-/-}$ mice compared with WT controls (Supplement 1, figure 3a and 3b). We also determined the mRNA levels of *K5*, *K14* and *K16*, as *K5* and *K14* is expressed in basal keratinocytes [136] and *K16* is expressed during situations of hyperproliferation [157]. These data showed that there is no difference in the expression of *K14* and *K16* between ACBP$^{-/-}$ or K14-ACBP$^{-/-}$ and their WT controls. However, the mRNA level of K5 was significantly increased (Supplement 1, figure 3c). These results indicate that the epidermal proliferation is elevated upon ACBP depletion.

In addition, we used immunohistochemistry to further elucidate the epidermal proliferation and differentiation status upon ACBP depletion and we found the staining of K10, K14 and loricrin to be similar between ACBP$^{-/-}$ and ACBP$^{+/+}$ mice (figure 15b).

Taken together, the presented results points towards an increase in epidermal differentiation and elevated proliferation upon ACBP depletion and we propose that the alterations might be initiated to counteract the impaired epidermal barrier observed in ACBP$^{-/-}$ mice.

2.1.4 ACBP DEPLETION RESULTS IN DECREASED LEVELS [OS] CERAMIDES IN STRATUM CORNEUM

As described in section 1.6, SC lipids such as ceramides, cholesterol and VLC FFA are important in maintaining the epidermal barrier integrity [139]. Ceramides are the most abundant lipid species in SC [239] and transgenic mouse models depleted of enzymes involved in SC [OS] ceramide synthesis such as CerS3, ELOVL1, ELOVL4, 12R-LOX, eLOX3, and Sap [250, 257, 259, 290, 292, 300] show impairment of the epidermal barrier due to alterations of the SC ceramides composition. These findings led us to investigate the SC ceramide composition in ACBP$^{-/-}$ mice using mass spectrometry (MS) and we found that only a few ceramide species within the [NS], [AS], ω-hydroxylated, and [EOS] ceramides were altered in ACBP$^{-/-}$ mice compared with ACBP$^{+/+}$ (figure 17a, b, c, d). In general, the ceramide species that were increased in amount had acyl chains ≤C22 whereas the species that were found decreased had acyl chain lengths ≥C24. Interestingly, all the [OS] ceramides with acyl chains ≥C30 were decreased in amount in SC from ACBP$^{-/-}$ mice (Supplement 1, figure 4a and 4b).

These findings suggest that ACBP depletion in mice impairs the [OS] ceramide synthesis pathway and possibly also the synthesis of other ceramide species with acyl chains ≥C24. This assumption is supported by the results presented in Supplement 2 where we show that ACBP significantly induces CerS3 and CerS2 activity *in vitro* (Supplement 2, figure 1B and 1C) [385]. Thus, ACBP depletion in mice is likely to result in decreased activities of both CerS2 and CerS3. CerS2 primarily utilizes C22-C24 acyl-CoA esters, whereas the affinity of CerS3 is acyl-CoA esters ≥C26 [90, 92], which is consistent with the length the acyl chains of those ceramides that are decreased in ACBP depleted mice SC. Furthermore, the solubility of acyl-CoA esters in aqueous solutions decreases when the chain length increases, thus ACBP may be more important to keep acyl-CoA esters ≥C26 available for synthesis of ceramides.

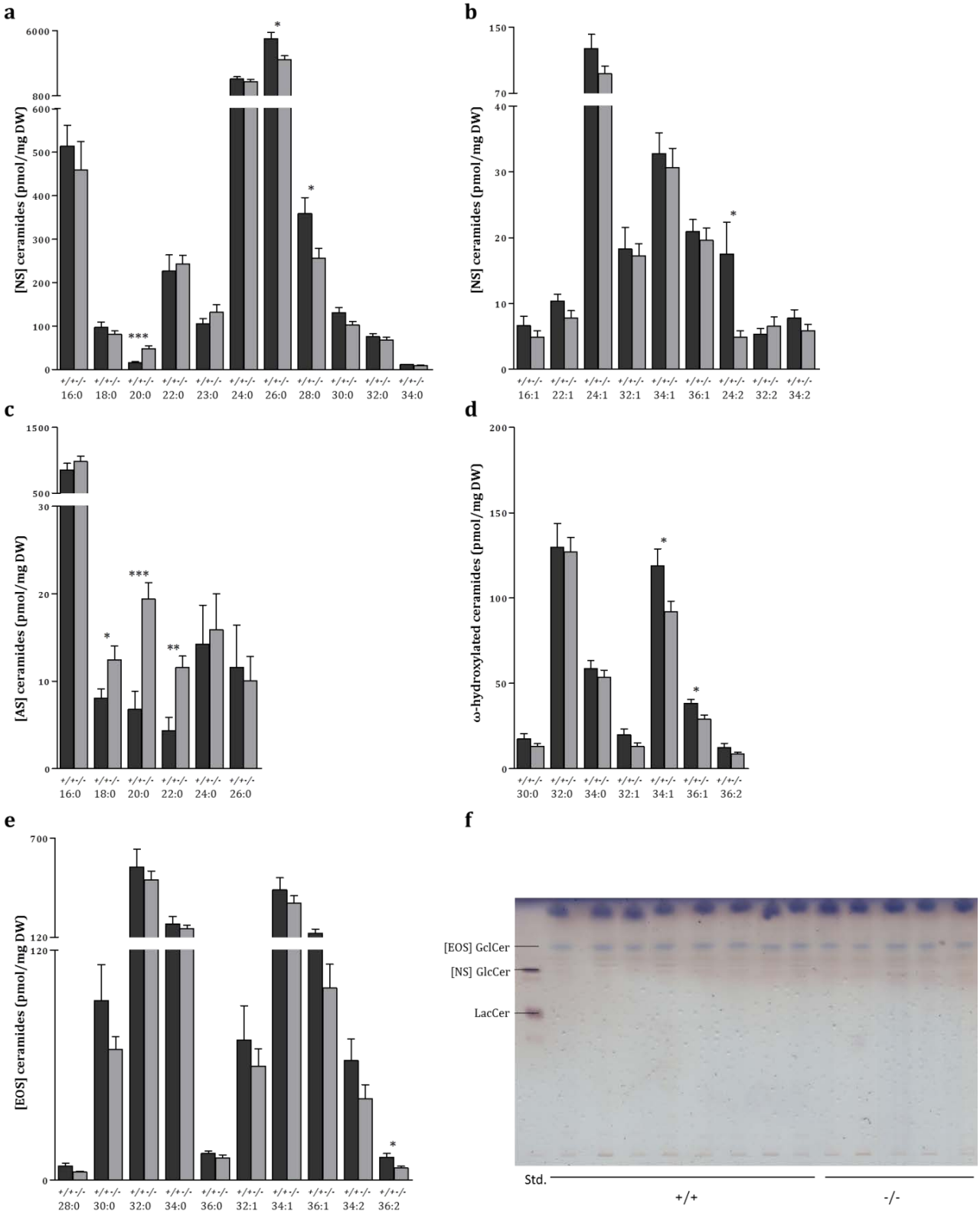
a
[NS] ceramides (pmol/mg DW)
16:0
18:0
20:0
22:0
23:0
24:0
26:0
28:0
30:0
32:0
34:0
b
[NS] ceramides (pmol/mg DW)
16:1
22:1
24:1
32:1
34:1
36:1
24:2
32:2
34:2
c
[AS] ceramides (pmol/mg DW)
16:0
18:0
20:0
22:0
24:0
26:0
d
ω-hydroxylated ceramides (pmol/mg DW)
30:0
32:0
34:0
32:1
34:1
36:1
36:2
e
[EOS] ceramides (pmol/mg DW)
28:0
30:0
32:0
34:0
36:0
32:1
34:1
36:1
34:2
36:2
f
[EOS] GclCer
[NS] GlcCer
LacCer
Std.
+/+
-/-

Figure 17: Stratum corneum ceramides. Stratum corneum was isolated from Veet® treated belly skin from 3 month old ACBP$^{+/+}$ (+/+) and ACBP$^{-/-}$ (-/-) mice using 0.25% Trypsin in PBS. Stratum corneum lipids were extracted using a modified Doering method as described in [250]. The different ceramide species were quantified using tandem mass spectrometry in collaboration with Dr. Roger Sandhoff, Lipid Pathobiochemistry group, German Research Center, Heidelberg. All the shown ceramide species composes of a sphingosine base with acyl chain length indicated. **a)** and **b)** display the levels of different [NS] ceramides species in SC. **c)** show the levels of different [NS] ceramides species in SC. **d)** show the levels of different ω-hydroxy ceramides in SC and **e)** display the [EOS] ceramides. Mean±SEM. n=7-9 mice/genotype/age. Unpaired parametric Students t-test: *P<0.05, **P<0.01, ***P<0.001. (f) Free SC ceramides were separated and developed according to [283], ceramides were identified using [NS] GlcCer (860549, Avanti) and LacCer (860597, Avanti).

Transgenic mouse models depleted of proteins, which are involved in the synthesis of [OS] ceramides, demonstrate the importance of [OS] ceramides in maintaining epidermal barrier integrity. Mice depleted of CerS3, ELOVL1, ELOVL4, 12R-LOX, eLOX3, and Sap all show decreased levels of [OS] ceramides in SC, which is accompanied by impaired barrier function [250, 257, 259, 290, 292, 300]. These observations indicate that the decreased level of [OS] ceramides in ACBP$^{-/-}$ mice SC might be causal for the reported impaired epidermal barrier. Furthermore, we speculate that the increased level of ceramides with acyl chain ≤C22 in ACBP depleted mice SC could potentially be a compensatory mechanism to counteract the impaired epidermal barrier.

As described in section 1.6, the synthesis of [OS] ceramides involves that acyl-CoA esters are elongated to ULC acyl-CoA esters before ω-hydroxylation, and subsequently ω-hydroxylated ceramides with ULC acyl chain are synthesized. The ω-hydroxylated ceramides becomes acylated to yield [EOS] ceramides, before glucosylation to form [EOS] GlcCer. Finally, the [EOS] GlcCer are processed and crosslinked to proteins of the cornified envelope in the SC (figure 12). The observed decreased level of [OS] ceramides in SC from ACBP$^{-/-}$ mice prompted us to further investigate the pathway of [OS] ceramide synthesis in these mice. Therefore, we analyzed the [EOS] GlcCer level by HPTLC in SC lipid extracts from ACBP$^{-/-}$ and ACBP$^{+/+}$ mice. However, we observed no alterations in the level of [EOS] GlcCer upon ACBP depletion (figure 15e). To further elucidate whether [EOS] GlcCer species might be reduced upon ACBP depletion, we need to apply a more sensitive method such as MS.

The assumption that the altered [OS] ceramide level is caused by reduced activity of CerS3, suggests that the level of intermediate ceramide products subsequent to *N*-acylation would be reduced. Surprisingly, only the level of a few species of ω-hydroxylated and [EOS] ceramides were reduced in SC upon ACBP depletion and this needs to be further elucidated.

The processing of [EOS] GlcCer into [OS] ceramides involves numerous enzymes including β-glucocerebrosidase (GBA1) and saposin (Sap). We set out to investigate whether the expression of *GBA1* and *proSap* (*pSap*) might be alternatively regulated upon ACBP depletion. We found the expression of *Sap* to be highly induced in ACBP$^{-/-}$ mice epidermis whereas the epidermal mRNA level of *GBA1* remained similar between ACBP$^{-/-}$ and ACBP$^{+/+}$ mice (figure 18). We speculate that the elevated expression of *GBA1* could potentially be a compensatory effect to counteract for the impaired epidermal barrier upon ACBP depletion.

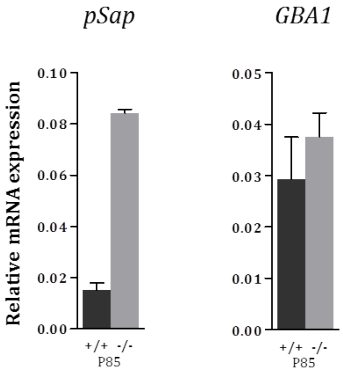

Figure 18: The mRNA level of *pSap* is increased in ACBP-/- epidermis. mRNA were isolated from epidermal splits (0.5 M ammonium thiocyanate in PBS) ACBP$^{+/+}$ (+/+) and ACBP$^{-/-}$ (-/-) mice at P85. mRNA extracted from five mice of each genotype were pooled, cDNA were synthesized and analyzed by RT-PCR using the following primers: *pSap* fwd.: 5'-AAGTGAAGCGGCGCCATGTA-3', *pSap* rev.: 5'-GAAGGGATTTCGCTGTGGGC-3', *GBA1* fwd.: 5'-TGGAGAGAAGTGTGCTGGTG-3', *GBA1* rev.: 5'-GGTAAGGTCACGGGGTCAAG-3', The expression was normalized to that of GAPDH: GAPDH fwd.: 5'-GCA CCAG TCA AGG CCG AGA AT-3', GAPDH rev.: 5'-TCT CGC TCC TGG AAG ATG GT-3'. RT-PCR results are presented as mean±SEM from duplicates.

2.1.5 THE EXPRESSION LEVELS OF CERS ISOFORMS IS ELEVATED UPON ACBP DEPLETION

As described in section 1.3.1 the different CerS enzymes display affinity towards acyl-CoA esters of different chain lengths and only CerS3 and CerS4 are expressed in high levels in skin [387]. Additionally, we found the SC ceramide profile to be altered upon ACBP depletion (Supplement 1, figure 4 and figure 17). We therefore analyzed the epidermal mRNA expression of different *CerS* and found the expression of *CerS2*, *CerS3*, *CerS4*, and *CerS5* to be elevated in epidermis from ACBP$^{-/-}$ mice compared with ACBP$^{+/+}$ (figure 19).

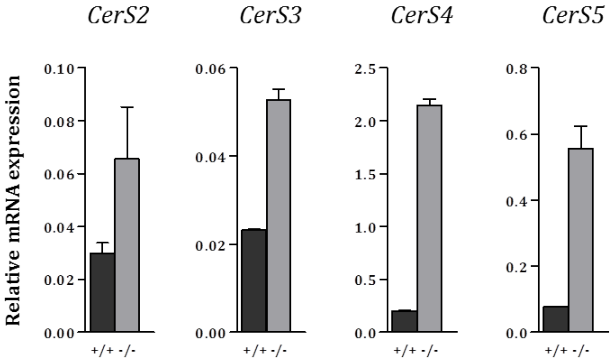

Figure 19: The levels of epidermal *CerS* expression are altered upon ACBP depletion.
mRNA were isolated from epidermal splits (0.5 M ammonium thiocyanate in PBS) from 5 + 5 ACBP$^{+/+}$ (+/+) and ACBP$^{-/-}$ (-/-) mice at P85 and equal amounts from each mice were pooled followed by cDNA synthesis. The mRNA levels were analyzed by RT-PCR using the following primers: *CerS2* fwd.: 5'-AGA GTG GGC TCT CTG GAC G-3', *CerS2* rev.: 5'-CCA GGG TTT ATC CAC AGT GAC-3', *CerS3* fwd.: 5'-CCT GGC TGC TAT TAG TCT GAT G-3', *CerS3* rev.: 5'-CTG CTT CCA TCC AGC ATA GG-3', *CerS4* fwd.: 5'-CTG TGG TAC TGT TGT TGC ATG AC-3', *CerS4* rev.: 5'-GCG CGT GTA GAA GAA GAC TAA G-3', *CerS5* fwd.: 5'-TGG CCA ATT ATG CCA GAC GTG AG-3', *CerS5* rev.: 5'-GGT AGG GCC CAA TAA TCT CCC AGC-3'. The expression was normalized to that of GAPDH: GAPDH fwd.: 5'-GCA CCAG TCA AGG CCG AGA AT-3', GAPDH rev.: 5'-TCT CGC TCC TGG AAG ATG GT-3'. RT-PCR results are presented as mean±SEM from duplicates. n=5 mice/genotype/age.

CerS2 has highest affinity towards C20-C26 acyl-CoA esters [90] and the increased expression of *CerS2* in ACBP$^{-/-}$ mice epidermis might therefore possibly be a compensatory mechanism to increase the level of ceramides and thereby help sustain the impaired epidermal barrier. However there are no reports of skin

defects in CerS2 depleted mice [388], which suggests that CerS2 only play a minor role in epidermal ceramide synthesis.
CerS3 produces ceramides with ≥C24 acyl chains [91-93] and is highly involved in the synthesis of epidermal ceramides in mice including glucosylated ceramides, [EOS] ceramides and [OS] ceramides [250].
We found the levels of [OS] ceramides to be decreased in SC of ACBP depleted mice, although the expression of *CerS3* was elevated. However, in Supplement 2 we showed that ACBP markedly (7-fold) induces CerS3 activity *in vitro [385]*. Taken together, these findings suggest that although the expression of *CerS3* is induced, the activity may be impaired, resulting in decreased levels of [OS] ceramides upon ACBP depletion.
CerS4 displays highest affinity towards C18-C22 acyl-CoA esters [94] and is highly involved in sebaceous gland homeostasis and lipid synthesis [381]. We therefore propose that the increased expression of *CerS4* is linked to the sebaceous gland hypertrophy observed in ACBP depleted mice.
CerS5 shows highest affinity towards C16 acyl-CoA esters [94] and we propose that the elevated expression of *CerS5* is a compensatory effect to counteract the barrier defect upon ACBP depletion. There are no reports of skin abnormalities in CerS5 depleted mice [389], which suggests that CerS5 only play a minor role in epidermal ceramide synthesis.
Taken together, the observed decreased level of [OS] ceramides in SC upon ACBP depletion possibly arises due to impaired activity of CerS2 and CerS3 as ACBP induces the activity of CerS2 and CerS3 *in vitro* (Supplement 2, figure 1B and 1C) [385]. We speculate whether the reduced level of SC [OS] ceramides causes elevated expression of CerS2-5 by a yet unknown mechanism.
In general we found ceramides species with acyl chain length ≤C22 to be increased in ACBP$^{-/-}$ SC, however ceramide species with acyl chain length ≥C24 were decreased upon ACBP depletion. This suggests that acyl-CoA esters might have an increasing need for ACBP as a carrier as their chain lengths increase. In keeping with that, ACBP only stimulates the activity of CerS2 and CerS3. Therefore, when taking the substrate specificities of the different CerS into account, these observations indicate that the lack of ACBP might impact the activity of CerS2 and CerS3 mostly due to their substrate specificity and thereby cause the reduced levels of the longer ceramide species.

2.1.6 EPIDERMAL LOCALIZATION OF ACBP, CERS3 and CERS4

In the skin ACBP is expressed in all live epidermal cells, with highest expression in SS, whereas the sebaceous glands display only low expression [16]. Furthermore, CerS3 and CerS4 are highly expressed in skin [387]. We have presented results, which indicate that ACBP depletion affects CerS3-directed synthesis of [OS] ceramides and alters the expression levels of *CerS3* and *CerS4*. These findings led us to investigate the localization of ACBP, CerS3 and CerS4 in the skin from ACBP$^{-/-}$ and ACBP$^{+/+}$ mice by immunohistochemistry. We noticed that ACBP is expressed in epidermis and in the PSU; especially the hair follicles displayed high expression and the expression was low in the sebaceous glands (figure 20), which is consistent with earlier reports [16]. CerS3 was expressed in the epidermis and also in the PSU, especially in the hair follicles, whereas CerS4 displayed high expression in the sebaceous glands and no noticeable expression in epidermis or hair follicles (figure 20). These findings confirm earlier reports regarding the epidermal expression of CerS3 and CerS4 [250, 382]. We did not observe any alterations in the localization of CerS3 and CerS4 upon ACBP depletion.

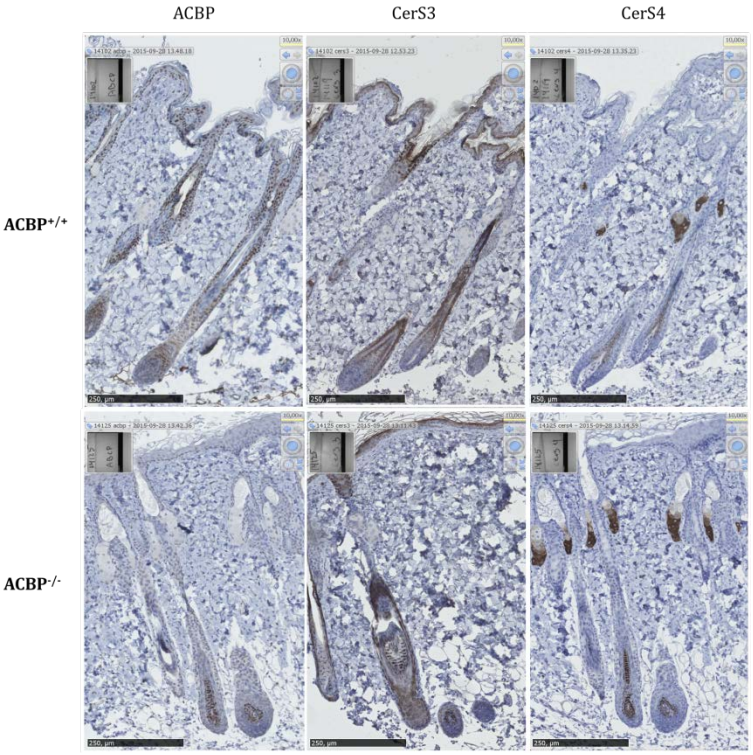

Figure 20: ACBP, CerS3 and CerS4 expression in ACBP$^{+/+}$ and ACBP$^{-/-}$mice epidermis. Three month old ACBP$^{+/+}$ and ACBP$^{-/-}$ mice were sacrificed, abdominal skin isolated and fixed in 10% formalin for 24h followed by paraffin embedding. Three sequential sections were stained against ACBP, CerS3 and CerS4 and subsequent visualized using diaminobenzidine (DAB). The ACBP antibody was generated in our lab, the CerS3 and CerS4 antibodies were kindly provided by Dr. Roger Sandhoff and Professor Klaus Willecke, respectively. The immunohistochemistry was conducted in collaboration with Professor Torben Steiniche, Department of Clinical Medicine, Patological institute, University Hospital Aarhus, Denmark and the pictures are representative of 4-5 individuals from each genotype.

2.1.7 ACBP DEPLETION IN MICE RESULTS IN SEBACEOUS GLAND HYPERTROPHY

When we investigated the morphological consequences of ACBP depletion we noticed that the sebaceous glands were enlarged in both ACBP$^{-/-}$ and K14-ACBP$^{-/-}$ mice. We explored these observations further and found the sebaceous glands to be 2-fold increased in size in both ACBP$^{-/-}$ and K14-ACBP$^{-/-}$ mice compared with WT control mice (Supplement 1, figure 5a and 5b). To evaluate whether the increase in sebaceous gland size were caused by elevated proliferation we quantified BrdU incorporation into sebaceous gland basal cells; however, there was no differences in proliferation of sebaceous glands basal cells between ACBP$^{-/-}$ mice and ACBP$^{+/+}$ (Supplement 1, figure 5c).

We have previously reported that the impaired epidermal barrier observed in ACBP$^{-/-}$ mice causes impairment of lipogenic gene expression in the liver [58] and Harderian gland hypertrophy [17]. Furthermore, both the liver and the Harderian gland phenotype could be rescued by applying an artificial barrier on the skin of ACBP$^{-/-}$ mice. These findings led us to analyze whether the enlargement of sebaceous glands in ACBP$^{-/-}$ mice could also be prevented by applying Vaseline twice a day from day 7 to 28 onto the skin of ACBP$^{-/-}$ mice. We found that the application of an artificial barrier was unable to prevent enlargement of the sebaceous glands in ACBP$^{-/-}$ mice (Supplement 1, figure 5d). This indicates that ACBP

depletion results in enlargement of the sebaceous glands and that the enlargement is possibly caused by ACBP depletion and not due to the impaired barrier function *per se*.

To further elucidate the cause of the enlarged sebaceous glands upon ACBP depletion, we investigated the differentiation status in ACBP$^{-/-}$ and ACBP$^{+/+}$ mice sebaceous glands. First we applied coherent anti-stokes raman scattering (CARS) microscopy to evaluate the lipid accumulation in sebaceous glands from ACBP$^{-/-}$ and ACBP$^{+/+}$ mice. This demonstrated that the whole gland in ACBP$^{-/-}$ mice were capable of accumulating lipids, just as in ACBP$^{+/+}$ mice and also confirmed the elevated size of the sebaceous glands in ACBP$^{-/-}$ mice (Supplement 1, figure 6a). SCD1 is a marker of sebaceous differentiation [390], and consistently we found the staining of SCD1 to be increased in size and intensity upon ACBP depletion (Supplement 1, figure 6b). Additionally, we found the mRNA expression level of *SCD1* to be elevated in epidermis from ACBP$^{-/-}$ mice compared with ACBP$^{+/+}$ (Supplement 1, figure 6c). Taken together, these results indicate that the enlarged sebaceous glands in ACBP depleted mice synthesize increased levels of lipids and consistently we found the mRNA expression levels of *HMG-CoA reductase* (*HMGCR*) and *squalene epoxidase* (*SQLE*) to be significantly increased in ACBP$^{-/-}$ mice epidermis (Supplement 1, figure 6c). Surprisingly, the expression of diacylglycerol acyltransferase 1 (*Dgat1*) was not significantly elevated upon ACBP depletion (Supplement 1, figure 6c). Collectively, these results indicate that the differentiation of the sebaceous glands in ACBP$^{-/-}$ mice is elevated and that the lipid production is increased, which results in sebaceous gland hypertrophy.

The elevated lipid production in the sebaceous glands of ACBP$^{-/-}$ mice and the greasy appearance of these mice, which is pronounced at P21, suggested that the glands might secrete increased amounts of lipids. Interestingly, we found the amount of lipids to be 2-fold increased on the fur of ACBP$^{-/-}$ mice at P21 compared with ACBP$^{+/+}$ (figure 21). Next we used HPTLC in combination with two different solvent systems to analyze the composition of the fur lipids. This revealed that there are increased levels of FFA, MADAG, CE, cholesterol, wax monoester, and wax diester on the fur of ACBP$^{-/-}$ mice compared with ACBP$^{+/+}$ when lipids extracted from equal amounts of fur were analyzed (Supplement 1, figure 7a and 7b). Taken together, these results demonstrate that both sebaceous gland lipid synthesis and sebum secretion are elevated upon ACBP depletion.

We next used the same method to investigate whether ACBP depletion, in addition to elevated sebocyte lipid synthesis, also resulted in alterations in the sebum lipid composition. We found that when analyzing the same amount of lipids from ACBP$^{-/-}$ and ACBP$^{+/+}$ mice fur, the levels of MADAG, wax diester and wax monoester were elevated in ACBP$^{-/-}$ mice fur (Supplement 1, figure 7c and 7d). These findings suggest that ACBP depletion, in addition to elevated sebum secretion, also alters the sebum lipid composition.

The increased MADAG level on the fur of ACBP depleted mice confirms previous findings by Bloksgaard *et al*. [16]. Additionally, we have previously shown that the Harderian glands of ACBP$^{-/-}$ mice secrete elevated amounts of MADAG [17]. We propose that the majority of the increased MADAG on the fur of ACBP depleted mice are synthesized by the hypertrophic sebaceous glands; however, the increased MADAG secretion from the Harderian glands may also contribute to the elevated fur MADAG level.

Wax esters may serve as a hydrophobic protective layer functioning to prevent dehydration and retain water as previously suggested [305, 391]. The sebum wax ester levels are also altered in mice depleted of ELOVL3, FA2H and CerS4 [365, 377, 381], but whether this is a compensatory mechanism to counteract impaired barrier integrity remain elusive.

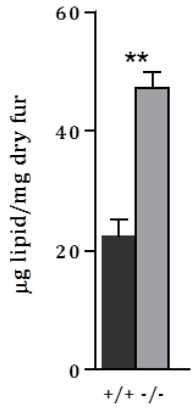

Figure 21: ACBP depletion results in increased level of sebum on the fur. The body fur from ACBP$^{+/+}$ (+/+) and ACBP$^{-/-}$ (-/-) mice at P21 were shaved off and collected, lipids were extracted 2x15 min with 3 mL acetone. The fur and the extracted lipids were dried under N_2 flow and weighed. Mean±SEM. n=3-5 mice/genotype. Unpaired parametric Students t-test: *P<0.05, **P<0.01, ***P<0.001.

2.1.8 THE EXPRESSION LEVEL OF *ELOVL* ISOFORMS IS ELEVATED UPON ACBP DEPLETION

The different ELOVL isoforms display differential substrate specificity and tissue distribution as discussed in section 1.6.2 and section 1.7.4 (reviewed by [392]). Especially, ELOVL1 and ELOVL4 are essential for the synthesis of epidermal VLC and ULC FAs, respectively, and for the survival in mice [257, 259]. ELOVL1 depleted mice show decreased levels of epidermal ceramides containing acyl chain ≥C26 (especially ω-hydroxylated ceramides) [259] and mice depleted of ELOVL4 are deficient in epidermal ceramides with ω-hydroxylated acyl chain ≥C28 in SC [256, 257]. Keeping that in mind, Bloksgaard *et al*. have previously shown that the ULC FFAs are decreased in ACBP$^{-/-}$ mice SC [16] and here we have shown that the level of [OS] ceramides in SC are decreased in ACBP$^{-/-}$ mice (Supplement 1, figure 4). Additionally, ELOVL3 is highly involved in sebaceous gland lipid synthesis and homeostasis and depletion of ELOVL3 in mice alters the sebum lipid composition [365]. Taken together, these findings made us investigate the expression of the various ELOVL isoforms and we found the mRNA level of *ELOVL1*, *ELOVL3*, *ELOVL4*, *ELOVL5*, *ELOVL6*, and *ELOVL7* to be elevated in ACBP$^{-/-}$ mice epidermis compared with ACBP$^{+/+}$ (figure 22).

When taking the substrate specificity of ELOVL1 and ELOVL4 into account, the increase in epidermal *ELOVL1* and *ELOVL4* expression does not correlate with the reported decrease of ULC FFA in ACBP$^{-/-}$ mice SC [16]. However, we have preliminary unpublished results showing that ACBP interacts with ELOVL1-7 *in vitro* (Master student Lisa Skov Baungaard). Additionally, which makes us speculate whether ACBP affects the activity of ELOVL1 and ELOVL4 as we have shown for CerS2 and CerS3 (Supplement 2, figure 1B and 1C) [385].

ELOVL3 is important for sebaceous gland homeostasis and lipid synthesis [365]. We propose that the increased *ELOVL3* mRNA level in epidermis from ACBP$^{-/-}$ mice might be a consequence of the sebaceous gland hypertrophy. ELOVL3 deficient mice display a fur/skin phenotype similar to that of ACBP depleted mice with tousled fur, alopecia and sebaceous gland hypertrophy [365]. These observations suggest that ACBP and ELOVL3 affect the sebaceous gland homeostasis in similar ways and may be involved in the same lipid synthesis pathways in sebaceous glands.

There have to the best of my knowledge not been reported any skin phenotypes linked to depletion of ELOVL5 and ELOVL6 in mice [393, 394]. Also, even though ELOVL7 display similar substrate specificity as ELOVL3 the expression of ELOVL7 in skin has not been investigated before [85]. However, it remains

elusive whether the elevated expression of *ELOVL5*, *ELOVL6* and *ELOVL7* upon ACBP depletion is linked to the sebaceous gland hypertrophy or to the impaired epidermal barrier.

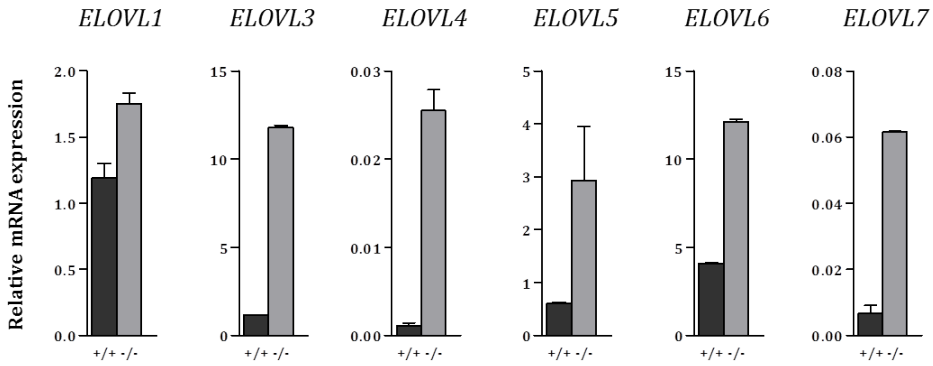

Figure 22: The levels of *ELOVL* expression in ACBP$^{-/-}$ and ACBP$^{+/+}$ mice epidermis. mRNA were isolated from epidermal splits (0.5 M ammonium thiocyanate in PBS) from ACBP$^{+/+}$ (+/+) and ACBP$^{-/-}$ (-/-) mice at P85 and were pooled. Followed by cDNA synthesis and the expression were analyzed by RT-PCR using the following primers: *ELOVL1* fwd.: 5'-TGT GAC CCC ATA GAC TTT TCC A-3', *ELOVL1* rew.: 5'-TCG AAC CAT CCG AAG TGC TT-3', *ELOVL3* fwd.: 5'-AGC AAG GTT GTT GAA CTG GGA-3', *ELOVL3* rev.: 5'-GAC GCT TAC GCA GGA TGA TGA-3', *ELOVL4* fwd.: 5'-AGG CGT TGA GTA TTT GGA CA-3', *ELOVL4* rev.: 5'-TTG AGG AAG AGG AAG ATG AAG C-3', *ELOVL5* fwd.: 5'-CCC CCG AGA TAC AAG AGT CAA A-3', *ELOVL5* rev.: 5'-GGG ATG TAA TTG TCC AGG AGG A-3', *ELOVL6* fwd.: 5'-TCA GCA AAG CAC CCG AAC TAG-3', *ELOVL6* rev.: 5'-CTG TTT CCT CAG AAT GAT GAA TAT CGT-3', *ELOVL7* fwd.: 5'-ATCTCCTCATGTCCTCGCCT-3', *ELOVL7* rev.: 5'-CCAGCCAGACATCACAAACTCA-3'. The expression was normalized to that of GAPDH: GAPDH fwd.: 5'-GCA CCAG TCA AGG CCG AGA AT-3', GAPDH rev.: 5'-TCT CGC TCC TGG AAG ATG GT-3'. RT-PCR results are presented as mean±SEM from duplicates. n=5 mice/genotype.

2.1.9 SUMMARY

In conclusion, Supplement 1 shows that targeted deletion of the *Acbp* gene in mice leads to slightly increased epidermal proliferation and differentiation. Furthermore, ACBP depletion causes an induced anagen-like state in the hair follicles. Moreover, we show that the level of [OS] ceramides is reduced upon ACBP depletion. Additionally, ACBP depletion in mice results in sebaceous gland hypertrophy due to elevated differentiation. The elevated differentiation causes increased sebum amounts on the fur of ACBP depleted mice. Finally, we show that application of an artificial barrier on the skin of ACBP depleted mice is unable to prevent the enlargement of the sebaceous glands. Taken together, these results indicate that ACBP is important in sustaining both epidermal and sebaceous gland homeostasis.

2.2 SUPPLEMENT 2

Supplement 2 describes our functional analysis of ACBP involvement in ceramide synthesis [385]. Information regarding mechanistic regulation of ceramide synthesis is sparse. However, CerS can be regulated by dimerization, phosphorylation and by interaction with ELOVL1 [84-86].

2.2.1 ACBP STIMULATES CERAMIDE SYNTHASE ACTIVITY

The different CerS isoforms utilizes acyl-CoA esters with differential chain lengths for *N*-acylation of sphinganine as discussed in section 1.3.1. Previous investigations show that ACBP binds C14-C22 acyl-CoA esters with high affinity and specificity. Taken together this made us speculate whether ACBP might be involved in the synthesis of ceramides, e.g. by delivering acyl-CoA esters, and we set out to investigate this further.

Initially, we investigated the activity of the different CerS isoforms in presence or absence of ACBP. We used homogenates from HEK293T cells overexpressing each of the six CerS isoforms and addressed the activity of the individual CerS isoforms using appropriate acyl-CoA esters in absence and in presence of increasing concentrations of recombinant rat ACBP (rACBP). This clearly demonstrated that ACBP increased the activity of CerS2 by 2-fold and the activity of CerS3 by 7-fold (Supplement 2, figure 1B and 1C, respectively); however, ACBP did not affect the activity of CerS1, CerS4, CerS5 and CerS6 (Supplement 2, figure 1A, 1D, 1E and 1F). Interestingly, Ohno and colleagues recently reported that CerS2 interacts with ELOVL1-7, but only affects the activity of ELOVL1 [85]. Taking into consideration the substrate specificity of CerS2 and ELOVL1, this suggests that CerS isoforms are likely to form functional complexes with ELOVL isoforms that produce the products they utilize. When taking into account that the solubility of acyl-CoA esters in aqueous solutions decreases when the chain length increases, and that CerS2 and CerS3 both utilizes VLC acyl-CoA esters, ACBP may be more important for keeping acyl-CoA esters available to CerS2 and CerS3 than to the other CerS isoforms that use shorter chain acyl-CoA esters.

We have investigated the activity of CerS3 in presence or absence of rACBP with increasing concentrations of C26 acyl-CoA ester and we found the activity of CerS3 to increase in a biphasic manner upon increasing C26 acyl-CoA ester level (Supplement 2, figure 1H). Further kinetic analysis revealed that the V_{max} of CerS3 towards sphinganine increased 4-fold in the presence of ACBP (Supplement 2, figure 2). Taken together, these results show that the activity of CerS3 increases upon increasing levels of substrate in an ACBP dependent manner.

We further confirmed that presence of ACBP increases the activity of CerS2 and CerS3, by showing that co-transfection of HEK293T cells with ACBP and either CerS2 or CerS3 stimulated the CerS activities in a similar manner as seen when rACBP was added (Supplement 2, figure 3).

ACBP is highly abundant in mouse hepatocyte cytosol and we showed that both low speed (10,000 x g) and high speed (100,000 x g) supernatants from $ACBP^{+/+}$ mice liver increased the activity of CerS3 to levels comparable with rACBP (Supplement 2, figure 4). However, importantly, cytosol from $ACBP^{-/-}$ mice liver did not affect the activity of CerS3, and these findings confirmed that it is the presence of ACBP in the cytosol that activates CerS3. In line with these findings we showed that addition of heterozygous ($ACBP^{+/-}$) mice liver stimulated CerS3 activity in a doze dependent manner to ~50% of the level seen with $ACBP^{+/+}$ cytosol (Supplement 2, figure 4).

The presented results clearly demonstrate that CerS2 and CerS3 activity is highly dependent of substrate availability mediated by ACBP and for the first time we show that ACBP is involved in the regulation of CerS2 and CerS3 activity.

The results presented above show that ACBP stimulates CerS2 and CerS3 activity *in vitro*; however, we wanted to investigate the activity of CerS2 and CerS3 in testis from $ACBP^{+/+}$ and $ACBP^{-/-}$ mice. Importantly, we showed that the activity of both CerS2 and CerS3 were significantly reduced in $ACBP^{-/-}$ mice testis homogenates compared with $ACBP^{+/+}$ (Supplement 2, figure 5), suggesting that ACBP stimulates CerS2 and CerS3 activity *in vivo*.

These findings are very interesting, as CerS3 is involved in the synthesis of epidermal [OS] ceramides [250] and we have showed that the SC [OS] ceramide level was reduced upon ACBP depletion in mice (Supplement 1, figure 4). However, we found the expression of CerS3 to be elevated in $ACBP^{-/-}$ mice epidermis (figure 19). Taken together, these observations suggests that ACBP depletion in mice reduces the activity of CerS3 which leads to decreased amounts of [OS] ceramide in SC, and that elevated mRNA expression levels of CerS3 are unable to compensate for the decreased activity.

To ensure that the altered ceramide synthase activities were not caused by differential expression of the different *CerS*, we showed that all *CerS* mRNAs are expressed at similar levels between $ACBP^{+/+}$ and $ACBP^{-/-}$ mice testis (Supplement 2, figure 6).

2.2.2 ACBP DEPLETION AFFECTS THE CERAMIDE COMPOSITION IN MICE TESTIS

Next, we wanted to address whether the altered activity of CerS2 and CerS3 affected the sphingolipid levels in $ACBP^{-/-}$ mice testis and we showed that the ceramide, dHCer, glucosylceramide, dihydroglucosylceramide, SM and dihydrosphingomyelin profiles were all altered upon ACBP depletion (Supplement 2, figure 7). As discussed in section 1.3.1, CerS2 displays substrate specificity towards C20-C26 acyl-CoA esters, whereas CerS3 is involved in the synthesis of ceramides with acyl moieties ≥C24. In mouse testis, we observed a decrease in the different sphingolipid species with acyl moieties ranging from C14 to C26, which was rather surprising. Laviad and colleagues have shown that CerS activity can be modulated by alterations in the dimer formations [84] and we suggests that the decreases in CerS2 and CerS3 activity may have altered the dimer formation and thereby the sphingolipid profile.

The ceramide profile in the SC of $ACBP^{-/-}$ mice was not altered to the same degree as the ceramide profile in $ACBP^{-/-}$ testis when compared with $ACBP^{+/+}$ levels. The skin is a more complex organ and the epidermal barrier is essential to mammalian survival, which made us speculate whether the impairment of the ceramide synthesis in epidermis upon ACBP depletion is to a higher degree protected by compensatory mechanisms than in testis. In keeping with this, we showed that the mRNA expression of *CerS2*, *CerS3*, *CerS4*, and *CerS5* were all elevated in $ACBP^{-/-}$ skin compared with that of $ACBP^{+/+}$ mice (figure 19) whereas *CerS1-6* were expressed in similar levels in testis between $ACBP^{-/-}$ and $ACBP^{+/+}$ mice (Supplement 2, figure 6).

2.2.3 CERS3 ACTIVATION BY ACBP REQUIRES LIGAND BINDING

As discussed in section 1.2.2, ACBP binds C14-C22 acyl-CoA esters with high affinity and specificity. The fact that ACBP activates CerS2 and CerS3 suggests that ACBP is capable of binding VLC acyl-CoA esters and in keeping with this, we showed that C12-C26 acyl-CoA esters shifted the mobility of ACBP using gel shift

assays (Supplement 2, figure 8), arguing that ACBP binds up to C26 acyl-CoA esters. However, the binding of C12 and C26 acyl-CoA esters to ACBP occur with lower affinity than that of C14-C24 acyl-CoA esters.
Next we wanted to investigate whether ligand binding to ACBP is required for the activation of CerS3. We therefore used a panel of ACBP mutants, which are incapable of binding acyl-CoA esters, and showed that none of the ACBP mutants stimulated CerS3 activity to a similar level as rACBP or $ACBP^{+/+}$ cytosol (Supplement 1, figure 9). These results convincingly show that ligand binding to ACBP is required for the ability of ACBP to stimulate CerS3 activity. In keeping with this, we also showed that recombinant rat FABP1 (rFABP1), which is abundant in cytosol and capable of binding acyl-CoA esters, was incapable of stimulating CerS3 activity, further sustaining that activation of CerS3 activity by ACBP is rather specific.

2.2.4 ACBP INTERACTS WITH CERAMIDE SYNTHASES

We have shown that ACBP stimulates CerS2 and CerS3 activity and we propose that ACBP delivers acyl-CoA esters to CerS2 and CerS3 via direct interaction. To further substantiate these findings, we used the proximity ligation assay (PLA) to show that ACBP interacts with CerS2-6 (Supplement 1, figure 10B). We hypothesize that the interaction between CerS and ACBP is likely to be very transient as we were unable to detect the interaction using gelshift assays or co-immunoprecipitation (results not shown). CerS localize to the outer ER membrane [75] and this is consistent with the observed localization of the interaction between ACBP and CerS in the PLA study.
ACBP interacts with CerS2-6 but only affects the activity of CerS2 and CerS3. In keeping with this, previous investigations show that CerS2 interacts with ELOVL1-7; however, only the activity of ELOVL1 is stimulated [85]. When keeping that in mind, the solubility of acyl-CoA esters decrease with increasing acyl chain length acyl chain length increases the. Thus, it makes logically sense that CerS2 and CerS3 with their preference for VLC acyl-CoA esters [72] are more dependent on ACBP for substrate delivery, whereas CerS1 and CerS4-6 prefers LC acyl-CoA esters that are relatively more soluble. Taken together, this suggests that ACBP maintains acyl-CoA esters readily available to all the CerS, and that this is particular important for CerS2 and CerS3 as they prefer acyl-CoA esters with longer acyl chain lengths.

2.2.5 SUMMARY

In conclusion, Supplement 2 shows that ACBP stimulates CerS2 activity by 2-fold and CerS3 activity by 7-fold *in vitro*; however, ACBP does not affect the activity of CerS1 and CerS4-6. Additionally, high-speed liver cytosol from $ACBP^{+/+}$ mice stimulates CerS3 activity whereas high-speed liver cytosol from $ACBP^{-/-}$ mice does not. Furthermore, the activity of CerS2 and CerS3 are significantly reduced in homogenates from $ACBP^{-/-}$ mice testis compared with $ACBP^{+/+}$ mice testis, and in line with this the level of long- and very-long chain ceramides are significant reduced. We also show that ACBP interacts with CerS2 and CerS3. Taken together, we report a novel importance for ACBP in the regulation of the synthesis of ceramides with VLC acyl moieties.

3 CONCLUSION AND FUTURE PERSPECTIVES

ACBP depleted mice display a disrupted epidermal barrier, which is accompanied by a distinct skin/fur phenotype. The mechanisms behind these phenotypical traits remain unknown and therefore we aimed to elucidate these further. We showed that the epidermal proliferation is slightly elevated upon ACBP depletion and we speculate that this might be due to compensatory mechanisms counteracting the impaired barrier. Additionally, depletion of ACBP in mice results in an induced anagen-like state of the hair follicles and sebum clotting of the infundibulum, which is likely to cause the reported alopecia.

Previous findings have shown that SC from ACBP$^{-/-}$ mice contains reduced levels of ULC FFA and here we found the level of [OS] ceramides in SC to be decreased. We propose that both the reduced ULC FFA and [OS] ceramides contribute to the reported impaired barrier in ACBP$^{-/-}$ mice. Surprisingly, we did not observe any alterations in intermediate ceramide classes in the synthesis pathway of [OS] ceramides in ACBP depleted mice. However, it is warranted to follow up the studies by MS analysis.

In Supplement 2 we show that ACBP activates CerS3 and based on this we conclude, that ACBP depletion leads to impaired activity of CerS3 and concomitant decreased levels of [OS] ceramides. However, we found the mRNA expression of *CerS3* to be elevated in epidermis upon ACBP depletion and we conclude that that increased expression of *CerS3* is unable to fully compensate for the decreased activity in ceramide synthesis. To test this hypothesis it is warranted to investigate the activity of CerS3 in epidermis isolated from ACBP$^{-/-}$ and ACBP$^{+/+}$ mice.

Importantly, we showed that ACBP depletion results in sebaceous gland hypertrophy i.e. a 2-fold increase in gland size. Additionally, we showed that the increased sebaceous gland size in ACBP$^{-/-}$ mice is due to elevated differentiation rather than increased proliferation. Interestingly, application of an artificial barrier to the skin of ACBP$^{-/-}$ mice was unable to prevent the enlargement of the glands, which suggests that it is specifically the ACBP depletion rather than the impaired barrier function that causes sebaceous gland enlargement. We used CARS microscopy to confirm that the sebaceous glands of ACBP$^{-/-}$ mice are enlarged and that they are fully capable of accumulating lipids. Additionally, we detected an increased SCD1 staining in sebaceous glands from ACBP$^{-/-}$ mice. These findings support the hypothesis that the elevated size of the sebaceous glands in ACBP$^{-/-}$ mice is due to increased differentiation and suggests that the sebum secretion is elevated. Consistently, we detected a 2-fold increase in the total amount of lipids on the fur of ACBP$^{-/-}$ mice. Additionally, when investigating the levels of the different lipid species on the fur we found several species to be elevated upon ACBP depletion. In thread with these findings, we reported the expression of several genes involved in sebaceous gland lipid synthesis including *SCD1*, *HMGCR* and *SQLE* to be elevated upon ACBP depletion.

To further elucidate the effects of ACBP depletion on epidermal and sebaceous gland lipid levels it would be highly relevant to use a combined proteomic and lipodomic approach on epidermal splits and isolated sebaceous glands.

ACBP binds acyl-CoA esters, which are utilized for ceramide synthesis; however to this end there is no the relationship of acyl-CoA esters to ceramide synthesis remains unknown. We therefore conducted functional analysis to study how ACBP is involved in ceramide synthesis and found that ACBP strongly activates CerS2 and CerS3 *in vitro*. However ACBP did not affect the activity of CerS4, CerS5 and CerS6. In keeping with this, we found that the activity of CerS3 is increased in the presence of rACBP and

importantly, we showed that addition of liver cytosol from ACBP$^{+/+}$ but not ACBP$^{-/-}$ mice stimulated CerS3 activity. Furthermore, we showed that CerS2 and CerS3 activity is decreased in testis from ACBP$^{-/-}$ mice. Taken together, these results clearly demonstrate that ACBP stimulates both CerS2 and CerS3 activity.

We used a panel of ACBP mutants to show that ligand binding to ACBP is required for the activation of CerS3. In addition, we used PLA to show that ACBP interacts with CerS2-6 although only the activity of CerS2 and CerS3 was induced in the presence of ACBP. These findings suggest that ACBP keeps a pool of acyl-CoA esters available to all the CerS. However, the solubility of acyl-CoA esters in aqueous solutions decreases with increased acyl chain length and when addressing the substrate specificity of CerS2 and CerS3, we find it likely that ACBP is more important for keeping acyl-CoA esters available to CerS2 and CerS3 than to the other CerS isoforms.

As ACBP interacts with and regulates CerS2 and CerS3, we speculate whether these proteins form a functional ACBP-CerS complex that drives ceramide synthesis. Previous findings show that ELOVL1 interacts with CerS2 [85], which suggest that ACBP, CerS and ELOVL may form a functional platform. We are currently investigating this assumption by conducting functional analysis of ACBP involvement I elongation of FA. Preliminary data from our lab (Lisa Skov Baungaard, unpublished) show that ACBP interacts with ELOVL1-7 *in vitro*; however, we also plan to address whether ACBP affects the activity of the different ELOVL isoforms.

REFERENCES

1. Faergeman, N.J. and J. Knudsen, *Role of long-chain fatty acyl-CoA esters in the regulation of metabolism and in cell signalling.* Biochem J, 1997. **323 (Pt 1)**: p. 1-12.
2. Neess, D., et al., *Long-chain acyl-CoA esters in metabolism and signaling: Role of acyl-CoA binding proteins.* Prog Lipid Res, 2015. **59**: p. 1-25.
3. Mogensen, I.B., et al., *A novel acyl-CoA-binding protein from bovine liver. Effect on fatty acid synthesis.* Biochem J, 1987. **241**(1): p. 189-92.
4. Knudsen, J., et al., *Acyl-CoA-binding protein in the rat. Purification, binding characteristics, tissue concentrations and amino acid sequence.* Biochem J, 1989. **262**(2): p. 513-9.
5. Mikkelsen, J. and J. Knudsen, *Acyl-CoA-binding protein from cow. Binding characteristics and cellular and tissue distribution.* Biochem J, 1987. **248**(3): p. 709-14.
6. Guidotti, A., et al., *Isolation, characterization, and purification to homogeneity of an endogenous polypeptide with agonistic action on benzodiazepine receptors.* Proc Natl Acad Sci U S A, 1983. **80**(11): p. 3531-5.
7. Yanagibashi, K., et al., *The regulation of intracellular transport of cholesterol in bovine adrenal cells: purification of a novel protein.* Endocrinology, 1988. **123**(4): p. 2075-82.
8. Chen, Z.W., et al., *Isolation and characterization of porcine diazepam-binding inhibitor, a polypeptide not only of cerebral occurrence but also common in intestinal tissues and with effects on regulation of insulin release.* Eur J Biochem, 1988. **174**(2): p. 239-45.
9. Herzig, K.H., et al., *Regulation of the action of the novel cholecystokinin-releasing peptide diazepam binding inhibitor by inhibitory hormones and taurocholate.* Regul Pept, 1998. **74**(2-3): p. 193-8.
10. Mandrup, S., et al., *Acyl-CoA-binding protein/diazepam-binding inhibitor gene and pseudogenes. A typical housekeeping gene family.* J Mol Biol, 1992. **228**(3): p. 1011-22.
11. Mandrup, S., et al., *Genome organization and expression of the rat ACBP gene family.* Mol Cell Biochem, 1993. **123**(1-2): p. 55-61.
12. Burton, M., et al., *Evolution of the acyl-CoA binding protein (ACBP).* Biochem J, 2005. **392**(Pt 2): p. 299-307.
13. Faergeman, N.J., et al., *Acyl-CoA binding proteins; structural and functional conservation over 2000 MYA.* Mol Cell Biochem, 2007. **299**(1-2): p. 55-65.
14. Burgi, B., et al., *Ontogeny of diazepam binding inhibitor/acyl-CoA binding protein mRNA and peripheral benzodiazepine receptor mRNA expression in the rat.* J Neuroendocrinol, 1999. **11**(2): p. 85-100.
15. Neess, D., et al., *ACBP--a PPAR and SREBP modulated housekeeping gene.* Mol Cell Biochem, 2006. **284**(1-2): p. 149-57.
16. Bloksgaard, M., et al., *The acyl-CoA binding protein is required for normal epidermal barrier function in mice.* J Lipid Res, 2012. **53**(10): p. 2162-74.
17. Bek, S., et al., *Compromised epidermal barrier stimulates Harderian gland activity and hypertrophy in ACBP-/- mice.* J Lipid Res, 2015. **56**(9): p. 1738-46.
18. Elholm, M., et al., *Regulatory elements in the promoter region of the rat gene encoding the acyl-CoA-binding protein.* Gene, 1996. **173**(2): p. 233-8.
19. Helledie, T., et al., *The gene encoding the Acyl-CoA-binding protein is activated by peroxisome proliferator-activated receptor gamma through an intronic response element functionally conserved between humans and rodents.* J Biol Chem, 2002. **277**(30): p. 26821-30.

20. Kolmer, M., et al., *Cloning and tissue-specific functional characterization of the promoter of the rat diazepam binding inhibitor, a peptide with multiple biological actions.* Proc Natl Acad Sci U S A, 1993. **90**(18): p. 8439-43.
21. Swinnen, J.V., et al., *Identification of diazepam-binding Inhibitor/Acyl-CoA-binding protein as a sterol regulatory element-binding protein-responsive gene.* J Biol Chem, 1998. **273**(32): p. 19938-44.
22. Sandberg, M.B., et al., *The gene encoding acyl-CoA-binding protein is subject to metabolic regulation by both sterol regulatory element-binding protein and peroxisome proliferator-activated receptor alpha in hepatocytes.* J Biol Chem, 2005. **280**(7): p. 5258-66.
23. Bhuiyan, J., et al., *Effects of high-fat diet and fasting on levels of acyl-coenzyme A binding protein in liver, kidney, and heart of rat.* Metabolism, 1995. **44**(9): p. 1185-9.
24. Hansen, H.O., et al., *Induction of acyl-CoA-binding protein and its mRNA in 3T3-L1 cells by insulin during preadipocyte-to-adipocyte differentiation.* Biochem J, 1991. **277 (Pt 2)**: p. 341-4.
25. Shimano, H., et al., *Sterol regulatory element-binding protein-1 as a key transcription factor for nutritional induction of lipogenic enzyme genes.* J Biol Chem, 1999. **274**(50): p. 35832-9.
26. Horton, J.D., et al., *Regulation of sterol regulatory element binding proteins in livers of fasted and refed mice.* Proc Natl Acad Sci U S A, 1998. **95**(11): p. 5987-92.
27. Andersen, K.V. and F.M. Poulsen, *Three-dimensional structure in solution of acyl-coenzyme A binding protein from bovine liver.* J Mol Biol, 1992. **226**(4): p. 1131-41.
28. Kragelund, B.B., et al., *Three-dimensional structure of the complex between acyl-coenzyme A binding protein and palmitoyl-coenzyme A.* J Mol Biol, 1993. **230**(4): p. 1260-77.
29. Teilum, K., et al., *Different secondary structure elements as scaffolds for protein folding transition states of two homologous four-helix bundles.* Proteins, 2005. **59**(1): p. 80-90.
30. Taskinen, J.P., et al., *High resolution crystal structures of unliganded and liganded human liver ACBP reveal a new mode of binding for the acyl-CoA ligand.* Proteins, 2007. **66**(1): p. 229-38.
31. Rosendal, J., P. Ertbjerg, and J. Knudsen, *Characterization of ligand binding to acyl-CoA-binding protein.* Biochem J, 1993. **290 (Pt 2)**: p. 321-6.
32. Faergeman, N.J., et al., *Thermodynamics of ligand binding to acyl-coenzyme A binding protein studied by titration calorimetry.* Biochemistry, 1996. **35**(45): p. 14118-26.
33. Knudsen, J., et al., *The function of acyl-CoA-binding protein (ACBP)/diazepam binding inhibitor (DBI).* Mol Cell Biochem, 1993. **123**(1-2): p. 129-38.
34. Mandrup, S., et al., *Effect of heterologous expression of acyl-CoA-binding protein on acyl-CoA level and composition in yeast.* Biochem J, 1993. **290 (Pt 2)**: p. 369-74.
35. Rasmussen, J.T., J. Rosendal, and J. Knudsen, *Interaction of acyl-CoA binding protein (ACBP) on processes for which acyl-CoA is a substrate, product or inhibitor.* Biochem J, 1993. **292 (Pt 3)**: p. 907-13.
36. Bhuiyan, A.K. and S.V. Pande, *Carnitine palmitoyltransferase activities: effects of serum albumin, acyl-CoA binding protein and fatty acid binding protein.* Mol Cell Biochem, 1994. **139**(2): p. 109-16.
37. Fyrst, H., et al., *Detection of acyl-CoA-binding protein in human red blood cells and investigation of its role in membrane phospholipid renewal.* Biochem J, 1995. **306 (Pt 3)**: p. 793-9.
38. Kerkhoff, C., et al., *Acyl-CoA binding protein (ACBP) regulates acyl-CoA:cholesterol acyltransferase (ACAT) in human mononuclear phagocytes.* Biochim Biophys Acta, 1997. **1346**(2): p. 163-72.
39. Chao, H., et al., *ACBP and cholesterol differentially alter fatty acyl CoA utilization by microsomal ACAT.* J Lipid Res, 2003. **44**(1): p. 72-83.
40. Kannan, L., J. Knudsen, and C.A. Jolly, *Aging and acyl-CoA binding protein alter mitochondrial glycerol-3-phosphate acyltransferase activity.* Biochim Biophys Acta, 2003. **1631**(1): p. 12-6.
41. Abo-Hashema, K.A., et al., *The interaction of acyl-CoA with acyl-CoA binding protein and carnitine palmitoyltransferase I.* Int J Biochem Cell Biol, 2001. **33**(8): p. 807-15.

42. Rasmussen, J.T., et al., *Acyl-CoA-binding protein (ACBP) can mediate intermembrane acyl-CoA transport and donate acyl-CoA for beta-oxidation and glycerolipid synthesis.* Biochem J, 1994. **299 (Pt 1)**: p. 165-70.
43. Faergeman, N.J. and J. Knudsen, *Acyl-CoA binding protein is an essential protein in mammalian cell lines.* Biochem J, 2002. **368**(Pt 3): p. 679-82.
44. Vock, C., et al., *ACBP knockdown leads to down-regulation of genes encoding rate-limiting enzymes in cholesterol and fatty acid metabolism.* Cell Physiol Biochem, 2010. **25**(6): p. 675-86.
45. Mandrup, S., et al., *Inhibition of 3T3-L1 adipocyte differentiation by expression of acyl-CoA-binding protein antisense RNA.* J Biol Chem, 1998. **273**(37): p. 23897-903.
46. Gaigg, B., et al., *Depletion of acyl-coenzyme A-binding protein affects sphingolipid synthesis and causes vesicle accumulation and membrane defects in Saccharomyces cerevisiae.* Mol Biol Cell, 2001. **12**(4): p. 1147-60.
47. Schjerling, C.K., et al., *Disruption of the gene encoding the acyl-CoA-binding protein (ACB1) perturbs acyl-CoA metabolism in Saccharomyces cerevisiae.* J Biol Chem, 1996. **271**(37): p. 22514-21.
48. Faergeman, N.J., et al., *Acyl-CoA-binding protein, Acb1p, is required for normal vacuole function and ceramide synthesis in Saccharomyces cerevisiae.* Biochem J, 2004. **380**(Pt 3): p. 907-18.
49. Knudsen, J., et al., *Yeast acyl-CoA-binding protein: acyl-CoA-binding affinity and effect on intracellular acyl-CoA pool size.* Biochem J, 1994. **302 (Pt 2)**: p. 479-85.
50. Feddersen, S., et al., *Transcriptional regulation of phospholipid biosynthesis is linked to fatty acid metabolism by an acyl-CoA-binding-protein-dependent mechanism in Saccharomyces cerevisiae.* Biochem J, 2007. **407**(2): p. 219-30.
51. Elle, I.C., et al., *Tissue- and paralogue-specific functions of acyl-CoA-binding proteins in lipid metabolism in Caenorhabditis elegans.* Biochem J, 2011. **437**(2): p. 231-41.
52. Huang, H., et al., *Acyl-coenzyme A binding protein expression alters liver fatty acyl-coenzyme A metabolism.* Biochemistry, 2005. **44**(30): p. 10282-97.
53. Oikari, S., et al., *Downregulation of PPARs and SREBP by acyl-CoA-binding protein overexpression in transgenic rats.* Pflugers Arch, 2008. **456**(2): p. 369-77.
54. Landrock, D., et al., *Acyl-CoA binding protein gene ablation induces pre-implantation embryonic lethality in mice.* Lipids, 2010. **45**(7): p. 567-80.
55. Lee, L., et al., *Loss of the acyl-CoA binding protein (Acbp) results in fatty acid metabolism abnormalities in mouse hair and skin.* J Invest Dermatol, 2007. **127**(1): p. 16-23.
56. Ohgami, R.S., et al., *nm1054: a spontaneous, recessive, hypochromic, microcytic anemia mutation in the mouse.* Blood, 2005. **106**(10): p. 3625-31.
57. Neess, D., et al., *Disruption of the acyl-CoA-binding protein gene delays hepatic adaptation to metabolic changes at weaning.* J Biol Chem, 2011. **286**(5): p. 3460-72.
58. Neess, D., et al., *Delayed hepatic adaptation to weaning in ACBP-/- mice is caused by disruption of the epidermal barrier.* Cell Rep, 2013. **5**(5): p. 1403-12.
59. Langaa, S., et al., *Mice with targeted disruption of the acyl-CoA binding protein display attenuated urine concentrating ability and diminished renal aquaporin-3 abundance.* Am J Physiol Renal Physiol, 2012. **302**(8): p. F1034-44.
60. Thudichum, J.L.W., *A treatise on the chemical constitution of the brain*. 1884, London: Bailliere, Tindall and Cox.
61. Carter, H.E., et al., *Biochemistry of the Sphingolipides .3. Structure of Sphingosine.* Journal of Biological Chemistry, 1947. **170**(1): p. 285-294.

62. Farwanah, H., et al., *Separation and mass spectrometric characterization of covalently bound skin ceramides using LC/APCI-MS and Nano-ESI-MS/MS.* J Chromatogr B Analyt Technol Biomed Life Sci, 2007. **852**(1-2): p. 562-70.
63. Stewart, M.E. and D.T. Downing, *Free sphingosines of human skin include 6-hydroxysphingosine and unusually long-chain dihydrosphingosines.* J Invest Dermatol, 1995. **105**(4): p. 613-8.
64. Karlsson, K.A., *On the chemistry and occurrence of sphingolipid long-chain bases.* Chem Phys Lipids, 1970. **5**(1): p. 6-43.
65. Karlsson, K.A., *Sphingolipid long chain bases.* Lipids, 1970. **5**(11): p. 878-91.
66. Gault, C.R., L.M. Obeid, and Y.A. Hannun, *An overview of sphingolipid metabolism: from synthesis to breakdown.* Adv Exp Med Biol, 2010. **688**: p. 1-23.
67. Zheng, W., et al., *Ceramides and other bioactive sphingolipid backbones in health and disease: lipidomic analysis, metabolism and roles in membrane structure, dynamics, signaling and autophagy.* Biochim Biophys Acta, 2006. **1758**(12): p. 1864-84.
68. Pruett, S.T., et al., *Biodiversity of sphingoid bases ("sphingosines") and related amino alcohols.* J Lipid Res, 2008. **49**(8): p. 1621-39.
69. Hannun, Y.A. and L.M. Obeid, *Many ceramides.* J Biol Chem, 2011. **286**(32): p. 27855-62.
70. Astudillo, L., et al., *Human genetic disorders of sphingolipid biosynthesis.* J Inherit Metab Dis, 2015. **38**(1): p. 65-76.
71. Wegner, M.S., et al., *The enigma of ceramide synthase regulation in mammalian cells.* Prog Lipid Res, 2016. **63**: p. 93-119.
72. Levy, M. and A.H. Futerman, *Mammalian ceramide synthases.* IUBMB Life, 2010. **62**(5): p. 347-56.
73. Mandon, E.C., et al., *Subcellular localization and membrane topology of serine palmitoyltransferase, 3-dehydrosphinganine reductase, and sphinganine N-acyltransferase in mouse liver.* J Biol Chem, 1992. **267**(16): p. 11144-8.
74. Mesicek, J., et al., *Ceramide synthases 2, 5, and 6 confer distinct roles in radiation-induced apoptosis in HeLa cells.* Cell Signal, 2010. **22**(9): p. 1300-7.
75. Hirschberg, K., J. Rodger, and A.H. Futerman, *The long-chain sphingoid base of sphingolipids is acylated at the cytosolic surface of the endoplasmic reticulum in rat liver.* Biochem J, 1993. **290 (Pt 3)**: p. 751-7.
76. Tidhar, R., et al., *Acyl chain specificity of ceramide synthases is determined within a region of 150 residues in the Tram-Lag-CLN8 (TLC) domain.* J Biol Chem, 2012. **287**(5): p. 3197-206.
77. Rost, B., *PHD: predicting one-dimensional protein structure by profile-based neural networks.* Methods Enzymol, 1996. **266**: p. 525-39.
78. Winter, E. and C.P. Ponting, *TRAM, LAG1 and CLN8: members of a novel family of lipid-sensing domains?* Trends Biochem Sci, 2002. **27**(8): p. 381-3.
79. Venkataraman, K. and A.H. Futerman, *Do longevity assurance genes containing Hox domains regulate cell development via ceramide synthesis?* FEBS Lett, 2002. **528**(1-3): p. 3-4.
80. Mesika, A., et al., *A new functional motif in Hox domain-containing ceramide synthases: identification of a novel region flanking the Hox and TLC domains essential for activity.* J Biol Chem, 2007. **282**(37): p. 27366-73.
81. Spassieva, S., et al., *Necessary role for the Lag1p motif in (dihydro)ceramide synthase activity.* J Biol Chem, 2006. **281**(45): p. 33931-8.
82. Kageyama-Yahara, N. and H. Riezman, *Transmembrane topology of ceramide synthase in yeast.* Biochem J, 2006. **398**(3): p. 585-93.
83. Jiang, J.C., et al., *Homologs of the yeast longevity gene LAG1 in Caenorhabditis elegans and human.* Genome Res, 1998. **8**(12): p. 1259-72.

84. Laviad, E.L., et al., *Modulation of ceramide synthase activity via dimerization.* J Biol Chem, 2012. **287**(25): p. 21025-33.
85. Ohno, Y., et al., *ELOVL1 production of C24 acyl-CoAs is linked to C24 sphingolipid synthesis.* Proc Natl Acad Sci U S A, 2010. **107**(43): p. 18439-44.
86. Sassa, T., T. Hirayama, and A. Kihara, *Enzyme Activities of the Ceramide Synthases CERS2-6 Are Regulated by Phosphorylation in the C-terminal Region.* J Biol Chem, 2016. **291**(14): p. 7477-87.
87. Pewzner-Jung, Y., S. Ben-Dor, and A.H. Futerman, *When do Lasses (longevity assurance genes) become CerS (ceramide synthases)?: Insights into the regulation of ceramide synthesis.* J Biol Chem, 2006. **281**(35): p. 25001-5.
88. Ginkel, C., et al., *Ablation of neuronal ceramide synthase 1 in mice decreases ganglioside levels and expression of myelin-associated glycoprotein in oligodendrocytes.* J Biol Chem, 2012. **287**(50): p. 41888-902.
89. Venkataraman, K., et al., *Upstream of growth and differentiation factor 1 (uog1), a mammalian homolog of the yeast longevity assurance gene 1 (LAG1), regulates N-stearoyl-sphinganine (C18-(dihydro)ceramide) synthesis in a fumonisin B1-independent manner in mammalian cells.* J Biol Chem, 2002. **277**(38): p. 35642-9.
90. Laviad, E.L., et al., *Characterization of ceramide synthase 2: tissue distribution, substrate specificity, and inhibition by sphingosine 1-phosphate.* J Biol Chem, 2008. **283**(9): p. 5677-84.
91. Rabionet, M., et al., *Male germ cells require polyenoic sphingolipids with complex glycosylation for completion of meiosis: a link to ceramide synthase-3.* J Biol Chem, 2008. **283**(19): p. 13357-69.
92. Mizutani, Y., A. Kihara, and Y. Igarashi, *LASS3 (longevity assurance homologue 3) is a mainly testis-specific (dihydro)ceramide synthase with relatively broad substrate specificity.* Biochem J, 2006. **398**(3): p. 531-8.
93. Mizutani, Y., et al., *2-Hydroxy-ceramide synthesis by ceramide synthase family: enzymatic basis for the preference of FA chain length.* J Lipid Res, 2008. **49**(11): p. 2356-64.
94. Riebeling, C., et al., *Two mammalian longevity assurance gene (LAG1) family members, trh1 and trh4, regulate dihydroceramide synthesis using different fatty acyl-CoA donors.* J Biol Chem, 2003. **278**(44): p. 43452-9.
95. Xu, Z., et al., *LASS5 is the predominant ceramide synthase isoform involved in de novo sphingolipid synthesis in lung epithelia.* J Lipid Res, 2005. **46**(6): p. 1229-38.
96. Becker, I., et al., *Differential expression of (dihydro)ceramide synthases in mouse brain: oligodendrocyte-specific expression of CerS2/Lass2.* Histochem Cell Biol, 2008. **129**(2): p. 233-41.
97. Ebel, P., et al., *Inactivation of ceramide synthase 6 in mice results in an altered sphingolipid metabolism and behavioral abnormalities.* J Biol Chem, 2013. **288**(29): p. 21433-47.
98. Castro, B.M., M. Prieto, and L.C. Silva, *Ceramide: a simple sphingolipid with unique biophysical properties.* Prog Lipid Res, 2014. **54**: p. 53-67.
99. Bikman, B.T. and S.A. Summers, *Ceramides as modulators of cellular and whole-body metabolism.* J Clin Invest, 2011. **121**(11): p. 4222-30.
100. Uchida, Y., *Ceramide signaling in mammalian epidermis.* Biochim Biophys Acta, 2014. **1841**(3): p. 453-62.
101. Chavez, J.A. and S.A. Summers, *A ceramide-centric view of insulin resistance.* Cell Metab, 2012. **15**(5): p. 585-94.
102. Raichur, S., et al., *CerS2 haploinsufficiency inhibits beta-oxidation and confers susceptibility to diet-induced steatohepatitis and insulin resistance.* Cell Metab, 2014. **20**(4): p. 687-95.
103. Kihara, A. and Y. Igarashi, *FVT-1 is a mammalian 3-ketodihydrosphingosine reductase with an active site that faces the cytosolic side of the endoplasmic reticulum membrane.* J Biol Chem, 2004. **279**(47): p. 49243-50.

104. Vanechten, G. and K. Sandhoff, *Ganglioside Metabolism - Enzymology, Topology, and Regulation.* Journal of Biological Chemistry, 1993. **268**(8): p. 5341-5344.
105. Cadena, D.L., R.C. Kurten, and G.N. Gill, *The product of the MLD gene is a member of the membrane fatty acid desaturase family: overexpression of MLD inhibits EGF receptor biosynthesis.* Biochemistry, 1997. **36**(23): p. 6960-7.
106. Ezoe, T., et al., *Biochemistry and neuropathology of mice doubly deficient in synthesis and degradation of galactosylceramide.* J Neurosci Res, 2000. **59**(2): p. 170-8.
107. Vacaru, A.M., et al., *Sphingomyelin synthase-related protein SMSr controls ceramide homeostasis in the ER.* J Cell Biol, 2009. **185**(6): p. 1013-27.
108. Hanada, K., et al., *Molecular machinery for non-vesicular trafficking of ceramide.* Nature, 2003. **426**(6968): p. 803-9.
109. Fukasawa, M., M. Nishijima, and K. Hanada, *Genetic evidence for ATP-dependent endoplasmic reticulum-to-Golgi apparatus trafficking of ceramide for sphingomyelin synthesis in Chinese hamster ovary cells.* J Cell Biol, 1999. **144**(4): p. 673-85.
110. Ichikawa, S., et al., *Expression cloning of a cDNA for human ceramide glucosyltransferase that catalyzes the first glycosylation step of glycosphingolipid synthesis.* Proc Natl Acad Sci U S A, 1996. **93**(10): p. 4638-43.
111. Huitema, K., et al., *Identification of a family of animal sphingomyelin synthases.* EMBO J, 2004. **23**(1): p. 33-44.
112. Ichikawa, S. and Y. Hirabayashi, *Glucosylceramide synthase and glycosphingolipid synthesis.* Trends Cell Biol, 1998. **8**(5): p. 198-202.
113. Stoffel, W., *Functional analysis of acid and neutral sphingomyelinases in vitro and in vivo.* Chem Phys Lipids, 1999. **102**(1-2): p. 107-21.
114. Bajjalieh, S.M., T.F. Martin, and E. Floor, *Synaptic vesicle ceramide kinase. A calcium-stimulated lipid kinase that co-purifies with brain synaptic vesicles.* J Biol Chem, 1989. **264**(24): p. 14354-60.
115. Moore, K.A. and I.R. Lemischka, *Stem cells and their niches.* Science, 2006. **311**(5769): p. 1880-5.
116. Tsuruta, D., et al., *Hemidesmosomes and focal contact proteins: functions and cross-talk in keratinocytes, bullous diseases and wound healing.* J Dermatol Sci, 2011. **62**(1): p. 1-7.
117. Ko, M.S. and M.P. Marinkovich, *Role of dermal-epidermal basement membrane zone in skin, cancer, and developmental disorders.* Dermatol Clin, 2010. **28**(1): p. 1-16.
118. Watt, F.M., *Role of integrins in regulating epidermal adhesion, growth and differentiation.* EMBO J, 2002. **21**(15): p. 3919-26.
119. Blanpain, C. and E. Fuchs, *Epidermal homeostasis: a balancing act of stem cells in the skin.* Nat Rev Mol Cell Biol, 2009. **10**(3): p. 207-17.
120. Fuchs, E. and S. Raghavan, *Getting under the skin of epidermal morphogenesis.* Nat Rev Genet, 2002. **3**(3): p. 199-209.
121. Fuchs, E., *Skin stem cells: rising to the surface.* J Cell Biol, 2008. **180**(2): p. 273-84.
122. Cangkrama, M., S.B. Ting, and C. Darido, *Stem cells behind the barrier.* Int J Mol Sci, 2013. **14**(7): p. 13670-86.
123. Pasparakis, M., I. Haase, and F.O. Nestle, *Mechanisms regulating skin immunity and inflammation.* Nat Rev Immunol, 2014. **14**(5): p. 289-301.
124. Koster, M.I. and D.R. Roop, *Mechanisms regulating epithelial stratification.* Annu Rev Cell Dev Biol, 2007. **23**: p. 93-113.
125. Stern, C.D., *Neural induction: old problem, new findings, yet more questions.* Development, 2005. **132**(9): p. 2007-21.

126. M'Boneko, V. and H.J. Merker, *Development and morphology of the periderm of mouse embryos (days 9-12 of gestation).* Acta Anat (Basel), 1988. **133**(4): p. 325-36.
127. Smart, I.H., *Variation in the plane of cell cleavage during the process of stratification in the mouse epidermis.* Br J Dermatol, 1970. **82**(3): p. 276-82.
128. Lechler, T. and E. Fuchs, *Asymmetric cell divisions promote stratification and differentiation of mammalian skin.* Nature, 2005. **437**(7056): p. 275-80.
129. Clayton, E., et al., *A single type of progenitor cell maintains normal epidermis.* Nature, 2007. **446**(7132): p. 185-9.
130. Koster, M.I., et al., *p63 induces key target genes required for epidermal morphogenesis.* Proc Natl Acad Sci U S A, 2007. **104**(9): p. 3255-60.
131. Hardman, M.J., et al., *Patterned acquisition of skin barrier function during development.* Development, 1998. **125**(8): p. 1541-52.
132. Hanson, J., *The histogenesis of the epidermis in the rat and mouse.* J Anat, 1947. **81**(Pt 2): p. 174-97.
133. Klein, A.M., et al., *Kinetics of cell division in epidermal maintenance.* Phys Rev E Stat Nonlin Soft Matter Phys, 2007. **76**(2 Pt 1): p. 021910.
134. Blanpain, C., V. Horsley, and E. Fuchs, *Epithelial stem cells: turning over new leaves.* Cell, 2007. **128**(3): p. 445-58.
135. Dobereiner, H.G., et al., *Force sensing and generation in cell phases: analyses of complex functions.* J Appl Physiol (1985), 2005. **98**(4): p. 1542-6.
136. Fuchs, E. and H. Green, *Changes in keratin gene expression during terminal differentiation of the keratinocyte.* Cell, 1980. **19**(4): p. 1033-42.
137. Bickenbach, J.R., et al., *Loricrin expression is coordinated with other epidermal proteins and the appearance of lipid lamellar granules in development.* J Invest Dermatol, 1995. **104**(3): p. 405-10.
138. Rassner, U., et al., *Coordinate assembly of lipids and enzyme proteins into epidermal lamellar bodies.* Tissue Cell, 1999. **31**(5): p. 489-98.
139. Feingold, K.R., *Thematic review series: skin lipids. The role of epidermal lipids in cutaneous permeability barrier homeostasis.* J Lipid Res, 2007. **48**(12): p. 2531-46.
140. Manabe, M., et al., *Interaction of filaggrin with keratin filaments during advanced stages of normal human epidermal differentiation and in ichthyosis vulgaris.* Differentiation, 1991. **48**(1): p. 43-50.
141. Candi, E., R. Schmidt, and G. Melino, *The cornified envelope: a model of cell death in the skin.* Nat Rev Mol Cell Biol, 2005. **6**(4): p. 328-40.
142. Eckhart, L., et al., *Cell death by cornification.* Biochim Biophys Acta, 2013. **1833**(12): p. 3471-80.
143. Henry, J., et al., *Update on the epidermal differentiation complex.* Front Biosci (Landmark Ed), 2012. **17**: p. 1517-32.
144. Green, K.J. and C.L. Simpson, *Desmosomes: new perspectives on a classic.* J Invest Dermatol, 2007. **127**(11): p. 2499-515.
145. Niessen, C.M., *Tight junctions/adherens junctions: basic structure and function.* J Invest Dermatol, 2007. **127**(11): p. 2525-32.
146. Mahoney, M.G., et al., *Delineation of diversified desmoglein distribution in stratified squamous epithelia: implications in diseases.* Exp Dermatol, 2006. **15**(2): p. 101-9.
147. Schafer, S., S. Stumpp, and W.W. Franke, *Immunological identification and characterization of the desmosomal cadherin Dsg2 in coupled and uncoupled epithelial cells and in human tissues.* Differentiation, 1996. **60**(2): p. 99-108.
148. Furukawa, F., et al., *Roles of E- and P-cadherin in the human skin.* Microsc Res Tech, 1997. **38**(4): p. 343-52.

149. Brandner, J.M., *Importance of Tight Junctions in Relation to Skin Barrier Function.* Curr Probl Dermatol, 2016. **49**: p. 27-37.
150. Presland, R.B. and B.A. Dale, *Epithelial structural proteins of the skin and oral cavity: function in health and disease.* Crit Rev Oral Biol Med, 2000. **11**(4): p. 383-408.
151. Homberg, M. and T.M. Magin, *Beyond expectations: novel insights into epidermal keratin function and regulation.* Int Rev Cell Mol Biol, 2014. **311**: p. 265-306.
152. Coulombe, P.A. and C.H. Lee, *Defining keratin protein function in skin epithelia: epidermolysis bullosa simplex and its aftermath.* J Invest Dermatol, 2012. **132**(3 Pt 2): p. 763-75.
153. Schweizer, J., et al., *New consensus nomenclature for mammalian keratins.* J Cell Biol, 2006. **174**(2): p. 169-74.
154. Fuchs, E. and K. Weber, *Intermediate filaments: structure, dynamics, function, and disease.* Annu Rev Biochem, 1994. **63**: p. 345-82.
155. Moll, R., et al., *The catalog of human cytokeratins: patterns of expression in normal epithelia, tumors and cultured cells.* Cell, 1982. **31**(1): p. 11-24.
156. Leigh, I.M., et al., *Keratins (K16 and K17) as markers of keratinocyte hyperproliferation in psoriasis in vivo and in vitro.* Br J Dermatol, 1995. **133**(4): p. 501-11.
157. Sano, T., et al., *Long-term alteration in the expression of keratins 6 and 16 in the epidermis of mice after chronic UVB exposure.* Arch Dermatol Res, 2009. **301**(3): p. 227-37.
158. McGowan, K. and P.A. Coulombe, *The wound repair-associated keratins 6, 16, and 17. Insights into the role of intermediate filaments in specifying keratinocyte cytoarchitecture.* Subcell Biochem, 1998. **31**: p. 173-204.
159. Coulombe, P.A., et al., *Point mutations in human keratin 14 genes of epidermolysis bullosa simplex patients: genetic and functional analyses.* Cell, 1991. **66**(6): p. 1301-11.
160. Lloyd, C., et al., *The basal keratin network of stratified squamous epithelia: defining K15 function in the absence of K14.* J Cell Biol, 1995. **129**(5): p. 1329-44.
161. DiGiovanna, J.J. and S.J. Bale, *Clinical heterogeneity in epidermolytic hyperkeratosis.* Arch Dermatol, 1994. **130**(8): p. 1026-35.
162. Reichelt, J., et al., *Formation of a normal epidermis supported by increased stability of keratins 5 and 14 in keratin 10 null mice.* Mol Biol Cell, 2001. **12**(6): p. 1557-68.
163. Dale, B.A., K.A. Holbrook, and P.M. Steinert, *Assembly of stratum corneum basic protein and keratin filaments in macrofibrils.* Nature, 1978. **276**(5689): p. 729-31.
164. Ishida-Yamamoto, A., H. Takahashi, and H. Iizuka, *Immunoelectron microscopy links molecules and morphology in the studies of keratinization.* Eur J Dermatol, 2000. **10**(6): p. 429-35.
165. Gan, S.Q., et al., *Organization, structure, and polymorphisms of the human profilaggrin gene.* Biochemistry, 1990. **29**(40): p. 9432-40.
166. Dale, B.A., K.A. Resing, and J.D. Lonsdale-Eccles, *Filaggrin: a keratin filament associated protein.* Ann N Y Acad Sci, 1985. **455**: p. 330-42.
167. Scott, I.R., C.R. Harding, and J.G. Barrett, *Histidine-rich protein of the keratohyalin granules. Source of the free amino acids, urocanic acid and pyrrolidone carboxylic acid in the stratum corneum.* Biochim Biophys Acta, 1982. **719**(1): p. 110-7.
168. Rawlings, A.V., et al., *Stratum corneum moisturization at the molecular level.* J Invest Dermatol, 1994. **103**(5): p. 731-41.
169. Presland, R.B., et al., *Evidence for specific proteolytic cleavage of the N-terminal domain of human profilaggrin during epidermal differentiation.* J Invest Dermatol, 1997. **108**(2): p. 170-8.
170. Palmer, C.N., et al., *Common loss-of-function variants of the epidermal barrier protein filaggrin are a major predisposing factor for atopic dermatitis.* Nat Genet, 2006. **38**(4): p. 441-6.

171. Sandilands, A., et al., *Prevalent and rare mutations in the gene encoding filaggrin cause ichthyosis vulgaris and predispose individuals to atopic dermatitis.* J Invest Dermatol, 2006. **126**(8): p. 1770-5.
172. Smith, F.J., et al., *Loss-of-function mutations in the gene encoding filaggrin cause ichthyosis vulgaris.* Nat Genet, 2006. **38**(3): p. 337-42.
173. Presland, R.B., et al., *Loss of normal profilaggrin and filaggrin in flaky tail (ft/ft) mice: an animal model for the filaggrin-deficient skin disease ichthyosis vulgaris.* J Invest Dermatol, 2000. **115**(6): p. 1072-81.
174. Lee, S.C., et al., *The structure of human trichohyalin. Potential multiple roles as a functional EF-hand-like calcium-binding protein, a cornified cell envelope precursor, and an intermediate filament-associated (cross-linking) protein.* J Biol Chem, 1993. **268**(16): p. 12164-76.
175. Yoneda, K., et al., *The human loricrin gene.* J Biol Chem, 1992. **267**(25): p. 18060-6.
176. Hohl, D., et al., *The small proline-rich proteins constitute a multigene family of differentially regulated cornified cell envelope precursor proteins.* J Invest Dermatol, 1995. **104**(6): p. 902-9.
177. Steinert, P.M. and L.N. Marekov, *Direct evidence that involucrin is a major early isopeptide cross-linked component of the keratinocyte cornified cell envelope.* J Biol Chem, 1997. **272**(3): p. 2021-30.
178. Koch, P.J., et al., *Lessons from loricrin-deficient mice: compensatory mechanisms maintaining skin barrier function in the absence of a major cornified envelope protein.* J Cell Biol, 2000. **151**(2): p. 389-400.
179. Green, H. and P. Djian, *Consecutive actions of different gene-altering mechanisms in the evolution of involucrin.* Mol Biol Evol, 1992. **9**(6): p. 977-1017.
180. Marekov, L.N. and P.M. Steinert, *Ceramides are bound to structural proteins of the human foreskin epidermal cornified cell envelope.* J Biol Chem, 1998. **273**(28): p. 17763-70.
181. Gibbs, S., et al., *Molecular characterization and evolution of the SPRR family of keratinocyte differentiation markers encoding small proline-rich proteins.* Genomics, 1993. **16**(3): p. 630-7.
182. Steinert, P.M. and L.N. Marekov, *The proteins elafin, filaggrin, keratin intermediate filaments, loricrin, and small proline-rich proteins 1 and 2 are isodipeptide cross-linked components of the human epidermal cornified cell envelope.* J Biol Chem, 1995. **270**(30): p. 17702-11.
183. Steinert, P.M., et al., *Small proline-rich proteins are cross-bridging proteins in the cornified cell envelopes of stratified squamous epithelia.* J Struct Biol, 1998. **122**(1-2): p. 76-85.
184. Candi, E., et al., *Transglutaminase cross-linking properties of the small proline-rich 1 family of cornified cell envelope proteins. Integration with loricrin.* J Biol Chem, 1999. **274**(11): p. 7226-37.
185. Hynes, N.E. and H.A. Lane, *ERBB receptors and cancer: the complexity of targeted inhibitors.* Nat Rev Cancer, 2005. **5**(5): p. 341-54.
186. Schneider, M.R., et al., *Beyond wavy hairs: the epidermal growth factor receptor and its ligands in skin biology and pathology.* Am J Pathol, 2008. **173**(1): p. 14-24.
187. Sibilia, M., et al., *The epidermal growth factor receptor: from development to tumorigenesis.* Differentiation, 2007. **75**(9): p. 770-87.
188. Pastore, S., et al., *The epidermal growth factor receptor system in skin repair and inflammation.* J Invest Dermatol, 2008. **128**(6): p. 1365-74.
189. Sibilia, M., et al., *The EGF receptor provides an essential survival signal for SOS-dependent skin tumor development.* Cell, 2000. **102**(2): p. 211-20.
190. Suzuki, Y., et al., *Targeted disruption of LIG-1 gene results in psoriasiform epidermal hyperplasia.* FEBS Lett, 2002. **521**(1-3): p. 67-71.
191. Guasch, G., et al., *Loss of TGFbeta signaling destabilizes homeostasis and promotes squamous cell carcinomas in stratified epithelia.* Cancer Cell, 2007. **12**(4): p. 313-27.
192. Franzke, C.W., et al., *Epidermal ADAM17 maintains the skin barrier by regulating EGFR ligand-dependent terminal keratinocyte differentiation.* J Exp Med, 2012. **209**(6): p. 1105-19.

193. Yang, A., et al., *p63, a p53 homolog at 3q27-29, encodes multiple products with transactivating, death-inducing, and dominant-negative activities.* Mol Cell, 1998. **2**(3): p. 305-16.
194. Laurikkala, J., et al., *p63 regulates multiple signalling pathways required for ectodermal organogenesis and differentiation.* Development, 2006. **133**(8): p. 1553-63.
195. Carroll, D.K., et al., *p63 regulates an adhesion programme and cell survival in epithelial cells.* Nat Cell Biol, 2006. **8**(6): p. 551-61.
196. Barbieri, C.E., C.E. Barton, and J.A. Pietenpol, *Delta Np63 alpha expression is regulated by the phosphoinositide 3-kinase pathway.* J Biol Chem, 2003. **278**(51): p. 51408-14.
197. Mills, A.A., et al., *p63 is a p53 homologue required for limb and epidermal morphogenesis.* Nature, 1999. **398**(6729): p. 708-13.
198. Yang, A., et al., *p63 is essential for regenerative proliferation in limb, craniofacial and epithelial development.* Nature, 1999. **398**(6729): p. 714-8.
199. Senoo, M., et al., *p63 Is essential for the proliferative potential of stem cells in stratified epithelia.* Cell, 2007. **129**(3): p. 523-36.
200. Menon, G.K., S. Grayson, and P.M. Elias, *Ionic calcium reservoirs in mammalian epidermis: ultrastructural localization by ion-capture cytochemistry.* J Invest Dermatol, 1985. **84**(6): p. 508-12.
201. Menon, G.K., et al., *Localization of calcium in murine epidermis following disruption and repair of the permeability barrier.* Cell Tissue Res, 1992. **270**(3): p. 503-12.
202. Elias, P.M., et al., *Formation of the epidermal calcium gradient coincides with key milestones of barrier ontogenesis in the rodent.* J Invest Dermatol, 1998. **110**(4): p. 399-404.
203. Hennings, H., et al., *Calcium regulation of growth and differentiation of mouse epidermal cells in culture.* Cell, 1980. **19**(1): p. 245-54.
204. Hennings, H. and K.A. Holbrook, *Calcium regulation of cell-cell contact and differentiation of epidermal cells in culture. An ultrastructural study.* Exp Cell Res, 1983. **143**(1): p. 127-42.
205. Zamansky, G.B., U. Nguyen, and I.N. Chou, *An immunofluorescence study of the calcium-induced coordinated reorganization of microfilaments, keratin intermediate filaments, and microtubules in cultured human epidermal keratinocytes.* J Invest Dermatol, 1991. **97**(6): p. 985-94.
206. Yuspa, S.H., et al., *Expression of murine epidermal differentiation markers is tightly regulated by restricted extracellular calcium concentrations in vitro.* J Cell Biol, 1989. **109**(3): p. 1207-17.
207. Pillai, S., et al., *Calcium regulation of growth and differentiation of normal human keratinocytes: modulation of differentiation competence by stages of growth and extracellular calcium.* J Cell Physiol, 1990. **143**(2): p. 294-302.
208. Su, M.J., et al., *1,25-Dihydroxyvitamin D3 potentiates the keratinocyte response to calcium.* J Biol Chem, 1994. **269**(20): p. 14723-9.
209. Rubin, A.L., N.L. Parenteau, and R.H. Rice, *Coordination of keratinocyte programming in human SCC-13 squamous carcinoma and normal epidermal cells.* J Cell Physiol, 1989. **138**(1): p. 208-14.
210. Hohl, D., et al., *Transcription of the human loricrin gene in vitro is induced by calcium and cell density and suppressed by retinoic acid.* J Invest Dermatol, 1991. **96**(4): p. 414-8.
211. Ng, D.C., et al., *Regulation of involucrin gene expression by calcium in normal human keratinocytes.* Front Biosci, 1996. **1**: p. a16-24.
212. Huff, C.A., S.H. Yuspa, and D. Rosenthal, *Identification of control elements 3' to the human keratin 1 gene that regulate cell type and differentiation-specific expression.* J Biol Chem, 1993. **268**(1): p. 377-84.
213. Dlugosz, A.A. and S.H. Yuspa, *Coordinate changes in gene expression which mark the spinous to granular cell transition in epidermis are regulated by protein kinase C.* J Cell Biol, 1993. **120**(1): p. 217-25.
214. Schepeler, T., M.E. Page, and K.B. Jensen, *Heterogeneity and plasticity of epidermal stem cells.* Development, 2014. **141**(13): p. 2559-67.

215. Rishikaysh, P., et al., *Signaling involved in hair follicle morphogenesis and development.* Int J Mol Sci, 2014. **15**(1): p. 1647-70.
216. Schmidt-Ullrich, R. and R. Paus, *Molecular principles of hair follicle induction and morphogenesis.* Bioessays, 2005. **27**(3): p. 247-61.
217. Hardy, M.H., *The secret life of the hair follicle.* Trends Genet, 1992. **8**(2): p. 55-61.
218. Millar, S.E., *Molecular mechanisms regulating hair follicle development.* J Invest Dermatol, 2002. **118**(2): p. 216-25.
219. Chase, H.B., *Growth of the hair.* Physiol Rev, 1954. **34**(1): p. 113-26.
220. Chase, H.B., R. Rauch, and V.W. Smith, *Critical stages of hair development and pigmentation in the mouse.* Physiol Zool, 1951. **24**(1): p. 1-8.
221. Stenn, K.S. and R. Paus, *Controls of hair follicle cycling.* Physiol Rev, 2001. **81**(1): p. 449-494.
222. Plikus, M.V. and C.M. Chuong, *Complex hair cycle domain patterns and regenerative hair waves in living rodents.* J Invest Dermatol, 2008. **128**(5): p. 1071-80.
223. Paus, R., et al., *A comprehensive guide for the recognition and classification of distinct stages of hair follicle morphogenesis.* J Invest Dermatol, 1999. **113**(4): p. 523-32.
224. St-Jacques, B., et al., *Sonic hedgehog signaling is essential for hair development.* Curr Biol, 1998. **8**(19): p. 1058-68.
225. Reddy, S., et al., *Characterization of Wnt gene expression in developing and postnatal hair follicles and identification of Wnt5a as a target of Sonic hedgehog in hair follicle morphogenesis.* Mech Dev, 2001. **107**(1-2): p. 69-82.
226. Andl, T., et al., *WNT signals are required for the initiation of hair follicle development.* Dev Cell, 2002. **2**(5): p. 643-53.
227. Atit, R., et al., *Beta-catenin activation is necessary and sufficient to specify the dorsal dermal fate in the mouse.* Dev Biol, 2006. **296**(1): p. 164-76.
228. Enshell-Seijffers, D., et al., *beta-catenin activity in the dermal papilla regulates morphogenesis and regeneration of hair.* Dev Cell, 2010. **18**(4): p. 633-42.
229. Lowry, W.E., et al., *Defining the impact of beta-catenin/Tcf transactivation on epithelial stem cells.* Genes Dev, 2005. **19**(13): p. 1596-611.
230. Bitgood, M.J. and A.P. McMahon, *Hedgehog and Bmp genes are coexpressed at many diverse sites of cell-cell interaction in the mouse embryo.* Dev Biol, 1995. **172**(1): p. 126-38.
231. Kobielak, K., et al., *Defining BMP functions in the hair follicle by conditional ablation of BMP receptor IA.* J Cell Biol, 2003. **163**(3): p. 609-23.
232. Botchkarev, V.A., et al., *Noggin is a mesenchymally derived stimulator of hair-follicle induction.* Nat Cell Biol, 1999. **1**(3): p. 158-64.
233. Horsley, V., et al., *NFATc1 balances quiescence and proliferation of skin stem cells.* Cell, 2008. **132**(2): p. 299-310.
234. Plikus, M.V., et al., *Cyclic dermal BMP signalling regulates stem cell activation during hair regeneration.* Nature, 2008. **451**(7176): p. 340-4.
235. Botchkarev, V.A., et al., *Noggin is required for induction of the hair follicle growth phase in postnatal skin.* Faseb j, 2001. **15**(12): p. 2205-14.
236. Blessing, M., et al., *Transgenic mice as a model to study the role of TGF-beta-related molecules in hair follicles.* Genes Dev, 1993. **7**(2): p. 204-15.
237. Kulessa, H., G. Turk, and B.L. Hogan, *Inhibition of Bmp signaling affects growth and differentiation in the anagen hair follicle.* Embo j, 2000. **19**(24): p. 6664-74.
238. Rendl, M., L. Polak, and E. Fuchs, *BMP signaling in dermal papilla cells is required for their hair follicle-inductive properties.* Genes Dev, 2008. **22**(4): p. 543-57.

239. Weerheim, A. and M. Ponec, *Determination of stratum corneum lipid profile by tape stripping in combination with high-performance thin-layer chromatography.* Arch Dermatol Res, 2001. **293**(4): p. 191-9.
240. Norlen, L., et al., *A new HPLC-based method for the quantitative analysis of inner stratum corneum lipids with special reference to the free fatty acid fraction.* Arch Dermatol Res, 1998. **290**(9): p. 508-16.
241. van Smeden, J., et al., *Combined LC/MS-platform for analysis of all major stratum corneum lipids, and the profiling of skin substitutes.* Biochim Biophys Acta, 2014. **1841**(1): p. 70-9.
242. Gray, G.M. and R.J. White, *Glycosphingolipids and ceramides in human and pig epidermis.* J Invest Dermatol, 1978. **70**(6): p. 336-41.
243. Wertz, P.W., et al., *The composition of the ceramides from human stratum corneum and from comedones.* J Invest Dermatol, 1985. **84**(5): p. 410-2.
244. Motta, S., et al., *Ceramide composition of the psoriatic scale.* Biochim Biophys Acta, 1993. **1182**(2): p. 147-51.
245. Breiden, B. and K. Sandhoff, *The role of sphingolipid metabolism in cutaneous permeability barrier formation.* Biochim Biophys Acta, 2014. **1841**(3): p. 441-52.
246. van Smeden, J., et al., *The important role of stratum corneum lipids for the cutaneous barrier function.* Biochim Biophys Acta, 2014. **1841**(3): p. 295-313.
247. Masukawa, Y., et al., *Comprehensive quantification of ceramide species in human stratum corneum.* J Lipid Res, 2009. **50**(8): p. 1708-19.
248. Masukawa, Y., et al., *Characterization of overall ceramide species in human stratum corneum.* J Lipid Res, 2008. **49**(7): p. 1466-76.
249. Rabionet, M., et al., *1-O-acylceramides are natural components of human and mouse epidermis.* J Lipid Res, 2013. **54**(12): p. 3312-21.
250. Jennemann, R., et al., *Loss of ceramide synthase 3 causes lethal skin barrier disruption.* Hum Mol Genet, 2012. **21**(3): p. 586-608.
251. Radner, F.P., et al., *Mutations in CERS3 cause autosomal recessive congenital ichthyosis in humans.* PLoS Genet, 2013. **9**(6): p. e1003536.
252. Eckl, K.M., et al., *Impaired epidermal ceramide synthesis causes autosomal recessive congenital ichthyosis and reveals the importance of ceramide acyl chain length.* J Invest Dermatol, 2013. **133**(9): p. 2202-11.
253. Beld, J., D.J. Lee, and M.D. Burkart, *Fatty acid biosynthesis revisited: structure elucidation and metabolic engineering.* Mol Biosyst, 2015. **11**(1): p. 38-59.
254. Kihara, A., *Very long-chain fatty acids: elongation, physiology and related disorders.* J Biochem, 2012. **152**(5): p. 387-95.
255. Sassa, T. and A. Kihara, *Metabolism of very long-chain Fatty acids: genes and pathophysiology.* Biomol Ther (Seoul), 2014. **22**(2): p. 83-92.
256. Li, W., et al., *Depletion of ceramides with very long chain fatty acids causes defective skin permeability barrier function, and neonatal lethality in ELOVL4 deficient mice.* Int J Biol Sci, 2007. **3**(2): p. 120-8.
257. Vasireddy, V., et al., *Loss of functional ELOVL4 depletes very long-chain fatty acids (> or =C28) and the unique omega-O-acylceramides in skin leading to neonatal death.* Hum Mol Genet, 2007. **16**(5): p. 471-82.
258. Cameron, D.J., et al., *Essential role of Elovl4 in very long chain fatty acid synthesis, skin permeability barrier function, and neonatal survival.* Int J Biol Sci, 2007. **3**(2): p. 111-9.
259. Sassa, T., et al., *Impaired epidermal permeability barrier in mice lacking elovl1, the gene responsible for very-long-chain fatty acid production.* Mol Cell Biol, 2013. **33**(14): p. 2787-96.

260. Li, W., et al., *Elovl4 haploinsufficiency does not induce early onset retinal degeneration in mice.* Vision Res, 2007. **47**(5): p. 714-22.
261. McMahon, A., et al., *Retinal pathology and skin barrier defect in mice carrying a Stargardt disease-3 mutation in elongase of very long chain fatty acids-4.* Mol Vis, 2007. **13**: p. 258-72.
262. Hsu, M.H., et al., *Human cytochrome p450 family 4 enzymes: function, genetic variation and regulation.* Drug Metab Rev, 2007. **39**(2-3): p. 515-38.
263. Lefevre, C., et al., *Mutations in a new cytochrome P450 gene in lamellar ichthyosis type 3.* Hum Mol Genet, 2006. **15**(5): p. 767-76.
264. Ohno, Y., et al., *Essential role of the cytochrome P450 CYP4F22 in the production of acylceramide, the key lipid for skin permeability barrier formation.* Proc Natl Acad Sci U S A, 2015. **112**(25): p. 7707-12.
265. Uchida, Y., et al., *Neutral lipid storage leads to acylceramide deficiency, likely contributing to the pathogenesis of Dorfman-Chanarin syndrome.* J Invest Dermatol, 2010. **130**(10): p. 2497-9.
266. Stone, S.J., et al., *Lipopenia and skin barrier abnormalities in DGAT2-deficient mice.* J Biol Chem, 2004. **279**(12): p. 11767-76.
267. Yamaguchi, T., et al., *CGI-58 facilitates lipolysis on lipid droplets but is not involved in the vesiculation of lipid droplets caused by hormonal stimulation.* J Lipid Res, 2007. **48**(5): p. 1078-89.
268. Fischer, J., et al., *The gene encoding adipose triglyceride lipase (PNPLA2) is mutated in neutral lipid storage disease with myopathy.* Nat Genet, 2007. **39**(1): p. 28-30.
269. Radner, F.P., et al., *Growth retardation, impaired triacylglycerol catabolism, hepatic steatosis, and lethal skin barrier defect in mice lacking comparative gene identification-58 (CGI-58).* J Biol Chem, 2010. **285**(10): p. 7300-11.
270. Haemmerle, G., et al., *Defective lipolysis and altered energy metabolism in mice lacking adipose triglyceride lipase.* Science, 2006. **312**(5774): p. 734-7.
271. Grond, S., et al., *Skin Barrier Development Depends on CGI-58 Protein Expression during Late-Stage Keratinocyte Differentiation.* J Invest Dermatol, 2017. **137**(2): p. 403-413.
272. Ohno, Y., et al., *PNPLA1 is a transacylase essential for the generation of the skin barrier lipid omega-O-acylceramide.* Nat Commun, 2017. **8**: p. 14610.
273. Vahidnezhad, H., et al., *Gene-Targeted Next Generation Sequencing Identifies PNPLA1 Mutations in Patients with a Phenotypic Spectrum of Autosomal Recessive Congenital Ichthyosis: The Impact of Consanguinity.* J Invest Dermatol, 2017. **137**(3): p. 678-685.
274. Hirabayashi, T., et al., *PNPLA1 has a crucial role in skin barrier function by directing acylceramide biosynthesis.* Nat Commun, 2017. **8**: p. 14609.
275. Grond, S., et al., *PNPLA1 Deficiency in Mice and Humans Leads to a Defect in the Synthesis of Omega-O-Acylceramides.* J Invest Dermatol, 2017. **137**(2): p. 394-402.
276. Ishibashi, Y., A. Kohyama-Koganeya, and Y. Hirabayashi, *New insights on glucosylated lipids: metabolism and functions.* Biochim Biophys Acta, 2013. **1831**(9): p. 1475-85.
277. Futerman, A.H. and R.E. Pagano, *Determination of the intracellular sites and topology of glucosylceramide synthesis in rat liver.* Biochem J, 1991. **280 (Pt 2)**: p. 295-302.
278. Jeckel, D., et al., *Glucosylceramide is synthesized at the cytosolic surface of various Golgi subfractions.* J Cell Biol, 1992. **117**(2): p. 259-67.
279. Gallala, H., et al., *Nitric oxide regulates synthesis of gene products involved in keratinocyte differentiation and ceramide metabolism.* Eur J Cell Biol, 2004. **83**(11-12): p. 667-79.
280. Madison, K.C. and E.J. Howard, *Ceramides are transported through the Golgi apparatus in human keratinocytes in vitro.* J Invest Dermatol, 1996. **106**(5): p. 1030-5.

281. Sando, G.N., E.J. Howard, and K.C. Madison, *Induction of ceramide glucosyltransferase activity in cultured human keratinocytes. Correlation with culture differentiation.* J Biol Chem, 1996. **271**(36): p. 22044-51.
282. Jennemann, R., et al., *Integrity and barrier function of the epidermis critically depend on glucosylceramide synthesis.* J Biol Chem, 2007. **282**(5): p. 3083-94.
283. Amen, N., et al., *Differentiation of epidermal keratinocytes is dependent on glucosylceramide:ceramide processing.* Hum Mol Genet, 2013. **22**(20): p. 4164-79.
284. Kelsell, D.P., et al., *Mutations in ABCA12 underlie the severe congenital skin disease harlequin ichthyosis.* Am J Hum Genet, 2005. **76**(5): p. 794-803.
285. Yanagi, T., et al., *Harlequin ichthyosis model mouse reveals alveolar collapse and severe fetal skin barrier defects.* Hum Mol Genet, 2008. **17**(19): p. 3075-83.
286. Zuo, Y., et al., *ABCA12 maintains the epidermal lipid permeability barrier by facilitating formation of ceramide linoleic esters.* J Biol Chem, 2008. **283**(52): p. 36624-35.
287. Grayson, S., et al., *Lamellar body-enriched fractions from neonatal mice: preparative techniques and partial characterization.* J Invest Dermatol, 1985. **85**(4): p. 289-94.
288. Madison, K.C., et al., *Lamellar granule biogenesis: a role for ceramide glucosyltransferase, lysosomal enzyme transport, and the Golgi.* J Investig Dermatol Symp Proc, 1998. **3**(2): p. 80-6.
289. Kolter, T., et al., *Lipid-binding proteins in membrane digestion, antigen presentation, and antimicrobial defense.* J Biol Chem, 2005. **280**(50): p. 41125-8.
290. Zheng, Y., et al., *Lipoxygenases mediate the effect of essential fatty acid in skin barrier formation: a proposed role in releasing omega-hydroxyceramide for construction of the corneocyte lipid envelope.* J Biol Chem, 2011. **286**(27): p. 24046-56.
291. Krieg, P., et al., *Aloxe3 knockout mice reveal a function of epidermal lipoxygenase-3 as hepoxilin synthase and its pivotal role in barrier formation.* J Invest Dermatol, 2013. **133**(1): p. 172-80.
292. Epp, N., et al., *12R-lipoxygenase deficiency disrupts epidermal barrier function.* J Cell Biol, 2007. **177**(1): p. 173-82.
293. Moran, J.L., et al., *A mouse mutation in the 12R-lipoxygenase, Alox12b, disrupts formation of the epidermal permeability barrier.* J Invest Dermatol, 2007. **127**(8): p. 1893-7.
294. Dick, A., et al., *Diminished Protein-Bound omega-Hydroxylated Ceramides In The Skin Of Ichthyosis Patients With 12r-Lox Or Elox-3 Deficiency.* Br J Dermatol, 2017.
295. Elias, P.M., et al., *Formation and functions of the corneocyte lipid envelope (CLE).* Biochim Biophys Acta, 2014. **1841**(3): p. 314-8.
296. Doering, T., R.L. Proia, and K. Sandhoff, *Accumulation of protein-bound epidermal glucosylceramides in beta-glucocerebrosidase deficient type 2 Gaucher mice.* FEBS Lett, 1999. **447**(2-3): p. 167-70.
297. Nemes, Z., et al., *A novel function for transglutaminase 1: attachment of long-chain omega-hydroxyceramides to involucrin by ester bond formation.* Proc Natl Acad Sci U S A, 1999. **96**(15): p. 8402-7.
298. Holleran, W.M., et al., *Consequences of beta-glucocerebrosidase deficiency in epidermis. Ultrastructure and permeability barrier alterations in Gaucher disease.* J Clin Invest, 1994. **93**(4): p. 1756-64.
299. Wilkening, G., T. Linke, and K. Sandhoff, *Lysosomal degradation on vesicular membrane surfaces. Enhanced glucosylceramide degradation by lysosomal anionic lipids and activators.* J Biol Chem, 1998. **273**(46): p. 30271-8.
300. Doering, T., et al., *Sphingolipid activator proteins are required for epidermal permeability barrier formation.* J Biol Chem, 1999. **274**(16): p. 11038-45.

301. Fujita, N., et al., *Targeted disruption of the mouse sphingolipid activator protein gene: a complex phenotype, including severe leukodystrophy and wide-spread storage of multiple sphingolipids.* Hum Mol Genet, 1996. **5**(6): p. 711-25.
302. Sidransky, E., D.M. Sherer, and E.I. Ginns, *Gaucher disease in the neonate: a distinct Gaucher phenotype is analogous to a mouse model created by targeted disruption of the glucocerebrosidase gene.* Pediatr Res, 1992. **32**(4): p. 494-8.
303. Grace, M.E., et al., *Non-pseudogene-derived complex acid beta-glucosidase mutations causing mild type 1 and severe type 2 gaucher disease.* J Clin Invest, 1999. **103**(6): p. 817-23.
304. Liu, Y., et al., *Mice with type 2 and 3 Gaucher disease point mutations generated by a single insertion mutagenesis procedure.* Proc Natl Acad Sci U S A, 1998. **95**(5): p. 2503-8.
305. Pappas, A., *Epidermal surface lipids.* Dermatoendocrinol, 2009. **1**(2): p. 72-6.
306. Kostyuk, V., et al., *Photo-oxidation products of skin surface squalene mediate metabolic and inflammatory responses to solar UV in human keratinocytes.* PLoS One, 2012. **7**(8): p. e44472.
307. Nagy, I., et al., *Propionibacterium acnes and lipopolysaccharide induce the expression of antimicrobial peptides and proinflammatory cytokines/chemokines in human sebocytes.* Microbes Infect, 2006. **8**(8): p. 2195-205.
308. Drake, D.R., et al., *Thematic Review Series: Skin Lipids. Antimicrobial lipids at the skin surface.* Journal of Lipid Research, 2008. **49**(1): p. 4-11.
309. Jenkinson, D.M., et al., *Comparative studies of the ultrastructure of the sebaceous gland.* Tissue Cell, 1985. **17**(5): p. 683-98.
310. Schneider, M.R. and R. Paus, *Sebocytes, multifaceted epithelial cells: lipid production and holocrine secretion.* Int J Biochem Cell Biol, 2010. **42**(2): p. 181-5.
311. Smith, K.R. and D.M. Thiboutot, *Thematic review series: skin lipids. Sebaceous gland lipids: friend or foe?* J Lipid Res, 2008. **49**(2): p. 271-81.
312. Niemann, C. and V. Horsley, *Development and homeostasis of the sebaceous gland.* Semin Cell Dev Biol, 2012. **23**(8): p. 928-36.
313. Thody, A.J. and S. Shuster, *Control and function of sebaceous glands.* Physiol Rev, 1989. **69**(2): p. 383-416.
314. Ehrmann, C. and M.R. Schneider, *Genetically modified laboratory mice with sebaceous glands abnormalities.* Cell Mol Life Sci, 2016. **73**(24): p. 4623-4642.
315. Nowak, J.A., et al., *Hair follicle stem cells are specified and function in early skin morphogenesis.* Cell Stem Cell, 2008. **3**(1): p. 33-43.
316. Frances, D. and C. Niemann, *Stem cell dynamics in sebaceous gland morphogenesis in mouse skin.* Dev Biol, 2012. **363**(1): p. 138-46.
317. Jensen, K.B., et al., *Lrig1 expression defines a distinct multipotent stem cell population in mammalian epidermis.* Cell Stem Cell, 2009. **4**(5): p. 427-39.
318. Niemann, C., et al., *Expression of DeltaNLef1 in mouse epidermis results in differentiation of hair follicles into squamous epidermal cysts and formation of skin tumours.* Development, 2002. **129**(1): p. 95-109.
319. Petersson, M., et al., *TCF/Lef1 activity controls establishment of diverse stem and progenitor cell compartments in mouse epidermis.* Embo j, 2011. **30**(15): p. 3004-18.
320. Nguyen, H., M. Rendl, and E. Fuchs, *Tcf3 governs stem cell features and represses cell fate determination in skin.* Cell, 2006. **127**(1): p. 171-83.
321. Han, G., et al., *Smad7-induced beta-catenin degradation alters epidermal appendage development.* Dev Cell, 2006. **11**(3): p. 301-12.
322. Allen, M., et al., *Hedgehog signaling regulates sebaceous gland development.* Am J Pathol, 2003. **163**(6): p. 2173-8.

323. Niemann, C., et al., *Indian hedgehog and beta-catenin signaling: role in the sebaceous lineage of normal and neoplastic mammalian epidermis.* Proc Natl Acad Sci U S A, 2003. **100 Suppl 1**: p. 11873-80.
324. Lapouge, G., et al., *Identifying the cellular origin of squamous skin tumors.* Proc Natl Acad Sci U S A, 2011. **108**(18): p. 7431-6.
325. Smith, T.M., et al., *Insulin-like growth factor-1 induces lipid production in human SEB-1 sebocytes via sterol response element-binding protein-1.* J Invest Dermatol, 2006. **126**(6): p. 1226-32.
326. Smith, T.M., et al., *IGF-1 induces SREBP-1 expression and lipogenesis in SEB-1 sebocytes via activation of the phosphoinositide 3-kinase/Akt pathway.* J Invest Dermatol, 2008. **128**(5): p. 1286-93.
327. Pochi, P.E., J.S. Strauss, and H. Mescon, *Sebum secretion and urinary fractional 17-ketosteroid and total 17-hydroxycorticoid excretion in male castrates.* J Invest Dermatol, 1962. **39**: p. 475-83.
328. Choudhry, R., et al., *Localization of androgen receptors in human skin by immunohistochemistry: implications for the hormonal regulation of hair growth, sebaceous glands and sweat glands.* J Endocrinol, 1992. **133**(3): p. 467-75.
329. Zouboulis, C.C., et al., *Androgens affect the activity of human sebocytes in culture in a manner dependent on the localization of the sebaceous glands and their effect is antagonized by spironolactone.* Skin Pharmacol, 1994. **7**(1-2): p. 33-40.
330. Ebling, F.J., *Hormonal factors influencing the response of the sebaceous gland to androgens.* Proc R Soc Med, 1969. **62**(9): p. 890-1.
331. Ebling, F.J., *The action of an anti-androgenic steroid, 17-alpha-methyl-B-nortestosterone, on sebum secretion in rats treated with testosterone.* J Endocrinol, 1967. **38**(2): p. 181-5.
332. Ebling, F.J. and J. Skinner, *The measurement of sebum production in rats treated with testosterone and oestradiol.* Br J Dermatol, 1967. **79**(7): p. 386-92.
333. Horsley, V., et al., *Blimp1 defines a progenitor population that governs cellular input to the sebaceous gland.* Cell, 2006. **126**(3): p. 597-609.
334. Arnold, I. and F.M. Watt, *c-Myc activation in transgenic mouse epidermis results in mobilization of stem cells and differentiation of their progeny.* Curr Biol, 2001. **11**(8): p. 558-68.
335. Zanet, J., et al., *Endogenous Myc controls mammalian epidermal cell size, hyperproliferation, endoreplication and stem cell amplification.* J Cell Sci, 2005. **118**(Pt 8): p. 1693-704.
336. Rosenfield, R.L., et al., *Mechanisms of androgen induction of sebocyte differentiation.* Dermatology, 1998. **196**(1): p. 43-6.
337. Chen, W., et al., *Expression of peroxisome proliferator-activated receptor and CCAAT/enhancer binding protein transcription factors in cultured human sebocytes.* J Invest Dermatol, 2003. **121**(3): p. 441-7.
338. Dozsa, A., et al., *PPARgamma-mediated and arachidonic acid-dependent signaling is involved in differentiation and lipid production of human sebocytes.* J Invest Dermatol, 2014. **134**(4): p. 910-20.
339. Rosenfield, R.L., et al., *Rat preputial sebocyte differentiation involves peroxisome proliferator-activated receptors.* J Invest Dermatol, 1999. **112**(2): p. 226-32.
340. Trivedi, N.R., et al., *Peroxisome proliferator-activated receptors increase human sebum production.* J Invest Dermatol, 2006. **126**(9): p. 2002-9.
341. Mao-Qiang, M., et al., *Peroxisome-proliferator-activated receptor (PPAR)-gamma activation stimulates keratinocyte differentiation.* J Invest Dermatol, 2004. **123**(2): p. 305-12.
342. Karnik, P., et al., *Hair follicle stem cell-specific PPARgamma deletion causes scarring alopecia.* J Invest Dermatol, 2009. **129**(5): p. 1243-57.
343. Picardo, M., et al., *Sebaceous gland lipids.* Dermatoendocrinol, 2009. **1**(2): p. 68-71.
344. Camera, E., et al., *Comprehensive analysis of the major lipid classes in sebum by rapid resolution high-performance liquid chromatography and electrospray mass spectrometry.* J Lipid Res, 2010. **51**(11): p. 3377-88.

345. Dahlhoff, M., et al., *Characterization of the sebocyte lipid droplet proteome reveals novel potential regulators of sebaceous lipogenesis.* Exp Cell Res, 2015. **332**(1): p. 146-55.
346. Downing, D.T., J.S. Strauss, and P.E. Pochi, *Variability in the chemical composition of human skin surface lipids.* J Invest Dermatol, 1969. **53**(5): p. 322-7.
347. Haahti, E. and E.C. Horning, *Isolation and characterization of saturated and unsaturated fatty acids and alcohols of human skin surface lipids.* Scand J Clin Lab Invest, 1963. **15**: p. 73-8.
348. James, A.T. and V.R. Wheatley, *Studies of sebum. 6. The determination of the component fatty acids of human forearm sebum by gas-liquid chromatography.* Biochem J, 1956. **63**(2): p. 269-73.
349. Nicolaides, N., *Skin lipids: their biochemical uniqueness.* Science, 1974. **186**(4158): p. 19-26.
350. Drake, D.R., et al., *Thematic review series: skin lipids. Antimicrobial lipids at the skin surface.* J Lipid Res, 2008. **49**(1): p. 4-11.
351. Wille, J.J. and A. Kydonieus, *Palmitoleic acid isomer (C16:1delta6) in human skin sebum is effective against gram-positive bacteria.* Skin Pharmacol Appl Skin Physiol, 2003. **16**(3): p. 176-87.
352. Ge, L., et al., *Identification of the delta-6 desaturase of human sebaceous glands: expression and enzyme activity.* J Invest Dermatol, 2003. **120**(5): p. 707-14.
353. Chen, H.C., et al., *Leptin modulates the effects of acyl CoA:diacylglycerol acyltransferase deficiency on murine fur and sebaceous glands.* J Clin Invest, 2002. **109**(2): p. 175-81.
354. Miyazaki, M., W.C. Man, and J.M. Ntambi, *Targeted disruption of stearoyl-CoA desaturase1 gene in mice causes atrophy of sebaceous and meibomian glands and depletion of wax esters in the eyelid.* J Nutr, 2001. **131**(9): p. 2260-8.
355. Cheng, J.B. and D.W. Russell, *Mammalian wax biosynthesis. I. Identification of two fatty acyl-Coenzyme A reductases with different substrate specificities and tissue distributions.* J Biol Chem, 2004. **279**(36): p. 37789-97.
356. Cheng, J.B. and D.W. Russell, *Mammalian wax biosynthesis. II. Expression cloning of wax synthase cDNAs encoding a member of the acyltransferase enzyme family.* J Biol Chem, 2004. **279**(36): p. 37798-807.
357. Yen, C.L., et al., *The triacylglycerol synthesis enzyme DGAT1 also catalyzes the synthesis of diacylglycerols, waxes, and retinyl esters.* J Lipid Res, 2005. **46**(7): p. 1502-11.
358. Yen, C.L., et al., *A human skin multifunctional O-acyltransferase that catalyzes the synthesis of acylglycerols, waxes, and retinyl esters.* J Lipid Res, 2005. **46**(11): p. 2388-97.
359. Faust, P.L. and W.J. Kovacs, *Cholesterol biosynthesis and ER stress in peroxisome deficiency.* Biochimie, 2014. **98**: p. 75-85.
360. Goldstein, J.L. and M.S. Brown, *Regulation of the mevalonate pathway.* Nature, 1990. **343**(6257): p. 425-30.
361. Oku, H., et al., *1-O-alkyl-2,3-diacylglycerols in the skin surface lipids of the hairless mouse.* Lipids, 1995. **30**(2): p. 169-72.
362. Lin, M.H., F.F. Hsu, and J.H. Miner, *Requirement of fatty acid transport protein 4 for development, maturation, and function of sebaceous glands in a mouse model of ichthyosis prematurity syndrome.* J Biol Chem, 2013. **288**(6): p. 3964-76.
363. Herrmann, T., et al., *Mice with targeted disruption of the fatty acid transport protein 4 (Fatp 4, Slc27a4) gene show features of lethal restrictive dermopathy.* J Cell Biol, 2003. **161**(6): p. 1105-15.
364. Sugawara, T., et al., *Reduced size of sebaceous gland and altered sebum lipid composition in mice lacking fatty acid binding protein 5 gene.* Exp Dermatol, 2012. **21**(7): p. 543-6.
365. Westerberg, R., et al., *Role for ELOVL3 and fatty acid chain length in development of hair and skin function.* J Biol Chem, 2004. **279**(7): p. 5621-9.
366. Sundberg, J.P., et al., *Asebia-2J (Scd1(ab2J)): a new allele and a model for scarring alopecia.* Am J Pathol, 2000. **156**(6): p. 2067-75.

367. Sampath, H., et al., *Skin-specific deletion of stearoyl-CoA desaturase-1 alters skin lipid composition and protects mice from high fat diet-induced obesity.* J Biol Chem, 2009. **284**(30): p. 19961-73.
368. Zheng, Y., et al., *Scd3--a novel gene of the stearoyl-CoA desaturase family with restricted expression in skin.* Genomics, 2001. **71**(2): p. 182-91.
369. Zheng, Y., et al., *Scd1 is expressed in sebaceous glands and is disrupted in the asebia mouse.* Nat Genet, 1999. **23**(3): p. 268-70.
370. Miyazaki, M., et al., *Reduced adiposity and liver steatosis by stearoyl-CoA desaturase deficiency are independent of peroxisome proliferator-activated receptor-alpha.* J Biol Chem, 2004. **279**(33): p. 35017-24.
371. Lee, S.H., et al., *Lack of stearoyl-CoA desaturase 1 upregulates basal thermogenesis but causes hypothermia in a cold environment.* J Lipid Res, 2004. **45**(9): p. 1674-82.
372. Binczek, E., et al., *Obesity resistance of the stearoyl-CoA desaturase-deficient (scd1-/-) mouse results from disruption of the epidermal lipid barrier and adaptive thermoregulation.* Biol Chem, 2007. **388**(4): p. 405-18.
373. Sampath, H., et al., *Stearoyl-CoA desaturase-1 mediates the pro-lipogenic effects of dietary saturated fat.* J Biol Chem, 2007. **282**(4): p. 2483-93.
374. Miyazaki, M., et al., *Stearoyl-CoA desaturase-1 deficiency attenuates obesity and insulin resistance in leptin-resistant obese mice.* Biochem Biophys Res Commun, 2009. **380**(4): p. 818-22.
375. Cases, S., et al., *Identification of a gene encoding an acyl CoA:diacylglycerol acyltransferase, a key enzyme in triacylglycerol synthesis.* Proc Natl Acad Sci U S A, 1998. **95**(22): p. 13018-23.
376. Uchida, Y., et al., *Fatty acid 2-hydroxylase, encoded by FA2H, accounts for differentiation-associated increase in 2-OH ceramides during keratinocyte differentiation.* J Biol Chem, 2007. **282**(18): p. 13211-9.
377. Maier, H., et al., *Normal fur development and sebum production depends on fatty acid 2-hydroxylase expression in sebaceous glands.* J Biol Chem, 2011. **286**(29): p. 25922-34.
378. Li, Y., et al., *Transgenic expression of human amphiregulin in mouse skin: inflammatory epidermal hyperplasia and enlarged sebaceous glands.* Exp Dermatol, 2016. **25**(3): p. 187-93.
379. Dahlhoff, M., et al., *Overexpression of epigen during embryonic development induces reversible, epidermal growth factor receptor-dependent sebaceous gland hyperplasia.* Mol Cell Biol, 2014. **34**(16): p. 3086-95.
380. Dahlhoff, M., et al., *Ligand-independent epidermal growth factor receptor hyperactivation increases sebaceous gland size and sebum secretion in mice.* Exp Dermatol, 2013. **22**(10): p. 667-9.
381. Ebel, P., et al., *Ceramide synthase 4 deficiency in mice causes lipid alterations in sebum and results in alopecia.* Biochem J, 2014. **461**(1): p. 147-58.
382. Peters, F., et al., *Ceramide synthase 4 regulates stem cell homeostasis and hair follicle cycling.* J Invest Dermatol, 2015. **135**(6): p. 1501-9.
383. van Ree, J.H., et al., *Increased response to cholesterol feeding in apolipoprotein C1-deficient mice.* Biochem J, 1995. **305 (Pt 3)**: p. 905-11.
384. Jong, M.C., et al., *Hyperlipidemia and cutaneous abnormalities in transgenic mice overexpressing human apolipoprotein C1.* J Clin Invest, 1998. **101**(1): p. 145-52.
385. Ferreira, N.S., et al., *Regulation of very-long acyl chain ceramide synthesis by Acyl-CoA binding protein.* J Biol Chem, 2017.
386. Fluhr, J.W., K.R. Feingold, and P.M. Elias, *Transepidermal water loss reflects permeability barrier status: validation in human and rodent in vivo and ex vivo models.* Exp Dermatol, 2006. **15**(7): p. 483-92.
387. Grosch, S., S. Schiffmann, and G. Geisslinger, *Chain length-specific properties of ceramides.* Prog Lipid Res, 2012. **51**(1): p. 50-62.

388. Imgrund, S., et al., *Adult ceramide synthase 2 (CERS2)-deficient mice exhibit myelin sheath defects, cerebellar degeneration, and hepatocarcinomas.* J Biol Chem, 2009. **284**(48): p. 33549-60.
389. Gosejacob, D., et al., *Ceramide Synthase 5 Is Essential to Maintain C16:0-Ceramide Pools and Contributes to the Development of Diet-induced Obesity.* J Biol Chem, 2016. **291**(13): p. 6989-7003.
390. Niemann, C., *Differentiation of the sebaceous gland.* Dermatoendocrinol, 2009. **1**(2): p. 64-7.
391. Yeats, T.H. and J.K. Rose, *The formation and function of plant cuticles.* Plant Physiol, 2013. **163**(1): p. 5-20.
392. Uchida, Y., *The role of fatty acid elongation in epidermal structure and function.* Dermatoendocrinol, 2011. **3**(2): p. 65-9.
393. Moon, Y.A., R.E. Hammer, and J.D. Horton, *Deletion of ELOVL5 leads to fatty liver through activation of SREBP-1c in mice.* J Lipid Res, 2009. **50**(3): p. 412-23.
394. Matsuzaka, T., et al., *Crucial role of a long-chain fatty acid elongase, Elovl6, in obesity-induced insulin resistance.* Nat Med, 2007. **13**(10): p. 1193-202.

SUPPLEMENT 1

Acyl-CoA binding protein sustains normal sebaceous gland differentiation and sebum production in mice.

Engelsby, H., Neess, D., Sandhoff, R., Niessen, C., Færgeman, N. J.

Manuscript in preparation

Sebaceous gland differentiation and sebum production depends on acyl-CoA binding protein in mice

Hanne Engelsby[1], Ditte Neess[1], Roger Sandhoff[2], Carien Niessen[3] and Nils J. Færgeman[1*]

[1]Villum Center for Bioanalytical Sciences, Department of Biochemistry and Molecular Biology, University of Southern Denmark, Campusvej 55, DK-5230 Odense M, Denmark

[2]Cellular & Molecular Pathology, Lipid Pathobiochemistry Group, INF 280, German Cancer Research Center, 69120, Heidelberg, Germany

[3]Department of Dermatology and CECAD Cologne, University of Cologne, CECAD Research Center, Joseph Stelzmannstrasse 26, 50931Cologne, Germany

Running title: Acyl-CoA binding protein sustains normal sebaceous gland differentiation and sebum production in mice

*To whom correspondence should be addressed:
Nils J. Færgeman
Villum Center for Bioanalytical Sciences, Department of Biochemistry and Molecular Biology,
University of Southern Denmark, Campusvej 55, DK-5230 Odense M, Denmark
Telephone +45 65502453, E-mail nils.f@bmb.sdu.dk

Keywords: Acyl-CoA, ACBP, epidermal barrier, sebaceous glands, sebocytes, sebum

---

ABSTRACT

Acyl-CoA binding protein (ACBP) is a highly conserved and ubiquitously expressed protein that binds C14-C22 acyl-CoA esters with high affinity and specificity. We recently reported that mice deficient in acyl-CoA binding protein ($ACBP^{-/-}$) display impaired epidermal barrier due to ACBP depletion in keratinocytes. This is accompanied by a marked decrease in very-long chain (VLC) free fatty acids (FFA) in stratum corneum (SC),

and increased levels of monoalkyl diacylglycerol (MADAG) in the fur, epidermis and SC. ACBP$^{-/-}$ mice experience difficulties during weaning due to delayed induction of SREBP-driven lipogenic and cholesterogenic gene programs in the liver, which is caused by accumulation of triacylglycerol (TAG) and cholesterol ester (CE) in the liver. Interesting, this liver phenotype is recapitulated in mice with keratinocyte specific deletion of *Acbp* (K14-ACBP$^{-/-}$) and is caused by the impaired epidermal barrier of these mice. Here we demonstrate that epidermal proliferation is induced in both ACBP$^{-/-}$ and K14-ACBP$^{-/-}$ mice compared with wild type (WT) control mice. Moreover, we demonstrate that disruption of ACBP leads to decreased amounts of protein bound ([OS]) ceramides in SC, and that the sebaceous glands are significantly enlarged and show increased sebum production with altered sebum lipid composition. These observations suggest an important role for ACBP in maintaining the integrity of the epidermal barrier function and in sebaceous gland homeostasis.

INTRODUCTION

The acyl-CoA binding protein (ACBP) is a 10 kDa intracellular protein, which binds C14-C22 acyl-CoA esters with high specificity and affinity [1-3]. ACBP is expressed in all cell types and is highly conserved in all eukaryotic species investigated [4-6]. The expression of ACBP varies between different cell types, with the highest expression in lipogenic cells [7]. Expression of the *Acbp* gene is controlled by lipogenic transcription factors, such as peroxisome proliferator activated receptor γ (PPARγ) and sterol regulatory element binding protein (SREBP) family members [8-11]. ACBP is able to function as an acyl-CoA ester pool former [12], and donate acyl-CoA esters to enzymes involved in lipid metabolism *in vitro* [13-17]. Furthermore, ACBP is capable of abolishing acyl-CoA product inhibition of a number of enzymes involved in lipid metabolism [1, 4, 12, 13, 18, 19]. Depletion of the ACBP analogue Acb1p in *Saccharomyces cerevisiae* causes altered membrane structures, vesicle accumulation and impaired synthesis of VLC fatty acids (FA) and sphingolipids [20, 21].

ACBP depleted mice (ACBP$^{-/-}$) are viable and born in a normal Mendelian ratio [22]. Around 16 days of age, ACBP$^{-/-}$ mice develop a characteristic skin/fur phenotype with greasy and tousled fur, which is accompanied with scaling and alopecia with age. ACBP is expressed in the epidermis and also at low levels in sebaceous glands [23]. Further investigations show that upon ACBP depletion, mice display an increased transepidermal water loss (TEWL), which is accompanied by a significantly reduced amount of very-long chain (VLC) free fatty acids (FFA) in stratum corneum (SC) and by increased levels of monoalkyl diacylglycerol (MADAG) in epidermis, SC and in fur lipids [23]. Tissue-specific loss of ACBP in keratinocytes (K14-ACBP$^{-/-}$) recapitulates the macroscopic phenotype of ACBP$^{-/-}$ mice and also results in an impaired epidermal barrier, arguing that the impaired barrier is due to specific loss of ACBP in the keratinocytes [24]. Additionally, both ACBP$^{-/-}$ and K14-ACBP$^{-/-}$ mice display delayed adaption to weaning with a late upregulation of hepatic lipogenic gene programs [22], which can be rescued by applying an artificial barrier to the mice [22, 24]. ACBP depletion causes

hypertrophy of Harderian glands in mice, which is accompanied with increased *de novo* MADAG synthesis and secretion [25].

The skin is the largest organ of the human body and the outermost layer, the epidermis, provides a barrier between the internal milieu and the external environment. The epidermis is subdivided into four different layers; stratum basale (SB), stratum spinosum (SS), stratum granulosum (SG) and stratum corneum (SC) [26]. Keratinocytes in SB express K5 and K14, whereas keratinocytes localized to SS express K1 and K10 [27]. In addition K16 is expressed during situations of hyperproliferation [28]. In the SG keratinocytes initiates the expression of differentiation markers such as filaggrin and loricrin [29]. When the keratinocytes reach the SC they become terminally differentiated as corneocytes. At this point the plasma membrane is replaced by a protein envelope, which is crosslinked with ceramides of the lipid envelope, together forming the cornified envelope. The corneocytes are surrounded by the lipid lamella, which contain mostly ceramides, cholesterol and FFA originating from the lamellar bodies [30]. In the SC a unique subclass of ceramides have been identified, namely the ω-hydroxy esterified ([EOS]) ceramides [31]. Due to their hydrophobicity these [EOS] ceramides are very important for maintaining the epidermal barrier. Furthermore, the [EOS] ceramides can be crosslinked to proteins in the cornified envelope such as involucrin, periplakin and envoplakin, yielding in [OS] ceramides, which serves as scaffold for the lipid lamella [32].

Within the epidermis the hair follicles reside, and together with the sebaceous gland, these form the pilosebaceous units (PSU). The hair follicles undergo continuous regeneration by cycling through phases of anagen (growth), catagen (regression) and telogen (rest) [33]. However, the sebaceous glands accumulate lipids that are secreted into the hair follicle through holocrine secretion and these lipids eventually reaches the skin surface [34]. Human sebum mainly consists of triacylglycerol (TAG), diacylglycerol (DAG), FFA, wax esters, squalene, cholesterol ester (CE), and cholesterol [35]. Several transgenic mouse models carrying a depletion of proteins involved in sebaceous gland lipid synthesis including stearoyl-CoA desaturase 1 (SCD1) [36], diacylglycerol acyltransferase 1 (DGAT1) [37], fatty acid elongase 3 (ELOVL3) [38], FA 2-hydroxylase (FA2H) [39] or ceramide synthase 4 (CerS4) [40], display alterations in the size of sebaceous glands.

In this study we aimed at understanding the molecular and cellular mechanisms governing the alterations in the skin of ACBP$^{-/-}$ mice. We demonstrate that loss of ACBP in mice results in increased epidermal proliferation. Furthermore, ACBP depletion in mice results in sebaceous glands hypertrophy, increased sebaceous gland differentiation and elevated sebum production. Finally, we show that the level of [OS] ceramides are decreased in ACBP$^{-/-}$ mice SC. Collectively, these results suggest that ACBP depletion in mice causes reduced levels of [OS] ceramides, which leads to the impairment of the epidermal barrier. This is likely counteracted by elevated

epidermal proliferation. Finally, we present results suggesting that ACBP might be involved in the regulation of sebaceous gland lipid biosynthesis and homeostasis.

RESULTS

ACBP depletion changes hair follicle cycling and causes enlarged sebaceous glands

ACBP$^{-/-}$ mice develop alopecia with age [23]. This prompted us to address how ACBP depletion affects the hair follicle cycling. Thus, we examined H&E stained sections from the back skin of both ACBP$^{-/-}$ and K14-ACBP$^{-/-}$ mice at different ages (P0, P15, P21, P33, P47, P58, and P85). During morphogenesis and the first synchronous hair cycle (P0, P21 and P33) we observed no differences in hair follicle morphology between ACBP$^{+/+}$ and ACBP$^{-/-}$ mice or between K14-ACBP$^{+/+}$ and K14-ACBP$^{-/-}$ mice (figure 1). Additionally, there were no differences in the ability of the hair follicles to enter the second catagen (P47) however, during the second telogen (P58) both ACBP$^{-/-}$ and K14-ACBP$^{-/-}$ mice exhibited approximately 1/3 of the hair follicles in an anagen-like state compared with ACBP$^{+/+}$ and K14-ACBP$^{+/+}$, respectively (figure 1). At P85 the hair cycling were no longer synchronized, yet both ACBP$^{-/-}$ and K14-ACBP$^{-/-}$ mice displayed more hair follicles in anagen than observed in WT control mice. These findings indicate that ACBP depletion affects the cycling of the hair follicles and causes an early anagen induction during the second telogen and that this induced anagen persists at P85 in both ACBP$^{-/-}$ and K14-ACBP$^{-/-}$ mice.

Interestingly, ACBP depletion caused enlargement of sebaceous glands at P15, P21, P33, P47, P58, and P85 in ACBP$^{-/-}$ and K14-ACBP$^{-/-}$ mice compared with WT control mice. Additionally, ACBP depletion caused sebum clotting of the hair follicle infundibulum where the sebaceous gland lipids are extruded into the hair follicle at P15 and P21 in ACBP$^{-/-}$ and K14-ACBP$^{-/-}$ mice (figure 1). Taken together, these results reveal that ACBP depletion affects the structure and function of the PSU and in particular the size of the sebaceous glands.

Inactivation of ACBP increases the epidermal proliferation

Mice depleted of CerS3 [41], UDP-glucose:ceramide glucosyltransferase (Ugcg) [42] or ELOVL4 [43] show impairment of the epidermal barrier integrity and concomitant alterations in the epidermal proliferation and differentiation status. Since ACBP depleted mice also display disruption of the epidermal barrier, we set out to thoroughly investigate the differentiation and proliferation status in ACBP$^{-/-}$ and K14-ACBP$^{-/-}$ mice skin. By preparing and investigating tissue sections, we determined the thickness of the interfollicular epidermis (IFE) (figure 2a and 2b). We found that the thickness of the IFE was slightly increased at P47 and P58 in ACBP$^{-/-}$ mice and at P85 in K14-ACBP$^{-/-}$ mice compared with WT control mice. This prompted us to examine the expression levels of genes encoding proteins involved in epidermal differentiation including K10, loricrin, involucrin and

profilaggrin by RT-PCR at P85 in ACBP$^{-/-}$ and ACBP$^{+/+}$ mice epidermis (figure 2c). However, we found no elevated mRNA levels of these markers in ACBP$^{-/-}$ mice compared with ACBP$^{+/+}$ mice.

We further investigated the epidermal proliferation in ACBP$^{-/-}$ and K14-ACBP$^{-/-}$ mice by bromodeoxyuridine (BrdU) labeling (figure 3a and 3b). BrdU is incorporated into the DNA of dividing cells and hence can be used to quantify the number of actively dividing cells. The BrdU incorporation into IFE basal cells were increased in ACBP$^{-/-}$ mice at P47 and P85 compared with ACBP$^{+/+}$, and at P33, P47, P58, and P85 in K14-ACBP$^{-/-}$ mice compared with K14-ACBP$^{+/+}$ mice. This led us to investigate the mRNA expression of genes encoding genes involved in epidermal proliferation and in situations of hyperproliferation including K5, K14 and K16. However, we only found the expression of *K5* significantly elevated in ACBP$^{-/-}$ mice epidermis compared with ACBP$^{+/+}$ (figure 3c).

Taken together, these results indicate that ACBP plays a role in maintaining the IFE since depletion of ACBP causes increased epidermal proliferation.

Deletion of *ACBP* results in decreased amounts of [OS] ceramides in stratum corneum

The epidermal barrier integrity is highly dependent on the SC lipid composition e.g. the ceramides, cholesterol and VLC FFA [44]. In particular [EOS] and [OS] ceramides are important for epidermal barrier integrity [41, 43]. We set out to analyze the SC ceramide content in ACBP$^{+/+}$ and ACBP$^{-/-}$ mice. We detected no overall differences in non-hydroxy ([NS]), α-hydroxy ([AS]), ω-hydroxy, or [EOS] ceramides species with sphingosine as long chain base (results not shown). However, [OS] ceramides with C30-C36 acyl chains, both saturated and unsaturated, were significantly reduced in SC from ACBP$^{-/-}$ mice compared with ACBP$^{+/+}$ (figure 4a and 4b). These findings show that ACBP depletion causes a decrease in SC [OS] ceramides by yet unknown mechanisms.

ACBP depletion causes sebaceous gland hypertrophy

As reported previously, ACBP depletion in mice causes a greasy and tousled appearance of the fur [22, 23]. We speculated whether this greasy appearance of the fur might be related to the enlarged sebaceous glands (figure 1). We therefore measured the sebaceous gland size at P15, P21, P33, P47, P58 and P85 in ACBP$^{-/-}$ and K14-ACBP$^{-/-}$ and compared with that of ACBP$^{+/+}$ and K14-ACBP$^{+/+}$, respectively. Interestingly, we found that sebaceous glands of both ACBP$^{-/-}$ and K14-ACBP$^{-/-}$ mice are 2-fold enlarged compared with WT controls at all ages examined (figure 5a and 5b). We wanted to investigate whether this enlargement was caused by increased proliferation of basal cells; however, this was not the case since we observed no differences in BrdU incorporation at P15 and P85 in ACBP$^{+/+}$ and ACBP$^{-/-}$ mice (figure 5c). We have previously reported that the impaired epidermal barrier observed in ACBP$^{-/-}$ mice results in perturbation of lipogenic gene expression in the liver at weaning, and that this is rescued by applying an artificial barrier on the skin [24]. Here we used the same

approach to analyze whether the epidermal barrier defect *per se* might be the cause of the sebaceous gland enlargement. The sebaceous gland area in $ACBP^{+/+}$ and $ACBP^{-/-}$ mice, which had been treated with Vaseline twice a day from day 7 to 28 (figure 5d), was determined. This revealed that applying Vaseline as an artificial barrier did not prevent enlargement of the sebaceous glands in $ACBP^{-/-}$ mice compared with $ACBP^{+/+}$ mice. These findings show that ACBP depletion leads to enlargement of the sebaceous glands independently of basal cell proliferation. Furthermore, the enlargement of the sebaceous glands is caused by an endogenous effect of ACBP deficiency and not as a compensatory effect due to an impaired barrier function.

Lack of ACBP increases lipid production in the sebaceous glands and alters the sebum lipid composition

As the enlargement of the sebaceous glands is not caused by elevated proliferation of the basal cells, we set out to investigate whether the cause might be increased differentiation of the sebaceous glands. During differentiation, the sebaceous glands accumulate lipids and we aimed at investigating whether this lipid accumulation might be affected by ACBP depletion. We applied coherent anti-stokes raman scattering (CARS) microscopy to visualize the neutral lipid content in sebaceous glands at P21 and P58 in $ACBP^{-/-}$ and $ACBP^{+/+}$ (figure 6a). As expected, we observed that sebaceous glands are lipid filled in both $ACBP^{-/-}$ and $ACBP^{+/+}$ mice. Furthermore, the increased size of the lipid filled sebaceous gland in $ACBP^{-/-}$ mice was pronounced. SCD1 is used as a marker of differentiation in sebaceous glands [45], and consistently we found the SCD1 staining to be increased in size and intensity in $ACBP^{-/-}$ mice compared with $ACBP^{+/+}$ mice (Figure 6b), indicating increased lipid biosynthesis in the sebaceous glands upon ACBP depletion. Furthermore, we detected that the expression of *SCD1* was increased, and in addition we found that the expression of *HMG-CoA reductase* (*HMGCR*) and *squalene epoxidase* (*SQLE*) was significantly increased in $ACBP^{-/-}$ mice. However, the expression level of diacylglycerol acyltransferase 1 (*Dgat1*) was not significantly altered upon ACBP depletion (figure 6c). Collectively, the data suggest that differentiation of sebaceous glands in $ACBP^{-/-}$ mice is elevated which results in an enlargement of the gland and increased lipid production,

Since $ACBP^{-/-}$ mice display enlarged sebaceous glands and signs of increased lipid secretion, we hypothesized that the greasy phenotype of the $ACBP^{-/-}$ mice might be caused by increased lipid secretion from the sebaceous glands. The greasy appearance of the fur is mostly pronounced around the time of weaning, therefor we extracted lipids from the fur of P21 $ACBP^{+/+}$ and $ACBP^{-/-}$ mice and analyzed the lipids using high performance thin layer chromatography (HPTLC). Interestingly, we extracted approximately twice as much lipids from the same amount of fur from $ACBP^{-/-}$ mice compared with $ACBP^{+/+}$ mice (results not shown). Using HPTLC and two different solvent systems we demonstrated that FFA, MADAG, CE, cholesterol, wax monoester, and wax diester were all significantly increased in fur lipids at P21 in $ACBP^{-/-}$ mice compared with $ACBP^{+/+}$ mice, while

the level of TAG and squalene were not significant altered (figure 7a and 7b). Taken together, these results indicates, that the sebum production and secretion is elevated upon ACBP depletion in mice.

To fully elucidate whether ACBP depletion not only resulted in elevated sebocyte lipid synthesis, but also altered composition of the synthesized lipids, we analyzed equal amounts of lipid extracted from the fur of ACBP$^{-/-}$ and ACBP$^{+/+}$ mice at P21 using HPTLC. This analysis revealed that there was an increase in MADAG, wax diester and wax monoester, and a concomitant decrease in FFA at P21 in ACBP$^{-/-}$ mice fur compared with ACBP$^{+/+}$ (figure 7c and 7d). These results indicate that ACBP depletion not only results in increased lipid production in sebocytes but also causes alterations in the lipid composition.

DISCUSSION

We previously reported that loss of ACBP in the epidermis results in an impaired epidermal barrier [24]. Here we show that disruption of ACBP results in increased proliferation of epidermal basal cells and slightly elevated epidermal differentiation, and that these alterations are caused by endogenous effects due to specific depletion of ACBP in keratinocytes.

We observed increased proliferation by incorporation of BrdU into K14 positive IFE cells in ACBP$^{-/-}$ and K14-ACBP$^{-/-}$ mice compared with WT controls. This was accompanied by elevated expression of *K5* in ACBP$^{-/-}$ and K14-ACBP$^{-/-}$ mice. These observations suggest that the proliferation of epidermal basal cells is increased in both ACBP$^{-/-}$ and K14-ACBP$^{-/-}$ mice, as *K5* is expressed in basal keratinocytes [27]. *K14* is also expressed in basal keratinocytes [27] whereas *K16* is expressed during situations of hyperproliferation [28]. However, the expression of *K14* and *K16* was not significant altered upon ACBP depletion. We suggest that the elevated proliferation upon ACBP depletion might be initiated to counteract the impaired epidermal barrier caused by ACBP depletion.

K10, *loricrin*, *involucrin* and *profilaggrin* are frequently used as markers of epidermal differentiation. Expression of *K10* is initiated in keratinocytes as they start to differentiate [27], and *loricrin*, *involucrin* and *filaggrin* are all part of the epidermal differentiation complex [29, 46]. The increased IFE thickness in ACBP$^{-/-}$ and K14-ACBP$^{-/-}$ mice is significant yet not very severe. However, the expression of *K10*, *loricrin*, *involucrin* and *profilaggrin* in epidermis is not altered upon ACBP depletion. We speculated that the slightly elevated epidermal differentiation in ACBP$^{-/-}$ and K14-ACBP$^{-/-}$ mice might counteract the disrupted epidermal barrier in both ACBP$^{-/-}$ and K14-ACBP$^{-/-}$ mice [24].

Epidermal barrier integrity relies on specialized [EOS] and [OS] ceramides with ULC acyl moieties. Decreased levels of [EOS] and/or [OS] ceramides causes disruption of the epidermal barrier function and is associated with

a number of human skin diseases e.g. neutral lipid storage disease, autosomal recessive congenital ichthyosis (ARCI) and Harlequin ichthyosis [47-49], which are recapitulated in mouse models depleted of CGI58, CerS3 and ABCA12, respectively [41, 49-52].

Importantly, CerS3 catalyzes the synthesis of ceramides with ULC acyl moieties [41, 53] and recently we reported that ACBP interacts with and highly stimulates CerS3 activity *in vitro* [54]. In this study, we showed that upon ACBP depletion the level of [OS] ceramides in SC was decreased, which is in keeping with the stimulatory effect of ACBP on ceramide synthesis. Furthermore, this indicate that ACBP might also stimulate the synthesis of ceramides with ULC acyl moiety *in vivo*. We speculate, that loss of ACBP may impact delivery of acyl-CoA esters to CerS3 and thereby reduce the activity of CerS3 and hence result in decreased level of [OS] ceramides in ACBP$^{-/-}$ mice SC, consequently resulting in an impaired epidermal barrier. To this end we have previously reported a decrease in VLC FFA in ACBP$^{-/-}$ mice SC [23], which may also contribute to the impaired epidermal barrier.

Importantly, in this study, we demonstrate that sebaceous glands are increased in size in ACBP$^{-/-}$ and K14-ACBP$^{-/-}$ mice skin at all ages investigated. This is consistent with previous findings in mice with a spontaneous deletion of 400 kb on chromosome 1 (*nm1054*) that includes the *Acbp* gene [55].

Interestingly, Harderian glands in ACBP$^{-/-}$ mice are enlarged compared with that of WT control animals and they both produce and secrete more lipids, primarily MADAG. Both the enlargement and the excess lipid secretion are reversed by applying an artificial epidermal barrier to ACBP$^{-/-}$ mice [25]. In contrast to these observations, we now show that the enlarged sebaceous glands are not normalized by application of an artificial barrier, indicating that the role of ACBP in sebocytes is independent of the barrier defect and that ACBP might be more directly involved in maintaining sebaceous gland homeostasis.

The sebaceous glands in ACBP$^{-/-}$ mice are not only enlarged but also accumulate lipids as visualized by CARS microscopy. Consistently, the mRNA expression levels of genes involved in lipid synthesis including *SCD1*, *HMGCR* and *SQLE* are elevated. Moreover, we found that levels of cholesterol, wax esters and MADAG on the fur are increased upon ACBP depletion, suggesting that increased amounts of lipids from the sebaceous glands are secreted on to the fur of ACBP$^{-/-}$ mice. In keeping with this, wax ester levels are elevated in sebum from ELOVL3, FA2H and CerS4 knock out mice [38, 40]. However, whether this is a compensatory mechanism to counteract impaired barrier integrity, or a more direct effect of the depletion of the different enzymes contributing to impaired epidermal barrier function remain elusive. In keeping with this study, we have previously reported that MADAG levels on the fur of ACBP$^{-/-}$ mice are elevated [23]. Furthermore, deletion of ACBP results in hypertrophy of the Harderian gland, accompanied by increased *de novo* synthesis and secretion

of MADAG [25]. Taken together, these studies suggest that ACBP regulates lipid biosynthesis in sebaceous glands including wax ester and MADAG biosynthesis.

Since incorporation of BrdU in to sebaceous basal cells is similar between $ACBP^{-/-}$ and $ACBP^{+/+}$ mice, hypertrophy of the sebaceous gland is unlikely to be due to elevated cellular proliferation. We therefor speculate whether the sebaceous gland hypertrophy is more likely caused by increased cellular differentiation since the sebaceous glands secrete more lipids while also displaying elevated SCD1 expression as well as SCD1 staining in sebaceous glands from $ACBP^{-/-}$ mice compared with that of $ACBP^{+/+}$ mice. Similarly, depletion of several enzymes including ELOVL3, FA2H or CerS4, which are all involved in sebaceous gland lipid synthesis in mice, also cause sebaceous gland hypertrophy in mice [38-40], whereas deletion of SCD1, DGAT1, FATP4 or FABP5 results in sebaceous gland atrophy [36, 37, 56, 57]. However, it is unclear why depletion of enzymes involved in sebaceous gland lipid synthesis in some cases causes hypertrophy and in other cases causes atrophy of the sebaceous glands.

$ACBP^{-/-}$ mice develop alopecia with age [23] and in the present study we show an induced anagen-like state in hair follicles at P58 and P85 in $ACBP^{-/-}$ and K14-$ACBP^{-/-}$ mice. A premature activation of hair follicle stem cells can drive the anagen-like state of hair follicles in ACBP deficient mice. In keeping with this, mice depleted of CerS4 display a similar anagen-like state in the hair follicles which causes exhaustion of hair follicle stem cells and leads to subsequent hair loss, through alterations in CerS4-directed epidermal ceramide composition [58]. Based on this we speculate whether the induced anagen-like state of the hair follicles in ACBP depleted mice might cause exhaustion of the hair follicle stem cells leading to hair loss.

CerS4 depleted mice, like $ACBP^{-/-}$ mice, display sebaceous gland hypertrophy, which is accompanied by altered lipid synthesis and secretion from sebocytes. This causes sebum clotting in the hair follicle infundibulum, which could potentially contribute to the hair loss [40]. Additionally, transgenic mouse models depleted of DGAT1, SCD1, ELOVL3 or FA2H also display hair loss [36-40]; however, in these cases the effect of the depleted enzyme on sebaceous gland homeostasis differs markedly. Depletion of ELOVL3 or FA2H causes enlargement of the sebaceous glands [38, 39], whereas SCD1 and DGAT1 disruption results in sebaceous gland atrophy [36, 37]. These findings indicate that alterations in sebaceous gland homeostasis and lipid synthesis affect the whole PSU and thereby in some cases contribute to hair loss. Here we show that ACBP depletion causes sebum clotting in the hair follicle infundibulum in mice at P15 and P21, and we hypothesize that this, together with the sebaceous gland hypertrophy, contributes to the alopecia observed in ACBP depleted mice.

EKSPERIMENTAL PROCEDURES

Mice strains

Mice with constitutive and keratinocyte-specific deletion of the *Acbp* gene has been described previously [22, 24]. Mice were housed under standard laboratory conditions (~55% relative humidity, 22 ± 3 °C, 12-h light/dark cycle and with ad libitum access to food and water) at the Biomedical Laboratory, University of Southern Denmark. Breeding of transgenic mice and animal experiments were approved by the Danish Animal Experiment Inspectorate.

Tissue collection

To investigate the cellular proliferation status, mice were injected intraperitoneally with BrdU (203806, Merck Millipore), 0.25 µg/mg bodyweight, 30 min before scarification by cervical dislocation. The mice were then shaved, and the fur was collected for lipid extraction. The upper part of the back skin was prepared for paraffin sectioning by fixation in 4% PFA (PBS) for 1 h. hereafter the tissues were perfused with TissueClean and paraffin followed by paraffin embedding. For cryo sections the upper part of the back skin was direct embedded in optimal cutting temperature (OCT) compound (TissueTek). For epidermal splits, the lower part of the back skin was placed floating in 0.5 M ammonium thiocyanate (PBS) for 30 min on ice, the epidermis were scraped off and snap frozed in liquid nitrogen in 500 mL Isol (2302700, PRIME) for subsequent RNA isolation.

Histology and immunohistochemistry

Paraffin sections were deparaffinized and H&E stained. For immunohistochemistry, paraffin sections were deparaffinized and antigens were retrieved with citrate buffer (S1699, Dako) and blocked with goat serum or fetal calf serum (10% in PBS), followed by incubation with indicated 1'ab, dilution and incubation time: Anti-K14 (1:1000) (2h) (PRB-155P, Covance); anti-BrdU (1:25) (2h) (347580, BD bioscience); anti-Loricrine (1:500) (2h) (PRB-145P, Covance); anti-K10 (1:500) (2h) (PRB-159P, Covance); anti-SCD1 (1:200) (overnight) (sc-14719, Santa Cruz) and indicated 2'ab, dilution and incubation time: Anti-mouse Alexa Flour 488 (1:500) (1 h) (A21121, life science), Anti-Rabbit Alexa Flour 594 (1:500) (1h) (A21207, life science); anti-Goat Alexa Flour 488 (1:500) (1h) (A21121, life science); DAPI (1:500) (1h) (D9542, Sigma). All antibodies were diluted in ab diluent (S302281, DAKO).

Microscopy

Fluorescent signals were visualized at ambient temperature on a Leica TCS SP8X confocal microscope with a hybrid detector using a HCX PL APO 100X/1.40 oil objective using Leica Application Suite software. Images

were processed using ImageJ. Coherent Anti-Stokes Raman Scattering (CARS) were carried out on a Leica TCS SP8 CARS microscope pumped to 816.4 nm. Pictures were processed using ImageJ.

Mass spectrometry of stratum corneum ceramides

The SC was isolated by placing abdominal skin samples from adult mice floating on 0.25% Trypsin (PBS) over night at room temperature. The ceramides were extracted as described in [59]. Mass spectrometry analysis was carried out as described in [41].

Real-Time PCR

Epidermal splits from $ACBP^{-/-}$ and $ACBP^{+/+}$ mice at P85 were homogenized in 500 mL Isol using Biorupter (5 min; 30 sec intervals, high level), followed by RNA isolation, cDNA synthesis and RT-PCR performed as previously described [22]. The following primers were used: *K10* fwd.: 5'-GACAACTGACAATGCCAACG-3', *K10* rev.: 5'-CAGGGTCACCTCATTCTCGT-3', *Loricrin* fwd.: 5'-GGTCACCGGGTTGCAACGGA-3', *Loricrin* rev.: 5'-GAGACACTAGAATTGGGAGG-3', *Involucrin* fwd.: 5'-GCAGCAGCAGCAACAGATAG-3', *Involucrin* rev.: 5'-GCACGTCTCCTTTCACTGGT-3', *profilaggrin* fwd.: 5'-AGGAGGAAGAAACACTGAGCAA-3', *profilaggrin* rev.: 5'-TGCTTTTGCCAGCTTTAGCAC-3', *K5* fwd.: 5'-CTC CAG GAA CCA TCA TGT CTC GCC AGT C-3', *K5* rev.: 5'-CAC CAC CGA AGC CAA AGC CAC TAC CAG-3', *K14* fwd.: 5'-GGA TGT GAA GAC AAG GCT GGA-3', *K14* rev.: 5'-AAG CCT GAG CAG CAT GTA GCA-3', *K16* fwd.: 5'-GAATGAGCTGTTCTTGCGGC-3', *K16* rev.: 5'-TCAAGGCAAGCATCTCCTCC-3', *SCD1* fwd.: 5'-ACA CCT GCC TCT TCG GGA TT-3', *SCD1* rev.: 5'-TGA TGC CCA GAG CGC TG-3', *HMGCR* fwd.: 5'-ACG CTC TTG TGG AAT GCC TT-3', *HMGCR* rev.: 5'-GGA CGC CTG ACA TGG TGC-3', *SQLE* fwd.: 5'-TGA ACA AAC GAG GCG TCC TT-3', *SQLE* rev.: 5'-GGT GCC TCA GGT TAT ACG CAT C-3', *Dgat1* fwd.: 5'-TTG CTC TGG CAT CAT ACT CC-3', *Dgat1* rev.: 5'-CCA CTG ACC TTC TTC CCT GT-3', *GAPDH* fwd.: 5'-GCA CCAG TCA AGG CCG AGA AT-3', *GAPDH* rev.: 5'-TCT CGC TCC TGG AAG ATG GT-3'.

HPTLC

The fur from P21 mice were shaved off and collected, lipids were extracted 2x15 min with 3 mL acetone. The fur and the extracted lipids were dried under N_2 flow. Lipids were re-suspended in 1:1 chloroform/methanol and loaded onto 10X20 cm silica gel 60 TLC plates. One plate was developed in 55:45 hexane/benzene and a second plate was developed in 80:30:1 hexane/diethyl ether/acetic acid. For identification we used Nu-Chek 18-4a (Nu-chek prep, inc.) with addition of squalene (S3626, Sigma), MADAG and a wax monoester (P0169, Sigma) as

standard. Plates were sprayed with 10% $CuSO_4$ in 8% H_3PO_4, where after the plates were heated to 185°C for 5 min to visualize the lipids. Lipid species were quantified using ImageJ.

Statistical analysis

Unpaired parametric Students t-test was used using GraphPad Prism (version 5). Data are presented as mean±SEM and asterisks indicate the following significance levels: *P<0.05, **P<0.01, ***P<0.001. Outliers were detected using GraphPad online outlier calculator: https://graphpad.com/quickcalcs/Grubbs1.cfm

References

1. Rasmussen, J.T., J. Rosendal, and J. Knudsen, *Interaction of acyl-CoA binding protein (ACBP) on processes for which acyl-CoA is a substrate, product or inhibitor.* Biochem J, 1993. **292 (Pt 3)**: p. 907-13.
2. Rosendal, J., P. Ertbjerg, and J. Knudsen, *Characterization of ligand binding to acyl-CoA-binding protein.* Biochem J, 1993. **290 (Pt 2)**: p. 321-6.
3. Faergeman, N.J., et al., *Thermodynamics of ligand binding to acyl-coenzyme A binding protein studied by titration calorimetry.* Biochemistry, 1996. **35**(45): p. 14118-26.
4. Mogensen, I.B., et al., *A novel acyl-CoA-binding protein from bovine liver. Effect on fatty acid synthesis.* Biochem J, 1987. **241**(1): p. 189-92.
5. Knudsen, J., et al., *Acyl-CoA-binding protein in the rat. Purification, binding characteristics, tissue concentrations and amino acid sequence.* Biochem J, 1989. **262**(2): p. 513-9.
6. Guidotti, A., et al., *Isolation, characterization, and purification to homogeneity of an endogenous polypeptide with agonistic action on benzodiazepine receptors.* Proc Natl Acad Sci U S A, 1983. **80**(11): p. 3531-5.
7. Neess, D., et al., *ACBP--a PPAR and SREBP modulated housekeeping gene.* Mol Cell Biochem, 2006. **284**(1-2): p. 149-57.
8. Helledie, T., et al., *The gene encoding the Acyl-CoA-binding protein is activated by peroxisome proliferator-activated receptor gamma through an intronic response element functionally conserved between humans and rodents.* J Biol Chem, 2002. **277**(30): p. 26821-30.
9. Mandrup, S., et al., *Acyl-CoA-binding protein/diazepam-binding inhibitor gene and pseudogenes. A typical housekeeping gene family.* J Mol Biol, 1992. **228**(3): p. 1011-22.
10. Sandberg, M.B., et al., *The gene encoding acyl-CoA-binding protein is subject to metabolic regulation by both sterol regulatory element-binding protein and peroxisome proliferator-activated receptor alpha in hepatocytes.* J Biol Chem, 2005. **280**(7): p. 5258-66.
11. Swinnen, J.V., et al., *Identification of diazepam-binding Inhibitor/Acyl-CoA-binding protein as a sterol regulatory element-binding protein-responsive gene.* J Biol Chem, 1998. **273**(32): p. 19938-44.
12. Knudsen, J., et al., *The function of acyl-CoA-binding protein (ACBP)/diazepam binding inhibitor (DBI).* Mol Cell Biochem, 1993. **123**(1-2): p. 129-38.
13. Chao, H., et al., *ACBP and cholesterol differentially alter fatty acyl CoA utilization by microsomal ACAT.* J Lipid Res, 2003. **44**(1): p. 72-83.
14. Fyrst, H., et al., *Detection of acyl-CoA-binding protein in human red blood cells and investigation of its role in membrane phospholipid renewal.* Biochem J, 1995. **306 (Pt 3)**: p. 793-9.

15. Kannan, L., J. Knudsen, and C.A. Jolly, *Aging and acyl-CoA binding protein alter mitochondrial glycerol-3-phosphate acyltransferase activity.* Biochim Biophys Acta, 2003. **1631**(1): p. 12-6.
16. Rasmussen, J.T., et al., *Acyl-CoA-binding protein (ACBP) can mediate intermembrane acyl-CoA transport and donate acyl-CoA for beta-oxidation and glycerolipid synthesis.* Biochem J, 1994. **299 (Pt 1)**: p. 165-70.
17. Abo-Hashema, K.A., et al., *Evaluation of the affinity and turnover number of both hepatic mitochondrial and microsomal carnitine acyltransferases: relevance to intracellular partitioning of acyl-CoAs.* Biochemistry, 1999. **38**(48): p. 15840-7.
18. Bhuiyan, A.K. and S.V. Pande, *Carnitine palmitoyltransferase activities: effects of serum albumin, acyl-CoA binding protein and fatty acid binding protein.* Mol Cell Biochem, 1994. **139**(2): p. 109-16.
19. Kerkhoff, C., et al., *Acyl-CoA binding protein (ACBP) regulates acyl-CoA:cholesterol acyltransferase (ACAT) in human mononuclear phagocytes.* Biochim Biophys Acta, 1997. **1346**(2): p. 163-72.
20. Faergeman, N.J., et al., *Acyl-CoA-binding protein, Acb1p, is required for normal vacuole function and ceramide synthesis in Saccharomyces cerevisiae.* Biochem J, 2004. **380**(Pt 3): p. 907-18.
21. Gaigg, B., et al., *Depletion of acyl-coenzyme A-binding protein affects sphingolipid synthesis and causes vesicle accumulation and membrane defects in Saccharomyces cerevisiae.* Mol Biol Cell, 2001. **12**(4): p. 1147-60.
22. Neess, D., et al., *Disruption of the acyl-CoA-binding protein gene delays hepatic adaptation to metabolic changes at weaning.* J Biol Chem, 2011. **286**(5): p. 3460-72.
23. Bloksgaard, M., et al., *The acyl-CoA binding protein is required for normal epidermal barrier function in mice.* J Lipid Res, 2012. **53**(10): p. 2162-74.
24. Neess, D., et al., *Delayed hepatic adaptation to weaning in ACBP-/- mice is caused by disruption of the epidermal barrier.* Cell Rep, 2013. **5**(5): p. 1403-12.
25. Bek, S., et al., *Compromised epidermal barrier stimulates Harderian gland activity and hypertrophy in ACBP-/- mice.* J Lipid Res, 2015. **56**(9): p. 1738-46.
26. Fuchs, E. and S. Raghavan, *Getting under the skin of epidermal morphogenesis.* Nat Rev Genet, 2002. **3**(3): p. 199-209.
27. Fuchs, E. and H. Green, *Changes in keratin gene expression during terminal differentiation of the keratinocyte.* Cell, 1980. **19**(4): p. 1033-42.
28. Sano, T., et al., *Long-term alteration in the expression of keratins 6 and 16 in the epidermis of mice after chronic UVB exposure.* Arch Dermatol Res, 2009. **301**(3): p. 227-37.
29. Bickenbach, J.R., et al., *Loricrin expression is coordinated with other epidermal proteins and the appearance of lipid lamellar granules in development.* J Invest Dermatol, 1995. **104**(3): p. 405-10.
30. Nemes, Z. and P.M. Steinert, *Bricks and mortar of the epidermal barrier.* Exp Mol Med, 1999. **31**(1): p. 5-19.
31. Wertz, P.W., et al., *The composition of the ceramides from human stratum corneum and from comedones.* J Invest Dermatol, 1985. **84**(5): p. 410-2.
32. Marekov, L.N. and P.M. Steinert, *Ceramides are bound to structural proteins of the human foreskin epidermal cornified cell envelope.* J Biol Chem, 1998. **273**(28): p. 17763-70.
33. Plikus, M.V. and C.M. Chuong, *Complex hair cycle domain patterns and regenerative hair waves in living rodents.* J Invest Dermatol, 2008. **128**(5): p. 1071-80.
34. Niemann, C. and V. Horsley, *Development and homeostasis of the sebaceous gland.* Semin Cell Dev Biol, 2012. **23**(8): p. 928-36.
35. Camera, E., et al., *Comprehensive analysis of the major lipid classes in sebum by rapid resolution high-performance liquid chromatography and electrospray mass spectrometry.* J Lipid Res, 2010. **51**(11): p. 3377-88.

36. Miyazaki, M., W.C. Man, and J.M. Ntambi, *Targeted disruption of stearoyl-CoA desaturase1 gene in mice causes atrophy of sebaceous and meibomian glands and depletion of wax esters in the eyelid.* J Nutr, 2001. **131**(9): p. 2260-8.
37. Chen, H.C., et al., *Leptin modulates the effects of acyl CoA:diacylglycerol acyltransferase deficiency on murine fur and sebaceous glands.* J Clin Invest, 2002. **109**(2): p. 175-81.
38. Westerberg, R., et al., *Role for ELOVL3 and fatty acid chain length in development of hair and skin function.* J Biol Chem, 2004. **279**(7): p. 5621-9.
39. Maier, H., et al., *Normal fur development and sebum production depends on fatty acid 2-hydroxylase expression in sebaceous glands.* J Biol Chem, 2011. **286**(29): p. 25922-34.
40. Ebel, P., et al., *Ceramide synthase 4 deficiency in mice causes lipid alterations in sebum and results in alopecia.* Biochem J, 2014. **461**(1): p. 147-58.
41. Jennemann, R., et al., *Loss of ceramide synthase 3 causes lethal skin barrier disruption.* Hum Mol Genet, 2012. **21**(3): p. 586-608.
42. Amen, N., et al., *Differentiation of epidermal keratinocytes is dependent on glucosylceramide:ceramide processing.* Hum Mol Genet, 2013. **22**(20): p. 4164-79.
43. Vasireddy, V., et al., *Loss of functional ELOVL4 depletes very long-chain fatty acids (> or =C28) and the unique omega-O-acylceramides in skin leading to neonatal death.* Hum Mol Genet, 2007. **16**(5): p. 471-82.
44. Feingold, K.R., *Thematic review series: skin lipids. The role of epidermal lipids in cutaneous permeability barrier homeostasis.* J Lipid Res, 2007. **48**(12): p. 2531-46.
45. Niemann, C., *Differentiation of the sebaceous gland.* Dermatoendocrinol, 2009. **1**(2): p. 64-7.
46. Henry, J., et al., *Update on the epidermal differentiation complex.* Front Biosci (Landmark Ed), 2012. **17**: p. 1517-32.
47. Uchida, Y., et al., *Neutral lipid storage leads to acylceramide deficiency, likely contributing to the pathogenesis of Dorfman-Chanarin syndrome.* J Invest Dermatol, 2010. **130**(10): p. 2497-9.
48. Radner, F.P., et al., *Mutations in CERS3 cause autosomal recessive congenital ichthyosis in humans.* PLoS Genet, 2013. **9**(6): p. e1003536.
49. Kelsell, D.P., et al., *Mutations in ABCA12 underlie the severe congenital skin disease harlequin ichthyosis.* Am J Hum Genet, 2005. **76**(5): p. 794-803.
50. Radner, F.P., et al., *Growth retardation, impaired triacylglycerol catabolism, hepatic steatosis, and lethal skin barrier defect in mice lacking comparative gene identification-58 (CGI-58).* J Biol Chem, 2010. **285**(10): p. 7300-11.
51. Yanagi, T., et al., *Harlequin ichthyosis model mouse reveals alveolar collapse and severe fetal skin barrier defects.* Hum Mol Genet, 2008. **17**(19): p. 3075-83.
52. Zuo, Y., et al., *ABCA12 maintains the epidermal lipid permeability barrier by facilitating formation of ceramide linoleic esters.* J Biol Chem, 2008. **283**(52): p. 36624-35.
53. Mizutani, Y., et al., *2-Hydroxy-ceramide synthesis by ceramide synthase family: enzymatic basis for the preference of FA chain length.* J Lipid Res, 2008. **49**(11): p. 2356-64.
54. Ferreira, N.S., et al., *Regulation of very-long acyl chain ceramide synthesis by Acyl-CoA binding protein.* J Biol Chem, 2017.
55. Lee, L., et al., *Loss of the acyl-CoA binding protein (Acbp) results in fatty acid metabolism abnormalities in mouse hair and skin.* J Invest Dermatol, 2007. **127**(1): p. 16-23.
56. Lin, M.H., F.F. Hsu, and J.H. Miner, *Requirement of fatty acid transport protein 4 for development, maturation, and function of sebaceous glands in a mouse model of ichthyosis prematurity syndrome.* J Biol Chem, 2013. **288**(6): p. 3964-76.

57. Sugawara, T., et al., *Reduced size of sebaceous gland and altered sebum lipid composition in mice lacking fatty acid binding protein 5 gene.* Exp Dermatol, 2012. **21**(7): p. 543-6.
58. Peters, F., et al., *Ceramide synthase 4 regulates stem cell homeostasis and hair follicle cycling.* J Invest Dermatol, 2015. **135**(6): p. 1501-9.
59. Doering, T., et al., *Sphingolipid activator proteins are required for epidermal permeability barrier formation.* J Biol Chem, 1999. **274**(16): p. 11038-45.

Figure legends

Figure 1**. ACBP dependent changes in skin morphology**. The upper back skin was isolated from $ACBP^{+/+}$, $ACBP^{-/-}$, K14-$ACBP^{+/+}$ and K14-$ACBP^{-/-}$ mice at indicated (P) days. The skin was fixed with 4% PFA in PBS followed by paraffin embedding. Skin sections were de-paraffinized and H&E stained. Black arrows indicate enlarged sebaceous glands, open arrows indicate sebum clotting in the hair follicle infundibulum and asterisks indicate hair follicles in anagen in P58. The pictures are representative of 3-5 mice from each genotype. Scale bars represent 100µm.

Figure 2. **ACBP depletion causes slightly increased epidermal differentiation**. (a) Quantification of interfollicular epidermis (IFE) thickness on H&E stained paraffin section from $ACBP^{+/+}$ and $ACBP^{-/-}$ mice skin at indicated (P) days. Mean±SEM. n=3-5 mice/genotype/age. *P<0.05, **P<0.01, ***P<0.001. (b) Quantification of IFE thickness on H&E stained paraffin section from K14-$ACBP^{+/+}$ and K14-$ACBP^{-/-}$ mice skin at indicated (P) days. Mean±SEM. n=3-5 mice/genotype/age. *P<0.05, **P<0.01, ***P<0.001. (c) Epidermis from P85 $ACBP^{+/+}$ and $ACBP^{-/-}$ mice were separated from dermis with 0.5 M ammonium thiocyanate in PBS, mRNA was isolated followed by cDNA synthesis and RT-PCR analysis. The mRNA expression of *K10*, *loricrin*, *involucrin* and *profilaggrin* in P85 $ACBP^{+/+}$ and $ACBP^{-/-}$ mice epidermis are normalized to GAPDH expression (n=5 of each genotype).

Figure 3. **ACBP depletion results in increased proliferation of epidermal basal cells**. (a) and (b) Mice were injected with BrdU 30 min. prior to scarification, the upper back skin were isolated, fixed with 4% PFA in PBS followed by paraffin embedding. Paraffin sections were de-paraffinized and incubated with 1' antibodies: Anti-BrdU (1:25) (347580, BD bioscience) and anti-K14 (1:1000) (PRB-155P, Covance) for 2h and 2' antibodies: Anti-mouse Alexa Flour 488 (1:500) (A21121, life science) and anti-Rabbit Alexa Flour 594 (1:500) (A21207, life science) for 1h. (a) BrdU positive cells relative to K14 positive cells were quantified in the interfollicular epidermis (IFE) of $ACBP^{+/+}$ and $ACBP^{-/-}$ mice at indicated (P) days. Mean±SEM. n=3-5 mice/genotype/age. *P<0.05, **P<0.01, ***P<0.001. (b) Quantification of BrdU positive cells relative to K14 positive cells in IFE of K14-$ACBP^{+/+}$ and K14-$ACBP^{-/-}$ mice at indicated (P) days. Mean±SEM. n=3-5 mice/genotype/age. *P<0.05, **P<0.01, ***P<0.001. (c) mRNA were isolated from epidermal splits (0.5 M ammonium thiocyanate in PBS) from P85 $ACBP^{+/+}$ and $ACBP^{-/-}$ mice, cDNA were synthesized and analyzed by RT-PCR using primers against K5, K14 and K16. The mRNA expression were normalized to GAPDH expression (n=5 of each genotype). Mean±SEM. *P<0.05, **P<0.01, ***P<0.001.

Figure 4. **Inactivation of ACBP results in decreased levels of protein bound ceramides in stratum corneum**. Stratum corneum was isolated from Veet® treated belly skin from 3 month old mice using 0.25% Trypsin in PBS. Stratum corneum lipids were extracted followed by extraction of the protein bounds lipids and de-salting. Protein bound ([OS]) ceramides were quantified by mass spectrometry. (a) Most abundant [OS] ceramides and (b) less abundant [OS] ceramides with sphingosine as long chain base and indicated acyl chain length. Mean±SEM. n=7-9 mice/genotype/age. *P<0.05, **P<0.01, ***P<0.001.

Figure 5. **Lack of ACBP causes significant enlargement of sebaceous glands, due to increased differentiation**. (a) Quantification of sebaceous gland area on H&E stained skin sections isolated from $ACBP^{+/+}$ and $ACBP^{-/-}$ mice at indicated P days. Mean±SEM. n=3-5 mice/genotype/age. *P<0.05, **P<0.01, ***P<0.001. (b) Quantification of sebaceous gland area in skin isolated from K14-$ACBP^{+/+}$ and K14-$ACBP^{-/-}$ mice at

indicated P days. Mean±SEM. n=3-5 mice/genotype/age. *P<0.05, **P<0.01, ***P<0.001. (c) Quantification of BrdU positive cells relative to K14 positive cells in sebaceous glands of $ACBP^{+/+}$ and $ACBP^{-/-}$ mice at indicated P days. Mean±SEM. n=3-5 mice/genotype/age. *P<0.05, **P<0.01, ***P<0.001. (d) Quantification of sebaceous gland area in skin isolated from $ACBP^{+/+}$ and $ACBP^{-/-}$ mice at P28 days. –vas indicates no Vaseline treatment, +vas indicates Vaseline treatment (twice a day from P7 to P28).

Figure 6. **Enlarged sebaceous glands in $ACBP^{-/-}$ mice are producing increased amounts of lipids**. (a) Cryo sections from $ACBP^{+/+}$ and $ACBP^{-/-}$ mice skin at indicated P days were analyzed using CARS microscopy to visualize lipids. Green color represents collagen and red color represents lipids. The displayed pictures are representative of at least 3 sebaceous glands from each of five mice, from each age and genotype. Scale bars represent 20 µm. (b) $ACBP^{+/+}$ and $ACBP^{-/-}$ mice at indicated P days were scarified, the upper back skin were isolated, fixed with 4% PFA in PBS followed by paraffin embedding. Paraffin sections were de-paraffinized and incubated with 1' antibodies: anti-SCD1 (1:200) (overnight) (sc-14719, Santa Cruz) and 2' antibodies: anti-Goat Alexa Flour 488 (1:500) (1h) (A21121, life science); DAPI (1:500) (1h) (D9542, Sigma). The blue color represents DAPI staining of cell nucleus and green color represents SCD1 staining in sebaceous glands. The displayed pictures are representative of at least 3 sebaceous glands from each of five mice, from each age and genotype. Scale bars represent 20 µm. (c) RT-PCR analysis of the expression level of *SCD1*, *SQLE*, *HMGCR* and *Dgat1* in epidermal splits isolated from $ACBP^{+/+}$ and $ACBP^{-/-}$ mice (n=5 of each genotype). Mean±SEM. n=5 mice/genotype. *P<0.05, **P<0.01, ***P<0.001.

Figure 7. **The enlarged sebaceous glands in $ACBP^{-/-}$ mice are secreting increased amounts of sebum**. The fur was isolated from P21 $ACBP^{+/+}$ and $ACBP^{-/-}$ mice, followed by extraction of the lipids 2x15 min (3 mL acetone) and subsequent drying under N_2 flow. The extracted lipids were re-suspended in 1:1 chloroform/methanol. (a) and (b) Lipid amounts extracted from equal amounts of dry fur were separated on 10x20 cm silica gel 60 TLC plates together with known standards using (a) 55:45 hexane/benzene and (b) 80:30:1 hexane/diethyl ether/acetic acid. (c) and (d) Equal amounts of lipids were separated on 10x20 cm silica gel 60 TLC plates using (c) 55:45 hexane/benzene and (d) 80:30:1 hexane/diethyl ether/acetic acid. n=3-5 mice. Lipids were visualized using 10% $CuSO_4$ in 8% H_3PO_4 and 5 min burning (185°C), separated lipids were quantified using ImageJ. n=3-5 of each genotype. Mean±SEM. *P<0.05, **P<0.01, ***P<0.001. Abbreviations: Free fatty acid (FFA), cholesterol (Chol), triacylglycerol (TAG), monoalkyl diacylglycerol (MADAG), and cholesterol ester (CE).

Figure 1

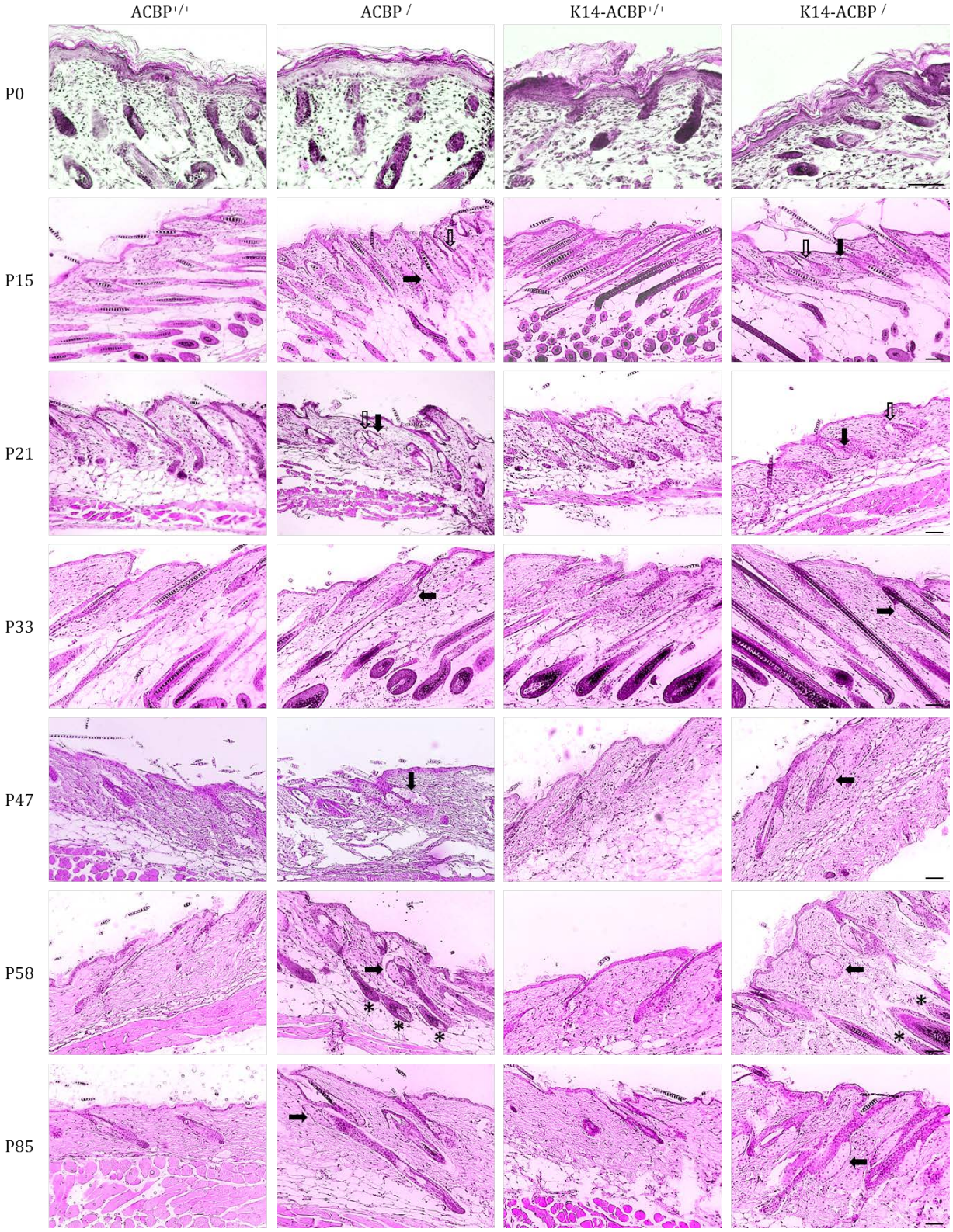

Figure 2

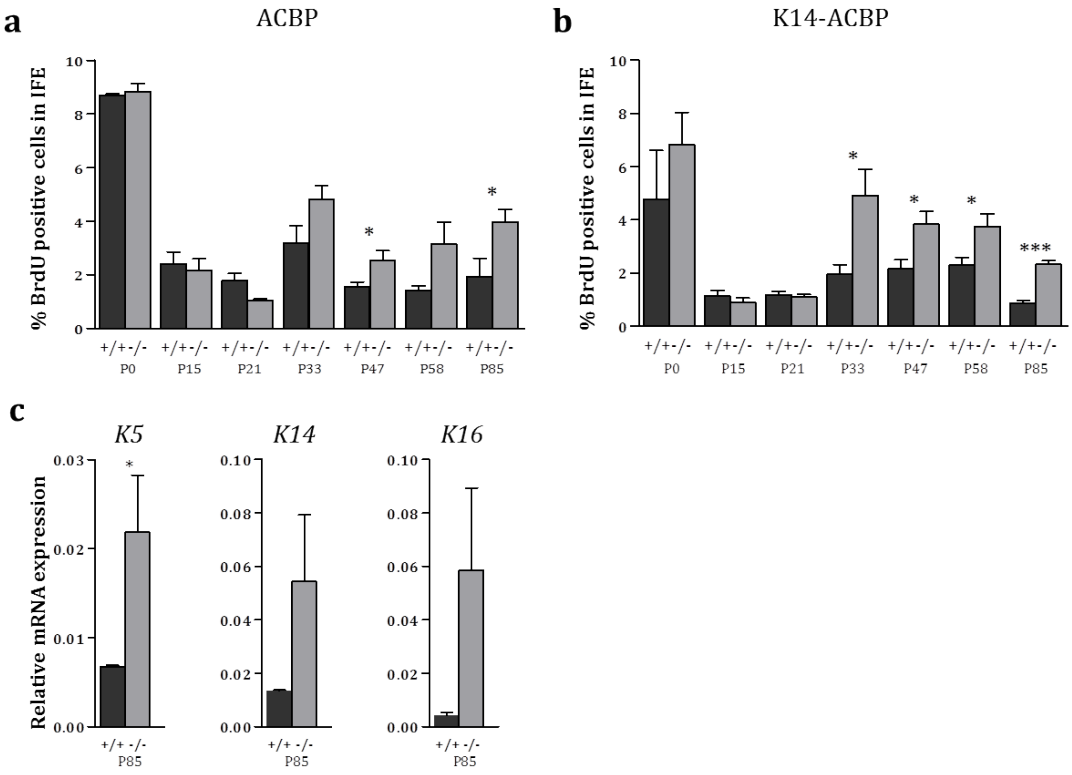
a
ACBP
% BrdU positive cells in IFE
+/+-/- P0
+/+-/- P15
+/+-/- P21
+/+-/- P33
+/+-/- P47
+/+-/- P58
+/+-/- P85
b
K14-ACBP
% BrdU positive cells in IFE
c
K5
K14
K16
Relative mRNA expression
+/+ -/- P85

Figure 3

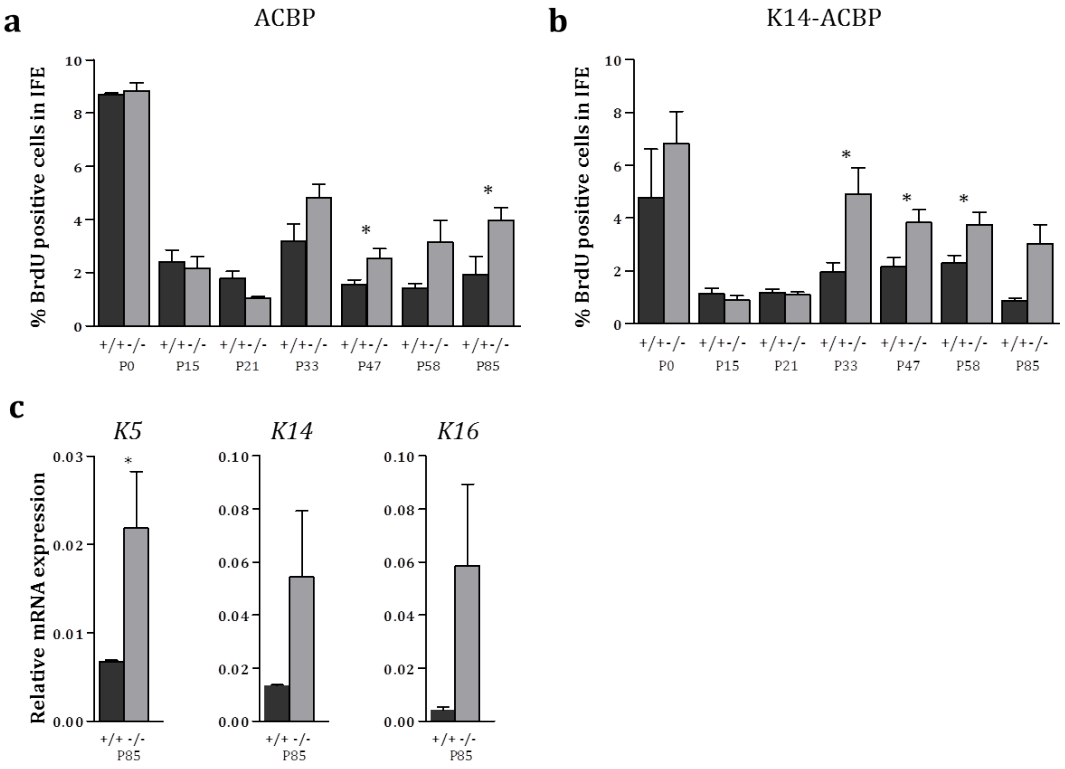
a
ACBP
% BrdU positive cells in IFE
+/+-/-
P0
P15
P21
P33
P47
P58
P85
b
K14-ACBP
% BrdU positive cells in IFE
c
K5
K14
K16
Relative mRNA expression
+/+ -/-
P85

Figure 4

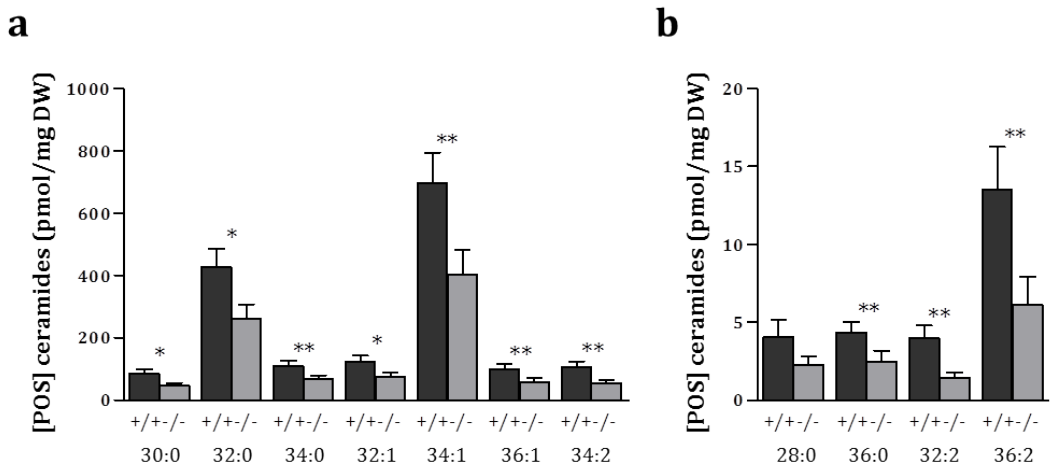
a
b
[POS] ceramides (pmol/mg DW)
1000
800
600
400
200
0
20
15
10
5
+/+-/-
30:0
32:0
34:0
32:1
34:1
36:1
34:2
28:0
36:0
32:2
36:2
*
**

Figure 5

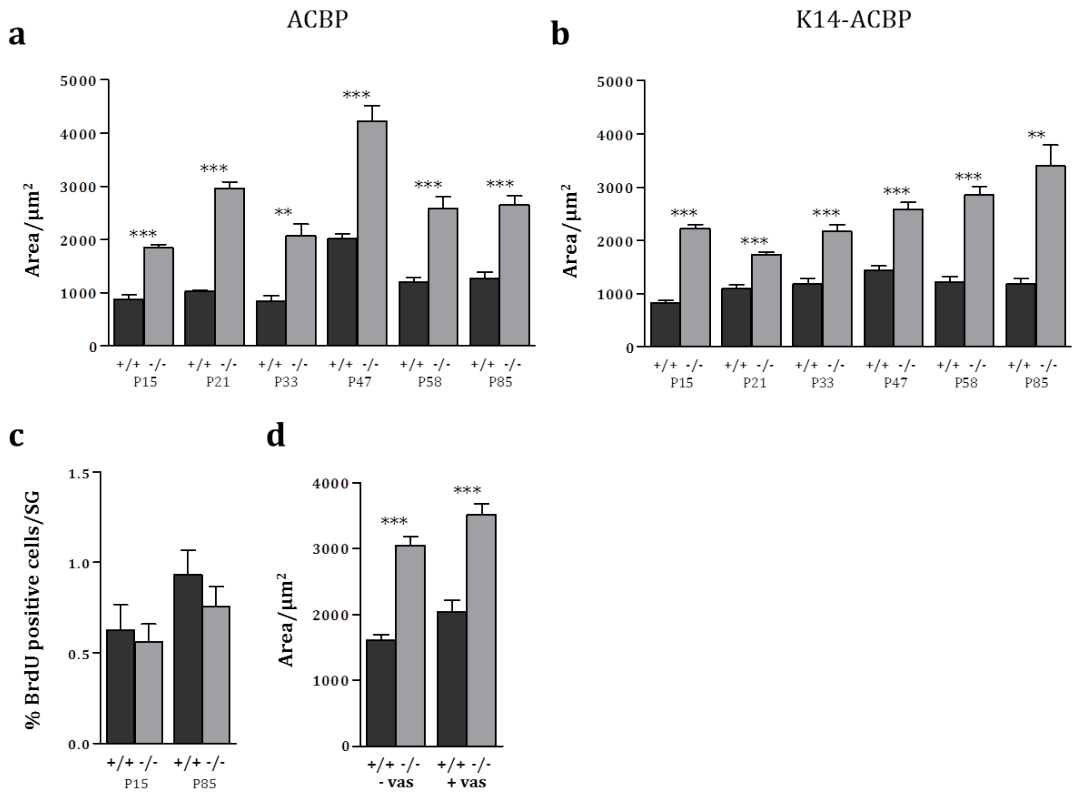
a
ACBP
b
K14-ACBP
Area/µm²
5000
4000
3000
2000
1000
0
***
**
+/+ -/-
P15
P21
P33
P47
P58
P85
c
% BrdU positive cells/SG
1.5
1.0
0.5
0.0
d
- vas
+ vas

Figure 6

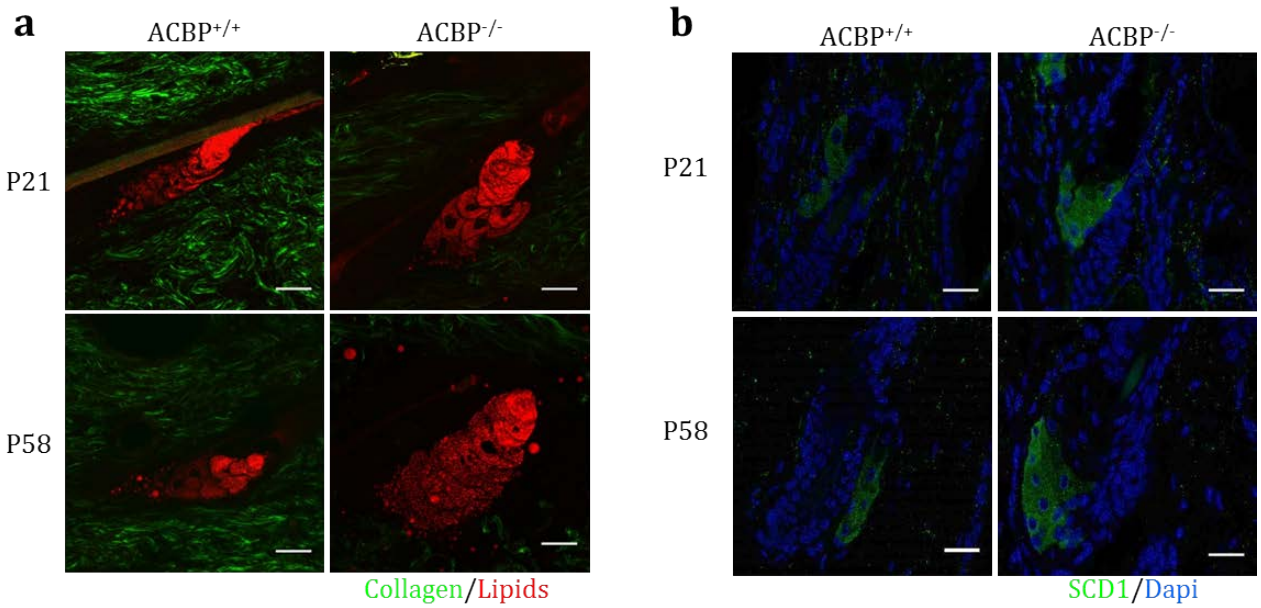
a
ACBP+/+
ACBP-/-
P21
P58
Collagen/Lipids
b
ACBP+/+
ACBP-/-
P21
P58
SCD1/Dapi

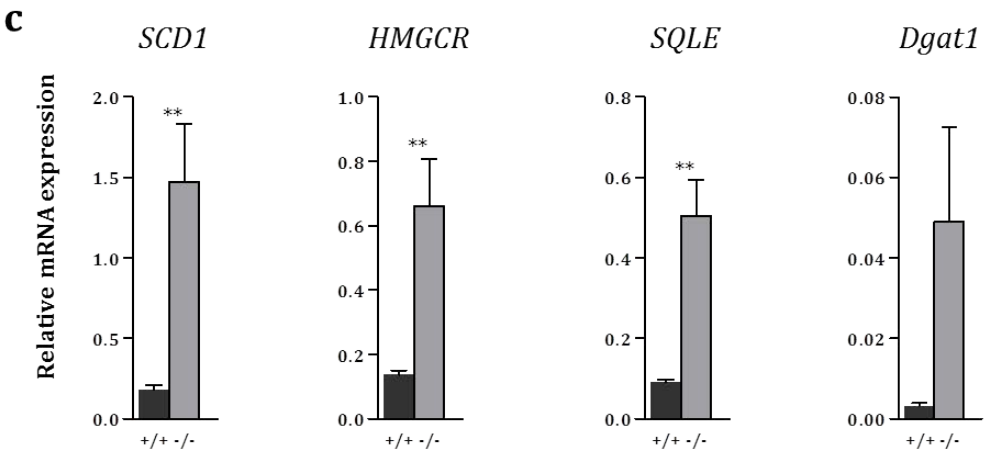
c
SCD1
HMGCR
SQLE
Dgat1
Relative mRNA expression
2.0
1.5
1.0
0.5
0.0
1.0
0.8
0.6
0.4
0.2
0.0
0.8
0.6
0.4
0.2
0.0
0.08
0.06
0.04
0.02
0.00
**
+/+ -/-

Figure 7

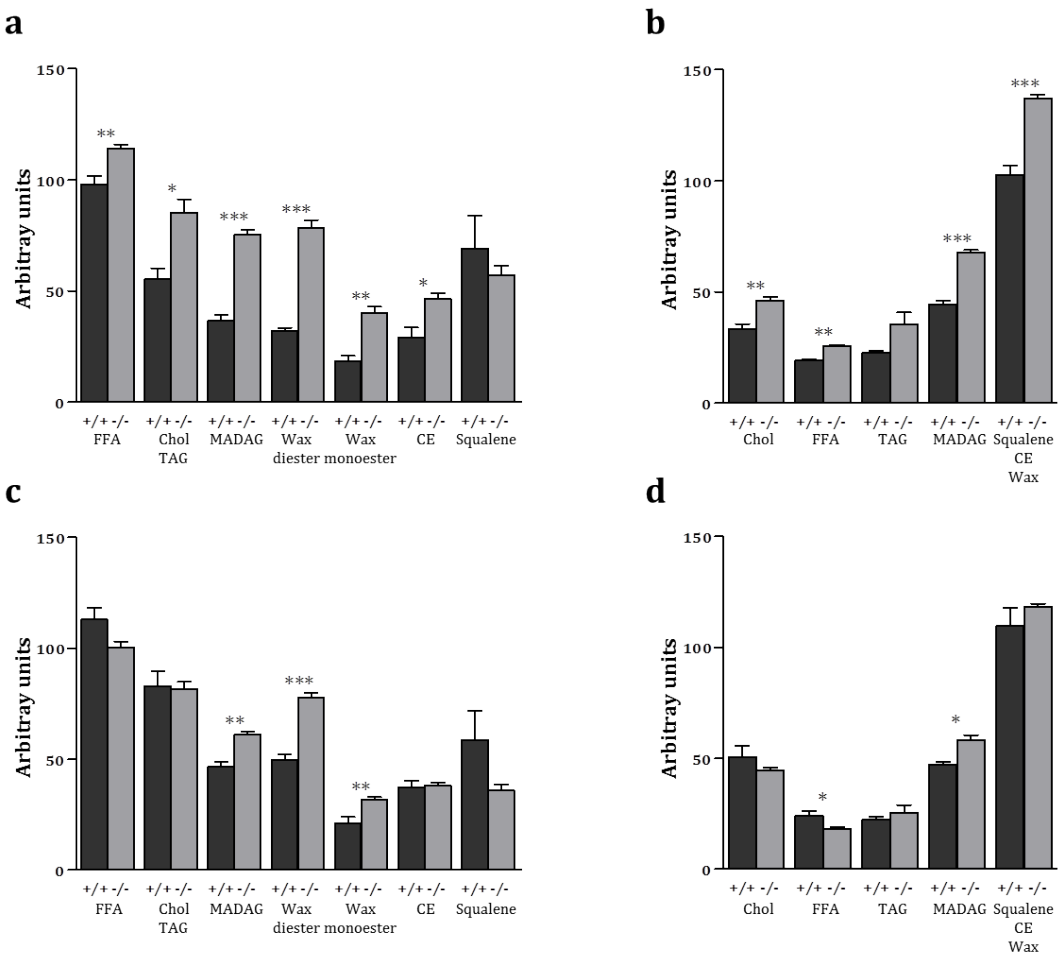
a
b
c
d
Arbitray units
150
100
50
0
+/+ -/-
FFA
Chol
TAG
MADAG
Wax diester
Wax monoester
CE
Squalene
Squalene CE Wax

SUPPLEMENT 2

Regulation of Very-Long Acyl Chain Ceramide Synthesis by Acyl-CoA Binding Protein

Natalia Santos Ferreira, **Hanne Engelsby,** Ditte Neess, Samuel L. Kelly, Giora Volpert, Alfred H. Merrill, Nils J. Færgeman and Anthony H. Futerman

The Journal of Biological Chemistry, in Press, Published on March 23, 2017 as Manuscript M117.785345

JBC Papers in Press. Published on March 23, 2017 as Manuscript M117.785345
The latest version is at http://www.jbc.org/cgi/doi/10.1074/jbc.M117.785345

Regulation of Very-Long Acyl Chain Ceramide Synthesis by Acyl-CoA Binding Protein

Natalia Santos Ferreira[1,4], Hanne Engelsby[2,4], Ditte Neess[2], Samuel L. Kelly[3], Giora Volpert[1], Alfred H. Merrill[3] Anthony H. Futerman[1,5], and Nils J. Færgeman[2,*]

[1]Department of Biomolecular Sciences, Weizmann Institute of Science, Rehovot 76100, Israel

[2]Villum Center for Bioanalytical Sciences, Department of Biochemistry and Molecular Biology, University of Southern Denmark, Campusvej 55, DK-5230 Odense M, Denmark

[3]School of Biology and Petit Institute for Bioengineering and Bioscience, Georgia Institute of Technology, Atlanta, Georgia 30332-0230, USA

[4]These authors contributed equally to this work

[5]The Joseph Meyerhoff Professor of Biochemistry at the Weizmann Institute of Science

Running title: ACBP is required for very-long acyl chain ceramide synthesis

[*]To whom correspondence should be addressed:
Nils J. Færgeman
Villum Center for Bioanalytical Sciences, Department of Biochemistry and Molecular Biology, University of Southern Denmark, Campusvej 55, DK-5230 Odense M, Denmark
Telephone +45 65502453, E-mail nils.f@bmb.sdu.dk

Keywords: Acyl-CoA, ACBP, Ceramides, Ceramide Synthase, Sphingolipid

ABSTRACT

Ceramide and more complex sphingolipids constitute a diverse group of lipids, which serve important roles as structural entities of biological membranes and as regulators of cellular growth, differentiation, and development. Thus, ceramides are vital players in numerous diseases including metabolic and cardiovascular diseases as well as neurological disorders. Here we show that acyl coenzyme A binding protein (ACBP) potently facilitates very-long acyl chain ceramide synthesis. ACBP increases the activity of ceramide synthase 2 (CerS2) by more than 2-fold and CerS3 activity by 7-fold. ACBP binds very long-chain acyl-CoA esters, which is required for its ability to stimulate CerS activity. We also show that high-speed liver cytosol from wild type mice activates CerS3 activity, while cytosol from ACBP knock out mice does not. Consistently, CerS2 and CerS3 activities are significantly reduced in the testes of $ACBP^{-/-}$ mice, concomitant with a significant reduction in long- and very-long chain ceramide levels. Importantly, we show that ACBP interacts with CerS2 and CerS3. Our data uncover a novel mode of regulation of very-long acyl chain ceramide synthesis by ACBP, which we anticipate is of crucial importance in understanding the regulation of ceramide metabolism in

pathogenesis.

Sphingolipids (SL) and in particular ceramides, mediate a number of cellular effects (1,2) including insulin resistance and are among the most deleterious lipids that perturb pancreatic β cell function, vascular reactivity and mitochondrial metabolism, which underlie the development of diabetes, obesity and cardiovascular disease (3-5). Importantly, inhibition of ceramide synthesis ameliorates many metabolic disorders in rodents (5). The ceramide *N*-acyl chain length significantly impacts the function of ceramides (6). For instance, ablation of ceramide synthase (CerS) 2, which catalyzes the formation of very-long (C22-24) acyl chain ceramides, results in hepatic insulin resistance in mice (7). Despite increased appreciation of the importance of ceramides, little information is available to allow delineation of the mechanism(s) of regulation of ceramide synthesis. Six CerS isoforms exist in mammals, each synthesizing ceramides with a specific acyl chain length (8). Thus, we only have limited knowledge about structure and function of the CerS isoforms; however, it is known that the active site resides in a sequence of 150 residues within the Tram-Lag-CLN8 domain (9), and that CerS can be regulated by phosphorylation, by homo- or heterodimerization and by interaction with fatty acid elongase, ELOVL1 (10-12). The CerS are highly homologous proteins, and reside in the endoplasmic reticulum where they have access to their two substrates, sphinganine and acyl-CoA esters.

A number of attempts have been made to model flux through the SL biosynthetic pathway (13,14). In contrast, experimental analysis of flux is limited to studies showing that the availability of fatty acids and serine can affect ceramide synthesis. This indicates that SL flux is coupled to other metabolic routes including synthesis and degradation of storage lipids like triacylglycerols (15,16), fatty acid elongation and fatty acid availability (12). Interestingly, acyl-CoA synthetase 5 (ACSL5) has recently been functionally coupled to ceramide synthesis via interaction with ceramide synthases (17). Acyl-CoA esters are generated in the cytosol via the action of acyl-CoA synthetases (18), and subsequently sequestered by high affinity acyl CoA binding domain proteins (ACBDs), which determine the metabolic routes and regulatory properties of acyl-CoA esters. The ACBDs comprise a highly conserved multi-gene family of intracellular lipid-binding proteins (19). Expression analyses confirm that ACBD1, also commonly known as ACBP, is by far the most abundantly expressed paralog (19). Recent genetic studies show that loss of ACBP in *Saccharomyces cerevisiae* and *C. elegans* abrogates fatty acid chain elongation and SL synthesis, resulting in compromised plasma membrane integrity and membrane function ((20) and our unpublished results).

We now show for the first time that ACBP potently activates CerS2 and CerS3 activity via direct interaction, and we show that ACBP ablation has deleterious effects on SL levels in mouse testis. We suggest that this novel interaction acts as a critical mode of regulation of very-long chain ceramide synthesis and as a putative site of interconnection between pathways of glycerolipid and SL synthesis. Hence, we suggest that the interaction between ACBP and CerS is important for directional channeling of acyl moieties in various cellular states.

RESULTS

ACBP stimulates CerS activity-Ceramide synthases catalyze the N-acylation of sphinganine using acyl-CoA esters as substrate. By virtue of its ability to bind acyl-CoA esters we speculated that CerS activity is determined by the availability of acyl CoA esters. We therefore assayed CerS activity in homogenates of HEK293T cells over-expressing each of the six CerS isoforms in the presence or absence of ACBP. These studies showed that recombinant ACBP potently stimulates both CerS2 and CerS3 activity. In the absence of ACBP, CerS2 activity was 82 ± 7 pmol/mg/min which increased more than 2-fold in the presence of as little as 0.25 nM ACBP (Fig. 1B). In the absence of ACBP, CerS3 activity was 16.0 ± 5.4 pmol/mg/min, which increased nearly 7-fold upon addition of ACBP (Fig. 1C). ACBP had no effect on the activity of the other CerS isoforms (Fig. 1) and did not affect the activity of a catalytic inactive form of CerS3 (Fig. 1). CerS activity increased in a biphasic manner (Fig 1) upon increasing $C_{26:0}$-CoA levels while keeping ACBP levels constant, indicating that CerS3 has

both low- and high-affinity binding components. Furthermore, the V_{max} of CerS3 towards sphinganine was increased from 55 to 235 pmol/mg/min in the presence of ACBP (Fig. 2).

To further substantiate the finding that ACBP stimulates CerS activity, HEK293T cells were cotransfected with ACBP and CerS2 or CerS3. The activities of both CerS2 and CerS3 significantly increased upon cotransfection to levels that were comparable to CerS activity upon addition of purified recombinant ACBP to cell lysates (Fig. 3). Moreover, since ACBP is a highly abundant cytosolic protein, we hypothesized that addition of cytosol would stimulate CerS3 activity. Indeed, we demonstrated that both low speed (10,000 x g) and high-speed (100,000 x g) supernatants from wild type mouse liver tissue stimulate CerS3 activity *in vitro* (Fig. 4). Importantly no stimulation of CerS3 activity was observed when using cytosol from an $ACBP^{-/-}$ mouse, confirming that ACBP is the main factor in liver cytosol capable of activating CerS. This was further supported by the dose dependent stimulation of CERS activity using cytosol from heterozygous $ACBP^{+/-}$ mouse liver resulting in ~50% activity relative to wild type cytosol (Fig. 4). Together, these observations demonstrate that the activity of both CerS2 and CerS3 is highly regulated by substrate availability mediated by ACBP.

ACBP ablation alters CerS activity and the sphingolipidome of mouse testis-Since ACBP potently stimulates CerS2 and CerS3 activity *in vitro*, we examined CerS2 and CerS3 activities in testis from ACBP depleted ($ACBP^{-/-}$) mice. Consistently, we observed significantly reduced CerS2 and CerS3 activity in testis from $ACBP^{-/-}$ mice (Fig. 5), which was not due to altered *Cers* mRNA expression (Fig. 6). This prompted us to examine the sphingolipidome in $ACBP^{-/-}$ mice. Thus, we analyzed the SL profile of testis from $ACBP^{+/+}$ and $ACBP^{-/-}$ mice by ESI-MS/MS, and found significant changes in ceramide, dihydroceramide, glucosylceramide, dihydroglucosylceramide, sphingomyelin, and dihydrosphingomyelin levels (Fig. 7). CerS2 utilizes primarily C_{22}-C_{24}-CoAs and C_{18}-CoA to a very minor extent (21), while CerS3 mainly uses $C_{26:0}$-CoA. Reduction in CerS2 and CerS3 activities might cause changes in levels of SLs containing other acyl chain lengths as we observe, due to altered dimer formation, which can significantly affect ceramide formation (10).

Activation of CerS3 requires ligand binding to ACBP-ACBP binds saturated and unsaturated C_{14}-C_{22} acyl-CoA esters with an affinity of 1-15 nM in a one-to-one binding mode, while free CoA binds with a much lower affinity (K_D of 2 mM) (22-24). The present finding that ACBP activates CerS2 and CerS3 suggests that ACBP can also bind very long-chain acyl-CoA esters. Using gel shift assays under non-denaturing conditions we observed that $C_{12:0}$-$C_{26:0}$-CoAs alter the mobility of ACBP (Fig. 8A), arguing that ACBP binds these acyl-CoA esters, although C12 and C_{26}-CoA is bound with lower affinity than the other acyl-CoA esters.

To test whether ligand binding to ACBP is required for CerS3 activation, we examined the effect of a panel of ACBP mutants, which do bind acyl-CoA ((23) and Fig. 8B), on CerS3 activity. CerS3 activity was not stimulated by ACBP in which Tyr28, Lys32 or Lys54 were mutated to alanine, which all interact with the 3′-phosphate on CoA and are required for ligand binding (Fig. 9). Moreover, altering the interaction between ACBP and the ω-end of the acyl-chain or the adenine ring by altering Leu25 or Phe5 to alanine, respectively, also abolishes the activating properties of ACBP (Fig. 9). Liver-type fatty acid binding protein-1 (FABP1), which also binds acyl-CoA esters and is highly abundant in liver (25), did not activate CerS3 (Fig. 9), which further substantiates that activation of ceramide synthase activity by ACBP is specific.

CerS interacts with ACBP-Our results clearly demonstrate that CerS2 and CerS3 are both activated by ACBP, suggesting that ACBP specifically target acyl-CoA esters to CerS2 or CerS3 via direct interaction. We were unable to detect such interactions by gelshift assays or by co-immunoprecipitation with or without cross-linking (not shown), likely due to the transient nature of this putative interaction. We therefore used a proximity ligation assay (PLA)(26) in which we co-expressed CerS3-HA and ACBP-FLAG in HEK293T cells and were able to detect an interaction between CerS3 and ACBP (Fig. 10). Consistent with the intracellular localization of CerS3, the CerS3-ACBP interaction localized to the perinuclear/ER. (Fig. 10A and 10B). We

demonstrate that ACBP also interacts with other members of the CerS family (Fig. 10B), even though their activity is not modulated by ACBP (Fig. 1), and also interacts with CerS2 and CerS3 even though they are catalytic inactive (Fig. 10C). Neither deletion of the HOX domain nor the C-terminus of CerS2 affected the interaction with ACBP (results not shown).

DISCUSSION

In the present study we show for the first time that CerS interact with and are regulated by ACBP, suggesting a novel mode of regulating sphingolipid synthesis. Despite the importance of ceramides and other sphingolipids as structural entities and as signaling molecules, the molecular mechanisms governing their synthesis remain unclear. In mammals, regulation of *de novo* ceramide synthesis may involve a complex balance between the six CerS isoforms as CerS activity can be modulated by reversible dimerization (10). Thus, different CerS isoforms physically interact, and the co-expression of one particular isoform can modulate the activity of another. Although the mechanisms driving dimerization remains unresolved, it is likely to be dynamic as pharmacologic stimulation of ceramide synthesis leads to an increase in CerS dimerization (10,27). Accordingly, the recently reported transcriptional and posttranscriptional regulation of CerS expression (28) may contribute to their dimerization and activity. Moreover, sphingosine-1-phosphate specifically inhibits CerS2 activity *in vitro* via a regulatory site, indicating an important regulatory interplay between sphingolipid metabolites (21).

The fact that CerS2 and CerS3 interact with and are regulated by ACBP suggests that these proteins might form a functional complex that drives ceramide synthesis. It is also interesting to note that fatty acid elongase (ELOVL) 1 interacts with CerS2, suggesting that synthesis of C_{24}-CoA by ELOVL1 is coordinated with the utilization of C_{24}-CoA by CerS2 for ceramide production (12). We therefore speculate that CerS2, ELOVL1 and ACBP form a functional platform, which promotes coordinated and directional synthesis of very-long chain acyl-CoA esters and ceramides. As a consequence, this interaction might determine the flux through the *de novo* ceramide synthesis pathway. To this end, generation of acyl-CoA esters by ACSL5 has recently been functionally coupled to ceramide synthesis (17), suggesting that ACSLs also could be part in such platforms. Notably, serine palmitoyl transferase, which catalyzes the first and rate-limiting step in sphingolipid synthesis, is also regulated by specific protein interactions by reversibly forming a 'SPOTS' complex with a family of conserved Orm proteins, the serine palmitoyltransferase accessory subunit Tsc3, and the phosphoinositide phosphatase Sac1 (29,30). However, even though CerS4-6 also interact with ACBP, their (and CerS1) kinetics are not affected by increasing levels of ACBP. Similarly, CerS2 also interacts with ELOVL1-7, although CerS2 only affects ELOVL1 activity (12). As the acyl chain length increases, the solubility of acyl-CoA esters in aqueous solutions decreases rapidly. Thus, while CerS1 and CerS4-6 all are characterized by having a preference for long-chain acyl-CoA esters, CerS2 and CerS3 both prefer very-long chain acyl-CoA (31). Thus, we speculate that ACBP interacts with all the CerS to maintain a critical level of available acyl-CoA substrates, which is in particularly important for CerS2 and CerS3.

Further kinetic analyses of CerS3 activation by ACBP revealed a biphasic saturation profile suggesting the presence of both low and high affinity-binding sites. Such a kinetic profile has been observed for a number of other enzymes, e.g. naproxen demethylation by CYP2C9 (32,33), CYP3A4-mediated metabolism of naphthalene (32), and 7-ethoxycoumarin *O*-deethylation and aminopyrine *N*-demethylation by NADPH-P450 reductase (34).

Even though the level of fatty acid binding protein 1 (FABP1), which also binds acyl-CoA esters, is approximately 10-fold higher than ACBP in liver, which also contains other acyl-CoA binding domain containing proteins (19), we show that ACBP is the primary factor in liver cytosol that stimulates CerS activity *in vitro*. This and the fact that ACBP mutants, incapable of binding ligand, cannot stimulate ceramide synthase activity, underline the suggestion that ACBP specifically channels acyl-CoA esters for activation of CerS2 and CerS3. Accordingly, ablation of ACBP in mice testis, in which both CerS2 and CerS3 are highly expressed (21), results in global alterations in ceramide and

sphingomyelin levels. This however does not affect reproduction of ACBP null mice (35). We previously reported that loss of ACBP in mice impairs the epidermal barrier function resulting in heat and water loss (36). Since synthesis of ceramides containing ultra very long-chain acyl chains generated by CerS3 in keratinocytes are required for the integrity of the epidermal barrier in both mice and humans (37-39), we speculate that the impaired epidermal barrier in ACBP knockout mice might be due to reduced levels of ceramides produced by CerS3 in the absence of ACBP.

In conclusion, we have identified a novel mode of regulating CerS2 and CerS3 activity *in vivo* via an interaction with ACBP. The present work and the genetic mice models that we have available provide an excellent framework to further delineate how ceramide synthases are regulated *in vivo* by acyl-CoA binding proteins and how this interaction affects mammalian physiology. By analogy to other lipid binding proteins involved in intra- and intercompartmental trafficking of sphingolipids like FAPP2 and CERT (40), we anticipate that ACBP constitutes a new regulatory lipid binding protein, which plays a central role in the sphingolipid network and is therefore important in our understanding of human diseases triggered by altered sphingolipid metabolism.

EXPERIMENTAL PROCEDURES

Materials-D-erythro-[4,5-^{3}H]-sphinganine was synthesized as described (41). Fatty acyl-CoAs, sphinganine, lipid standards for thin layer chromatography (TLC), and internal standards for liquid chromatography electrospray ionization tandem mass spectrometry (LC-ESI-MS/MS) were from Avanti Polar Lipids (Alabaster, AL). Silica gel 60 TLC plates were from Merck. All solvents were of analytical grade and were from Biolab (Jerusalem, Israel). Defatted bovine serum albumin and a protease inhibitor mixture were from Sigma-Aldrich.

Mice-Acbp knock out mice have been described previously (35,36). Mice were housed under standard conditions (36). Animal experiments and breeding of transgenic mice were approved by the Danish Animal Experiment Inspectorate. Tissues were dissected and processed according to previously described procedures (36).

Cell Culture-Human embryonic kidney (HEK) 293T cells were cultured in Dulbecco's modified Eagle's medium (Gibco) supplemented with 10% fetal calf serum, 100 IU/ml penicillin and 100µg/ml streptomycin. HEK293T cells were transfected with human CerS with an HA tag at the C terminus (CerS-HA) and/or murine ACBP (ACBD1) with a Flag tag at the C terminus using a jetPEIa^{TM}, DNA in vitro transfection reagent (Polypus transfection) (8 µg DNA per 10 cm culture dish). Forty-eight hours after transfection, cells were collected by trypsinization and stored at -80 °C.

Expression and purification of recombinant rat ACBP-Protein expression and purification of rat ACBP was performed as described (42). Selected residues in rat ACBP were replaced with alanine by site-directed mutagenesis (43).

CerS assays and SL measurements-CerS was assayed in homogenates as described using [4,5-^{3}H]-sphinganine, 15 µM sphinganine, 20 µM defatted bovine serum albumin and 50 µM fatty acyl-CoA (Avanti Polar Lipids, Alabster, AL) (44). For CerS1 and CerS4 assays 150 µg of protein was used, for CerS2, CerS5 and CerS6 100 µg of protein was used, and for CerS3 assays 250 µg of protein was used. When effects of high-speed cytosols on CerS activity were examined, 6 mg cytosol protein was added for each ml assay. SL levels were measured by ESI MS/MS using a PE-Sciex API 3000 triple quadrupole mass spectrometer and an ABI 4000 quadrupole-linear ion trap mass spectrometer (45,46).

Proximity ligation assay-The interaction between ACBP and CerS was examined by proximity ligation assay (PLA) in HEK293T cells essentially as described previously (47). Briefly, 0.48 µg DNA was mixed with 1 µg polyethylenimine, diluted with 20 µL DMEM and incubated for 10 min at room temperature. Cells were grown to 90-95 % confluence in a 10 cm petri dish, detached by incubation with 500 µL trypsin and neutralized with 5.5 mL DMEM, mixed with the transfection mixture and seeded into 16 chambered cover glass (C37000, Thermo®). Cells were incubated as described above for 48 h. DMEM was aspirated, cells were washed with PBS, chambers were removed and cells fixed with 4 % paraformaldehyde in H_2O for

10 min at room temperature. Cells were washed 3x for 5 min each in PBS in a 10 cm petri dish with gentle agitation. Cells were permeabilized with 0.5 % Triton X-100 in PBS for 10 min, followed by 3 washes in 0.05 % Tween 20 in TBS for 5 min each in a 10 cm petri dish with gentle agitation. Cells were blocked with 1 drop Duolink® In Situ Blocking Solution (DUO82007, Sigma-Aldrich®) for 1 h at 37°C in a humidity chamber. Cells were incubated with 40 µL primary antibodies: anti-DDK (TA50011, Origene®) and anti-HA (H6908, Sigma-Aldrich®), 1 µg/mL diluted in Duolink® Antibody Diluent (DUO82008, Sigma-Aldrich®), 1 h at 37°C in a humidity chamber. Cells were washed for 2 min followed by two 10 min washes in Duolink® In Situ Wash Buffer A (DUO82047, Sigma-Aldrich®) in a 10 cm petri dish with gentle agitation and incubated with 40 µL Duolink® In Situ PLA® probes, anti-rabbit (DUO82002, Sigma-Aldrich®), anti-mouse (DUO82004, Sigma-Aldrich®) diluted 5x in Duolink® Antibody Diluent (DUO82008, Sigma-Aldrich®), for 1 h at 37°C in a humidity chamber. Cells were washed for 2 min followed by two 10 min washes in Duolink® In Situ Wash Buffer A in a 10 cm petri dish with gentle agitation. PLA® probes were ligated by incubation with 40 µL Duolink® In Situ Ligase diluted 1:40 in Duolink® In Situ Ligation (DUO82009, Sigma-Aldrich®) for 30 min at 37°C in a humidity chamber followed by two washes for 2 min in Duolink® In Situ Wash Buffer A in a 10 cm petri dish with gentle agitation. PLA® probes were amplified by incubation with 40 µL Duolink® In Situ Amplification Red diluted 1:40 in 1 x Duolink® In Situ Ligation (DUO82011, Sigma-Aldrich®) for 100 min at 37°C in a humidity chamber and washed twice for 10 min in Duolink® In Situ Wash Buffer B (DUO82048, Sigma-Aldrich®) in a 10 cm petri dish with agitation (30 rpm). The cover slides were dipped in 10x diluted Duolink® In Situ Wash Buffer B (DUO82048, Sigma-Aldrich®), the silicone membrane around the cells was removed and the cover slides were mounted on microscopy slides with Duolink® In Situ Mounting Medium with DAPI (DUO82040, Sigma-Aldrich®). Florescent signals were visualized at ambient temperature on a Leica TCS SP8X confocal microscope with a hybrid detector using a HCX PL APO 100X/1.40 oil objective using Leica Application Suite software. Images were processed using ImageJ (48).

RNA isolation and real-time PCR-Isolation of total RNA and determination of mRNA levels by real-time PCR were carried out as described (36). TFIIB expression was used for normalization. The following real-time primers were used: TfIIb fwd: 5-GTTCTGCTCCAACCTTTGCCT-3', TfIIb rev: 5-TGTGTAGCTGCCATCTGCACTT-3'. CerS1 fwd: 5'-GCC ACC ACA CAC ATC TTT CGG-3', CerS1 rev: 5'-GGA GCA GGT AAG CGC AGT AG-3', CerS2 fwd: 5'-AGA GTG GGC TCT CTG GAC G-3', CerS2 rev: 5'-CCA GGG TTT ATC CAC AGT GAC-3', CerS3 fwd: 5'-CCT GGC TGC TAT TAG TCT GAT G-3', CerS3 rev: 5'-CTG CTT CCA TCC AGC ATA GG-3', CerS4 fwd: 5'-CTG TGG TAC TGT TGT TGC ATG AC-3', CerS4 rev: 5'-GCG CGT GTA GAA GAA GAC TAA G-3', CerS5 fwd: 5'-TGG CCA ATT ATG CCA GAC GTG AG-3', CerS5 rev: 5'-GGT AGG GCC CAA TAA TCT CCC AGC-3', CerS6 fwd: 5'-GCA TTC AAC GCT GGT TTC GAC-3', CerS6 rev: 5'-TTC AAG AAC CGG ACT CCG TAG-3'

Western blotting-Transfected HEK293T cells were harvested in SDS lysis buffer and protein extracts were prepared as described in (36). The protein concentration was determined using Pierce BCA Protein Assay kit, followed by SDS-PAGE protein separation, blotting and ECL as described in (36). The following antibodies were used: Anti-HA (H6908, Sigma), anti-DDK (TA50011, Origene), anti-GAPDH (sc-25778, Santa Cruz), and horseradish peroxidase-conjugated anti-rabbit and anti-mouse antibodies (W4011 and W4021, Promega).

Statistics-Statistical analysis was performed using the Student's t-test, and differences among groups were considered significant for $p<0.05$ (*), $p< 0.01$ (**), $p< 0.001$ (***) and $p< 0.0001$ (****).

Acknowledgements

We thank Dr. Elad L. Laviad (Weizmann Institute of Science) for help with the initial part of this study.

Conflict of interest

The authors declare that they have no conflicts of interest with the contents of this article.

Author Contributions

NSF performed CerS assays, HE performed the proximity ligation assays and Western blotting, DN managed all mice work, GV analyzed the enzyme kinetic analyses, KLS and AHM carried out the ESI-MS/MS analyses of sphingolipids, NJF expressed and purified all recombinant ACBP proteins, and NJF and AHF managed and funded the studies and wrote the manuscript.

REFERENCES

1. Hannun, Y. A., and Obeid, L. M. (2008) Principles of bioactive lipid signalling: lessons from sphingolipids. *Nat Rev Mol Cell Biol* **9**, 139-150
2. Maceyka, M., and Spiegel, S. (2014) Sphingolipid metabolites in inflammatory disease. *Nature* **510**, 58-67
3. Astudillo, L., Sabourdy, F., Therville, N., Bode, H., Segui, B., Andrieu-Abadie, N., Hornemann, T., and Levade, T. (2015) Human genetic disorders of sphingolipid biosynthesis. *J Inherit Metab Dis* **38**, 65-76
4. Hla, T., and Kolesnick, R. (2014) C16:0-ceramide signals insulin resistance. *Cell Metab* **20**, 703-705
5. Chaurasia, B., and Summers, S. A. (2015) Ceramides - Lipotoxic Inducers of Metabolic Disorders. *Trends Endocrinol Metab* **26**, 538-550
6. Raichur, S., Wang, S. T., Chan, P. W., Li, Y., Ching, J., Chaurasia, B., Dogra, S., Ohman, M. K., Takeda, K., Sugii, S., Pewzner-Jung, Y., Futerman, A. H., and Summers, S. A. (2014) CerS2 haploinsufficiency inhibits beta-oxidation and confers susceptibility to diet-induced steatohepatitis and insulin resistance. *Cell Metab* **20**, 687-695
7. Park, J. W., Park, W. J., Kuperman, Y., Boura-Halfon, S., Pewzner-Jung, Y., and Futerman, A. H. (2013) Ablation of very long acyl chain sphingolipids causes hepatic insulin resistance in mice due to altered detergent-resistant membranes. *Hepatology* **57**, 525-532
8. Tidhar, R., and Futerman, A. H. (2013) The complexity of sphingolipid biosynthesis in the endoplasmic reticulum. *Biochim Biophys Acta* **1833**, 2511-2518
9. Tidhar, R., Ben-Dor, S., Wang, E., Kelly, S., Merrill, A. H., Jr., and Futerman, A. H. (2012) Acyl chain specificity of ceramide synthases is determined within a region of 150 residues in the Tram-Lag-CLN8 (TLC) domain. *J Biol Chem* **287**, 3197-3206
10. Laviad, E. L., Kelly, S., Merrill, A. H., Jr., and Futerman, A. H. (2012) Modulation of ceramide synthase activity via dimerization. *J Biol Chem* **287**, 21025-21033
11. Sassa, T., Hirayama, T., and Kihara, A. (2016) Enzyme Activities of the Ceramide Synthases CERS2-6 Are Regulated by Phosphorylation in the C-terminal Region. *J Biol Chem*
12. Ohno, Y., Suto, S., Yamanaka, M., Mizutani, Y., Mitsutake, S., Igarashi, Y., Sassa, T., and Kihara, A. (2010) ELOVL1 production of C24 acyl-CoAs is linked to C24 sphingolipid synthesis. *Proc Natl Acad Sci U S A* **107**, 18439-18444
13. Alvarez-Vasquez, F., Sims, K. J., Cowart, L. A., Okamoto, Y., Voit, E. O., and Hannun, Y. A. (2005) Simulation and validation of modelled sphingolipid metabolism in Saccharomyces cerevisiae. *Nature* **433**, 425-430
14. Wronowska, W., Charzynska, A., Nienaltowski, K., and Gambin, A. (2015) Computational modeling of sphingolipid metabolism. *BMC Syst Biol* **9**, 47

15. Rajakumari, S., Rajasekharan, R., and Daum, G. (2010) Triacylglycerol lipolysis is linked to sphingolipid and phospholipid metabolism of the yeast Saccharomyces cerevisiae. *Biochim Biophys Acta* **1801**, 1314-1322
16. Radner, F. P., Grond, S., Haemmerle, G., Lass, A., and Zechner, R. (2011) Fat in the skin: Triacylglycerol metabolism in keratinocytes and its role in the development of neutral lipid storage disease. *Dermatoendocrinol* **3**, 77-83
17. Senkal, C. E., Salama, M. F., Snider, A. J., Allopenna, J. J., Rana, N. A., Koller, A., Hannun, Y. A., and Obeid, L. M. (2017) Ceramide Is Metabolized to Acylceramide and Stored in Lipid Droplets. *Cell Metab* **25**, 686-697
18. Grevengoed, T. J., Klett, E. L., and Coleman, R. A. (2014) Acyl-CoA metabolism and partitioning. *Annu Rev Nutr* **34**, 1-30
19. Neess, D., Bek, S., Engelsby, H., Gallego, S. F., and Faergeman, N. J. (2015) Long-chain acyl-CoA esters in metabolism and signaling: Role of acyl-CoA binding proteins. *Prog Lipid Res* **59**, 1-25
20. Gaigg, B., Neergaard, T. B., Schneiter, R., Hansen, J. K., Faergeman, N. J., Jensen, N. A., Andersen, J. R., Friis, J., Sandhoff, R., Schroder, H. D., and Knudsen, J. (2001) Depletion of acyl-coenzyme A-binding protein affects sphingolipid synthesis and causes vesicle accumulation and membrane defects in *Saccharomyces cerevisiae*. *Mol Biol Cell* **12**, 1147-1160
21. Laviad, E. L., Albee, L., Pankova-Kholmyansky, I., Epstein, S., Park, H., Merrill, A. H., Jr., and Futerman, A. H. (2008) Characterization of ceramide synthase 2: tissue distribution, substrate specificity, and inhibition by sphingosine 1-phosphate. *J Biol Chem* **283**, 5677-5684
22. Faergeman, N. J., Sigurskjold, B. W., Kragelund, B. B., Andersen, K. V., and Knudsen, J. (1996) Thermodynamics of ligand binding to acyl-coenzyme A binding protein studied by titration calorimetry. *Biochemistry* **35**, 14118-14126
23. Kragelund, B. B., Poulsen, K., Andersen, K. V., Baldursson, T., Kroll, J. B., Neergard, T. B., Jepsen, J., Roepstorff, P., Kristiansen, K., Poulsen, F. M., and Knudsen, J. (1999) Conserved residues and their role in the structure, function, and stability of acyl-coenzyme A binding protein. *Biochemistry* **38**, 2386-2394
24. Fulceri, R., Knudsen, J., Giunti, R., Volpe, P., Nori, A., and Benedetti, A. (1997) Fatty acyl-CoA-acyl-CoA-binding protein complexes activate the Ca2+ release channel of skeletal muscle sarcoplasmic reticulum. *Biochem J* **325 (Pt 2)**, 423-428
25. Rolf, B., Oudenampsen-Kruger, E., Borchers, T., Faergeman, N. J., Knudsen, J., Lezius, A., and Spener, F. (1995) Analysis of the ligand binding properties of recombinant bovine liver-type fatty acid binding protein. *Biochim Biophys Acta* **1259**, 245-253
26. Soderberg, O., Leuchowius, K. J., Gullberg, M., Jarvius, M., Weibrecht, I., Larsson, L. G., and Landegren, U. (2008) Characterizing proteins and their interactions in cells and tissues using the in situ proximity ligation assay. *Methods* **45**, 227-232
27. Jensen, S. A., Calvert, A. E., Volpert, G., Kouri, F. M., Hurley, L. A., Luciano, J. P., Wu, Y., Chalastanis, A., Futerman, A. H., and Stegh, A. H. (2014) Bcl2L13 is a ceramide synthase inhibitor in glioblastoma. *Proc Natl Acad Sci U S A* **111**, 5682-5687
28. Wegner, M. S., Wanger, R. A., Oertel, S., Brachtendorf, S., Hartmann, D., Schiffmann, S., Marschalek, R., Schreiber, Y., Ferreiros, N., Geisslinger, G., and Grosch, S. (2014) Ceramide synthases CerS4 and CerS5 are upregulated by 17beta-estradiol and GPER1 via AP-1 in human breast cancer cells. *Biochem Pharmacol* **92**, 577-589
29. Breslow, D. K., Collins, S. R., Bodenmiller, B., Aebersold, R., Simons, K., Shevchenko, A., Ejsing, C. S., and Weissman, J. S. (2010) Orm family proteins mediate sphingolipid homeostasis. *Nature* **463**, 1048-1053
30. Han, S., Lone, M. A., Schneiter, R., and Chang, A. (2010) Orm1 and Orm2 are conserved endoplasmic reticulum membrane proteins regulating lipid homeostasis and protein quality control. *Proc Natl Acad Sci U S A* **107**, 5851-5856
31. Levy, M., and Futerman, A. H. (2010) Mammalian ceramide synthases. *IUBMB Life* **62**, 347-356

32. Korzekwa, K. R., Krishnamachary, N., Shou, M., Ogai, A., Parise, R. A., Rettie, A. E., Gonzalez, F. J., and Tracy, T. S. (1998) Evaluation of atypical cytochrome P450 kinetics with two-substrate models: evidence that multiple substrates can simultaneously bind to cytochrome P450 active sites. *Biochemistry* **37**, 4137-4147
33. Hutzler, J. M., Hauer, M. J., and Tracy, T. S. (2001) Dapsone activation of CYP2C9-mediated metabolism: evidence for activation of multiple substrates and a two-site model. *Drug Metab Dispos* **29**, 1029-1034
34. Inouye, K., Mizokawa, T., Saito, A., Tonomura, B., and Ohkawa, H. (2000) Biphasic kinetic behavior of rat cytochrome P-4501A1-dependent monooxygenation in recombinant yeast microsomes. *Biochim Biophys Acta* **1481**, 265-272
35. Neess, D., Bloksgaard, M., Bek, S., Marcher, A. B., Elle, I. C., Helledie, T., Due, M., Pagmantidis, V., Finsen, B., Wilbertz, J., Kruhoffer, M., Faergeman, N., and Mandrup, S. (2011) Disruption of the acyl-CoA-binding protein gene delays hepatic adaptation to metabolic changes at weaning. *The Journal of biological chemistry* **286**, 3460-3472
36. Neess, D., Bek, S., Bloksgaard, M., Marcher, A. B., Faergeman, N. J., and Mandrup, S. (2013) Delayed hepatic adaptation to weaning in ACBP-/- mice is caused by disruption of the epidermal barrier. *Cell Rep* **5**, 1403-1412
37. Jennemann, R., Rabionet, M., Gorgas, K., Epstein, S., Dalpke, A., Rothermel, U., Bayerle, A., van der Hoeven, F., Imgrund, S., Kirsch, J., Nickel, W., Willecke, K., Riezman, H., Grone, H. J., and Sandhoff, R. (2012) Loss of ceramide synthase 3 causes lethal skin barrier disruption. *Hum Mol Genet* **21**, 586-608
38. Eckl, K. M., Tidhar, R., Thiele, H., Oji, V., Hausser, I., Brodesser, S., Preil, M. L., Onal-Akan, A., Stock, F., Muller, D., Becker, K., Casper, R., Nurnberg, G., Altmuller, J., Nurnberg, P., Traupe, H., Futerman, A. H., and Hennies, H. C. (2013) Impaired epidermal ceramide synthesis causes autosomal recessive congenital ichthyosis and reveals the importance of ceramide acyl chain length. *J Invest Dermatol* **133**, 2202-2211
39. Radner, F. P., Marrakchi, S., Kirchmeier, P., Kim, G. J., Ribierre, F., Kamoun, B., Abid, L., Leipoldt, M., Turki, H., Schempp, W., Heilig, R., Lathrop, M., and Fischer, J. (2013) Mutations in CERS3 cause autosomal recessive congenital ichthyosis in humans. *PLoS Genet* **9**, e1003536
40. Yamaji, T., and Hanada, K. (2015) Sphingolipid metabolism and interorganellar transport: localization of sphingolipid enzymes and lipid transfer proteins. *Traffic* **16**, 101-122
41. Hirschberg, K., Rodger, J., and Futerman, A. H. (1993) The long-chain sphingoid base of sphingolipids is acylated at the cytosolic surface of the endoplasmic reticulum in rat liver. *Biochem J* **290 (Pt 3)**, 751-757
42. Wadum, M. C., Villadsen, J. K., Feddersen, S., Moller, R. S., Neergaard, T. B., Kragelund, B. B., Hojrup, P., Faergeman, N. J., and Knudsen, J. (2002) Fluorescently labelled bovine acyl-CoA-binding protein acting as an acyl-CoA sensor: interaction with CoA and acyl-CoA esters and its use in measuring free acyl-CoA esters and non-esterified fatty acids. *Biochem J* **365**, 165-172
43. Fisher, C. L., and Pei, G. K. (1997) Modification of a PCR-based site-directed mutagenesis method. *Biotechniques* **23**, 570-571, 574
44. Lahiri, S., Lee, H., Mesicek, J., Fuks, Z., Haimovitz-Friedman, A., Kolesnick, R. N., and Futerman, A. H. (2007) Kinetic characterization of mammalian ceramide synthases: determination of K(m) values towards sphinganine. *FEBS Letters* **581**, 5289-5294
45. Sullards, M. C., Liu, Y., Chen, Y., and Merrill, A. H., Jr. (2011) Analysis of mammalian sphingolipids by liquid chromatography tandem mass spectrometry (LC-MS/MS) and tissue imaging mass spectrometry (TIMS). *Biochim Biophys Acta* **1811**, 838-853
46. Shaner, R. L., Allegood, J. C., Park, H., Wang, E., Kelly, S., Haynes, C. A., Sullards, M. C., and Merrill, A. H., Jr. (2009) Quantitative analysis of sphingolipids for lipidomics using triple quadrupole and quadrupole linear ion trap mass spectrometers. *J Lipid Res* **50**, 1692-1707
47. Thymiakou, E., and Episkopou, V. (2011) Detection of signaling effector-complexes downstream of bmp4 using PLA, a proximity ligation assay. *J Vis Exp*

48. Schneider, C. A., Rasband, W. S., and Eliceiri, K. W. (2012) NIH Image to ImageJ: 25 years of image analysis. *Nat Methods* **9**, 671-675

FOOTNOTES

This work was supported by the Israel Science Foundation (0888/11) and The Danish Council for independent Research-Natural Science (23459) and the Novo Nordisk Foundation.

The abbreviations used are: ACBP, acyl-coenzyme A binding protein; ACBD, acyl CoA binding domain proteins; CerS, ceramide synthase; ELOVL, elongase; LC ESI-MS/MS, liquid chromatography electrospray ionization tandem mass spectrometry; PLA, proximity ligation assay; TLC, thin layer chromatography;

FIGURE LEGENDS

FIGURE 1. ACBP stimulates CerS2 and CerS3 activity *in vitro*. Homogenates were prepared from HEK293T cells overexpressing Cers1 (A), CerS2 (B), CerS3 (C), CerS4 (D), CerS5 (E), CerS6 (F) or a catalytic inactive form of CerS3 (W15R) (G) and CerS activity was determined using $C_{18:0}$-CoA (A), $C_{24:1}$-CoA (B), $C_{26:0}$-CoA (C, G, H), $C_{20:0}$-CoA (D), $C_{16:0}$-CoA (E and F), respectively, in the presence of increasing amounts of ACBP. (H) CerS3 activity was assayed in the presence of increasing amounts of $C_{26:0}$-CoA in the presence or absence of 1 nM recombinant ACBP. Results are mean values ± S.D, n = 3 for A-G and N = 6 for H.

FIGURE 2. ACBP increases CerS3 activity. Homogenates were prepared from HEK293T cells overexpressing CerS3 and CerS3 activity was determined using $C_{26:0}$-CoA in the presence of increasing amounts of sphinganine. Results are shown as means ± S.D, n = 3.

FIGURE 3. Co-expression of ACBP in HEK293T cells increases CerS2 and CerS3 activity. CerS2-HA (A) or CerS3-HA (B) were co-expressed in HEK293T cells with Flag-tagged ACBP, and CerS2 or CerS3 activity was assayed. CerS2 or CerS3 activity was also assayed in cell lysates from cells transfected with CerS2 or CerS3 after addition of purified, recombinant ACBP. Data shown represent means ± S.D, n = 3. Statistical analyses were performed using unpaired t-test, *, $p < 0.05$; **, $p < 0.01$, ***, $p < 0.001$, ****, $p < 0.0001$.

FIGURE 4. CerS3 activity is activated by high-speed cytosol. Homogenates were prepared from HEK293T cells overexpressing CerS3 and CerS3 activity was determined using $C_{26:0}$-CoA after addition of purified recombinant ACBP or liver 10.000 x g cytosol (A) or liver 100.000 x g cytosol (B) prepared from $ACBP^{+/+}$, $ACBP^{+/-}$ or $ACBP^{-/-}$ mice. Data shown represent means ± S.D, n = 3. Statistical analyses were performed using unpaired t-test, *, $p < 0.05$; **, $p < 0.01$, ***, $p < 0.001$, ****, $p < 0.0001$.

FIGURE 5. Loss of ACBP in mice reduces CerS activity *in vivo*. CerS2 and CerS3 activities were determined in homogenates from testes from either $ACBP^{+/+}$ mice (black bars) or $ACBP^{-/-}$ mice (grey bars) using $C_{22:0}$-CoA and $C_{26:0}$-CoA as substrates, respectively. Values are mean values ± S.D, n = 3. Statistical analyses were performed using unpaired t-test, *, $p < 0.05$; **, $p < 0.01$, ***, $p < 0.001$, ****, $p < 0.0001$.

FIGURE 6. *Cers1-6* expression is unaffected in testis of $ACBP^{-/-}$ mice. (A) Total RNA was isolated from testis from $ACBP^{+/+}$ (black bars) or $ACBP^{-/-}$ mice (grey bars) and expression levels of *Cers1-6* were determined by qPCR. Data shown are mean values ± SD, n = 9. Statistical analyses were performed using unpaired t-test, *($P < 0.05$), **($P < 0.01$), and ***($P < 0.001$).

FIGURE 7. Ablation of ACBP affects the testis sphingolipidome. LC-ESI MS/MS analysis of ceramide (A), dihydroceramide (B), glucosylceramide (C), dihydroglucosylceramide (D), sphingomyelin (E), dihydrosphingomyelin (F) and sphingoid bases (G) from testis from $ACBP^{+/+}$ mice (black bars) or $ACBP^{-/-}$ mice (grey bars). Values represent mean ± SD, n = 3. Statistical analyses were performed using unpaired t-test, *, $p < 0.05$; **, $p < 0.01$, ***, $p < 0.001$, ****, $p < 0.0001$.

FIGURE 8. ACBP binds long-chain and very long-chain acyl-CoA esters. (A) Recombinant rat ACBP was incubated with the indicated saturated acyl-CoA (1:1 molar ratio), and apo- and holo ACBP were subsequently separated by native gel electrophoresis and protein bands were visualized by Coomassie staining. (B) Recombinant rat ACBP (WT) or ACBP Y28A were incubated with $C_{16:0}$-CoA and subsequently separated by native gel electrophoresis and protein bands visualized by Coomassie staining.

FIGURE 9. CerS3 activity is activated by ACBP and depends on ligand binding to ACBP. Homogenates were prepared from HEK293T cells overexpressing CerS3 and CerS3 activity was determined using $C_{26:0}$-CoA after addition of (A) purified recombinant ACBP or a mutated form of ACBP, which binds ligand with very low affinity, or (B) purified recombinant liver fatty acid binding protein 1 (FABP1). Values are shown as mean ± SD, n = 3. Statistical analyses were performed using unpaired t-test, *, $p < 0.05$; **, $p < 0.01$, ***, $p < 0.001$, ****, $p < 0.0001$.

FIGURE 10. CerS and ACBP interact *in situ*. FLAG-tagged ACBP was co-expressed in HEK293T cells together with (A) HA-tagged CerS2 or CerS3, (B) the indicated HA-tagged CerS, and (C) HA-tagged wild-type and mutated (both W15R) forms of CerS2 or CerS3. PLA using primary antibodies against HA and FLAG tags and secondary antibodies carrying PLA probes were applied to visualize the ACBP-CerS interaction. DAPI was used to detect nuclei. Scale bar, 10 µm or 20 µm (ACBP/CerS2 in B). Controls were cells transfected with empty plasmids alone or in combination with either ACBP or CerS3 plasmids. Other controls received either only one primary antibody or none. (D) Western blots shows expression of FLAG-tagged ACBP and HA-tagged CerS in HEK293T cells transfected with the indicated plasmid. GAPDH was used as loading control. The arrows mark the CerS. 2_m and 3_m indicate cells expressing CerS2 W15R and CerS3 W15R, respectively.

Figure 1

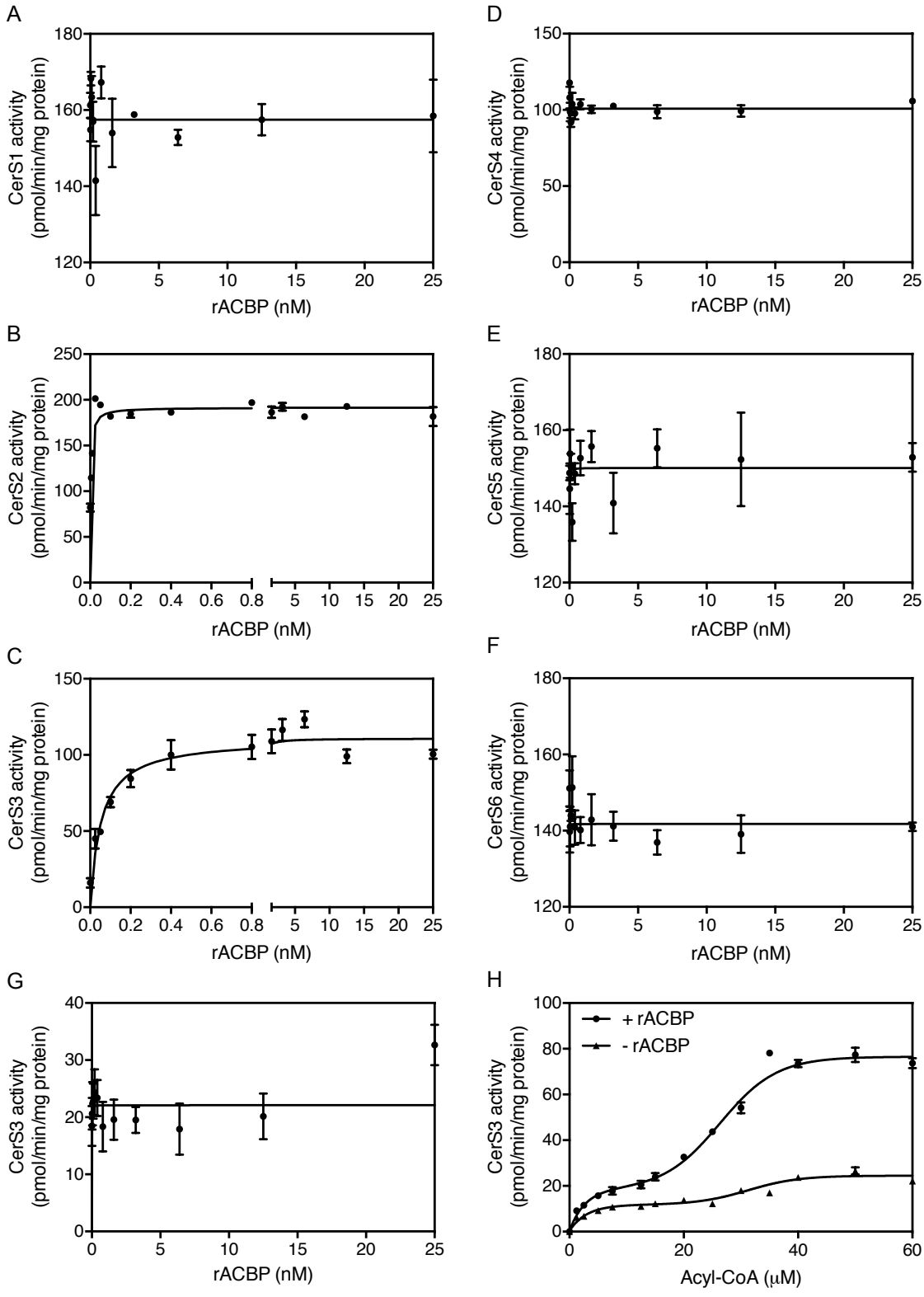
A
CerS1 activity (pmol/min/mg protein)
rACBP (nM)
B
CerS2 activity (pmol/min/mg protein)
rACBP (nM)
C
CerS3 activity (pmol/min/mg protein)
rACBP (nM)
D
CerS4 activity (pmol/min/mg protein)
rACBP (nM)
E
CerS5 activity (pmol/min/mg protein)
rACBP (nM)
F
CerS6 activity (pmol/min/mg protein)
rACBP (nM)
G
CerS3 activity (pmol/min/mg protein)
rACBP (nM)
H
CerS3 activity (pmol/min/mg protein)
+ rACBP
- rACBP
Acyl-CoA (μM)

Figure 2

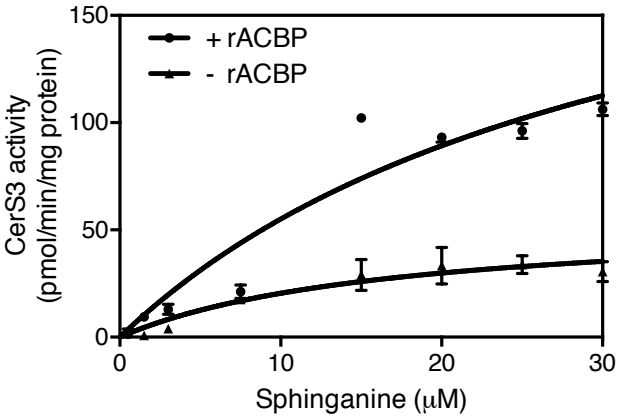
150
100
50
0
0
10
20
30
+ rACBP
- rACBP
CerS3 activity
(pmol/min/mg protein)
Sphinganine (μM)

Figure 3

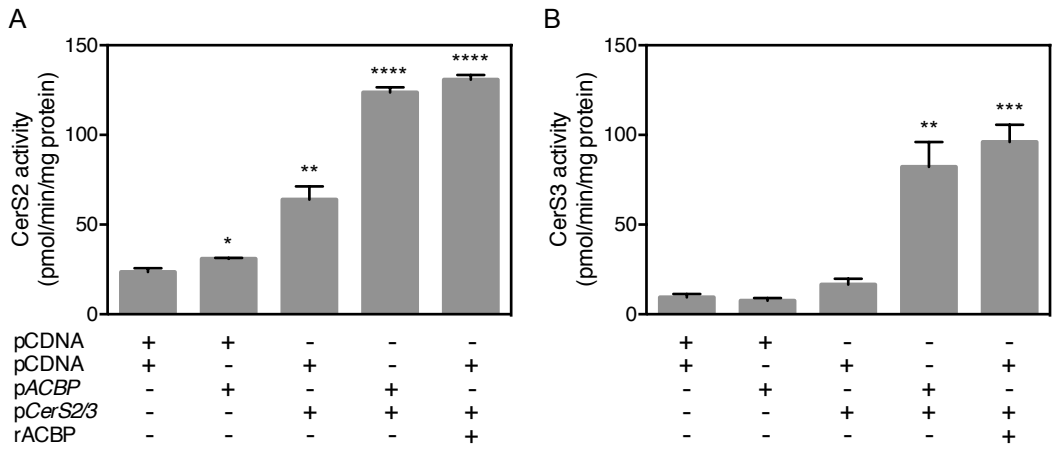
A
CerS2 activity
(pmol/min/mg protein)
150
100
50
0
*
**
****
****
pCDNA + + - - -
pCDNA + - + - +
pACBP - + - + -
pCerS2/3 - - + + +
rACBP - - - - +
B
CerS3 activity
(pmol/min/mg protein)
150
100
50
0
**
***
+ + - - -
+ - + - +
- + - + -
- - + + +
- - - - +

Figure 4

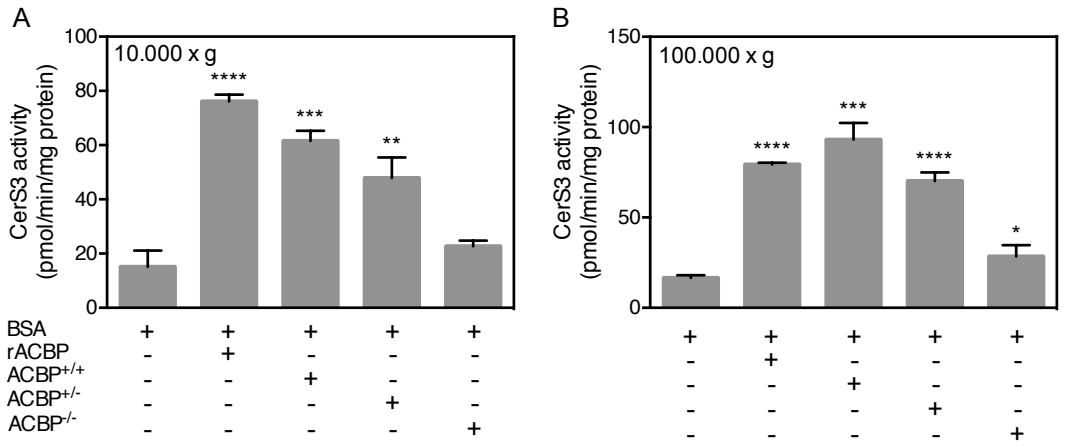
A
10.000 x g
CerS3 activity (pmol/min/mg protein)
100
80
60
40
20
0
****
***
**
BSA + + + + +
rACBP - + - - -
ACBP+/+ - - + - -
ACBP+/- - - - + -
ACBP-/- - - - - +
B
100.000 x g
CerS3 activity (pmol/min/mg protein)
150
100
50
0
****
***
****
*
+ + + + +
- + - - -
- - + - -
- - - + -
- - - - +

Figure 5

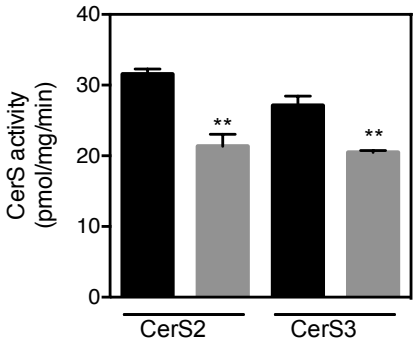

Figure 6

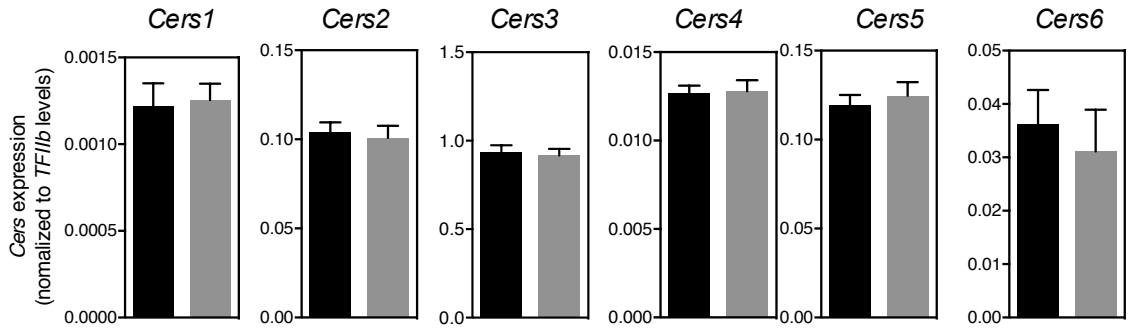
Cers1
Cers2
Cers3
Cers4
Cers5
Cers6
Cers expression
(nomalized to TFIIb levels)
0.0015
0.0010
0.0005
0.0000
0.15
0.10
0.05
0.00
1.5
1.0
0.5
0.0
0.015
0.010
0.005
0.000
0.15
0.10
0.05
0.00
0.05
0.04
0.03
0.02
0.01
0.00

Figure 7

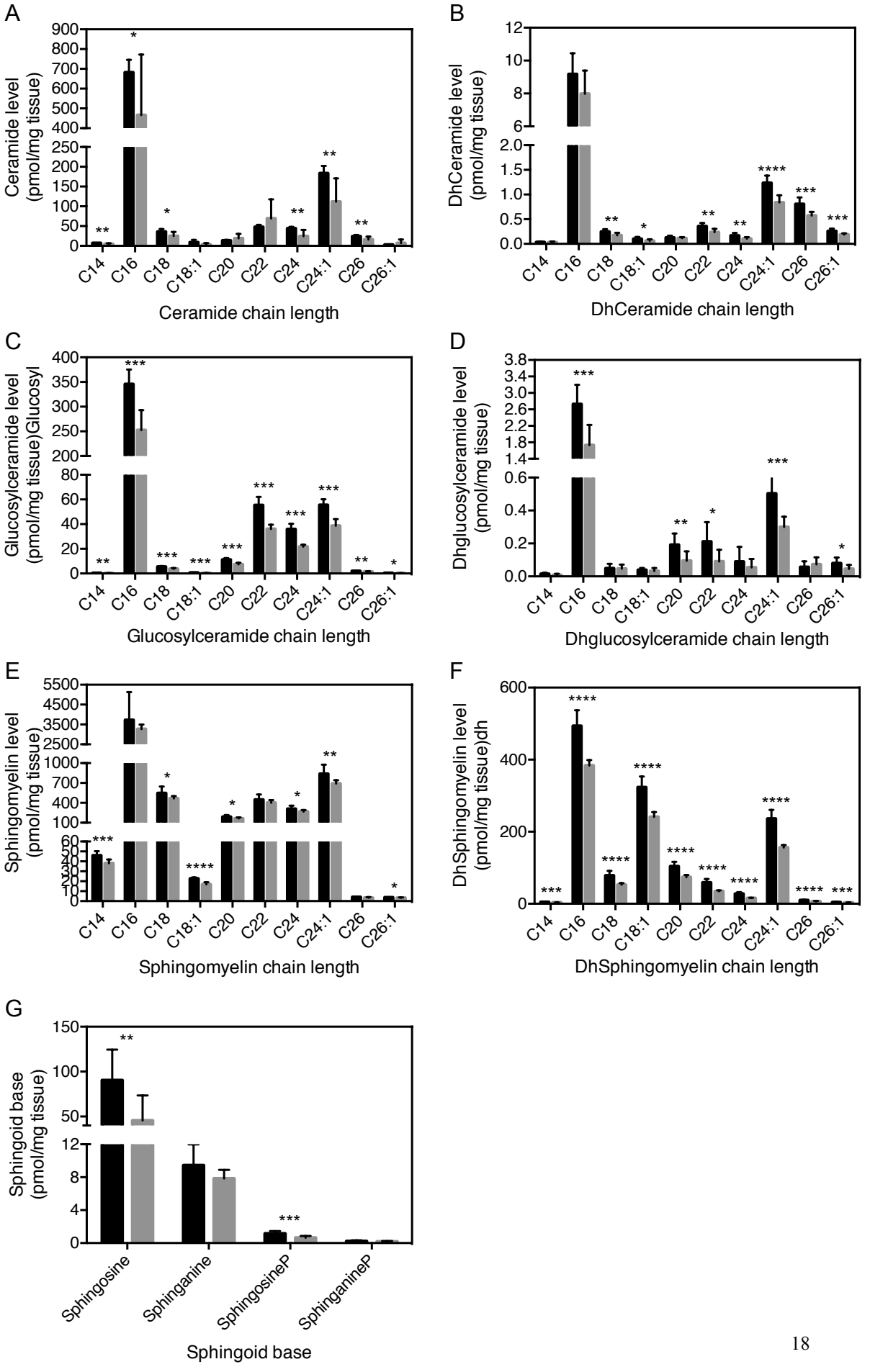
A
Ceramide level (pmol/mg tissue)
Ceramide chain length
B
DhCeramide level (pmol/mg tissue)
DhCeramide chain length
C
Glucosylceramide level (pmol/mg tissue)Glucosyl
Glucosylceramide chain length
D
Dhglucosylceramide level (pmol/mg tissue)
Dhglucosylceramide chain length
E
Sphingomyelin level (pmol/mg tissue)
Sphingomyelin chain length
F
DhSphingomyelin level (pmol/mg tissue)dh
DhSphingomyelin chain length
G
Sphingoid base (pmol/mg tissue)
Sphingosine
Sphinganine
SphingosineP
SphinganineP
Sphingoid base
C14
C16
C18
C18:1
C20
C22
C24
C24:1
C26
C26:1

Figure 8

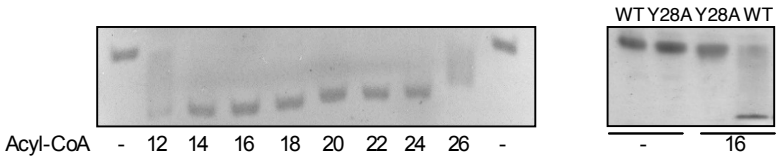

Figure 9

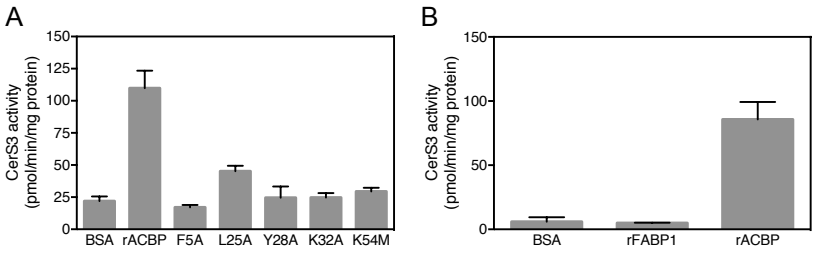
A
CerS3 activity (pmol/min/mg protein)
150
125
100
75
50
25
0
BSA
rACBP
F5A
L25A
Y28A
K32A
K54M
B
CerS3 activity (pmol/min/mg protein)
150
100
50
0
BSA
rFABP1
rACBP

Figure 10

A

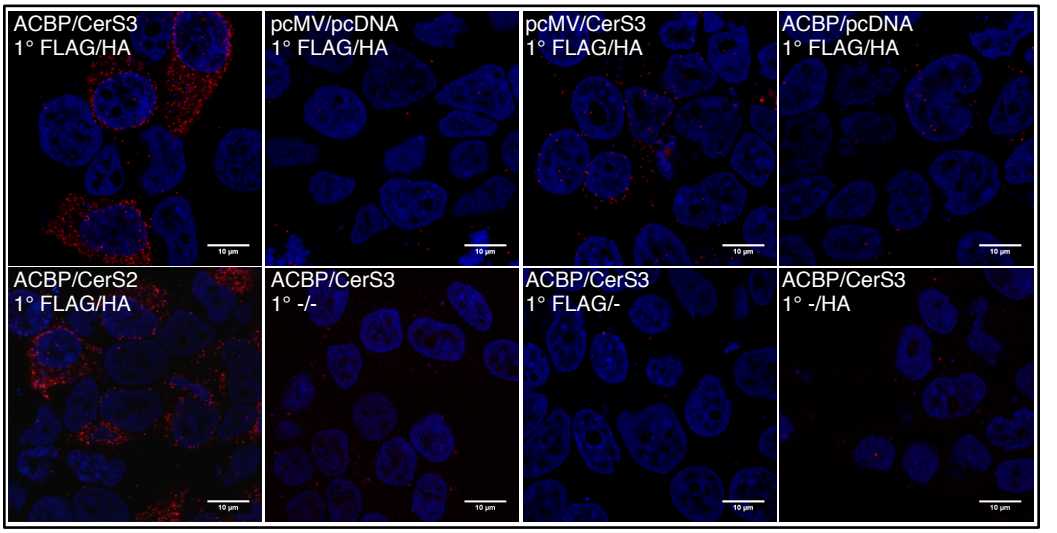

B

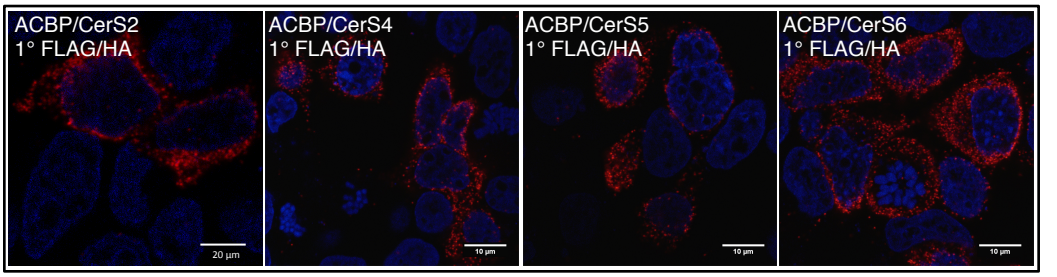

C

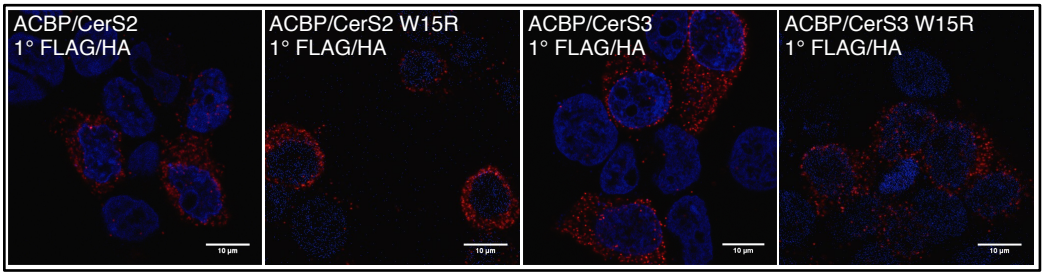

D

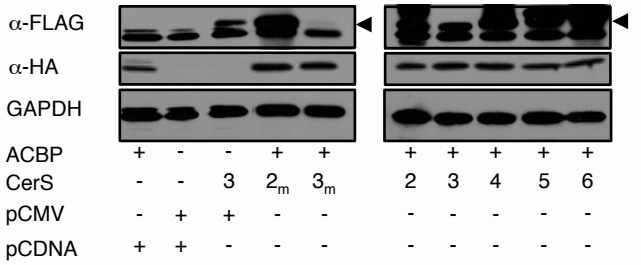

Regulation of very-long acyl chain ceramide synthesis by Acyl-CoA binding protein

Natalia Santos Ferreira, Hanne Engelsby, Ditte Neess, Samuel L. Kelly, Giora Volpert, Alfred H. Merrill, Jr., Anthony H. Futerman and Nils J. Faergeman

J. Biol. Chem. published online March 19, 2017 originally published online March 19, 2017